DETECTING CLIMATE CHANGE IMPACTS THROUGH SOIL BACTERIAL COMMUNITIES IN ALPINE REGIONS OF GANGOTRI NATIONAL PARK, WESTERN HIMALAYA

Thesis submitted for the award of the degree of

Doctor of Philosophy

in

Wildlife Science

by

PAMELA BHATTACHARYA

to

Saurashtra University

Rajkot - 360005 (Gujarat)

Under the supervision of

Dr. Gopal Singh Rawat, Research Affiliate and former Dean

भारतीय वन्यजीव संस्थान
Wildlife Institute of India

July 2022

Citation:

Bhattacharya, P. (2022). Detecting climate change impacts through soil bacterial communities in alpine regions of Gangotri National Park, Western Himalaya. Ph.D. Thesis, Wildlife Institute of India, Dehradun, India and Saurashtra University, Rajkot, India. pp. 1-120.

भारतीय वन्यजीव संस्थान
Wildlife Institute of India

DECLARATION

I hereby declare that the work conducted under the thesis entitled "**Detecting climate change impacts through soil bacterial communities in alpine regions of Gangotri National Park, western Himalaya",** is a record of original and independent research work done by me and subsequently submitted for the award of degree of **Doctor of Philosophy in Wildlife Science** to **Saurashtra University, Rajkot (Gujarat).** This research work has been carried out under the guidance and supervision of Dr. Gopal Singh Rawat, Ex Dean and Research Affiliate and co-supervision of Dr. Gautam Talukdar, Scientist E of Wildlife Institute of India, Dehradun. The work has not formed the basis for the award of any other degree, diploma or any other qualification. I also declare that the thesis embodies my own work, analysis, observation, understanding and the particulars given in it are true to the best of my knowledge.

Pamela Bhattacharya

(Pamela Bhattacharya)

Place: Dehradun

Date: 6.07.2022

(Dr. Gopal Singh Rawat)

Supervisor

पत्रपेटी सं0 18, चन्द्रबनी, देहरादून – 248 001, भारत
Post Box No. 18, Chandrabani, Dehra Dun - 248001, INDIA
ई.पी.ए.बी.एक्स : + 91-135-2640111 से 2640115 फैक्स : 0135-2640117, तार : WILDLIFE
EPABX : + 91-135-2640111 to 2640115 Fax : 0135-2640117; GRAM : WILDLIFE
ई–मेल / E-mail : wii@wii.gov.in

भारतीय वन्यजीव संस्थान
Wildlife Institute of India

CERTIFICATE

This is to certify that the thesis by Ms. Pamela Bhattacharya entitled "**Detecting climate change impacts through soil bacterial communities in alpine regions of Gangotri National Park, western Himalaya**", is an original and independent research work submitted to the **Saurashtra University, Rajkot (Gujarat)**, for the award of the degree of **Doctor of Philosophy in Wildlife Science.**

Ms. Pamela Bhattacharya has put more than six semesters of research work embodied in this thesis under my guidance and supervision. The work presented in this thesis has not been submitted to any other University or Institute for the award of any degree, diploma or distinction.

(Dr. Gopal Singh Rawat)
Supervisor

(Dr. Yadvendradev Jhala)
Dean
Faculty of Wildlife Science

संकायाध्यक्ष / Dean
भारतीय वन्यजीव संस्थान
WILDLIFE INSTITUTE OF INDIA
देहरादून / Dehradun

पत्रपेटी सं0 18, चन्द्रबनी, देहरादून – 248 001, भारत
Post Box No. 18, Chandrabani, Dehra Dun - 248001, INDIA
ई.पी.ए.बी.एक्स : + 91-135-2640111 से 2640115 फैक्स : 0135-2640117, तार : WILDLIFE
EPABX : + 91-135-2640111 to 2640115 Fax : 0135-2640117, GRAM : WILDLIFE
ई–मेल / E-mail : wii@wii.gov.in

Accredited Grade "A" by NAAC

SAURASHTRA UNIVERSITY
P.G.T.R Section
Main Office, First Floor
University Road
Rajkot – 360 005 (Gujarat)
Phone No.: 2578501
Fax : (0281)2856983
www.saurashtrauniversity.edu

CERTIFICATE FOR PRE-Ph.D. PRESENTATION

This is to certify that **Ms. Pamela Bhattacharya** has made Pre-Ph.D. presentation as per UGC guideline "University Grant Commission (Minimum Standard and Procedure for award of Ph.D. Degree) Regulation-2016" and Saurashtra University Ordinance for Ph.D. Programme (O.Ph.D. 8.3), on her research work entitled "**Detecting climate change impacts through soil bacterial communities in alpine regions of Gangotri National Park, western Himalaya",** at Wildlife Institute of India, Dehradun, Research Centre of Saurashtra University, Rajkot on 11th October 2021 before all the faculty members and students of the Department for getting feedback and comments.

I certify that the research work was appreciated by all who were present, and the comments made by the faculty and researchers have been appropriately included in the thesis.

(Dr. Gopal Singh Rawat)
Supervisor

(Dr. Yadvendradev Jhala)
Dean
Faculty of Wildlife Science

संकायाध्यक्ष / Dean
भारतीय वन्यजीव संस्थान
WILDLIFE INSTITUTE OF INDIA
देहरादून / Dehradun

भारतीय वन्यजीव संस्थान
Wildlife Institute of India

CERTIFICATE OF PLAGIARISM CHECK

This is to certify that the Ph.D. thesis titled "**Detecting climate change impacts through soil bacterial communities in alpine regions of Gangotri National Park, western Himalaya**", submitted by Ms. Pamela Bhattacharya has been examined by us for plagiarism check as per UGC (Promotion of Academic Integrity and Presentation of Plagiarism in Higher Educational Institutions) Regulations. The following inference are drawn from the check:

a) Thesis has significant new work/knowledge as compared to already published work or work under consideration for publication elsewhere.
b) No sentence, equation, diagram, table, paragraph or section id found to have been copied verbatim from previous work unless it was placed under quotation marks and source was duly cited.
c) The work presented is original work of the author (i.e., there is no plagiarism) and there is no fabrication or by changing or by omitting data or results such that the research is not accurately represented.

The similarity percentage for the thesis as reported by the software iThenticate is 10%. Two papers already published from this thesis with Ms. Pamela Bhattacharya as the first author have been excluded from the plagiarism check.

(Smt. Sunita Agarwal)
Librarian

(Sunita Agarwal)
Librarian
Wildlife Institute of India
Dehradun

(Dr. Gopal Singh Rawat)
Supervisor

पत्रपेटी सं0 18, चन्द्रबनी, देहरादून – 248 001, भारत
Post Box No. 18, Chandrabani, Dehra Dun - 248001, INDIA
ई.पी.ए.बी.एक्स : + 91-135-2640111 से 2640115 फैक्स : 0135-2640117, तार : WILDLIFE
EPABX : + 91-135-2640111 to 2640115 Fax : 0135-2640117; GRAM : WILDLIFE
ई–मेल / E-mail : wii@wii.gov.in

DETECTING CLIMATE CHANGE IMPACTS THROUGH SOIL B...

By: Pamela BHATTACHARYA

As of: Jan 18, 2022 8:10:46 PM
16,951 words - 151 matches - 94 sources

Similarity Index

10%

Mode: Summary Report

sources:

119 words / 1% - Internet from 29-Oct-2021 12:00AM
www.frontiersin.org

36 words / < 1% match - Internet from 10-Oct-2021 12:00AM
www.frontiersin.org

27 words / < 1% match - Internet from 09-Mar-2019 12:00AM
www.frontiersin.org

23 words / < 1% match - Internet from 28-Oct-2021 12:00AM
www.frontiersin.org

20 words / < 1% match - Internet from 16-Oct-2021 12:00AM
www.frontiersin.org

20 words / < 1% match - Internet from 29-Nov-2021 12:00AM
www.frontiersin.org

12 words / < 1% match - Internet from 16-Apr-2020 12:00AM
www.frontiersin.org

11 words / < 1% match - Internet from 13-Nov-2021 12:00AM
www.frontiersin.org

10 words / < 1% match - Internet from 13-Nov-2021 12:00AM
www.frontiersin.org

9 words / < 1% match - Internet from 11-Oct-2021 12:00AM
www.frontiersin.org

9 words / < 1% match - Internet from 27-Dec-2021 12:00AM
www.frontiersin.org

CONTENTS

Acknowledgements

This Ph.D. work has come to its completion today with the support and guidance of many individuals to whom I am immensely thankful. I would like to acknowledge Dr. Dhananjay Mohan (Director), Dr. V.B. Mathur (former Director), Dr. Ruchi Badola (Dean), Dr. Monali Sen (Registrar), Dr. Bitapi Sinha (Research coordinator), and Dr. S. Sathyakumar (Nodal Officer, DST project National Mission for Sustaining the Himalayan Ecosystem), Wildlife Institute of India, for providing me the opportunity to conduct this Ph.D. research work in the institute.

I am grateful to my supervisor Dr. Gopal Singh Rawat, for accepting me as his student and giving me his support, guidance, and encouragement throughout this research work. His immense knowledge and valuable advice has helped me to develop good work ethics and conduct this research work independently with confidence. I cannot thank him enough for all that I have learnt from him. I would like to thank my co-supervisor Dr. Gautam Talukdar for his continuous support, guidance and time during this Ph.D. work. He has given me all the freedom and motivation to explore several aspects of research life and shape this thesis and the manuscripts.

I would like to thank all funding agencies for supporting this Ph.D. work. This work had been a part of the project National Mission for Sustaining the Himalayan Ecosystem (NMSHE) that was funded by the Department of Science and Technology, Government of India (Grant no. DST/SPLICE/CCP/NMSHE/TF-2/WII/2014[G]). Partial funding for the bacterial Next Generation Sequencing was provided by the United Nations Development Programme and the Ministry of Environment, Forest and Climate Change Government of India through the Third National Communication project (Grant no. 7/2/2015-CC). I would like to acknowledge the Council of Scientific and Industrial Research, Government of India (Award no. 09/668(0012)/2019– EMR–I) for supporting me with Senior Research Fellowship.

I am immensely thankful to Pankaj Tiwari for his unparalleled support during this work. His ideas were crucial to develop the novel concepts and theories of the studies. The constructive arguments and discussions I had with him have improved the work quality and took this thesis in the right direction resulting in two good publications in renowned journals. His involvement have made it possible to bring this thesis to finalization. It was a memorable experience to work with him and gain knowledge.

I would also like to thank Dr. Punyasloke Bhadury for his valuable input regarding in-depth sequencing, Dr. Awadhesh Pandit and Tejali Naik for their support in Next Generation Sequencing work. I am grateful to Sitendu Goswami, who is no less than a mentor to me. He has taught me data analysis in R, troubleshoot data analysis difficulties time to time and fine tune the study design. I would also like to thank Dr. Raman Kumar for his valuable guidance regarding statistics and data analysis. My thanks to Dr. S.K. Gupta (Nodal Officer of Wildlife Forensics and Conservation Genetics Cell) and Dr. J.A. Johnson (Nodal Officer of Analytical laboratory) of Wildlife Institute of India for facilitating this work. I am also thankful to Madhan Raj, Mr. Rakesh and Arun Kumar for their support in the genetics and analytical laboratory. I also acknowledge help from Dr. Ishwari Dutt Rai, Dr. Devendra Kumar and Umed S. Rana for their field assistance. I sincerely thank Dr. Samrat Mondol for motivating and supporting me to execute the work in the Institute and NCBS where I conducted the sequencing. His constant guidance and vital inputs have helped me to fine tune the work.

I would also like to thank Principal Chief Conservator of Forests of Uttarakhand, Divisional Forest Officers (DFOs), Uttarkashi for providing necessary permits to conduct the research in Gangotri National Park. I would like to acknowledge the wardens, range officers, deputy range officers, foresters, and forest guards for their support during the field work.

Finally, I would like to acknowledge dadu, baba, ma, Sonali di, and Debajyoti da for encouraging and keeping faith in me throughout this journey.

List of publications:

Bhattacharya, P., Tiwari, P., Talukdar, G., Rawat, G.S. (2022). Shifts in bacterial community composition and functional traits at different time periods post-deglaciation of Gangotri glacier, Himalaya. Current Microbiology, 79(3):91. https://doi.org/10.1007/s00284-022-02779-8

Bhattacharya, P., Tiwari, P., Rai, I.D., Talukdar, G., Rawat, G.S. (2022). Edaphic factors override temperature in shaping soil bacterial diversity across an elevation-vegetation gradient in Himalaya. Applied Soil Ecology, 170, 104306. https://doi.org/10.1016/j.apsoil.2021.104306

Tiwari, P., **Bhattacharya, P**., Rawat, G.S., Talukdar, G. (2021). Equilibrium in soil respiration across a climosequence indicates its resilience to climate change in a glaciated valley, western Himalaya. Scientific Reports, 11, 23038. https://doi.org/10.1038/s41598-021-02199-x

Tiwari, P., **Bhattacharya, P**., Rawat, G.S., Rai, I.D., Talukdar, G. (2021). Experimental warming increases ecosystem respiration by increasing above-ground respiration in alpine meadows of Western Himalaya. Scientific Reports, 11, 2640. https://doi.org/10.1038/s41598-021-82065-y

Bhattacharya, P., Talukdar, G., Rawat, GS., Mondol, S. (2017). Importance of monitoring soil microbial community responses to climate change in the Indian Himalayan region. Current Science, 112: 1622 – 1623. IF: 0.883.

Bhattacharya, P., Priyadarshani, S., Kumar, D., & Rai, I. D. (2016). Bibliography on microflora (lichens, fungi and bacteria) of the Indian Himalayan Region. Bibliography on the Fauna and Micro flora of the Indian Himalayan Region, 17, 264.

List of conferences: *International*

Bhattacharya P (2021) Oral presentation titled "Experimental warming impacts on soil bacterial community in an alpine meadow, Western Himalaya " in Summer Field School (online) on "Mountain ecosystems and resource management", Grassroots Institute, Canada, September 2021.

Bhattacharya P (2020) Abstract selected for oral presentation titled "Patterns of soil bacterial diversity, community composition and function along glacial foreland in Gangotri National Park, Western Himalaya" in 36th International Geological Congress.

Bhattacharya P (2015) Training course on "Monitoring Greenhouse Gas Fluxes from Natural and Agro-ecosystems", Chengdu Institute of Biology, Chengdu, China, December 2015.

List of conferences: *National*

Bhattacharya P (2018) Oral presentation titled "Influence of environmental parameters on soil microbial community function across alpine habitats in Indian Himalayan region" in 3rd Himalayan Internal Annual Research seminar in Wildlife Institute of India, Dehradun.

Bhattacharya P (2017) Oral presentation titled "Soil microbial community composition and function across alpine habitats of Gangotri National Park, Uttarakhand" in 2nd Himalayan Internal Annual Research seminar in Wildlife Institute of India, Dehradun.

Bhattacharya P (2016) Oral presentation titled "Soil microbial communities and lichens as indicator systems for monitoring climate change impacts in alpine regions of the Indian Himalayan Region" in National Conference on "Recent Advances in Remote Sensing and GIS with Special Emphasis on Mountain Ecosystems" organized at Indian Institute of Remote Sensing, Dehradun.

Bhattacharya P (2016) Oral presentation titled "Response of soil bacterial communities to changes in climate in the Indian Himalayan Region – standardization of methods" in 1st Himalayan Internal Annual Research seminar in Wildlife Institute of India, Dehradun.

Bhattacharya P (2015) Poster presentation titled "Detecting climate change impacts on mycorrhizal communities in the Indian Himalayan region" at the annual meeting of Cryptogam research in India, National Botanical Research Institute, Lucknow.

List of figures

List of tables

Chapter 1

Background

1.1 Introduction

Increasing emission of greenhouse gases since industrialization has substantially changed the atmospheric composition and is the primary cause of climate change (Krishnan et al., 2020). Warming since 1950 has contributed significantly to weather and climate extremities, including heat waves, heavy precipitation, droughts, global monsoon pattern change, melting of glaciers, rise in sea level that have led to changes in marine and terrestrial ecosystems (Krishnan et al., 2020). In this regard, terrestrial microbial communities hold great significance as they play a crucial role in carbon (C) and nitrogen (N) cycles and lead to the emission of greenhouse gases like carbon dioxide (CO_2), methane (CH_4), and nitrous oxide (N_2O) through decomposition of organic matter (Chatterjee and Saha, 2018; Dutta and Dutta, 2016; Singh et al., 2010). Therefore, soil microbial communities can provide positive feedback to climate change, and hence understanding the response of these communities to climate change requires much attention.

The global mean surface temperature has increased by 1.5 ºC in the last century and is predicted to rise by 5 ºC at the end of the 21st century ("IPCC Climate Change 2013," 2013). However, the temperature rise will not be uniform globally, where some regions, including the high latitudes and mountains, will experience greater warming than the global average (Krishnan et al., 2020; Mountain Research Initiative EDW Working Group, 2015) (Figure 1.1). Among the mountain ecosystems, Himalaya is predicted to experience a temperature increase of about 5.2 °C under the RCP8.5 scenario by the 21st century (Shrestha et al., 2012a). Earlier studies prove that western Himalaya has already warmed by 0.9 °C from 1901–2003 (Dash et al., 2007). Moreover, it has been projected that warming will be more prominent in alpine regions (Chen and Tian, 2005; Mountain Research Initiative EDW Working Group, 2015). Almost one-third of India's soil organic

C is present in the Himalaya (Bhattacharyya et al., 2008), of which alpine regions store a large proportion due to low decomposition and low turnover rate under extremely cold conditions (Budge et al., 2011). The alpine regions being C-rich and temperature-sensitive, there are major concerns that rising temperature can deplete C store triggered by enhanced microbial decomposition, eventually reducing substrate for microbes and increasing C in the atmospheric pool (Bardgett et al., 2008; Donhauser and Frey, 2018; Trivedi et al., 2013).

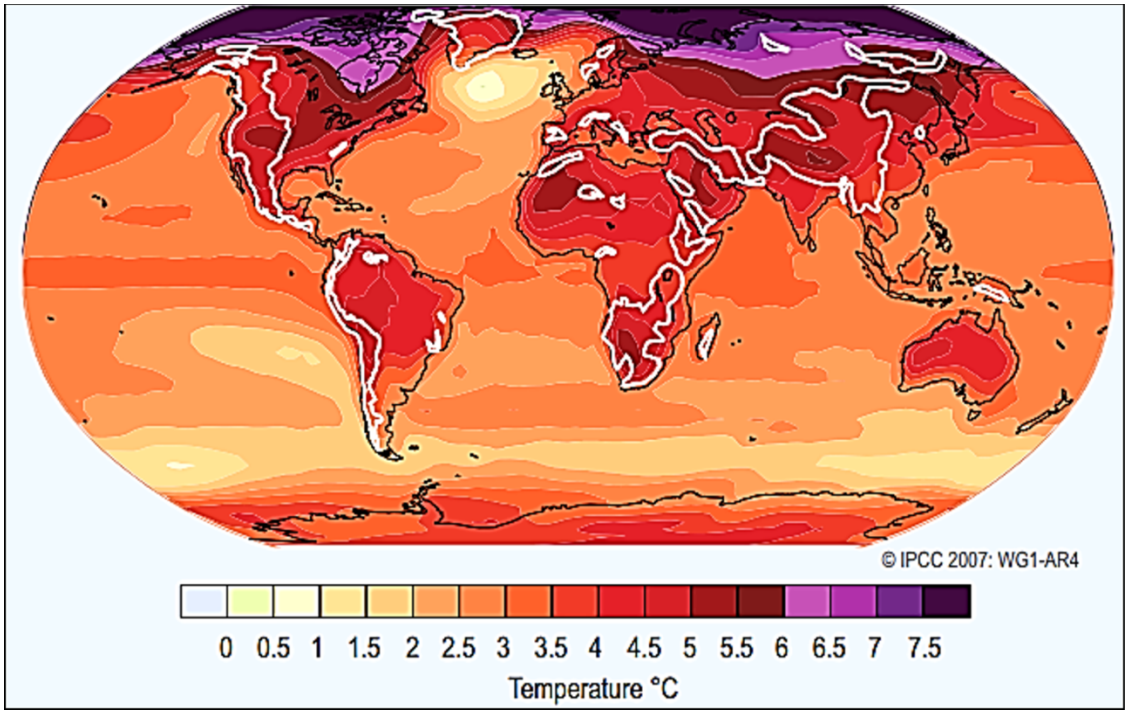

Figure 1.1 Projected temperature increase by the end of 21st across the globe. The white contour line depicts important mountain regions of the world (IPCC Climate Change 2007).

Plant communities sequester the atmospheric CO_2 through photosynthesis, of which most are stored in the plant tissues, and the excess is excreted out as root exudates (Figure 1.2) (Trivedi et al., 2013). C from both root exudates and plant dead leaves and stems become

food for the microbes in the soil (Trivedi et al., 2013). The microbes degrade the SOC for sustaining their life processes and, in the process, liberate CO_2 (Trivedi et al., 2013). The remaining C gets accumulated in the soil. The balance in the nature is such that soil acts as a C sink and currently stores about 2500 petagrams of C, which is 3 times that of the atmospheric pool (Figure 1.2) (Trivedi et al., 2013). There are two types of microbial communities in the soil, one that feeds on root exudates directly, and the other depends on the SOC store (Figure 1.3). The respiration from plant and microbial communities are termed autotrophic, and heterotrophic respiration,

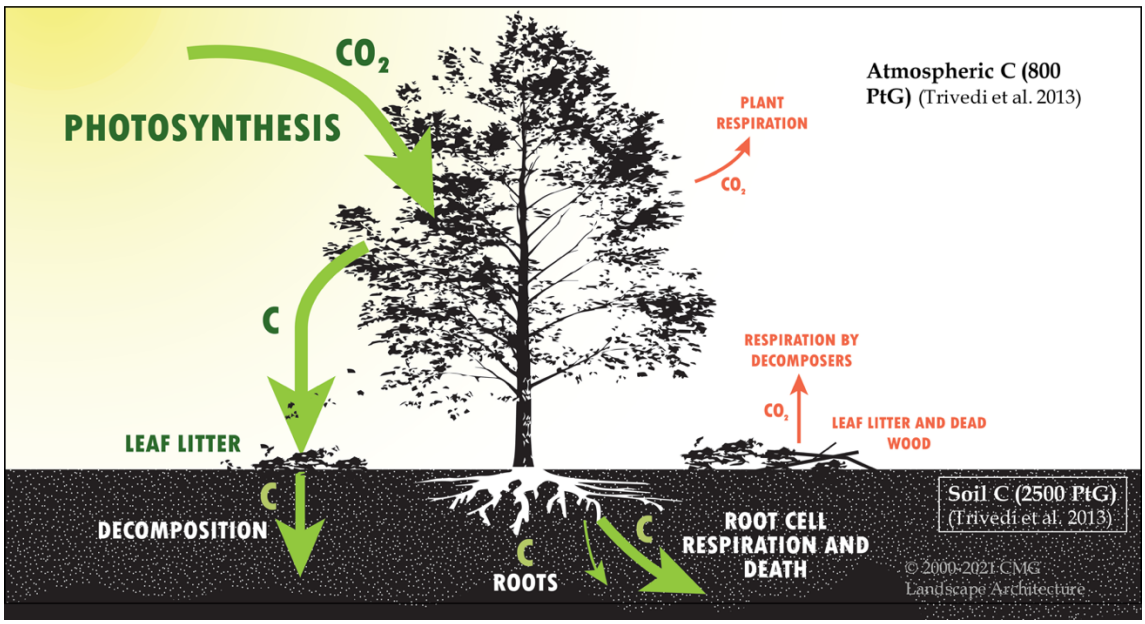

Figure 1.2 The role of plants and microbial decomposition in terrestrial carbon cycle. Background image courtesy to CMG Landscape Architecture (2000-2021).

respectively, and together constitutes soil respiration (Trivedi et al., 2013). Soil respiration is the largest land-to-air CO_2 flux estimated to be 10 times more than the C liberated by anthropogenic sources (Hashimoto et al., 2015). Climate warming is

expected to increase C decomposition by microbes and, in turn, soil respiration providing positive feedback to climate warming (Bardgett et al., 2008).

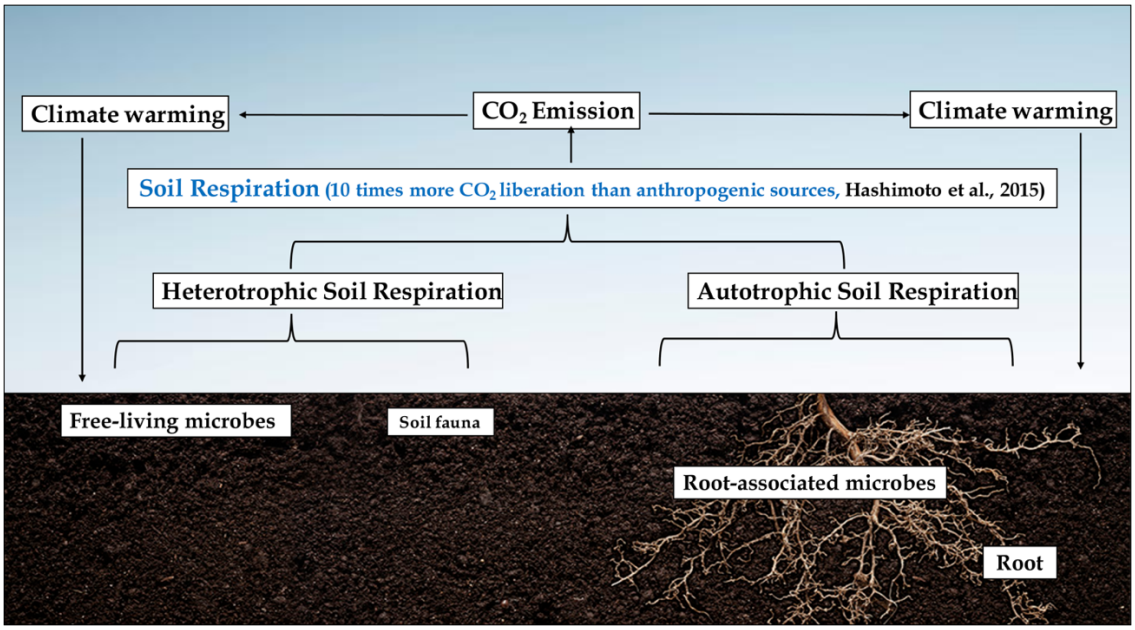

Figure 1.3 Effects of climate warming on soil microbial community and respiration and feed back to global climate warming.

1.2 Review of literature

The primary focus of this study was alpine bacterial communities. Upon in-depth review, it was found that studies have been conducted in some alpine ecosystems of the world, including Tibetan Plateau, Swiss, Italian, and European Alps, Colorado Rocky mountain, Peruvian Andes, Austrian Alps, Mount Fuji, Changbai Mountain and Mount Gongga (Donhauser and Frey, 2018) to understand the response of these communities to climate change (Figure 1.4, Appendix Table A1). These studies reveal a considerable bacterial diversity despite harsh and cold condition in the alpine environment. While it is well established that plant and animal diversity decreases with increasing elevation due to extreme climatic conditions at high altitudes, soil microbes are more adapted to cold

oligotrophic nutrient-limited conditions and follow distribution pattern that varied from place to place (Bryant et al., 2008). Different environmental factors, including climate, vegetation and edaphic properties were found to primarily influence the community composition in the alpine soil (Donhauser and Frey, 2018).

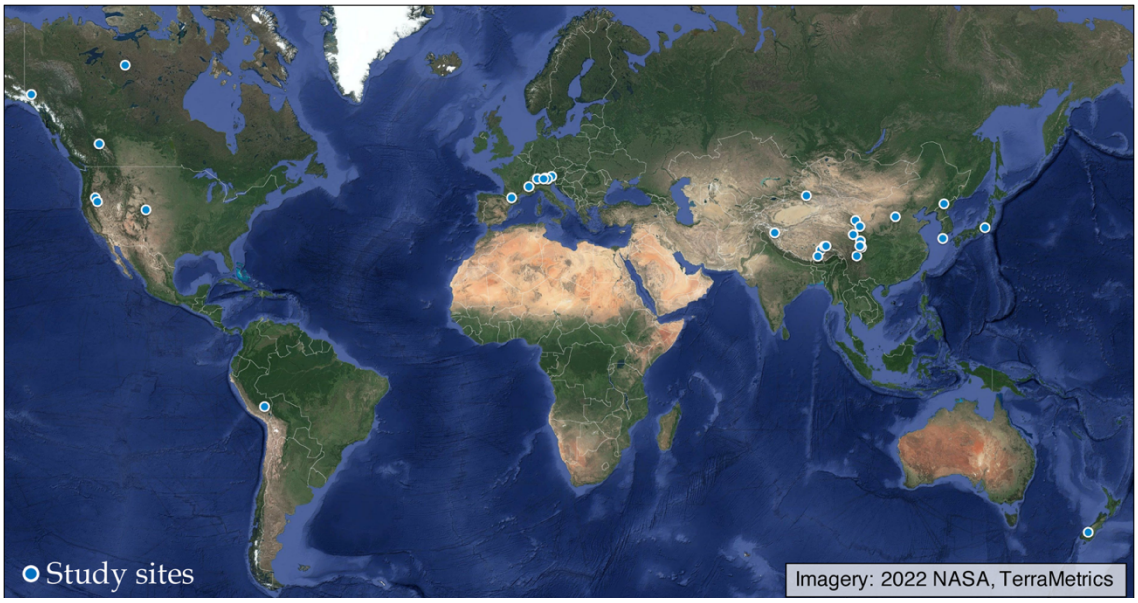

Figure 1.4 Climate change impact studies on alpine soil bacterial communities. The map was generated in Google maps and the satellite imagery used is a base map.

The inconsistency in distribution patterns is mainly due to local edaphic conditions and climate variability (Singh et al., 2014; Yashiro et al., 2016). It is only when more studies on bacterial diversity patterns from alpine ecosystems having similar geological and climatic conditions are performed over spatial and temporal scales, appropriate conclusions can be made regarding their response to climate change.

Current knowledge regarding soil bacterial community response to climate change is based mainly on studies conducted in the Tibetan Plateau (as can be seen by the high density of study points in the Figure 1.4), while the nearby Himalayan region entirely

lacks any such study. Major subject focus on soil bacterial research has been on applied and functional research, taxonomy, ecology, bacterial genetics/genomics and biodiversity conservation. Applied and functional research include investigation of soil bacterial diversity in different ecological niches along altitudinal gradients for isolation and identification of biotechnologically and agriculturally potential strains and novel species (Kasana and Yadav, 2007; Duraipandiyan et al., 2010; Bharti et al., 2010; Saba et al., 2012; Sharma et al., 2014; Kshetri et al., 2015).

Encompassing the world's highest mountain ranges, the Himalaya represents diverse ecosystems with immense biodiversity (Padma, 2014). In addition, it retains about 33% of India's C stock (Bhattacharyya et al., 2008) and has a critical role in the global carbon cycle and climate warming (Longbottom et al., 2014; Yang et al., 2008). However, our knowledge on soil bacterial community is limited to only their diversity and composition based on cloning techniques. Furthermore, studies based on metagenomics are at its nascent stage and no effort have been taken till date to understand the influence of environmental factors on these communities (Bhattacharya et al., 2016).

Earlier studies on climate change impacts on soil bacterial communities involved laboratory incubation of soil samples at different temperatures (Figure 1.5) (Bradford et al., 2010). However, this approach led to changes in the microclimate and edaphic properties, and the results were unreliable. Recent strategies include the assessment of bacterial communities at their natural sites (Figure 1.5) (Donhauser and Frey, 2018). Some efforts have been made to use the deglaciation event for understanding patterns in the bacterial communities at different time periods of glacier retreat induced by climate change (Figure 1.5) (Ciccazzo et al., 2016; Hotaling et al., 2017) Another popular approach involves using elevation gradients as a proxy for climate change, where decreasing elevation represented increasing temperature (Figure 1.5) (Margesin and

Niklinska, 2019). The most recent approach consists of the use of open-top chambers (OTCs) to simulate climate warming in the field (Figure 1.5) (Donhauser and Frey, 2018; Marion et al., 1997).

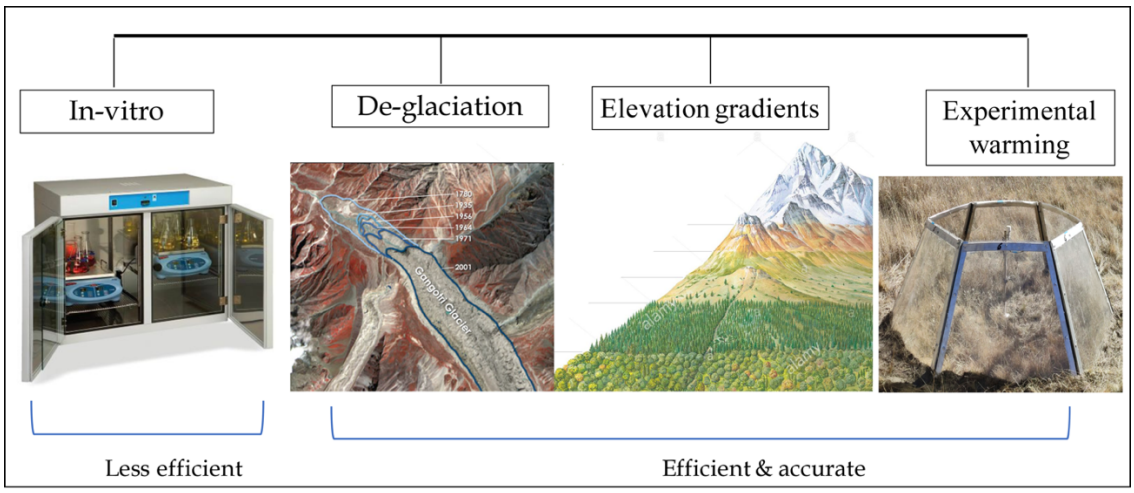

Figure 1.5 Different approaches to study climate change impacts on soil microbial communities.

Microbial communities can be analysed through two different techniques, i.e., culture-dependent and culture-independent, to estimate their diversity and taxonomic composition (Figure 1.6) (Botta and Cocolin, 2012). With the development of technology, we have now shifted from laborious culture dependent to fast and efficient next generation sequencing (NGS) (Suyal et al., 2019). Using this technique not only we can identify a large number of microbial taxa at species level in a community but also the metagenome functional potential by virtue of computational methods (Shendure and Ji, 2008). NGS has several advantages over sanger sequencing (Figure 1.7) (Shendure and Ji, 2008). Unlike sanger sequencing, NGS does not require cloning of microbial marker genes. Moreover NGS can generate millions of reads per sample at once and 96 samples can be sequence parallelly which saves both time and cost (Shendure and Ji, 2008).

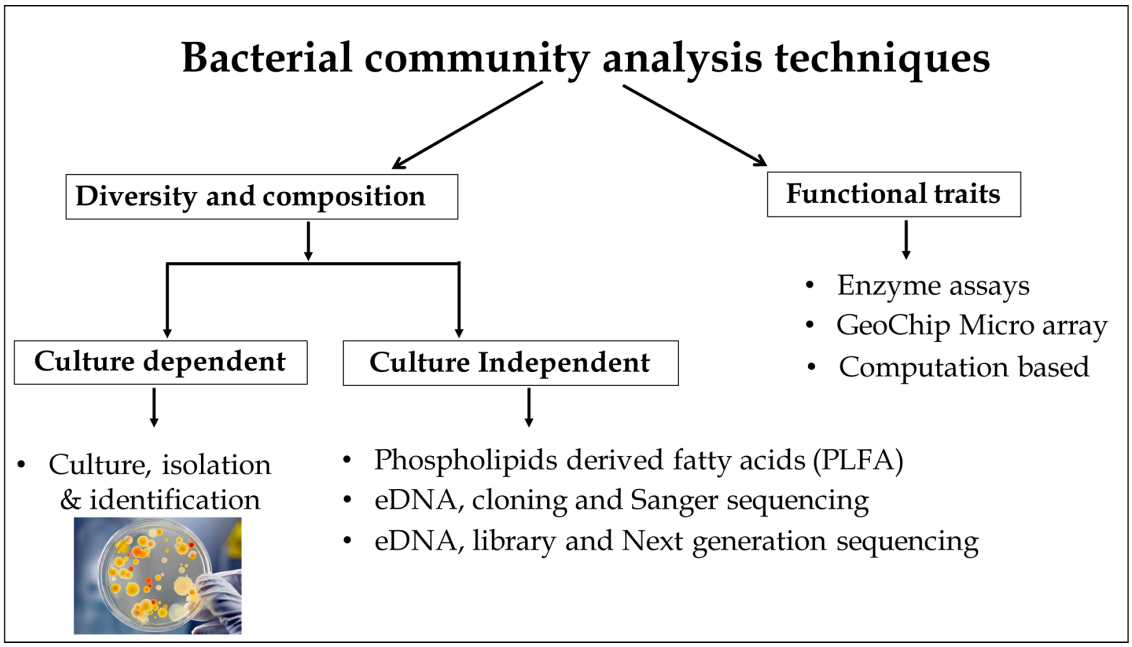

Figure 1.6 Different techniques to analyse bacterial community diversity and functions.

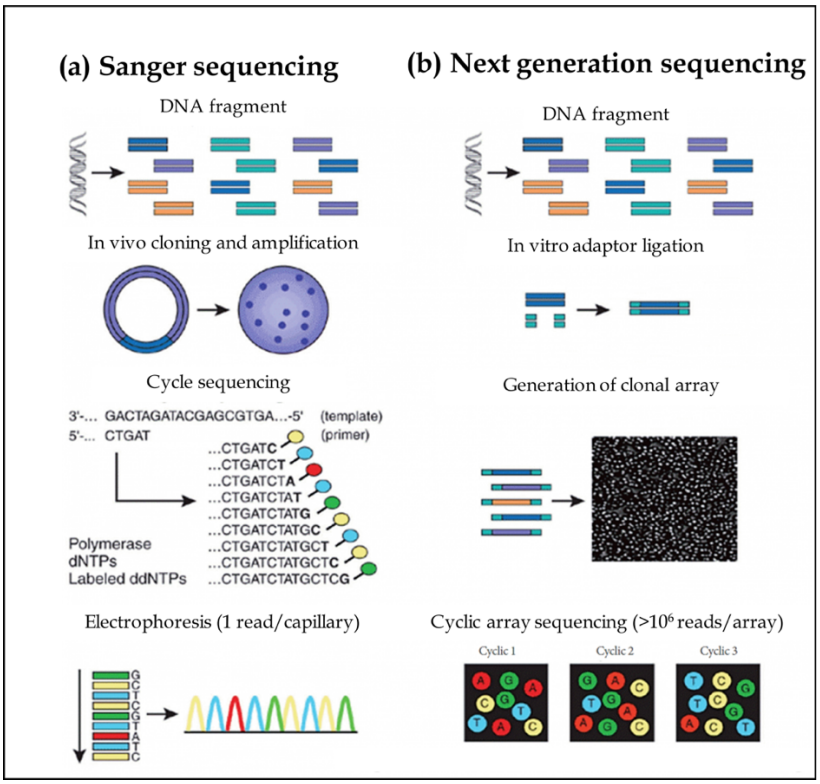

Figure 1.7 Work flow of (a) Sanger sequencing and (b) Next generation sequencing.

1.3 Research objectives

The proposed study aims to use molecular data to understand the ecology of bacterial community including variation in their diversity, composition and functions in response to climate warming in alpine region of Gangotri National Park, western Himalaya. Earlier to this study, knowledge regarding the ecological traits of these communities and the impact of climate warming was entirely lacking. The primary focus of this thesis work was to generate baseline data on alpine soil bacterial community in the Himalaya.

The objectives of this doctoral research are:

1. Understanding the shifts in soil bacterial diversity and ecological traits at different periods post deglaciation of Gangotri glacier, western Himalaya.
2. Assessing climate change impacts on soil bacterial diversity and functional traits using alpine elevation-vegetation gradient as proxy.
3. Evaluating the role of temperature and edaphic factors in shaping the community diversity and composition along the elevation-vegetation gradient.
4. Investigating bacterial community response to experimental warming in an alpine meadow.

1.4 Research questions

The specific questions of this doctoral research are:

1. How soil bacterial communities respond to climate change in alpine region of Himalaya?
2. What are the environmental parameters that influence the community diversity and composition ?

1.5 Study area

The study was conducted along a recently deglaciated valley in the upper Bhagirathi basin towards the snout of the Gaumukh glacier in Gangotri National Park, western Himalaya (30.95–30.99° N, 78.99–79.06° E) (Figure 1.8). We selected an elevation gradient of ~ 700 m starting from 3373 m to 4020 m along the valley. The entire gradient encompasses a ~14 km trail of 7 km^2 area where anthropogenic interference is limited and livestock grazing is banned. In our study we have divided the gradient into low (3373-3564 m), mid (3645-3770 m) and high (3890-4020m) elevation ranges as represented in figure 1.8 for ease in result interpretation.

The Gangotri glacier is the largest in Himalaya, having a total ice cover of 200 km^2 (Rao and Patil, 2017). From 1935 to 1996, the glacier has retreated on an average of 19 m/year, double that of the previous century exposing 2.25 km^2 (Rao and Patil, 2017). The deglaciated foreland now supports alpine and subalpine vegetation rich in high altitude flora that has been legally protected in the form of Gangotri National Park (Pusalkar and Singh, 2012). To understand the bacterial community succession with respect to plant community development after glacier retreat we selected three sites representing recent (~ 17 yrs.), intermediate (~ 120 yrs.), and late (~ 326 yrs.) post-deglaciation periods located at increasing distance from the snout of Gangotri glacier (three sites in high elevation zone in Figure 1.8). The recently deglaciated site represented a bare surface of sand, gravel, and small rocks. The intermediate site was characterized by fresh alluvial soil with sparse vegetation represented by pioneer communities such as *Calamagrostis emodensis* and other herbs. The late-stage represented herbaceous formation where the soil was well developed.

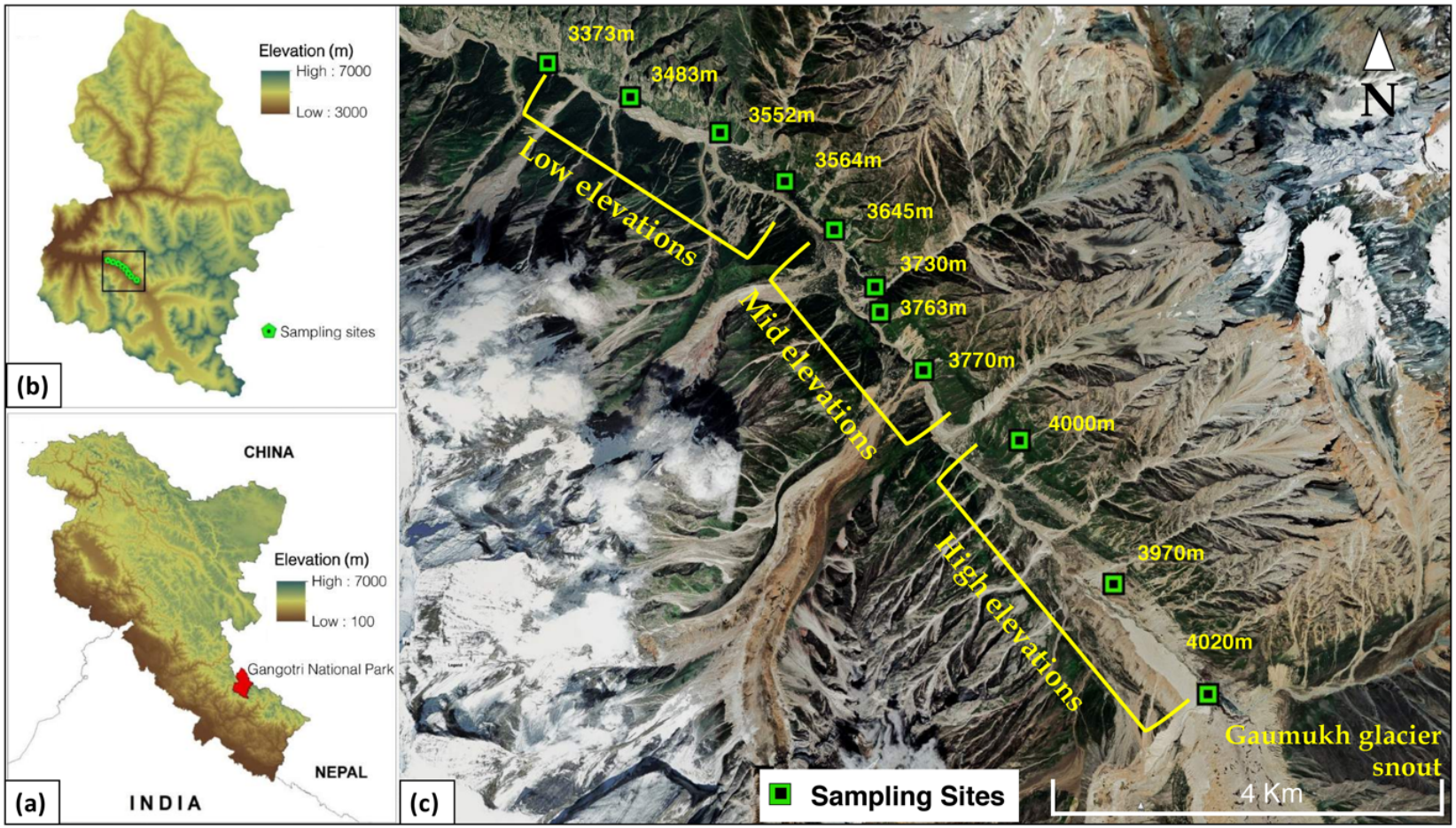

Figure 1.8 Map of the study area (a) Western Himalaya, India, (b) Gangotri National Park, and (c) soil sampling sites along a elevation gradient of ~ 700 m in Gangotri National Park. All maps were generated in ArcGIS version 10.7 (ESRI, CA, USA, https://desktop.arcgis.com/en/arcmap/).

High altitude habitats in the Himalaya, due to their ongoing formation in terms of soil and vegetation climax (Shrestha et al., 2012b), provide climate-vegetation gradient across short elevation ranges and are ideal for studies on bacterial community dynamics. To understand the impact of climate change on these communities we selected twelve altitudinal sites across the gradient on the south west facing slope of the valley for bacterial community analysis. Vegetation in this region changes with increasing elevation forming elevation-vegetation gradient from a subalpine forest in lower elevations to alpine scrub in mid and alpine meadow at the higher elevations (Pusalkar and Singh, 2012).

Majority of alpine meadows are covered by herbaceous meadows dominated by graminoids i.e., grasses and sedges (Tiwari et al., 2021b). The ability of the graminoid plant communities to adapt to harsh climate, translocate carbon compounds to the belowground parts and sensitivity to climatic conditions make these meadows ecologically important (Tiwari et al., 2021b). Soil bacterial community diversity and composition in these habitats are expected to change with rising temperature leading to change in their organic carbon decomposition rate setting positive feedback to climate warming. To understand the impact of increasing temperature on the bacterial communities we conducted experimental warming using open top chambers to simulate climate warming in the alpine meadow (Marion et al., 1997).

1.6 Thesis Structure

This thesis focuses on understanding the response of soil bacterial community to climate warming along elevation-vegetation gradient in the alpine region of a recently deglaciated valley towards Gangotri Glacier in Gangotri National Park, western Himalaya. To the best of my knowledge, this is the first study that provides baseline on soil bacterial community and the major environmental regulators along elevation-vegetation gradient in the high altitude of the Himalaya.

- The thesis 1st chapter provides insight into the ecological traits of the bacterial community during succession at different time periods post-deglaciation of Gangotri glacier, using 16S metagenomics.
- The 2nd and 3rd chapter aims to understand the impact of climate warming on the community along an alpine elevation-vegetation gradient and identify the direct and indirect impacts of temperature and edaphic properties using metagenomics and statistical models.
- The 4th chapter aims to confirm the impact of rising temperature on the community through experimental warming using open-top-chambers at an alpine meadow.
- In the thesis conclusion, the key findings of each chapter have been highlighted, and the implications regarding the impact of climate warming on alpine soil bacterial community have been discussed.

This work substantially enhances our understanding of the relationship of soil bacterial community to temperature and edaphic properties in the western Himalaya. Overall, the study will assist in the prediction of the soil bacterial response to future climate warming.

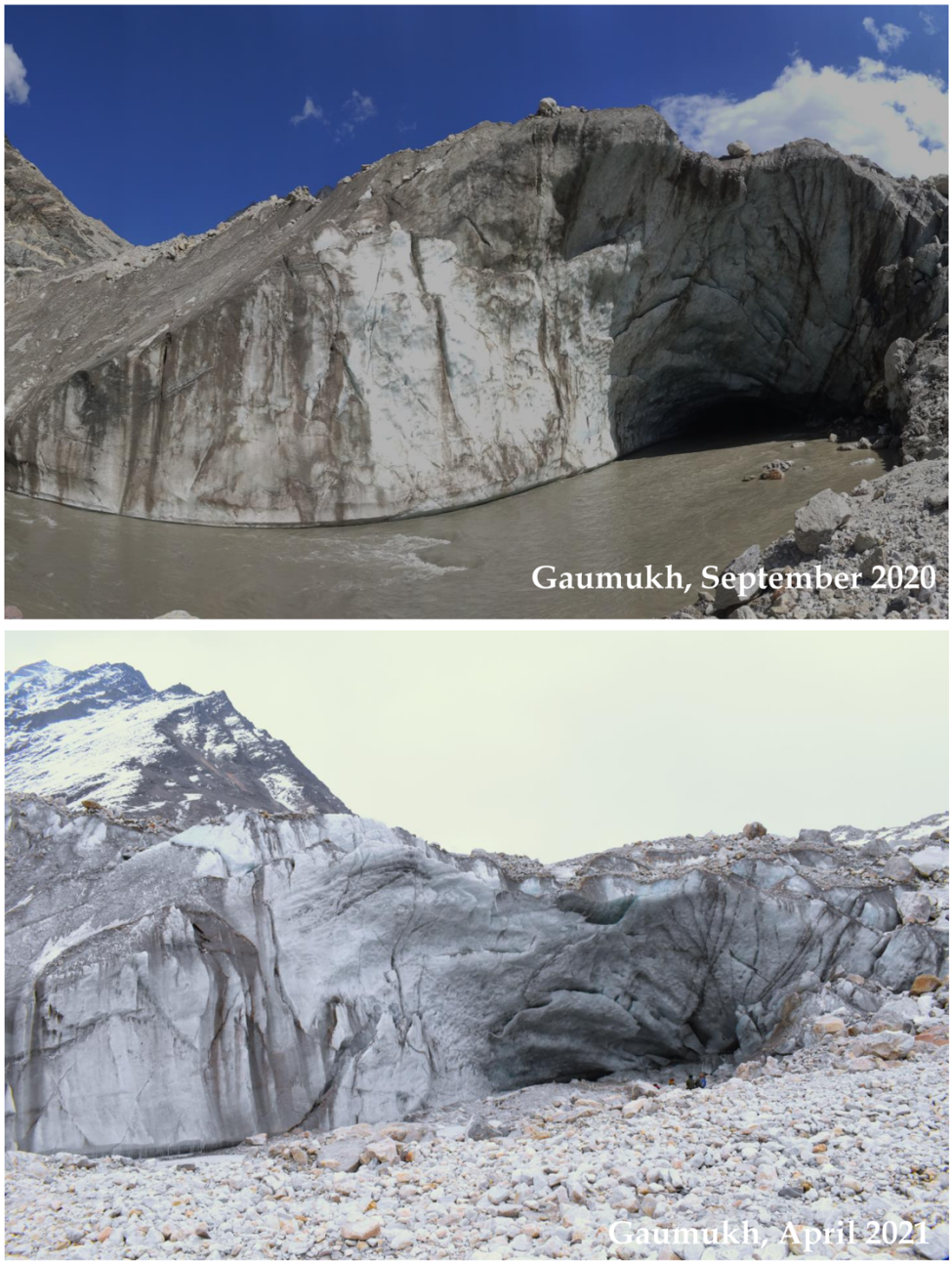

©Pankaj Tiwari

Chapter 2

Shifts in soil bacterial community diversity, composition and functional traits along glacial foreland

2.1 Introduction

Increasing global average surface temperature since the past decade has led to rapid changes in terrestrial ecosystems (Cramer et al., 2001). The high altitude ecosystems and polar regions have particularly experienced higher warming rates, leading to rapid melting of ice and retreat of glaciers (SchüTte et al., 2010; Venkatachalam et al., 2021; Wu et al., 2012). As the glaciers retreat, new lands are exposed for colonization by pioneer bacterial communities capable of surviving in cold oligotrophic environments primarily by utilizing atmospheric carbon (C) and nitrogen (N) depositions as energy sources (Hotaling et al., 2017; Schütte et al., 2009). Increasing bacterial activity promotes mineral weathering leading to nutrient mobilization and soil formation (Alfaro et al., 2020; Hotaling et al., 2017; Kim et al., 2017; Schütte et al., 2009). Availability of essential nutrients such as phosphorus (P), calcium, and potassium facilitates the recruitment and growth of other microbial communities and plant colonization (Alfaro et al., 2020; Frkova et al., 2021). Microbial activity and primary production eventually drive biogeochemical transformations in recently exposed soils leading to the gradual accumulation of organic matter and ecosystem maturation (Alfaro et al., 2020; Bradley et al., 2017). Despite the critical role of bacterial communities in initiating soil and ecosystem development, there is limited understanding of the ecological attributes of the community, including the relationship between their composition and functional traits, interspecies interactions, and environmental control on the diversity. Understanding the ecological characteristics of abundant bacterial taxa is required for insight into the crucial microbial process involved in ecosystem development.

Taxonomic classification of bacterial meta-genome is gradually progressing with cost-effective next-generation sequencing techniques (Gilbert and Dupont, 2011). However, the functional traits of bacterial communities are poorly characterized due to the low

similarity of environmental 16S rRNA sequence with the existing meta-genome databases (Gilbert and Dupont, 2011). Additionally, functional characterization of the meta-genomes using meta-transcriptomics is expensive (Feng et al., 2020; Gilbert and Dupont, 2011). Therefore, this has inhibited understanding the functional potential of the newly evolving ecosystems post-deglaciation. Recently, efforts have been made to predict bacterial meta-genome functions using various less expensive computational approaches based on 16S rRNA sequences (Ortiz-Estrada et al., 2019). PICRUST platform is one of the effective computational tools to predict soil bacterial functions taking into account the relationship between phylogeny and function (Langille et al., 2013). Although these metagenome function prediction tools are widely used for environmental bacterial community function prediction, they have certain limitations (S. Sun et al., 2020). Since the microbial metagenome database used for alignment of the 16S rDNA sequences majorly represent microorganisms associated with human microbiota, the predictive power of these tools for environmental samples is compromised and needs to be used with caution (S. Sun et al., 2020).

The Himalayan region, representing the highest mountain ranges globally, has warmed significantly in the past years and is predicted to experience a temperature rise of 3 °C by 2050 (Shrestha et al., 2012b). Almost 17% of the Himalayan landscape is glaciated, of which 21% have retreated over the last 50 years (Rao and Patil, 2017). The Gangotri glacier is the largest in Himalaya, having a total ice cover of 200 km^2 (Rao and Patil, 2017). This glacier is the primary source of the river Ganga on which 42% of the Indian population is dependent (Misra, 2011). From 1935 to 1996, the glacier has retreated on an average of 19 m/year, double that of the previous century exposing 2.25 km^2 (Rao and Patil, 2017). The deglaciated foreland now supports sub-alpine and alpine vegetation rich in high altitude flora that has been legally protected in the form of Gangotri National Park

(Pusalkar and Singh, 2012). Quantification of soil microbial community along a temporal sequence in glacial forelands advances our understanding of the past and future trends in ecosystem functioning during deglaciation. In this study, we investigated the succession in soil bacterial community at different periods in the forelands of Gangotri glacier with the following objectives: i) assessment of the shift in bacterial community richness, diversity, and composition at different taxonomic levels (phyla, class, and genera), ii) assessment of bacterial co-occurrence pattern, iii) evaluation of the shifts in the community traits associated with a) most abundant functions and b) biogeochemical cycles, i.e., C, N, P and sulphur (S), and iv) evaluate the impact of environmental factors on the community diversity and composition.

2.2 Study area

The study was conducted along an alpine glacier foreland on the southwest-facing slope of the Gangotri glacier located in western Himalaya, India (30.95-30.99° N, 78.99-79.06° E, 4000 m above mean sea level) (Figure 2.1). We selected three sites representing recent (~ 17 yrs.), intermediate (~ 120 yrs.), and late (~ 326 yrs.) post-deglaciation periods located at increasing distance from the snout of Gangotri glacier (Figure 2.2). We calculated the age of each site by calculating the average rate of glacier retreat via Google earth imagery from 2010 to 2016 (Figure 2.2 and Table 2.1). Using the images the distance between the glacier snout at different time periods were used to estimate the rate of glacier retreat (Rao and Patil, 2017) (Figure 2.2 and Table 2.1). The recently deglaciated site was 340 m away from the snout and represented a bare surface of sand, gravel, and small rocks (Figure 2.2 and Table 2.1). The intermediate site was 1.96 km away from the snout, characterized by fresh alluvial soil with sparse vegetation

represented by pioneer communities such as *Calamagrostis emodensis* and other herbs (Table 2.2). The late stage was 3.8 km away from the snout, where the soil

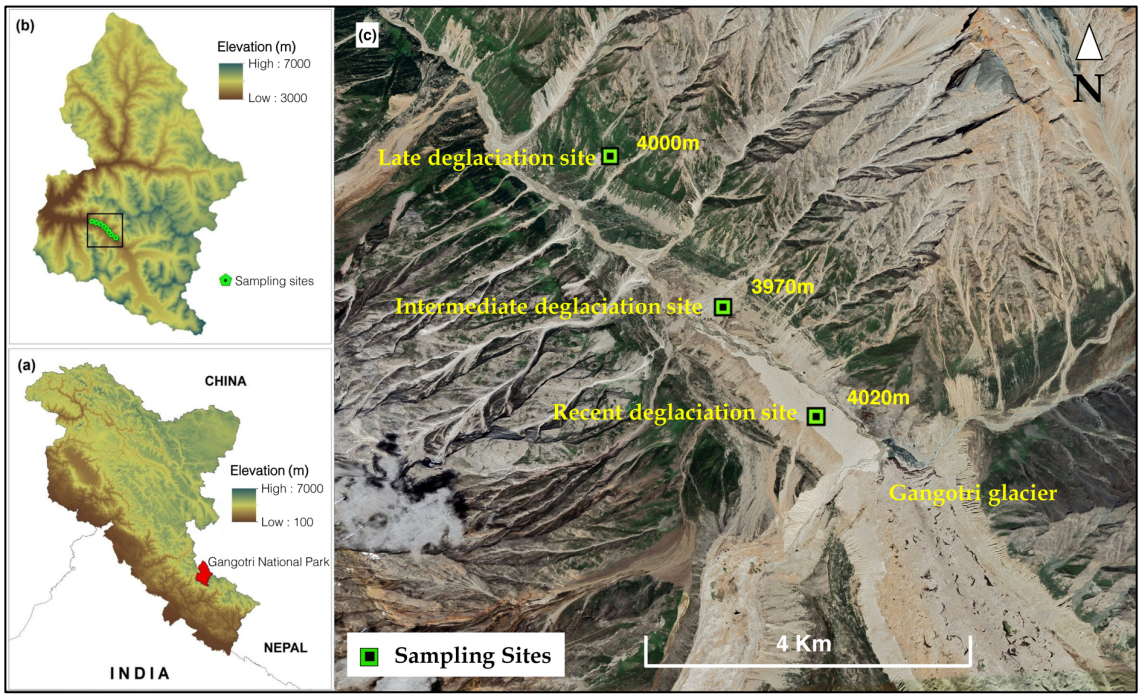

Figure 2.1 Map of the study area (a) Western Himalaya, India, (b) Gangotri National Park, and (c) soil sampling sites representing three post-deglaciation periods in Gangotri National Park. All maps were generated in ArcGIS version 10.7 (ESRI, CA, USA, https://desktop.arcgis.com/en/arcmap/).

was well developed, representing herbaceous formation. From the recent to the late stage, the soil pH ranged from 6.7 ± 0.3 to 4.9 ± 0.3 (Table 2.2). Soil organic carbon (SOC) and total nitrogen (TN) ranged from 0.4 ± 0.03 to 56.2 ±11.8 g Kg^{-1} and 0.1 ± 0.01 to 4.2 ± 0.3 g Kg^{-1}, respectively (Table 2.2). The region is completely covered with snow from December to mid-May (Pusalkar and Singh, 2012; Tiwari et al., 2021c). Mean annual precipitation (MAP) and mean annual temperature (MAT) close to the study sites were around 1500 mm and 2.92 ± 0.36 °C, respectively (Sanyal et al., 2013; Tiwari et al., 2021b).

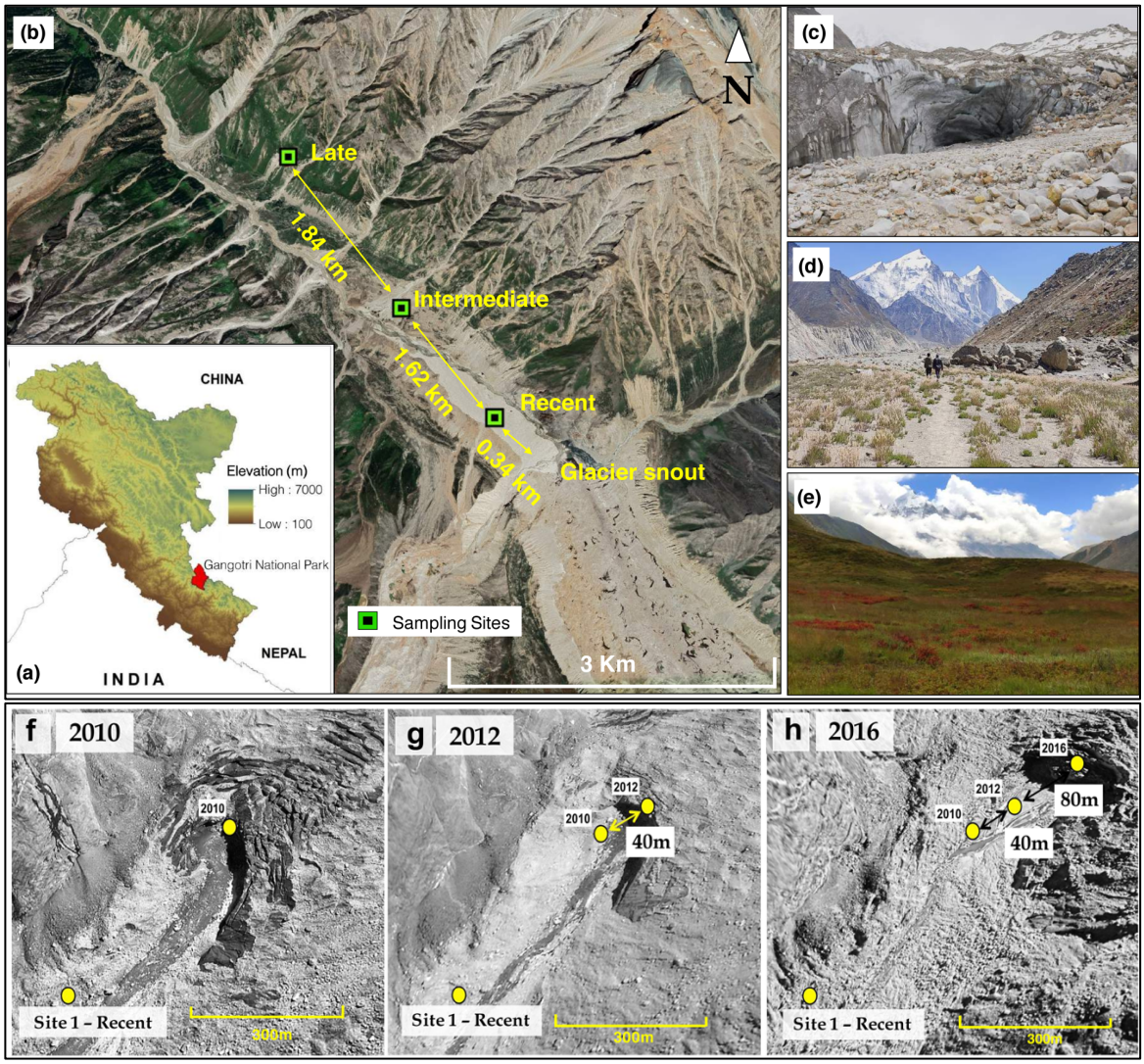

Figure 2.2 Soil sampling sites at different post-deglaciation periods of gangotri glacier and google earth images showing retreat of Gangotri glacier since 2010. (a) Gangotri National Park in western Himalaya, (b) soil sampling sites representing three post-deglaciation periods in Gangotri National Park, (c) recent deglaciation site (~ 17 yrs), (d) intermediate deglaciation site (~ 120 yrs), (e) late deglaciation site (~ 326 yrs), (f) location of the glacier in 2010, (g) location of the glacier in 2012, and (g) location of the glacier in 2016. S represents our first soil sampling site in the year 2016.

Table 2.1 Distance and deglaciation time of each site from the snout of the Gangotri glacier.

Deglaciation period	Distance from glacier snout (m)	Rate of deglaciation (m/year)	Years of deglaciation	References for rate of deglaciation
Recent	340	20	17	Google earth images (Figure 2.2)
Intermediate	1960	19	120	Rao and Patil, 2017
Late	3800	7.3	326	Rao and Patil, 2017

2.3 Materials and Methods

2.3.1 Site selection and soil sampling

We selected four 5 × 5 m plots (approximately 50 m apart) at each site. In each plot, five 1 × 1 m sub-plots were selected randomly to better represent habitat heterogeneity before vegetation analysis and soil sampling (Figure 2.3). Sampling was performed in autumn of 2016 between 24th to 27th October. Vegetation was estimated at each subplot by the quadrat method (Gleason, 1920). At each subplot, five soil cores (~ 1 g each) were collected at four corners and center from 5 cm depth using hand-held sterile soil corer (50 ml centrifuge tube of diameter 2.5 cm, Tarsons Products Pvt. Ltd, India). Before soil collection, aboveground vegetation and leaf litter were removed if present. Based on the design of Lanzén et al. (2016) (Lanzén et al., 2016), soil cores at each plot (n = 25) were pooled in a sterile zip-lock bag homogenized. We aliquoted 5 g soil from this pool and preserved it in 100% ethanol (Merck, Germany) for molecular analysis (Harry et al., 2000). The remaining soil was kept for soil physicochemical analyses. All samples (n = 4 per site) were transported in a cool box containing dry ice within 48 hours of sampling to the laboratory for downstream analysis.

Table 2.2 Dominant plants and edaphic properties including soil moisture content (SMC), pH, soil organic carbon (SOC), total nitrogen (TN), and carbon to nitrogen ratio (C/N) across three sites post-deglaciation of Gangotri glacier, Himalaya. Values are mean ± SE of mean, n = 4.

Deglaciation period	**Altitude (m.a.s.l)**	**Vegetation**	**MAT**	**SMC (%)**	**SOC (g Kg^{-1})**	**TN (g Kg^{-1})**	**C/N ratio**	**pH**
Recent	3940 – 4036 m	Barren land	1.8 ± 0.16^{a}	5.8 ± 1.9^{a}	0.4 ± 0.03^{a}	0.1 ± 0.01^{a}	4.3 ± 0.7^{a}	6.7 ± 0.3^{a}
Intermediate	3930 – 3970 m	*Calamagrostis emodensis, Saxifraga brunoniana, Anaphalis contorta, Chamerion speciosum*	2.2 ± 0.07^{a}	6.7 ± 2.9^{a}	1.5 ± 0.5^{b}	0.14 ± 0.03^{b}	10.4 ± 0.7^{b}	5.8 ± 0.4^{ab}
Late	3980 – 4020 m	*Geranium himalayense*, *Aconogonum tortuosum*, *Nepeta discolor, Potentilla atrisanguinea*	1.9 ± 0.05^{a}	20.1 ± 2.2^{b}	56.2 ± 11.8^{c}	4.2 ± 0.3^{c}	13.2 ± 2.2^{b}	4.9 ± 0.3^{b}

2.3.2 Measurement of soil properties

We estimated soil properties, including soil moisture content (SMC), pH, SOC, TN, and carbon to nitrogen ratio (C/N). SMC was measured gravimetrically using 5 g soil sample immediately after soil transport to the laboratory (Rayment and Lyons, 2011). The remaining soil was air-dried and made free of gravels, plant roots, and leaf litter by sieving through a 1 mm sieve. We measured soil pH using a glass electrode pH meter (Sension 7, Hach Company, USA) in a suspension (1:2.5 (w/v)) of soil in deionized water (Blakemore et al., 1987). SOC and TN were measured using the potassium dichromate ($K_2Cr_2O_7$) oxidation method (Walkley and Black, 1934) and Kjeldahl method (Bremner, 2018) using Kjeltec 8400 (Foss India Pvt. Ltd), respectively. C/N ratio was estimated from the SOC and TN values.

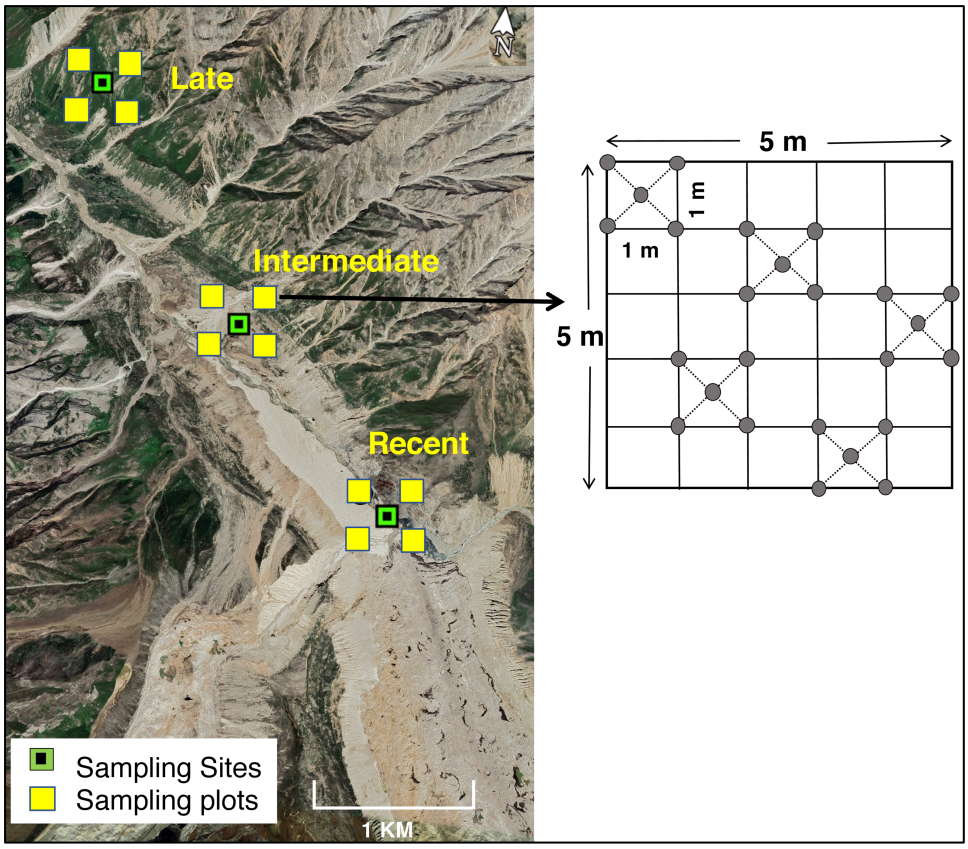

Figure 2.3 Soil sampling site and sampling design.

2.3.3 DNA extraction, PCR amplification, and Illumina sequencing

Approximately 0.25 g of each soil sample was taken to extract environmental genomic DNA using a Nucleopore GDNA soil kit (Genetix Biotech Asia Pvt. Ltd, India) following the manufacturer's instructions. DNA concentrations were estimated using Qubit dsDNA HS Assay Kit (Life Technologies, USA). The bacterial V3 and V4 regions were amplified using the primer pair 338F (5′-CCTACGGGNGGCWGCAG-3′) and 806R (5′-GACTACHVGGGTATCTAATCC-3′) (Luo et al., 2019) with Illumina 16S Metagenomics Sequencing library preparation protocol. The PCR reaction was conducted with 12.5 µl of 2X Kappa Hifi Hotstart ReadyMix (Kappa Biosystems, Roche Sequencing and Life Science, USA), 1 µl each of 5 µM forward and reverse primer and 10.5 µl of the template (12.5 ng of microbial DNA). The conditions for PCR reaction included an initial denaturation of 95 °C for 3 min, followed by 25 cycles of 95 °C for 30 s, 55 °C for 30 s, and 72 °C for 30 s, followed by a final extension for 10 min at 72 °C. A negative PCR (no template DNA) was included to monitor contamination. We purified and barcoded PCR products using Nextera XT kit (Illumina Inc., United States) and normalized amplicons to 2 nM for each library. An equal volume of each library was pooled, denatured, and diluted to 4 pM before loading onto the MiSeq flow cell (Illumina Inc., United States). Sequencing was performed at the Next Generation Genomics Facility at Center for Cellular, and Molecular Platforms (C-CAMP), Bangalore, India, using a 2×300 bp paired-end protocol on the Illumina MiSeq platform.

2.3.5 Sequence Data Processing

We used the MiSeq S.O.P. pipeline in Mothur v.1.40.5 to process Illumina-generated raw sequences (Kozich et al., 2013; Schloss et al., 2009). We prepared full-length sequences from which good reads (> 460 bp length with no homopolymer stretches longer than 8bp)

were identified and clustered (based on ≥ 97% similarity) using 16S rRNA reference database Greengenes (v.13_5). Subsequently, chimeric sequences were removed using Uchime, followed by all singletons, chloroplasts, archaea, mitochondria, and unknown origin sequences (Edgar et al., 2011). We used high-quality sequences to estimate pair-wise distances and generate single-linkage clusters with ≥ 97% sequence similarity. The longest read from each cluster was used as the reference sequence for a taxonomic assignment against the Greengenes database (v.13_5). Quantitative estimates of individual reads per taxonomic unit were generated from all sequences in each cluster and their replicates (≥ 97% similarity). The dataset was normalized by rarefying the sequences to the lowest sample-specific sequencing depth with maximum Good's coverage (Kozich et al., 2013). Finally, the sequences were clustered into different taxonomic levels for operational taxonomic unit (OTU) abundance and composition analysis. The data were sorted to separate the abundant and rare taxa based on their relative abundances. OTUs with ≥1% relative abundance was considered abundant, whereas ≤0.1% was considered rare (Pedrós-Alió, 2006).

2.3.6 Co-occurrence network construction

Bacterial interspecies interactions were identified by constructing co-occurrence ecological networks using Random Matrix Theory (RMT)-based method in Molecular Ecological Network Analysis (MENA) pipeline (Deng et al., 2012; Zhou et al., 2011). We performed Pearson correlation ($p<0.05$) between OTUs at genus level having relative abundances > 0.1% in all samples during network construction at an identical similarity threshold of 0.87 between recent and intermediate communities (network-RI) and intermediate and late communities (network-IL). Two networks (RI and IL) were constructed to understand the shift in interspecies interaction during bacterial succession

from one period to the other. Various indices were calculated, including node and link numbers, average degree (avgK), average clustering coefficient (avgCC), average path distance (GD), density (D), modularity (M), and connectedness (Con) to evaluate and compare the overall topological features of the networks (Deng et al., 2012). The networks were separated into different modules using fast greedy modularity optimization (Deng et al., 2012) and a submodule structure layout for the network graphs were visualized using Cytoscape 3.8.2 (Shannon et al., 2003). In the graphs, each node represents one genus, and each link represents one significant correlation.

2.3.7 Functional analysis of the bacterial community

The genetic functional potential of the bacterial community was predicted using PICRUST (Phylogenetic Investigation of Communities by Reconstruction of Unobserved States) pipeline on the galaxy server (Langille et al., 2013) (https://galaxyproject.org/use/langille-lab/). Taxonomic classification of 16S sequences at ≥ 97% similarity was conducted against the Greengenes database. Each 16S sequence was processed to pre-computed closed-reference OTUs against the Greengenes database 13.5 to find the "nearest neighbour of the reference sequence". The OTU. table was normalized according to the 16S rRNA gene copy number. The functional prediction was performed using the normalized OTU table against the Kyoto Encyclopedia of Genes and Genomes (KEGG) orthology database. The KEGG orthology (KO) assignments were performed at level 1 and 2 categories. The nearest sequence taxon index assessed the accuracy of the predicted metagenome. For our analysis, we classified the predicted functions into most abundant traits having relative abundance ≥1% at KO levels 1 and 2. Relative abundance of genes (Table 2.3) involved in C, N, S, and P cycles were calculated from the predicted functions of the meta-genome.

Table 2.3 Genes involved in biogeochemical cycles.

Biogeochemical cycle	Pathways	Genes involved
Carbon	Carbon fixation	Carbon-monoxide dehydrogenase,acetyl-CoA decarbonylase/synthase, formate dehydrogenase and formate-tetrahydrofolate ligase
	Chitin decomposition	Chitinase, bifunctional chitinase/lysozyme, alpha-N-acetylglucosaminidase, beta-hexosaminidase and beta-N-acetylhexosaminidase
	Lignin decomposition	Tyrosinase
	Pectin decomposition	Polygalacturonase and alpha-L-rhamnosidase
	Cellulose decomposition	Endoglucanase, beta-glucosidase, cellulose 1,4-beta-cellobiosidase, 6-phospho-beta-glucosidase and glucan 1,3-beta-glucosidase
	Hemi-cellulase decomposition	Endo-1,4-beta-xylanase
	Starch decomposition	Alpha-amylase, pullulanase, glucoamylase, cyclomaltodextrinase and isoamylase
Nitrogen	Nitrogen fixation	Nitrogenase
	Nitrification	Ammonia monooxygenase, hydroxylamine oxidase and nitrate reductase
	Dissimilatory nitrate reduction	Nitrate reductase, periplasmic nitrate reductase, nitrite reductase and cytochrome c-552
	Assimilatory nitrate reduction	Ferredoxin-nitrate reductase and nitrate reductase
	Denitrification	Nitrate reductase, periplasmic nitrate reductase, nitrite reductase, nitric oxide reductase and nitrous-oxide reductase
	Nitrogen mineralization	Leucyl aminopeptidase, urease and arginase
Phosphorus	Phosphorus mineralization	Alkaline phosphatase, phosphodiesterase, acid phosphatase and 4-phytase acid phosphatase
Sulphur	Dissimilatory sulfate reduction	Sulfate adenylyltransferase, adenylylsulfate reductase and sulfite reductase
	Assimilatory sulfate reduction	3'-phosphoadenosine 5'-phosphosulfate synthase, sulfate adenylyltransferase, bifunctional enzyme, sulfate adenylyltransferase, adenylylsulfate kinase, phosphoadenosine phosphosulfate reductase and sulfite reductase

2.3.8 Data analysis

We calculated bacterial alpha diversity through three indices: species richness (Sobs), evenness, and diversity based on Shannon's Index (H) (Spellerberg and Fedor, 2003) for each sample using the Mothur platform. Before the analysis, we tested normality and heteroscedasticity of data by the Shapiro-Wilk and Levene tests, respectively. We used One-way analysis of variance (ANOVA) to determine significant differences in environmental variables, alpha diversity indices, and functional traits between the sites. Further, Tukey's honest significance difference (HSD) post-hoc test was applied for pair-wise comparisons of mean at 95% confidence intervals where differences were significant.

We calculated the Bray-Curtis dissimilarity matrix for beta diversity estimation after Hellinger transformation of rarefied abundance data at phyla, class, and genus levels. For visual interpretation of differences in the bacterial community, composition principal coordinates analysis (PCoA) using the Bray-Curtis dissimilarity matrix was used. We used Multi-Response Permutation Procedure (MRPP) analysis (Oksanen et al., 2019) with 9,999 permutations to test any significance in compositional differences.

We performed multiple ordinary least square (OLS) regression analyses with stepwise forward selection to assess the relationship of environmental variables with bacterial richness, evenness, and diversity. Since SOC and TN showed high correlation ($r = 0.94$, $p < 0.001$) (Figure 2.4), regressions were performed with SOC only. Based on Akaike's information criterion, the most parsimonious model was selected (Johnson and Omland, 2004). We performed the Mantel test with Pearson correlation to test the relationship of bacterial community composition with environmental variables. A forward selection was performed with environmental variables using stepwise regression (with 999 permutations), followed by Redundancy analysis (RDA) using Hellinger transformed

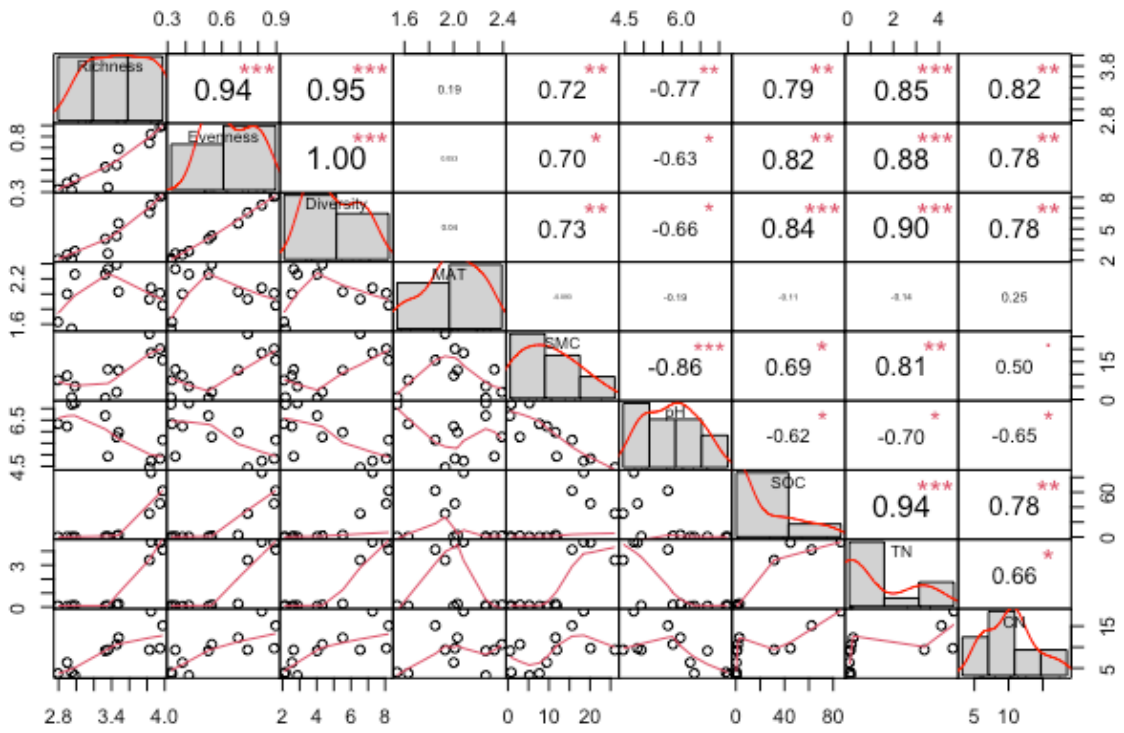

Figure 2.4 Correlogram showing Pearson correlation between bacterial richness, evenness, diversity, and environment variables.

bacterial abundance data to identify environmental variables that significantly explained the variation in abundant phyla. Only those environmental variables having VIF value less than 10 were included in the analysis. The RDA model and the environmental variables were tested by permutation test using ANOVA. Finally, we performed a structural equation model (SEM) analysis to determine both direct and indirect effects of environmental variables on bacterial richness, α-diversity, and composition. We used the first axis of PCoA of the Bray-Curtis dissimilarity matrix for the community composition (Li et al., 2015). We developed a path model based on theoretical knowledge to relate environmental variables including vegetation, MAT, SMC, SOC, C/N, and pH with bacterial richness, diversity, and composition. To improve the fit between the model and the data, the initial theoretical model was modified for the correct specification of

theoretical causal relationships between variables before analysis. Maximum likelihood estimation was used to compare the SEM model with the observations. The model fitness with the data was tested using Comparative Fit Index (CFI), Akaike Information Criteria (AIC), and Root Square Mean Errors of Approximation (RMSEA). Good model fits were indicated by a high CFI (> 0.90), low AIC, and low RMSEA(< 0.05) ("Structural Equation Modeling and Natural Systems by J. B. GRACE," 2007). All analyses were conducted in R 4.0.3 (http://www.R-project.org/) through RStudio 1.3.1093, 2020 (https://rstudio.com/products/rstudio/) using vegan 2.5-7 (https://cloud.r-project.org/package=vegan), lavaan 0.6-9 (https://cloud.r-project.org/package=lavaan), dplyr 1.0.5 (https://cloud.r-project.org/package=dplyr) and ggplot2 3.3.3 (https://cloud.r-project.org/package=ggplot2) (Oksanen et al., 2019; R Core Team, 2020).

2.3.9 Availability of data and material

The DNA sequence data set has been deposited to the National Centre for Biotechnology Information (NCBI) Short Read Archive (https://www.ncbi.nlm.nih.gov/sra). The BioProject accession number is PRJNA754406.

2.4 Results

2.4.1 Variation in soil properties

Soil properties varied significantly across the sites (Table 2.2). SMC, SOC, TN, and C/N significantly increased ($p < 0.05$), while pH significantly decreased ($p < 0.05$) from the recent to late stage. MAT showed no significant difference ($p = 0.079$).

2.4.2 Variation in bacterial α-diversity

Illumina sequencing across 12 samples resulted in a total of 654,842 high-quality sequences averaging 54,570 ± 8,940 sequence reads per sample (Table 2.4). Good's coverage ranged from 92% to 99.9% (Table 2.4), indicating that the sequencing was adequate and represented most of the bacterial communities at the study sites.

The alpha diversity indices indicated that bacterial community richness, evenness, and Shannon diversity increased significantly from 816 to 8008, 0.36 to 0.83, and 2.42 to 7.52, respectively, from the recent to late-stage post-deglaciation ($p < 0.05$) (Figure 2.5).

Table 2.4 Number of sequences and Good's coverage at all sampling sites.

Sample number	Altitude (m)	Date of sampling	Sample ID	Total paired end reads	Total quality reads	Good's coverage (%)
1	4036	October_2016	RS1	168068	58742	0.99
2	4025	October_2016	RS2	144905	50092	0.99
3	3975	October_2016	RS3	164238	40601	0.99
4	3940	October_2016	RS4	163849	56245	0.99
5	3970	October_2016	IS1	151220	42596	0.99
6	3940	October_2016	IS2	213886	73403	0.98
7	3930	October_2016	IS3	188478	60673	0.98
8	3922	October_2016	IS4	188389	60044	0.98
9	4020	October_2016	LS1	235374	56467	0.94
10	4000	October_2016	LS2	285827	53606	0.92
11	3990	October_2016	LS3	301118	56241	0.93
12	3980	October_2016	LS4	311183	46132	0.93

2.4.3 Variation in bacterial β-diversity

Considering a ≥ 97% sequence similarity, we identified 42794 OTUs that were classified into 37 phyla (97% of the OTUs), 93 classes (96.9%), 168 orders (72.4%), 332 families (68.5%), 452 genera (57%) and 86 species (1%). Due to the low classification percentage at the species level, all further diversity analyses were conducted at phyla, class, and genera level only.

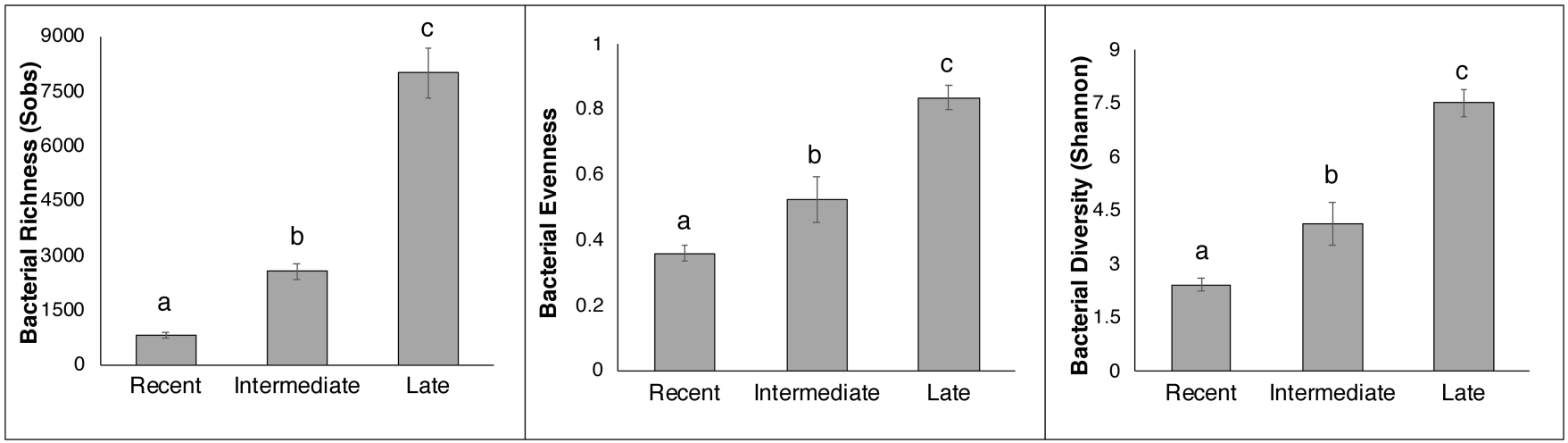

Figure 2.5 Variation in bacterial alpha diversity indices at different deglaciation periods. Significant differences in alpha diversity indices was assessed by one way ANOVA followed by Tukey's honest significance difference (HSD) post-hoc test. Bars represent mean ± SE of mean, n = 4. Different letters (above each bar) indicate a significant difference between the periods ($p < 0.05$).

The number of abundant bacterial taxa and their relative abundances increased drastically from recent to late stages at all three taxonomic levels (Figure 2.6a). At phyla level the increasing abundant taxa were *Proteobacteria* (relative abundance from recent to intermediate to late-stage: 6.8-27.2-14.5%), *Firmicutes* (1.4-0.9-24.2%), *Planctomycet*es (0.01-0.36-7.6%), *Acidobacteria* (0-1.3-6%), *Verrucomicrobia* (0.01-0.5-5.8%), Candidatus TM6 (0.003-0.12-4.1%), and *Chloroflexi* (0.04-0.17-3.6%), while the decreasing abundant taxa was *Actinobacteria* (89%-62%-27.5%). Increasing abundant taxa at class level were *Bacilli* (0.53-0.6-22.9%), *Thermoleophilia* (0.09-0.5-9.3%), *Alphaproteobacteria* (1.4-14.5-10.44%), *Planctomycetia* (0.01-0.27-5.5%), and *Spartobacteria* (0.01-0.43-5.4%), while *Actinobacteria* (90-62-15.7%) decreased inabundance. At genus level *Bacillus* (0.08-0.04-16.5%), Candidatus DA101 (0.01-0.375-5.11%), *Sporosarcina* (0-0.38-3.2%), *Rhodoplanes* (0.01-1.03-3.3%), and *Pseudonocardia* (0.07-0.07-2%) became more abundant, while *Mycobacterium* decreased (89%-62%-0.9%). This increase in abundance of bacterial taxa led to a more evenly distributed community in the late stage compared to the recent stage, which was dominated by a single bacterial taxon at different taxonomic levels viz., *Actinobacteria* at phyla and class level (89% and 90%, respectively) and *Mycobacterium* (89%) at the genus level.

Bacterial beta-diversity varied significantly between the three habitats as indicated by the MRPP analysis at phyla ($A = 0.439$ and $p < 0.001$), class ($A = 0.398$ and $p < 0.001$) and genus levels ($A = 0.357$ and $p < 0.001$). The significant change in bacterial beta diversity is visually represented by PCoA analysis (Figure 2.6b), where three distinct clusters were formed at three levels.

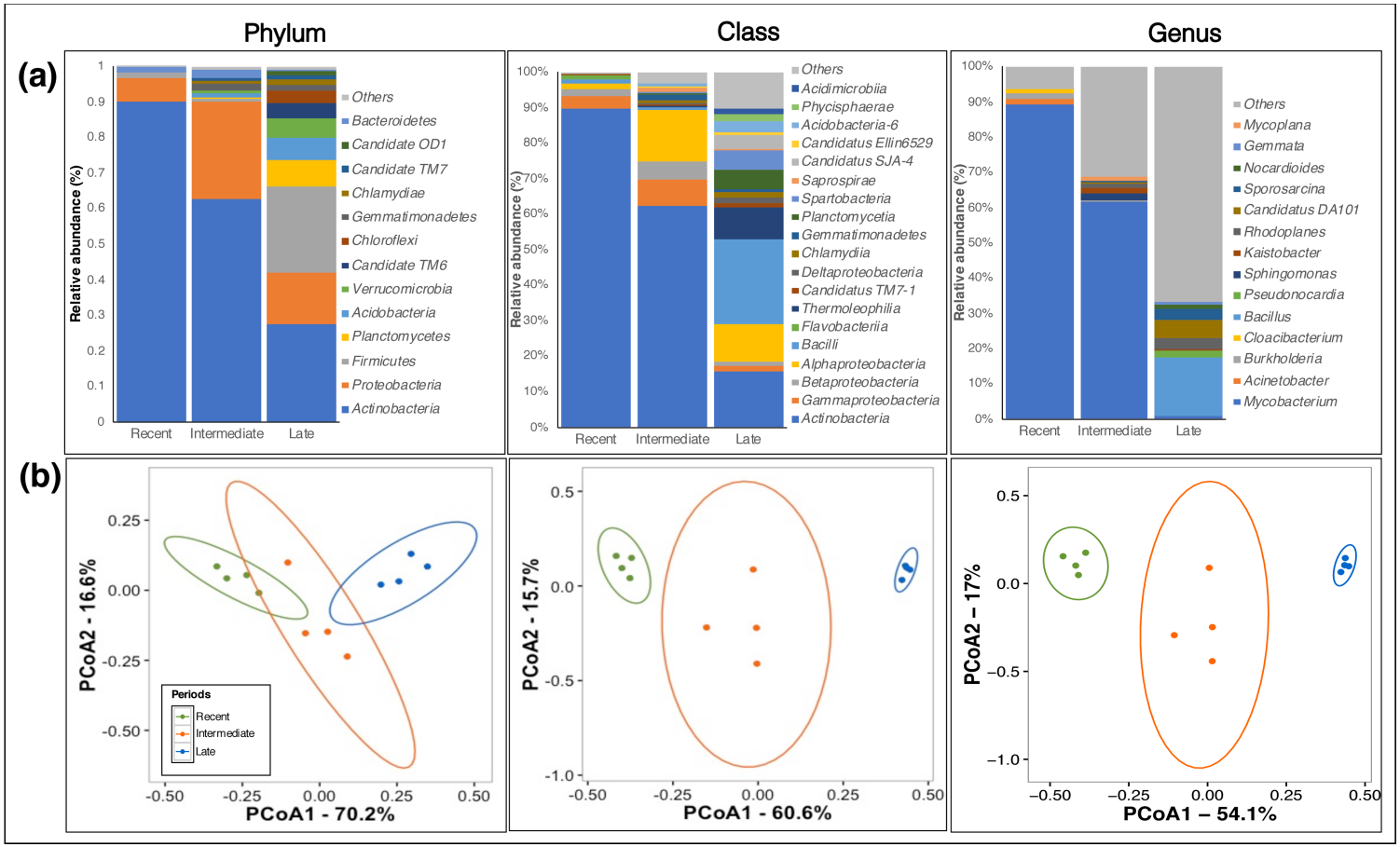

Figure 2.6 Variation in bacterial beta diversity at different post-deglaciation periods. (a) Relative abundances of bacterial phyla, class, and genera across the periods. Here "Others" represent all taxa with relative abundances < 1% and (b) Principal coordinates analysis (PCoA) based on Bray-Curtis dissimilarity of bacterial communities at phyla, class, and genera levels.

2.4.4 Bacterial co-occurrence pattern across the site

The bacterial co-occurrence networks between the sites showed all features of ecological networks, including scale-free (R^2 of power-law ranged from 0.57 to 0.61), small world (GD ranged from 3.1 to 3.5), non-random, and modular (modularity = 0.53) (Table 2.5). Comparison of topological features showed that the number of nodes, links, and links per node was greater in the network-IL than network-RI by 168%, 455%, and 110%, respectively (Supplementary Table S4 and Fig. 3). In both the networks, 4 joint modules having nodes ≥6 were observed within the bigger network (Fig. 2.7 and Appendix Figure A1). The modules in network-IL showed 15% more positive interactions than network-RI. In network-RI, most genera belonging to the phyla *Proteobacteria*, *Actinobacteria, Verrucomicrobia,* and *Bacteroidetes* showed more negative interactions than positive. In network-IL, most genera of the phyla *Proteobacteria*, *Actinobacteria, Planctomycetes, Gemmatimonadetes,* and *Bacteroidetes* showed more positive interactions, while *Verrucomicrobia*, *Acidobacteria*, and *Firmicutes* showed more negative interactions. The avgK, avgCC, GD, and Con increased by 102%, 28%, 12%, and 5%, respectively, from network-RI to network-IL, whereas D decreased by 24%.

Table 2.5 Co-occurrence network topological properties for networks between recent and intermediate communities (Network-RI) and intermediate and late communities (Network-IL).

	Network Indices	Network-RI	Network-IL
Empirical network	R square of power-law	0.614	0.577
	Total nodes	45	121
	Total links	86	478
	Links per node	1.9	4
	Positive co-occurrence (%)	35	50
	Modularity(fast greedy)	0.525	0.529
	Connectedness (Con)	0.756	0.798
	Average degree (avgK)	3.822	7.901
	Average clustering coefficient (avgCC)	0.371	0.476
	Average path distance (GD)	3.08	3.46
	Density (D)	0.087	0.066
Random network	Average path distance (GD)	2.825 +/- 0.088	2.630 +/- 0.029
	Average clustering coefficient (avgCC)	0.130 +/- 0.031	0.112 +/- 0.013
	Modularity(fast greedy)	0.391 +/- 0.015	0.280 +/- 0.009
	Connectedness (Con)	0.980 +/- 0.039	0.994 +/- 0.013

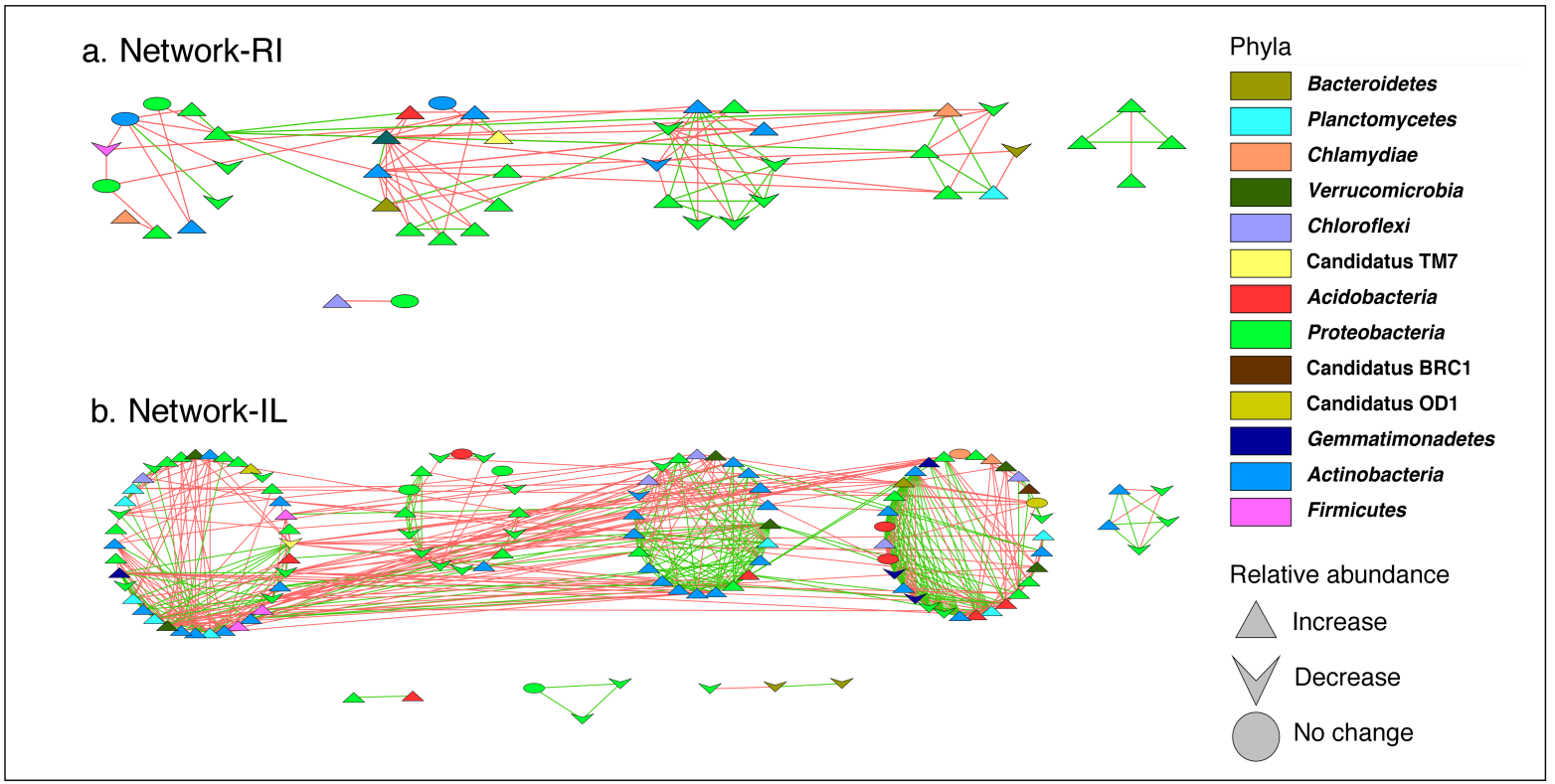

Figure 2.7 Submodule structure layout of bacterial co-occurrence networks of (a) recent and intermediate communities (Network-RI) and (b) intermediate and late communities (Network-IL) based on Random Matrix Theory. Each node represents a genera, and each straight line (link) represent a significant ($p < 0.05$) correlation. Nodes of the same color represent the same phyla the genera belong to. Nodes with triangle shapes represent genera with increasing abundance, inverted triangle shapes represent decreasing abundance, and oval shapes represent genera with no change in their relative abundance. Green and red lines indicate positive and negative correlations between nodes, respectively. Each module in the network is represented by a circle composed of nodes.

2.4.5 Shifts in abundant functional traits of the bacterial community

PICRUST predicted metagenome functions are shown in Figure 2.8 and 2.9, representing the most abundant traits and biogeochemical cycles, respectively, at levels 1 and 2 KO categories. The nearest taxon sequence index (NSTI) value of the samples ranged from 0.008 to 0.24. At level 1 KO category, we identified four abundant functional pathways of the metagenome, i.e., metabolism, environmental information processing, genetic information processing, and cellular processes. Of these functions, the relative abundances of the environmental and genetic information processing (6.8-12% and 4-10%, respectively) and cellular processes (0.12-1.4%) increased significantly from the

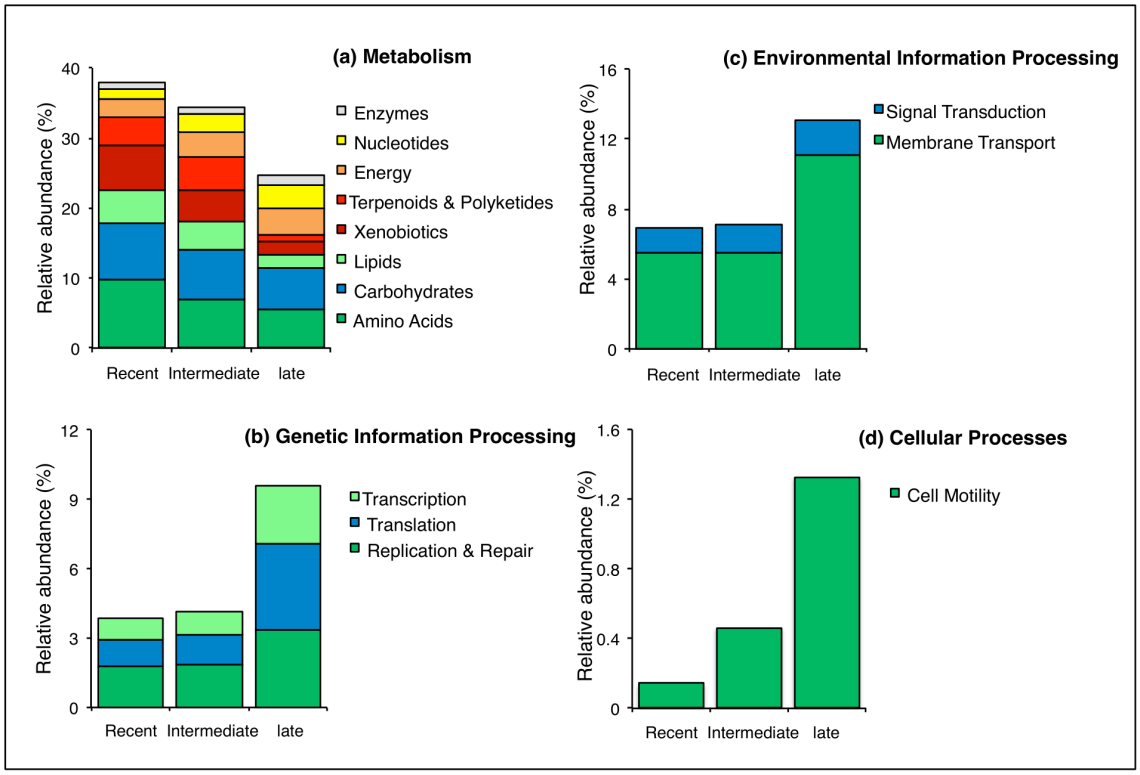

Figure 2.8 Relative abundance of most abundant predicted metagenome functions at level 1 KO category across different post-deglaciation periods. Each bar represents the relative abundances of all pathways associated with the abundant functions at the level 2 KO category.

recent to late-stage ($p < 0.05$). In contrast, the relative abundance of metabolism, the dominant pathway at the recent stage, decreased drastically in the later stage (38-24%, $p < 0.05$) (Figure 2.8). However, we observed an increase in the relative abundance of energy and enzymes metabolism at the level 2 KO category.

2.4.6 Shifts in biogeochemical pathways of the bacterial community

The overall relative abundance of genes involved in each of C, S, and P cycles increased significantly ($p < 0.05$), whereas that of N remained the same from recent to late-stage at level 1 KO category ($p = 0.92$) (Figure 2.9). Relative abundance of both labile (cellulose, hemicellulose, and starch) and recalcitrant (chitin and pectin) C decomposition and C

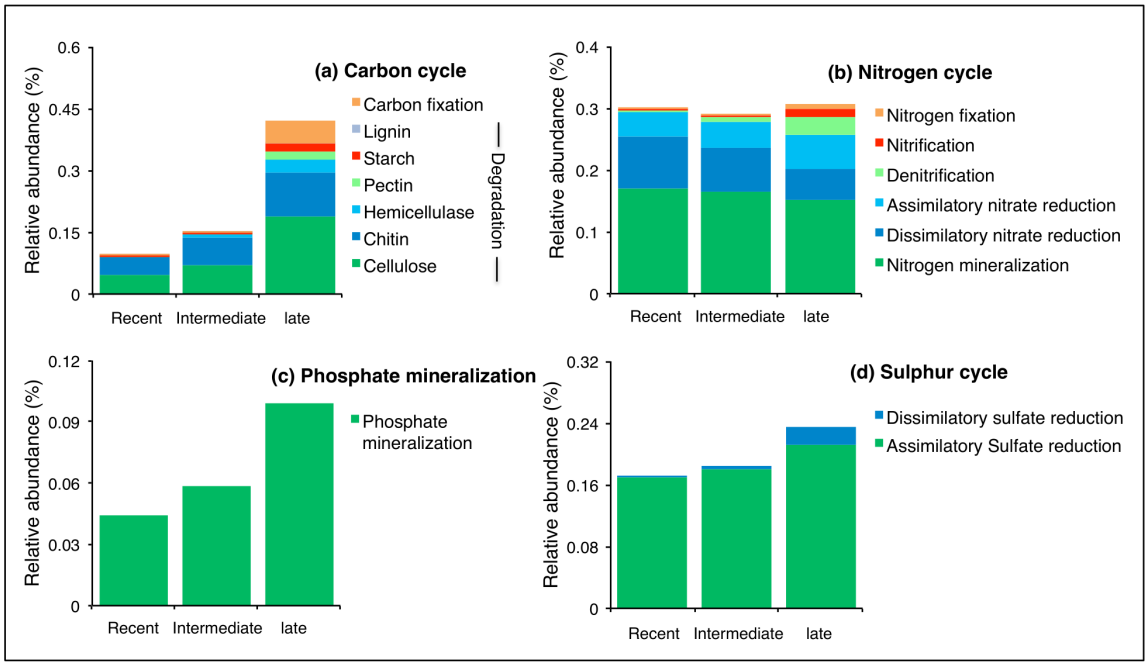

Figure 2.9 Relative abundance of genes involved in carbon (C), nitrogen (N), phosphorus (P), and sulfur (S) cycles across different post-deglaciation periods. Each bar represents relative abundances of all pathways of the C, N, S, and P cycles at the level 2 KO category.

fixation pathways significantly increased ($p < 0.05$) post-deglaciation at level 2 KO. Although the overall relative abundance of N cycling genes showed no change, N fixation, nitrification, and denitrification relative abundances increased. On the other hand, the relative abundance of dissimilatory N reduction pathways decreased ($p < 0.05$).

2.4.7 Factors affecting α and β-diversity

Multiple linear regressions showed that SMC, SOC and C/N ratio positively affected α-diversity across the sites (Table 2.6). Variability in richness ($R^2 = 0.8$, $p < 0.001$) was significantly explained by SMC and CN ratio, while that in evenness ($R^2 = 0.67$, $p < 0.001$) and diversity ($R^2 = 0.7$, $p < 0.001$) were significantly explained by SOC. We found no significant relationships between α-diversity and pH, CN, and MAT. The mantel test showed that β-diversity was significantly correlated to all the measured soil properties (SMC: $r = 0.565$, $p < 0.001$; SOC: $r = 0.66$, $p < 0.01$; TN: $r = 0.715$, $p < 0.01$; C/N: $r = 0.419$, $p < 0.05$, and pH: $r = 0.365$, $p < 0.05$) and not MAT.

Table 2.6 Multiple linear regression models show a significant relationship between richness, evenness, diversity, and environmental variables.

α-diversity	Predictor variables	R^2	α	β	F	p	AIC
Richness	SMC CN	0.8	2.6 (0.14)	0.022 (0.01) 0.056 (0.02)	17.97	<0.0007	-34.65
Evenness	SOC	0.67	0.46 (0.05)	0.006 (0.001)	20.53	< 0.001	-46.38
Diversity	SOC	0.7	3.42 (0.46)	0.066 (0.01)	23.9	< 0.001	8.72

Values within parenthesis indicate standard error. α and β are constants. Significant at $p < 0.001$.

The Redundancy Analysis showed that SMC and C/N explained 65% ($F(2,9) = 8.5$, $p < 0.001$) of the variability in the relative abundances of the abundant phyla across the sites, except *Proteobacteria*, *Actinobacteria*, *Chlamydiae*, and Candidatus OD1 (Figure 2.10). The SEM model (CFI = 0.95, AIC = 78.4, RMSEA = 0.2, $p < 0.05$) explained 80%, 93%, and 95% of the variation in bacterial richness, α-diversity and composition, respectively (Figure 2.11). Diversity was strongly related to SOC ($\lambda = 0.24$, $p < 0.05$) and richness ($\lambda = 0.77$, $p < 0.001$) which was influenced directly by SMC ($\lambda = 0.42$, $p < 0.01$) and C/N ($\lambda = 0.59$, $p < 0.001$) and indirectly by SOC ($\lambda = 0.47$, $p < 0.01$), vegetation type ($\lambda = -0.33$, $p < 0.01$). Community composition was related to richness ($\lambda = 0.34$, $p < 0.001$) and affected directly by SOC ($\lambda = 0.46$, $p < 0.001$), SMC ($\lambda = -0.46$, $p < 0.001$), and C/N ($\lambda = -0.2$, $p < 0.05$). The standardized path coefficients of direct, indirect and total effects is shown in (Table 2.7).

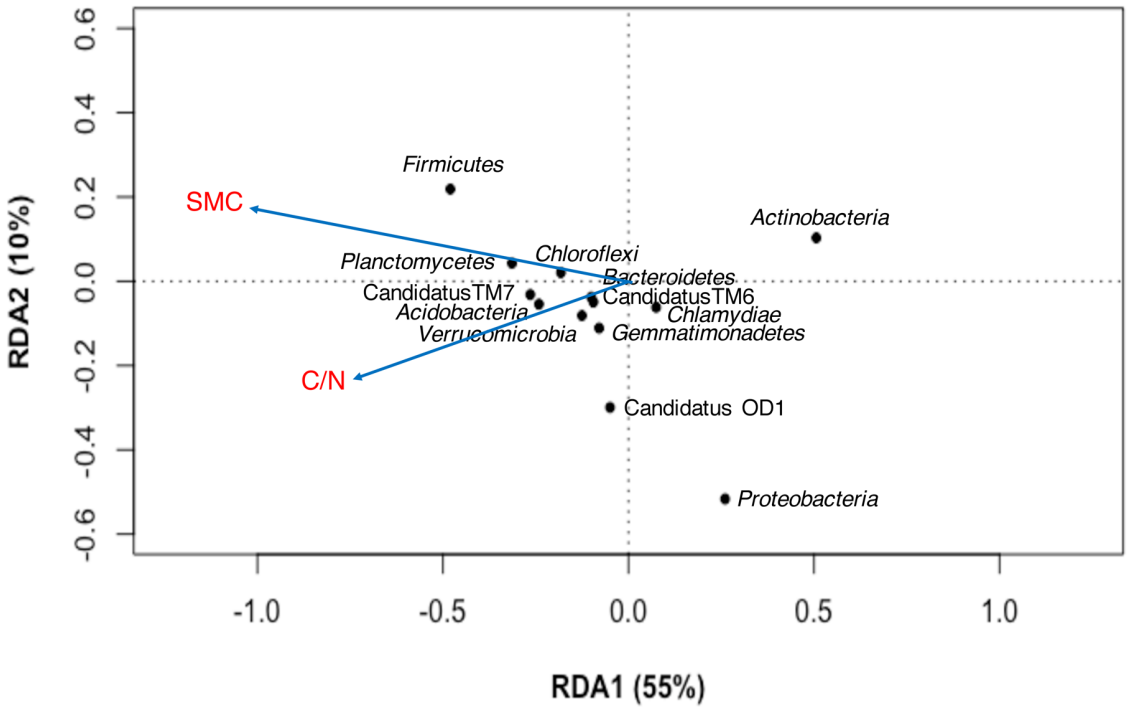

Figure 2.10 Redundancy analysis (RDA) showing significant relationships between abundant bacterial phyla and environmental variables. The figure is generated in R 4.0.3 (http://www.R-project.org/) using vegan 2.5-7 (https://cloud.r-project.org/package=vegan).

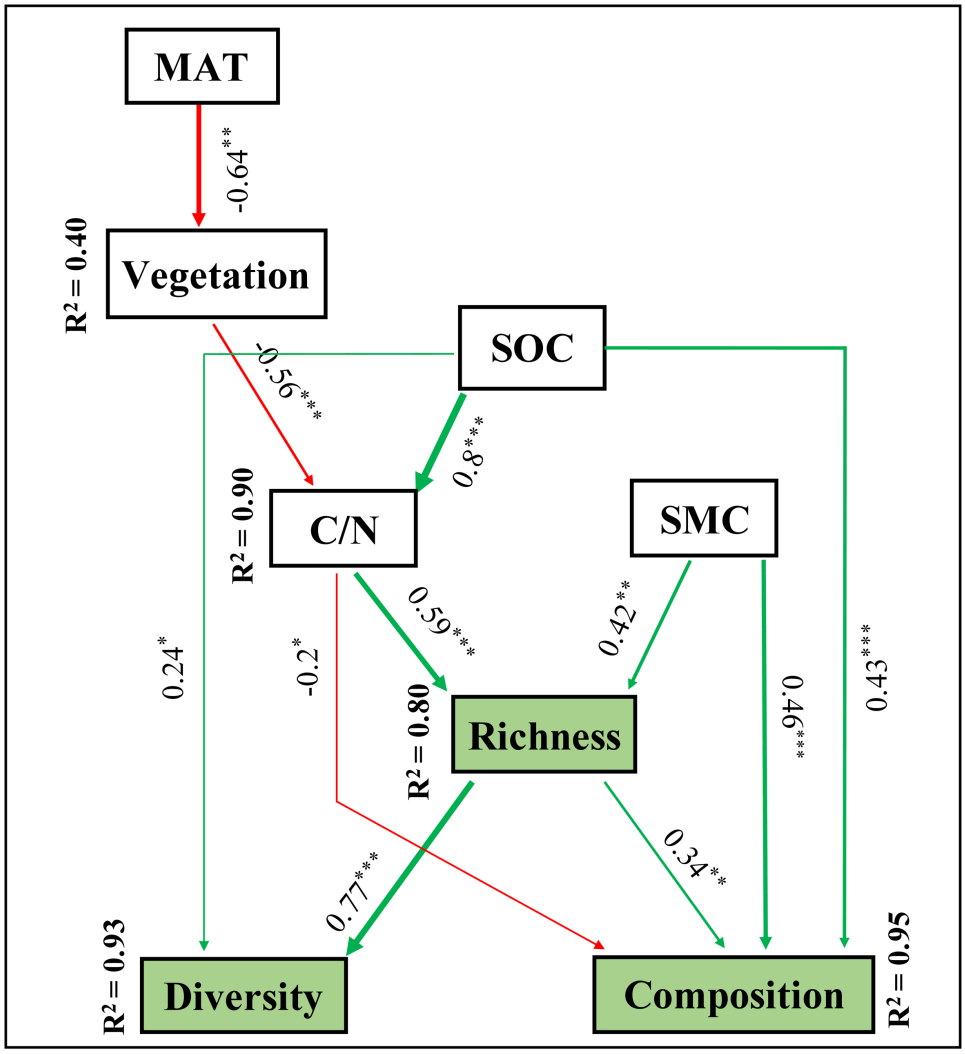

Figure 2.11 Structural equation model (SEM) showing the causal influences of vegetation, MAT, SMC, SOC, and C/N ratio on bacterial richness, α-diversity, and composition. Red and green lines, respectively, represent significant negative and positive effects. The width of the arrows is based on the standardized path coefficients indicating the strength of the causal effect. The standardize coefficients are marked above each path (* indicates significant ($p < 0.05$) effects, ** indicates significant ($p < 0.01$) effects, *** indicates significant ($p < 0.001$) effects). R^2 values represent the percentage of variance explained for each variable.

Table 2.7 Direct, indirect and total effect coefficients of each variable in the structural model.

Variable	Direct effect	Indirect effect	Total effect
Richness			
SMC	0.42	-	0.42
CN	0.59	-	0.59
SOC		0.47	0.47
Vegetation	-	-0.33	-0.33
MAT	-	0.21	0.21
Diversity			
Richness	0.77	-	0.77
SOC	0.24	0.36	0.6
SMC	-	0.32	0.32
Vegetation	-	0.25	0.25
MAT	-	0.16	0.16
Composition			
Richness	0.34	-	0.34
SMC	0.46	0.14	0.6
CN	-0.20		-0.20
SOC	0.43	-0.16	0.27
Vegetation	-	0.11	0.11
MAT	-	0.07	0.07
Vegetation			
MAT	-0.64	-	-0.64

Effects were calculated using standardized path coefficients for significant relations ($p<0.05$, $p<0.01$ and $p<0.001$).

2.5 Discussion

This study on bacterial community succession across a temporal sequence ranging from ~ 20 to 300 years in the foreland of the Gangotri glacier provides an in-depth understanding of changes in the community diversity and functional traits during different periods post-deglaciation. Alpha diversity measurements indicated that the community in the recently exposed site had low richness and diversity. This community possibly originates from atmospheric depositions of dust particles through precipitation and wind or from supraglacial snow (a glacier zone where sunlight penetrates) and subglacial sediments (bedrock at ice-melt water interface) through glacial runoff (Ciccazzo et al., 2016; Hotaling et al., 2017; Stres et al., 2014). In the cold, nutrient-poor

environment, the community focuses on cell metabolism (Figure 2.8) rather than growth, probably acquiring energy from atmospheric deposition of C and N sources or trace gases such as H_2 and CO (Hotaling et al., 2017; Ji et al., 2017). With time the bacterial community shifted towards a richer and evenly distributed community from the recently deglaciated stage to late. A substantial increase in bacterial OTUs and their relative abundances resulted in a highly diverse community during the transition. Our results are in agreement with previous studies from other glaciated regions of the world reporting an increase in bacterial diversity during progressive stages post-deglaciation (Jangid et al., 2013; Nemergut et al., 2007; SchüTte et al., 2010; Wu et al., 2012).

The linear increase in alpha diversity suggests that environmental factors increasing across the sites might control the bacterial community diversity. In our study, the barren land in the recent stage developed into a sparsely vegetated area in the intermediate stage and a well-developed meadow in the late phase (Table 2.1). The increase in alpha diversity corresponds to the increase in SOC, C/N ratio, and SMC associated with developing vegetation (Figure 2.5 and Table 2.1), indicating that soil nutrients and their availability influence bacterial diversity post-deglaciation. This assumption was supported by the regression analysis where the majority of variability in bacterial richness (80%), evenness (67%), and diversity (70%) were explained by SMC, SOC (and in turn TN for its high correlation with SOC, $r = 0.94$, $p < 0.001$) and C/N ratio (Table 2.6). The SEM analysis established the positive influence of soil nutrients and their availability on bacterial richness and diversity (Figure 2.11). Previous studies have shown the critical role of soil nutrients in regulating bacterial diversity post deglaciation due to its direct influence on bacterial growth, metabolism, and reproduction (Bhattacharya et al., 2022; Tarlera et al., 2008). It is well known that soil microorganisms have a C/N ratio of 8:1 and grow optimally in soil with a C/N ratio close to 24:1 (Brady, N.C. and Weil, R.R.,

2002). The increasing C/N ratio from recent to late-stage supported more bacterial taxa to increase due to more available organic C, which resulted in greater bacterial diversity. The crucial role of the C/N ratio was also reported by earlier studies (Lanzén et al., 2016). The community composition showed rapid turnover during 300 years post-deglaciation. The community shifted from a single bacterial taxa-dominated community in the recent stage to a diverse one in the late stage, where several taxa become relatively abundant (Figure 2.6). This shift in the bacterial composition is most likely related to vegetation development and an adequate supply of nutrients (Bhattacharya et al., 2022; Qiang et al., 2021). Under nutrient-limited conditions, communities compete for substrate resulting in the dominance of specific taxa (Zhu et al., 2020). In the recent and intermediate communities, negative and competitive interactions led to the dominance of *Actinobacteria,* followed by an increasing abundance of *Proteobacteria* and *Verrucomicrobia* (Figure 2.6 and 2.7). With adequate nutrient supply, communities become cooperative, favoring the growth of multiple taxa (Zhu et al., 2020). This cooperative nature was observed in the co-occurrence pattern between intermediate and late-stage, where positive interactions led to an increase in abundance of different bacterial phyla *Planctomycetes, Gemmatimonadetes,* and *Bacteroidetes* (Figure 2.6 and 2.7). The positive feedback influence of vegetation development and nutrients on community composition was established by mantel test, RDA, and SEM analysis (Figure 2.10 and 2.11).

The taxonomic analysis showed the genus *Mycobacterium* belonging to *Actinobacteria* phyla was the pioneer bacterial taxa dominating the recent stage. This genus is abundant in many natural ecosystems, including soil, lakes, and rivers (Santos et al., 2015). They have also been found in inorganic sediments, rocks, and dust particles and are the most stress-tolerant bacteria so far identified (Santos et al., 2015). Due to their exceptional

stress tolerance, they are ubiquitous in nature and can survive extreme environments such as hot springs, permafrost, and glaciers (Santos et al., 2015). They generally colonize environments with low microbial diversity (Santos et al., 2015) and, in this study, have been found to inhabit an active moraine solely. This contrasts to earlier studies from polar and alpine glaciers where it co-inhabited with other abundant taxa such as *Methylobacterium, Rhodococcus, Sphingomonas, Arthrobacter, and Frigoribacterium* (Miteva et al., 2004; Santos et al., 2015). The phyla *Actinobacteria* is the oldest living organism with extraordinary temperature stress tolerance (Santos et al., 2015). *Actinobacteria* can predominate cold oligotrophic environments by forming mycelia required to acquire nutrients (Gupta et al., 2015). In addition, they play a crucial role in soil development through N and P mobilization, chitin degradation, and inhibition of plant pathogenic fungal species growth (Shao et al., 2019). Consequently, they create favorable soil conditions by establishing C, N, and P pools to assist the growth of other microbes and eventually plant colonization. The role of *Actinobacteria* was evident in our study as different bacterial phyla *Proteobacteria*, *Firmicutes*, *Planctomycetes*, *Acidobacteria*, *Verrucomicrobia*, and *Chloroflexi,* gradually increased in abundance in the intermediate and late-stage with the concurrent development of soil and plants communities. *Actinobacteria* was earlier reported from polar and alpine glacial forelands and lakes (Mapelli et al., 2011; Philippot et al., 2011; SchüTte et al., 2010; Venkatachalam et al., 2021; Wu et al., 2012), cryoconite holes (Edwards et al., 2013), and glacial meltwater (Ahmad et al., 2021), suggesting their ubiquitous nature in diverse cold habitats. Their ability to utilize atmospheric trace gases as energy sources make them efficient to adapt and survive in low nutrient cold habitats (Ji et al., 2017).

The high degree of shift in bacterial diversity and composition post-deglaciation led to considerable variation in the functional traits (Figure 2.8 and 2.9). The community in the

recent stage mainly depended on metabolic functions to develop resting cellular forms for sustaining life in the cold oligotrophic environment (Dube et al., 2019). As the community diversified in the later stages, they focused more on functions that allowed them to gain mobility, sense environmental signals, and import nutrients to reproduce and grow faster for their co-existence with soil development and plant growth (Ahmad et al., 2021; Kazemi et al., 2016). The functional progression was evident from the high relative abundance of *Proteobacteria, Firmicutes, Planctomycetes*, and *Acidobacteria* at the later stages that are well-known copiotrophs having efficient membrane transport and signaling pathways, stress response regulatory system, and carbohydrate metabolism (Ahmad et al., 2021; Koch, 2001).

Nutrient availability is well known to impact bacterial succession (Ortiz-Álvarez et al., 2018). We observed a substantial increase in relative abundances of functional pathways along with the development of new ones involved in C, N, S, and P cycles post-deglaciation (Figure 2.9). The increase in labile and recalcitrant C decomposition suggests functional adaptation of the bacterial community to utilize new nutrient resources such as cellulose, hemicellulose, starch, pectin, and chitin, accumulating in soil due to the growth of plants and other microbial communities (Jangid et al., 2013; Kazemi et al., 2016). The community in the later stages increased their C fixation ability, coinciding with the increase in abundance of the genus *Clostridia*, known to fix atmospheric CO_2 using the Wood-Ljungdahl pathway (Drake et al., 2008).

N mineralization and assimilatory N reduction relative frequencies showed no variation, suggesting a functional similarity between the communities. On the contrary, N fixation, nitrification, and denitrification increased from the intermediate to late-stage, indicating that specific bacterial taxa display these functional abilities. For instance, bacterial genera *Allorhizobium*, *Mesorhizobium, Bradyrhizobium* known to fix N, and *Pseudomonas* and

Bacillus known for denitrification (Kuypers et al., 2018; Mancinelli, 1996; Zahran, 1999) increased in abundance from the intermediate to late periods. The increase in N fixation processes most likely led to N accumulation in the ecosystem, promoting microbial and plant growth in the late stage (Brankatschk et al., 2011; Wang et al., 2021). Similarly, an increase in phosphate mineralization can enhance phosphate availability for microbial and plant growth (Tiwari and Singh, 2017), whereas sulfur reduction pathways are used to fulfil increasing energy demand (Florentino et al., 2016).

Chapter 3

Soil bacterial diversity, composition, and interspecies interactions along an elevation-vegetation gradient

3.1 Introduction

Alpine ecosystems, despite having extreme cold environments, harbour a considerable bacterial diversity (Adamczyk et al., 2019; Donhauser and Frey, 2018). The alpine bacterial communities play crucial role in soil development and cycling of nutrients essential for plant colonization, growth, and survival (Donhauser and Frey, 2018). The community diversity and functions are largely dependent on the soil physicochemical properties, vegetation types, nutrient contents, temperature, and other climatic variables (Donhauser and Frey, 2018). The ongoing higher rate of climate change in the alpine regions, is expected to induce change in plant communities and nutrient contents which may further alter bacterial community diversity and composition (Djukic et al., 2010). However, knowledge regarding impacts of climate change on bacterial communities associated with different vegetation types is limited.

Earlier studies have mostly used elevation gradients in alpine ecosystems to study the patterns in bacterial community diversity as a response to climate change. However, the distribution patterns reported in these studies are contrasting and site-specific. For instance, studies from the Italian and Swiss Alps (Adamczyk et al., 2019; Siles and Margesin, 2017), Mount Gongga, Changbai Mountain, and Colorado Rocky Mountains (Bryant et al., 2008; Shen et al., 2015; Zhu et al., 2020) showed decreasing bacterial diversity across elevation. In contrast, Tibetan Plateau and Mount Wutai exhibited an increasing trend (Luo et al., 2019; Zhang et al., 2019), and Mt Fuji showed a hump-back trend in bacterial diversity (Singh et al., 2012). Additionally, studies also observed no definite trends along elevation (Siles and Margesin, 2016; Yashiro et al., 2016). The inconsistency in elevation patterns is mainly due to local edaphic conditions and climate variability (Singh et al., 2014; Yashiro et al., 2016). It is only when more studies on bacterial diversity patterns from alpine ecosystems having similar geological and climatic

conditions are performed over spatial and temporal scales, appropriate conclusions can be made regarding their response to climate change.

To account for spatial and temporal variability simultaneously, we take advantage of a short elevation gradient with vegetation shift in the Himalaya to investigate the patterns in bacterial diversity across three years. Encompassing the world's highest mountain ranges, the Himalaya represents diverse ecosystems with immense biodiversity (Padma, 2014). In addition, it retains about 33% of India's carbon stock (Bhattacharyya et al., 2008) and has a critical role in the global carbon cycle and climate warming (Longbottom et al., 2014; Yang et al., 2008). Recent assessments predict a 4.6 °C temperature rise in Himalaya by 2050 (R. Krishnan et al., 2020). High altitude habitats in the Himalaya, due to their ongoing formation in terms of soil and vegetation climax (Shrestha et al., 2012b), provide climate-vegetation gradient across short elevation ranges and are ideal for studies on bacterial community dynamics. The objectives of our study were to (i) assess the patterns in bacterial α and β-diversity across an elevation-vegetation gradient, (ii) determine seasonal and inter-annual variability in bacterial diversity, and (iii) assess bacterial co-occurrence pattern across the gradient. We hypothesized an increasing co-operative interactions between the bacterial communities with a decreasing diversity across the elevation-vegetation gradient.

3.2 Study Area

The study was conducted along an elevation gradient on a southwest-facing slope of a glaciated valley in Western Himalaya, India (30.95–30.99° N, 78.99–79.06° E) (Figure 3.1). The entire gradient (3373–4020 m) encompasses a ~10 km trail inside a protected area (Gangotri National Park) where anthropogenic interference is limited and livestock grazing is banned. Vegetation in this region changes with increasing elevation forming

elevation-vegetation gradient from a subalpine forest in lower elevations to alpine scrub in mid and alpine meadow at the higher elevations (Figure 3.2). The ground vegetation cover in the forest, alpine scrub, and meadow was estimated ca. 40 ± 14%, 22.5 ± 3.5%, and 70 ± 14%, respectively. Table 3.1 details the dominant plant species in each vegetation type. The soil is poorly formed and slightly acidic (Table 3.1). Mean annual precipitation is around 1500 mm, which occurs in the form of rainfall during June to September and snowfall from December to May (Sanyal et al., 2013) while, mean annual air temperature (MAT) range from 1.85 ± 0.22 °C to 6.13 ± 0.16 °C (Table 3.1).

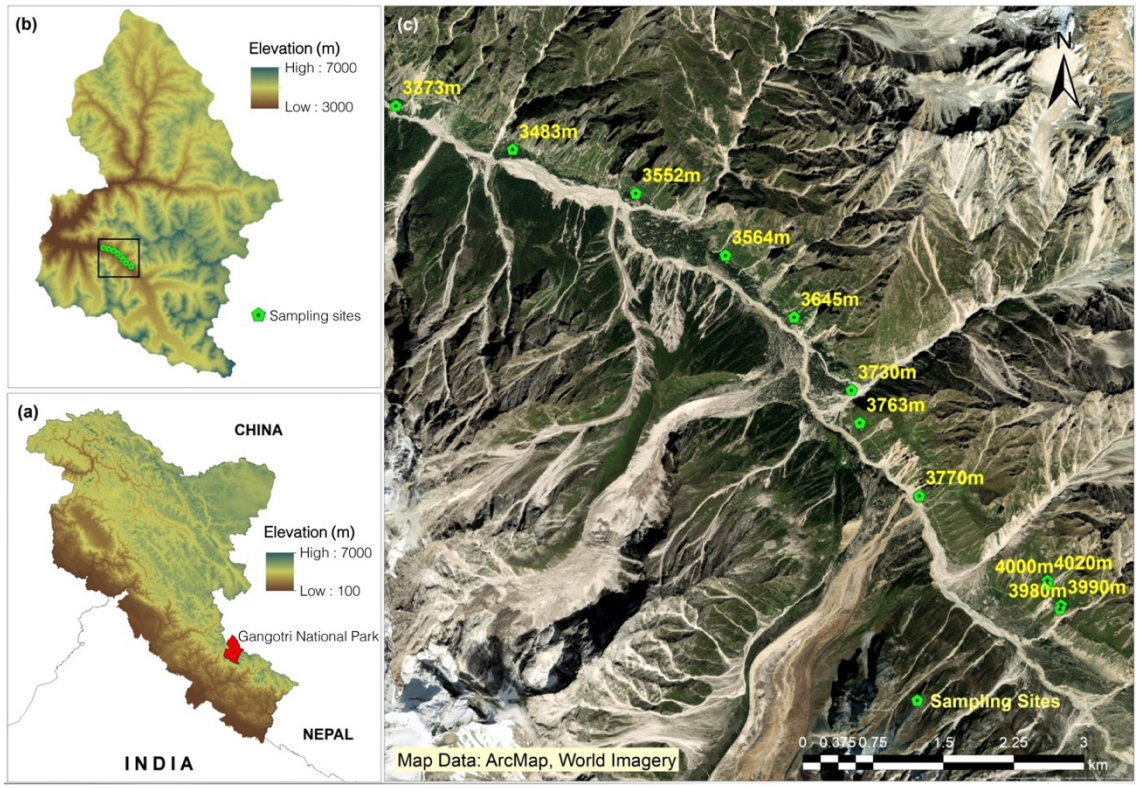

Figure 3.1 Map of the study area (a) Western Himalaya, India, (b) Gangotri National Park, and (c) sampling sites along an elevation-vegetation gradient in Gangotri National Park. All maps were generated in ArcGIS version 10.7 (ESRI, CA, USA, https://desktop.arcgis.com/en/arcmap/).

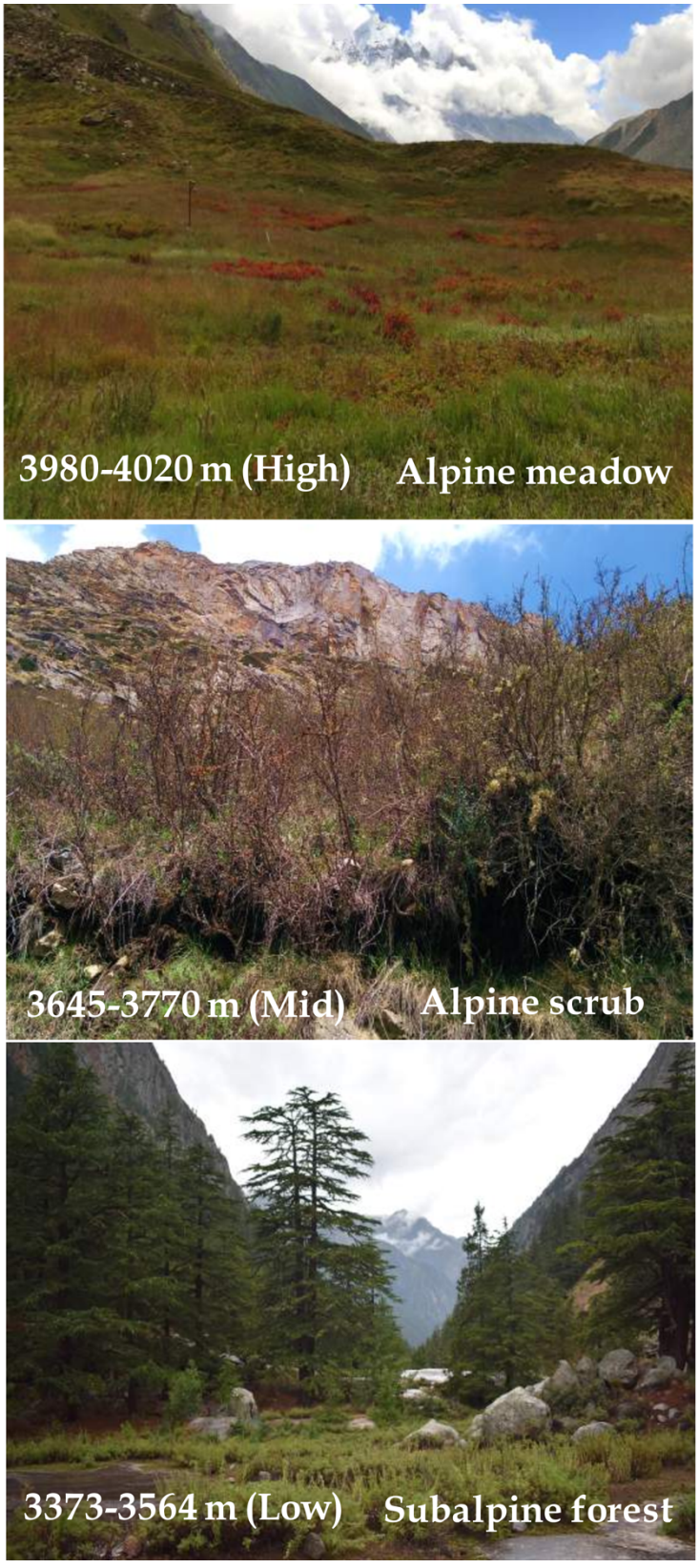

Figure 3.2 Dominant vegetation types across the elevation-vegetation gradient.

Table 3.1 Vegetation, mean annual air temperature (MAT), and soil pH, at sampling sites across elevation.

Altitude (m.a.s.l)	Vegetation	Dominant Plants	MAT (°C)	pH
3373	Subalpine forest	**Tree species:** *Betula utilis, Populus ciliata, Acer caesium, Sorbaria tomentosa* **Ground vegetation:** *Astragalus candolleanus*, *Anaphalis triplinervis*, *Rosularia alpestris*, *Calamogrostis emodensis,*	6.13 ± 0.16^{e}	5.34 ± 0.2^{a}
3483			6.04 ± 0.03^{e}	5.77 ± 0.19^{a}
3552			5.48 ± 0.01^{de}	5.19 ± 0.42^{a}
3564			5.32 ± 0.13^{de}	5.07 ± 0.35^{a}
3645	Alpine scrub	*Rosa sericea, Spiraea canescens, Artemisia santolinifolia, Lonicera obovata, Viburnum cotinifolium, Berberis jaeschkeana, Juniperus communis*	4.73 ± 0.05^{cd}	5.96 ± 0.26^{a}
3730			4.04 ± 0.09^{bc}	5.8 ± 0.39^{a}
3763			3.42 ± 0.19^{b}	5.5 ± 0.39^{a}
3770			3.71 ± 0.11^{bc}	5.11 ± 0.3^{a}
3980	Alpine meadow	*Geranium himalayense*, *Aconogonum tortuosum*, *Nepeta discolor, Potentilla atrisanguinea*	2.01 ± 0.21^{a}	5.34 ± 0.4^{a}
3990			1.93 ± 0.22^{a}	5.14 ± 0.42^{a}
4000			1.85 ± 0.22^{a}	5.54 ± 0.37^{a}
4020			2.08 ± 0.43^{a}	5.22 ± 0.32^{a}

Values are mean ± S.E of mean, n = 5. Mean values followed by different letters are significantly different ($p < 0.05$).

3.3 Material and methods

3.3.1 Site selection and soil sampling

We selected twelve altitudinal sites across the gradient (Figure 3.1c) and marked a 5 × 5 m plot at each altitude (Figure 3.3). In each plot, we randomly selected five 1 × 1 m sub-plots for soil sampling (Figure 3.3). Five soil cores (~1 g each) were collected from 5 cm depth at four corners and center of the sub-plot using hand-held sterile soil corer (50 ml centrifuge tube of diameter 2.5 cm, Tarsons Products Pvt. Ltd, India). Before soil collection, ground vegetation was clipped, and litter was removed. Then, following the

design of (Lanzén et al., 2016), soil core at each altitude (n = 25) were pooled in a sterile ziplock bag and homogenized. From this pool, 5 g soil was aliquoted and preserved

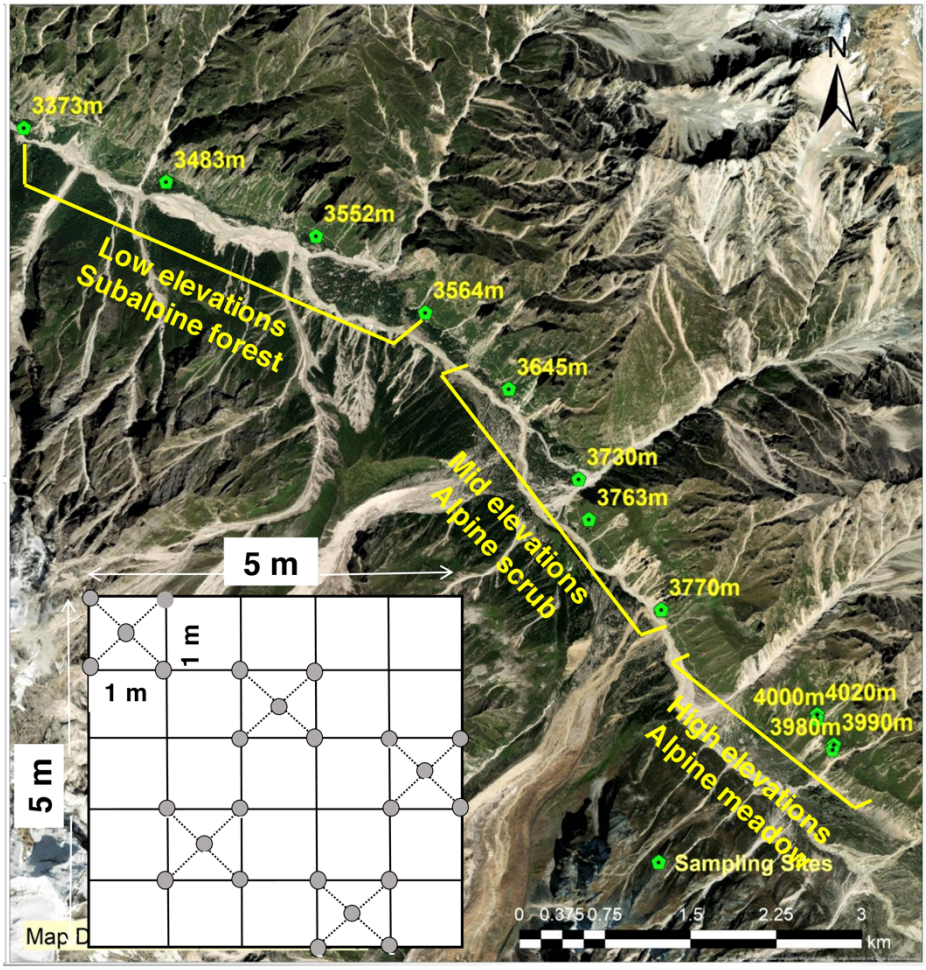

Fig. 3.3 Site selection and soil sampling strategy along the elevation-vegetation gradient in Gangotri National Park.

in 100% ethanol (Merck, Germany) to prevent the environmental DNA from hydrolytic damage before molecular analyses (Harry et al., 2000).

Both samples (one for molecular analysis and the other for soil physicochemical analyses) were transported to the laboratory in a cool box containing dry ice. Soil sampling was performed during spring (May) and autumn (October) at five time-points

during October 2016, May and October 2017, and May and October 2018, giving us a total sample size of 60 (n = 5 for each altitude).

3.3.3 DNA extraction, PCR amplification, and Illumina sequencing

We extracted soil genomic DNA from approximately 0.25 g of each soil sample using a Nucleopore GDNA soil kit (Genetix Biotech Asia Pvt. Ltd, India) following the manufacturer's kit protocol. We quantified DNA concentrations using Qubit dsDNA HS Assay Kit (Life Technologies, USA). We used Illumina 16S Metagenomics Sequencing library preparation protocol to prepare sequencing libraries for bacterial V3 and V4 regions using the primers 338F (5′-CCTACGGGNGGCWGCAG-3′) and 806R (5′-GACTACHVGGGTATCTAATCC-3′) (Luo et al., 2019). The PCR reaction contained 12.5 µl of 2×Kappa Hifi Hotstart ReadyMix (Kappa Biosystems, Roche Sequencing and Life Science, USA), 1 µl each of 5 µM forward and reverse primer, and 10.5 µl of the template (12.5 ng of microbial DNA), respectively. PCR conditions included an initial denaturation of 95 °C for 3 min, followed by 25 cycles of 95 °C for 30 s, 55 °C for 30 s, and 72 °C for 30 s, followed by a final extension for 10 min at 72 °C. PCR negative (no template DNA) was included to monitor any contamination. PCR products were purified, barcoded using Nextera XT kit (Illumina Inc., United States), and normalized to 2 nM for each library. The equal volume of these libraries was pooled, denatured, and diluted to 4 pM before loading onto the MiSeq flow cell (Illumina Inc., United States). Sequencing was performed on Illumina MiSeq platform using a 2 × 300 bp paired-end protocol at the Next Generation Genomics Facility at Center for Cellular and Molecular Platforms (C-CAMP), Bangalore, India.

3.3.4 Sequence data processing

We processed the raw sequences using the MiSeq SOP pipeline in Mothur v.1.40.5 (Kozich et al., 2013; Masse et al., 2017; Schloss et al., 2009). Full-length sequences were prepared, and good reads (>460 bp length with no homopolymer stretches longer than 8 bp) were identified and clustered (based on ≥97% similarity) using 16S rRNA database SILVA 132 SSU SEED (Quast et al., 2012). Uchime was used to remove chimeric sequences, followed by eliminating all singletons, chloroplasts, archaea, mitochondria, and unknown origin sequences (Edgar et al., 2011). Only high-quality sequences were used to estimate pairwise distances and generate single-linkage clusters with ≥97% sequence similarity. The longest read from each cluster was used as the reference sequence for taxonomic assignments against the SILVA SSU NR Ref database (Quast et al., 2012). All sequences in each cluster and their replicates (≥97% similarity) provided the quantitative estimates of individual reads per taxonomic unit. The dataset was normalized by rarefying the sequences to the lowest sample-specific sequencing depth with maximum Good's coverage (Kozich et al., 2013). Four samples with a sequence read less than the rarefaction depth were excluded from the downstream analyses. Finally, we clustered the sequences to phylum levels for operational taxonomic unit (OTU) abundance and composition analysis. We further classified the data into abundant taxa based on their relative abundances. OTUs with ≥1% relative abundance were considered abundant (Pedrós-Alió, 2006).

3.3.5 Co-occurrence network construction

To identify bacterial interspecies interactions, we constructed co-occurrence ecological networks following Random Matrix Theory (RMT)-based method through Molecular Ecological Network Analysis (MENA) pipeline (Deng et al., 2012; Zhou et al., 2011).

Pearson correlation between OTUs at genus level having relative abundances >0.1% in all samples were used to construct the network with an identical similarity threshold 0.7 at three elevation ranges low (3373–3564 m), mid (3645–3770 m), and high (3980–4020 m). We calculated various indices, including node and link numbers, average degree (avgK), average clustering coefficient (avgCC), average path distance (GD), density (D), modularity (M), and connectedness (Con) to evaluate and compare the overall topological features of the networks (Deng et al., 2012). The networks were separated into different modules using fast greedy modularity optimization (Deng et al., 2012). The network graphs were visualized using Cytoscape 3.8.2 (Shannon et al., 2003), where each node represents one genus, and each link represents one significant correlation.

3.3.6 Data analysis

We calculated three bacterial α-diversity indices: richness (Sobs), evenness, and Shannon diversity index for each sample using the Mothur platform. We used one-way analysis of variance (ANOVA) to determine significant differences in α-diversity indices, MAT, and edaphic factors (SMC, SOC, total nitrogen, pH, and C/N) between altitudinal sites. Where differences were significant, Tukey's honest significance difference (HSD) post-hoc test was applied for pairwise comparisons of mean at 95% confidence intervals. Seasonal and inter-annual variability in α-diversity was evaluated by grouping the data into low (3373–3564 m), mid (3645–3770 m), and high elevation ranges (3980–4020 m) followed by independent sample *t*-test and ANOVA, respectively. Before the analysis, we tested normality and heteroscedasticity of data by the Shapiro-Wilk and Levene tests, respectively. We calculated the Bray-Curtis dissimilarity matrix after Hellinger transformation of rarefied abundance data at the phyla level for β-diversity estimation. Principal Coordinate Analysis (PCoA) using the Bray- Curtis dissimilarity matrix was

used to interpret differences in bacterial community composition visually. To test any significant compositional differences, we used Multi-Response Permutation Procedure (MRPP) analysis (Oksanen et al., 2019) with 9999 permutations, where chance corrected within-group agreement (a measure of effect size presented as *A* value) was calculated. The *A* value ranges between 0 and 1, where $A = 0$ indicates samples within a group are heterogeneous, and $A = 1$ depicts they are identical. We evaluated seasonal and inter-annual variability in β-diversity by grouping the data into low (3373–3564 m), mid (3645–3770 m), and high elevation ranges (3980–4020 m) followed by MRPP analysis. All analyses were conducted in R 4.0.3 (http://www.R-project.org/) through RStudio 1.3.1093, 2020 (https://rstudio.com/products/rstudio/) using vegan 2.5-7 (https://cloud.r-project.org/package=vegan), dplyr 1.0.5 (https://cloud.r-project.org/package=dplyr) and ggplot2 3.3.3 (https://cloud.r-project.org/package=ggplot2) (Oksanen et al., 2019; Wickham, 2011; Wickham and Wickham, 2017).

3.3.7 Accession number

The DNA sequence data set has been deposited to National Centre for Biotechnology Information (NCBI) Short Read Archive (https://www.ncbi.nlm.nih.gov/sra). The BioProject accession number PRJNA705032.

3.4 Results

3.4.1 Taxonomic overview

A total of 2,542,679 high-quality sequences across 60 samples were generated, averaging 42,378 ± 14,204 sequences per sample (Appendix Table A2). Rarefaction based on sequence reads of one of the samples (23,821) provided maximum Good's coverage (>82%) (Appendix Table A2) for 56 samples. The remaining four samples (at altitudes

3645 m, 3730 m, 3763 m, and 3770 m in May 2018) having sequence reads less than the rarefaction depth were eliminated, and downstream analyses were performed only with 56 samples. We identified 126,667 OTUs at ≥97% similarity and were grouped into 35 phyla. Out of these 35 phyla, 34 were classified, of which 12 were abundant (relative abundance ≥1%), accounting for 98% of the total bacterial sequences (Figure. 3.4a).

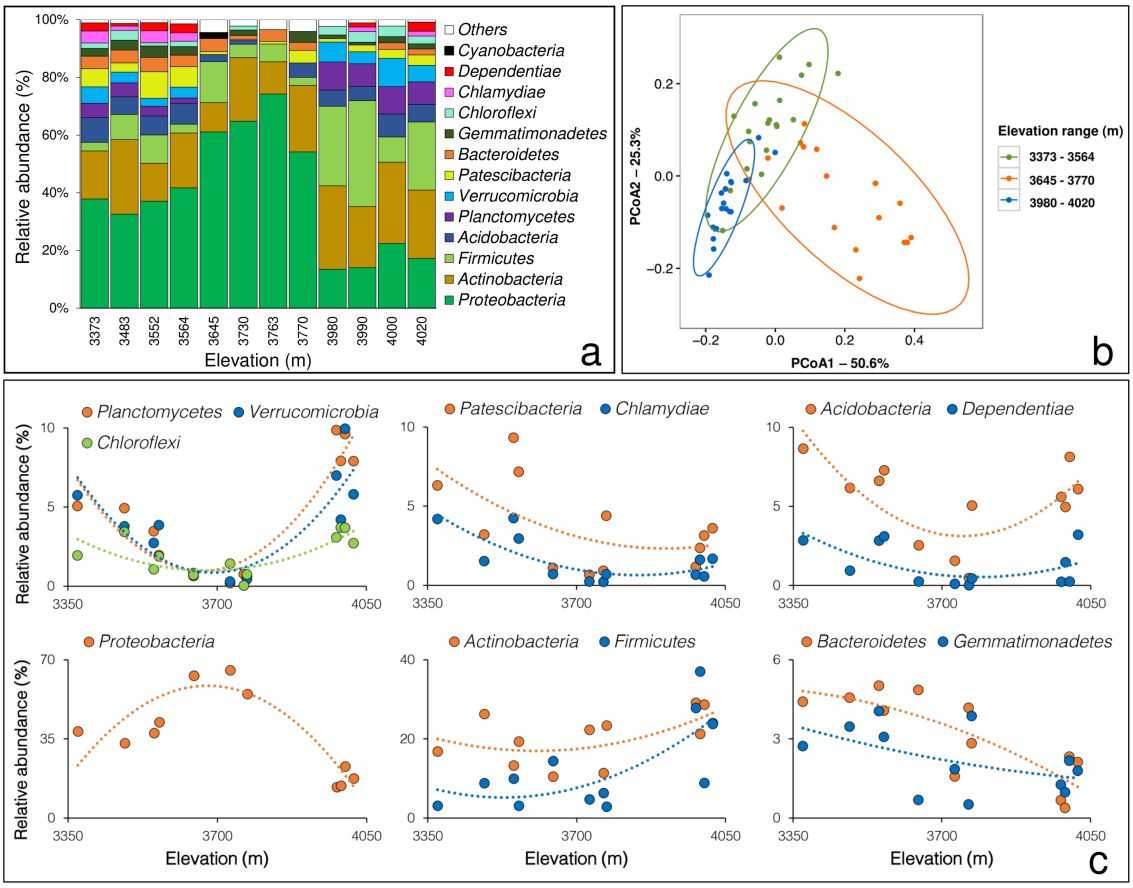

Figure 3.4 Bacterial β-diversity across elevation-vegetation gradient (a) variation in relative abundances of bacterial phyla where "Others" _represent all phyla with relative abundances <1%, (b) Principal Co-ordinates Analysis (PCoA) based on Bray-Curtis dissimilarity of bacterial communities and (c) variation in relative abundance of individual abundant bacterial phyla. b was generated in R 4.0.3 (http://www.R-project.org/) using vegan 2.5-7 (https://cloud.r-project.org/package=vegan), dplyr 1.0.5 (https://cloud.r-project.org/package=dplyr) and ggplot2 3.3.3 (https://cloud.r-project.org/package=ggplot2).

These abundant phyla were *Proteobacteria* (relative abundance 39.22%), *Actinobacteria* (20.3%), *Firmicutes* (12.4%), *Acidobacteria* (5.17%), *Planctomycetes* (4.37%), *Verrucomicrobia* (3.66%), *Patescibacteria* (3.56%), *Bacteroidetes* (3.02%), *Gemmatimonadetes* (2.17%), *Chloroflexi* (2%), *Chlamydiae* (1.58%) and *Dependentiae* (1.28%).

3.4.2. Bacterial α and β-diversity across elevation-vegetation gradient

Bacterial α-diversity (richness, evenness and, Shannon diversity) followed a similar trend as edaphic properties (SMC, SOC, and total nitrogen) with similarities at low and high elevation and dip in mid-elevations (Figure. 3.5). As a result, three distinct groups encompassing four altitudes each were visible across the gradient.

Bacterial β-diversity also showed the influence of mid-elevations. The abundant phyla decreased from 12 in the low elevations (3373–3564 m) to 5–7 across 3645–3770 m, then regained to 9–12 in higher elevations (Figure. 3.4a). As the number of abundant phyla decreased in mid-elevations, the communities showed less even distribution. *Proteobacteria* dominated community composition up to 3770 m with relative abundance ranging from 33 to 75%. However, *Actinobacteria* (21–29%) and *Firmicutes* (8–36%) seemed to dominate the community at higher elevations equally. We also observed the presence of *Cyanobacteria* with a relative abundance of 1.98% at only 3645 m. Three significantly distinct ($A = 0.26$, $p < 0.001$) community clusters were observed at low, mid, and high elevation ranges (Figure. 3.4b). However, we observed high overlaps between the clusters at low and high elevations.

Figure. 3.4c shows trends in the relative abundance of abundant phyla across the elevation-vegetation gradient. Except for the most abundant *Proteobacteria*, which

peaked in mid-elevations and dipped at higher elevations, several bacterial phyla showed a mid-elevation dip. Three types of curves with such mid-elevation dips were observed,

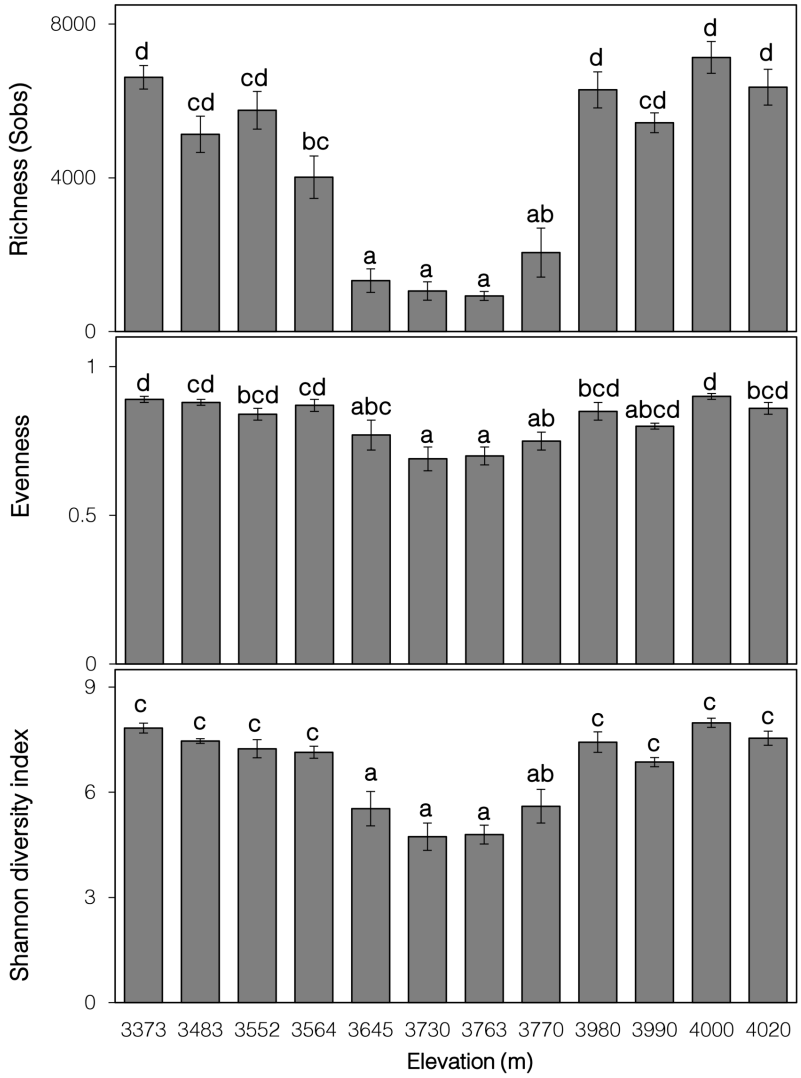

Figure 3.5 Variation in bacterial richness, evenness, and diversity across the elevation-vegetation gradient. Bars represent mean ± S.E of mean, n = 5 at each altitude. Different letters (above each bar) indicate significant difference between altitudes ($p < 0.05$). Bacterial β-diversity also showed the influence of mid-elevations. The abundant phyla

one, with similar abundances at low and high elevations (*Acidobacteria* and *Dependentiae*), second, with a gradual decrease up to mid-elevations and then an abrupt increase in higher elevations (*Planctomycetes*, *Verrucomicrobia*, *Chloroflexi*), and thirdly with the highest abundance at low elevations with a dip in mid and stable towards

higher elevations (*Patescibacteria*, *Chlamydiae*). On the contrary, *Actinobacteria* and *Firmicutes* increased, whereas *Bacteroidetes* and *Gemmatimonadetes* decreased across elevation.

3.4.3 Bacterial α and β-diversity across seasons and years

We assessed the variability in α and β-diversity across seasons (spring and autumn) and years (2016, 2017, and 2018) within 3373–3564 m, 3645–3770 m, and 3980–4020 m elevation ranges. We observed no significant difference ($p > 0.05$) in both α and β-diversity across seasons and years except for a decrease in richness during spring in the elevation range 3980–4020 m (Fig. 3.6, Table 3.2, 3.3 and 3.4).

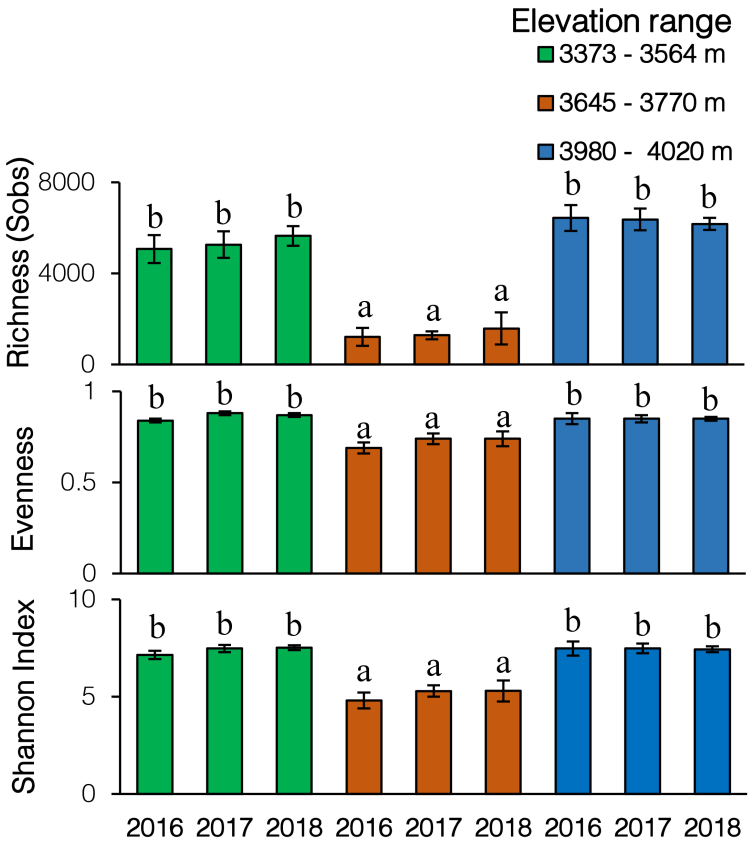

Figure 3.6 Inter-annual variations in bacterial richness, evenness, and diversity. Bars represent mean ± S.E of mean, n = 5 at each altitude. Different letters (above each bar) indicate significant difference between altitudes ($p < 0.05$).

Table 3.2 Results of independent sample t-test for bacterial community α-diversity comparison between two seasons (Spring and Autumn) at different elevation ranges (3373-3564 m), (3645-3770 m), and (3890-4020 m).

Elevation range	**Richness (Sobs)**			**Evenness**			**Diversity (Shannon Index)**		
	Spring	Autumn	p-value	Spring	Autumn	p - value	Spring	Autumn	p-value
(3373-3564 m)	5365 ± 534	5391 ± 382	0.96	0.86 ± 0.02	0.87 ±0.01	0.83	7.4 ± 0.18	7.4 ± 0.18	0.86
(3645-3770 m)	1008 ± 220	1452 ± 257	0.36	0.74 ± 0.03	0.72 ± 0.02	0.773	5.1 ± 0.33	5.2 ± 0.27	0.79
(3890-4020 m)	5644 ± 226	6745 ± 301	0.016	0.84 ± 0.02	0.86 ± 0.014	0.26	7.2 ± 0.2	7.6 ± 0.2	0.143

Values are mean ± S.E of the mean. n = 8 and12 for spring and autumn, respectively. Significant at $p < 0.05$.

Table 3.3 Results of MRPP analyses for bacterial community composition comparison between two seasons (Spring and Autumn) at low (3373-3564 m), mid (3645-3770 m) and high (3890-4020 m) elevation ranges.

Elevation range	Seasons	A value	p value
3373-3564 m	Spring &Autumn	0.0067	0.266
3645-3770 m	Spring &Autumn	0.01632	0.215
3890-4020 m	Spring &Autumn	0.001549	0.3723

Table 3.4 Results of MRPP analyses for bacterial community composition comparison between three years at low (3373-3564 m), mid (3645-3770 m) and high (3890-4020 m) elevation ranges.

Elevation range	Year	A value	p value
3373-3564 m	2016, 2017 & 2018	0.03885	0.0984
3645-3770 m	2016, 2017 & 2018	-0.03968	0.8083
3890-4020 m	2016, 2017 & 2018	-0.009465	0.5645

3.4.4 Bacterial co-occurrence pattern across elevation-vegetation gradient

The bacterial co-occurrence networks at the three elevation ranges showed scale-free (connectivity distribution obeyed power-law model, R^2 ranged from 0.3 to 0.92), non-random, small world (average path distance ranged from 3.1 to 4.5), and modular (modularity ranged from 0.45 to 0.57) features of ecological networks (Table 3.5) (Deng et al., 2012; Zhou et al., 2011). Comparison of topological features between the three networks revealed a dip in the number of nodes and links at the mid-elevation range with the highest value at the high-elevation range (Table 3.5 and Fig. 3.7). The low and high elevation range consisted of eleven and five modules, respectively, with most nodes connected positively (63–86%). In contrast, the mid-elevation range showed mainly

negative relation (70%) among nodes of the four constructed modules. A dip in network modularity (connectivity within a module) was observed in the mid-elevation range (0.45), where the density (0.084) and connectedness (1) peaked. The average degree (3.3–4.6) and clustering coefficient (0.14–0.23) increased linearly across the elevation ranges.

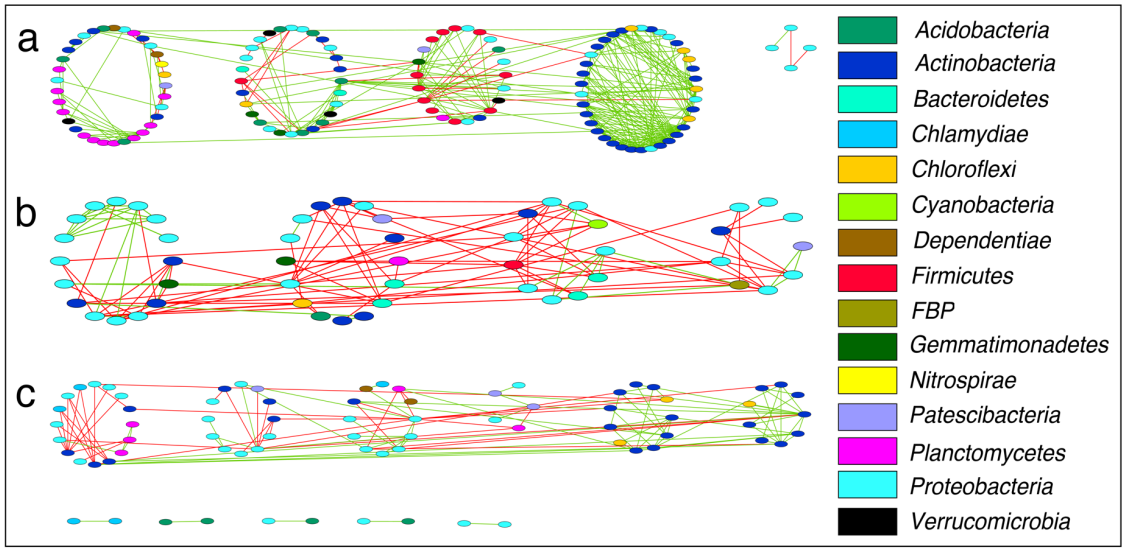

Figure 3.7 Co-occurrence networks of bacterial genera at (a) high (3980-4020 m), (b) mid (3645-3770 m), and (c) low (3373-3564) elevation range based on Random Matrix Theory. Each genus is represented as a node having an oval shape, and each significant ($p<0.05$) correlation (link) is represented as a straight line. Nodes of the same color represent the same phyla the genera belong to. Green and red lines indicate positive and negative correlations between nodes, respectively. Each module in the network is represented by a circle composed of nodes. The figure was generated in Cytoscape 3.2.8.

3.5 Discussion

Earlier studies on soil bacterial communities from various mountain ecosystems of the world have described different elevation patterns of α-diversity, such as increasing (Luo et al., 2019; Zhang et al., 2019), decreasing (Adamczyk et al., 2019; Bryant et al., 2008;

Table 3.5 Co-occurrence network topological properties at low, mid, and high elevation ranges.

	Network Indexes	Low (3373-3564 m)	Mid (3645-3770 m)	High (3980-4020 m)
Empirical	R square of power-law	0.92	0.3	0.864
	Total nodes	75	52	124
	Total links	122	112	285
	Links per node	1.6	2.2	2.3
	Positive co-occurrence (%)	63	30	86
	Average path distance (GD)	3.47	3.08	4.5
	Modularity	0.55	0.45	0.57
	Average degree (avgK)	3.25	4.31	4.6
	Average clustering coefficient	0.14	0.17	0.233
	Density (D)	0.044	0.084	0.037
	Connectedness	0.751	1	0.937
Randomized	Average clustering coefficient	0.06 ± 0.02	0.08 ± 0.03	0.06 ± 0.01
	Average path distance (GD)	3.36 ± 0.11	2.81 ± 0.05	3.23 ± 0.05
	Modularity(fast greedy)	0.49 ± 0.02	0.39 ± 0.02	0.41 ± 0.01
	Connectedness (Con)	0.90 ± 0.07	0.99 ± 0.02	0.98 ± 0.03

Shen et al., 2015; Siles and Margesin, 2017; Zhu et al., 2020) and unimodal trends (Singh et al., 2012). In contrast, α-diversity in our study followed a hollow trend, which dipped in the mid-elevations (Figure 3.5). The same trend was found across all three sampling years (Figure 3.6). Upon an in-depth literature review, we came across only a single study reporting a similar mid-elevation dip in bacterial α-diversity in the southwest and northeast slopes of Mt Halla, both at 700–1300 m elevation range (Singh et al., 2014). This suggests that there are factors other than elevation or temperature that control the bacterial richness and diversity. The major factors responsible for this trend is possibly the underlying gradient in soil properties caused by the variation in vegetation types along the studied gradient. In our study, the vegetation types in the low and high elevations were subalpine forest and alpine meadow, respectively, having moist soil and equally high organic carbon content, whereas in the mid elevations the vegetation was alpine scrub having dry soil and low organic carbon content. The dry and less nutrient soil in

the mid elevations probably led to a decrease in the bacterial richness, evenness and diversity.

Similar mid elevation dip pattern was observed in relative abundance of most abundant bacterial phyla (Figure 3.4a & c). This led to a different community composition in the mid elevations compared to similar compositions at low and high elevations (Figure 3.4b). The difference in community composition at mid-elevations was reflected in most phyla's relative abundances (*Acidobacteria*, *Dependentiae*, *Planctomycetes*, *Verrucomicrobia*, *Chloroflexi*, *Patescibacteria*, and *Chlamydiae*) showing mid-elevation dips (Figure. 3.4c, Chapter 3). Such mid elevation dip pattern has rarely been observed in nature, apart from a study in China where decrease in phylogenetic diversity of biofilm bacterial community was observed in the mid elevations (Wang et al., 2012). The observed pattern in our study suggests that the abundance of most abundant phyla are possibly dependent on soil properties and not climatic factors. The low moisture in the mid elevations probably led to low nutrient availability giving rise to a competitive community where members compete for nutrients (Figure 3.7). On the other hand, the high moisture and nutrient availability in the low and high elevation the communities were co-operative in nature (Figure 3.7).

The patterns observed in our study indicates that the bacterial community diversity and composition may be majorly regulated by soil properties and vegetation types along elevation gradient.

©Pankaj Tiwari

Chapter 4

Factors governing soil bacterial community diversity and composition

4.1 Introduction

Bacterial communities play a crucial role in soil formation, nutrient cycling, and plant colonization (Donhauser and Frey, 2018). These communities also regulate soil carbon storage through decomposition and mediate feedbacks between climate change and ecosystem functioning by heterotrophic respiration (Trivedi et al., 2013). Recent studies have demonstrated that incorporating trophic level information of these communities in carbon dynamic-based ecosystem models has enhanced predictive power (Treseder et al., 2012; Wieder et al., 2015). However, despite their pivotal role in ecosystem functioning and environmental susceptibility (Xu et al., 2014), knowledge regarding their environmental drivers has been inconclusive due to considerable variability in observed diversity patterns (Crowther et al., 2019).

Earlier studies understanding the factors regulating bacterial diversity patterns have primarily used elevation gradient in mountain ecosystems to proxy environmental change (Donhauser and Frey, 2018). However, the distribution patterns reported in these studies are contrasting and site-specific. For instance, studies from the Italian and Swiss Alps (Adamczyk et al., 2019; Siles and Margesin, 2016), Mount Gongga, Changbai Mountain, and Colorado Rocky Mountains (Bryant et al., 2008; Shen et al., 2015; Zhu et al., 2020) showed decreasing bacterial diversity across elevation. In contrast, Tibetan Plateau and Mount Wutai exhibited an increasing trend (Luo et al., 2019; Zhang et al., 2019), and Mt Fuji showed a hump-back trend in bacterial diversity (Singh et al., 2012). Additionally, studies also observed no definite trends along elevation (Siles and Margesin, 2016; Yashiro et al., 2016). The inconsistency in elevation patterns is mainly due to local edaphic and climate variability (Singh et al., 2014; Yashiro et al., 2016).

Seasonal and interannual variations in climatic and edaphic factors influence bacterial community diversity and composition (Siles et al., 2017, 2016). However, earlier studies

have been conducted across either a single time-point or seasons within a year across different spatial scales. Small scale studies (<1000 m elevation gradient) with relatively uniform vegetation have identified the role of climate but have masked the influence of edaphic factors (H. Sun et al., 2020). While large scale studies (>1000 m elevation gradient) have accounted for both climatic as well as edaphic factors (Xue et al., 2018; Yashiro et al., 2016) however are limited in numbers due to logistic feasibility. To account for spatial and temporal variability simultaneously, we take advantage of a short elevation gradient with vegetation shift in the Himalaya to investigate the influence of both edaphic and climatic factors on bacterial diversity across three years. These gradients provide an array of environmental factors within small distances and are easy to monitor across multiple time points (Djukic et al., 2010; Tang et al., 2020; Zhu et al., 2020).

Encompassing the world's highest mountain ranges, the Himalaya represents diverse ecosystems with immense biodiversity (Padma, 2014). In addition, it retains about 33% of India's carbon stock (Bhattacharyya et al., 2008) and has a critical role in the global carbon cycle and climate warming (Longbottom et al., 2014; Yang et al., 2008). Recent assessments predict a 3 °C temperature rise in Himalaya by 2050 (Shrestha et al., 2012b). High altitude habitats in the Himalaya, due to their ongoing formation in terms of soil and vegetation climax (Shrestha et al., 2012b), provide climate-vegetation gradient across short elevation ranges and are ideal for studies on bacterial community dynamics. The objectives of our study were to evaluate the role of temperature and edaphic factors in shaping the community diversity and composition. We hypothesized increasing co-operative interactions between the bacterial communities with a decreasing diversity across the elevation-vegetation gradient mainly regulated by temperature.

4.2 Study Area

As described in Chapter 3.

4.3 Material and methods

4.3.1 Site selection and soil sampling

Temperature and edaphic factors were estimated at the same twelve altitudinal sites selected across the gradient as in Chapter 3 (Figure 3.1c). At each site the soil samples collected for bacterial community analysis in Chapter 3 were also used for edaphic factor estimation. At each site a 5 × 5 m plot was marked and soil sampling was performed as described earlier (Figure 3.3). Samples were transported to the laboratory in a cool box containing dry ice. Soil sampling was performed during spring (May) and autumn (October) at five time-points during October 2016, May and October 2017, and May and October 2018, giving us a total sample size of 60 (n = 5 for each altitude).

4.3.2 Measurement of air temperature and edaphic factors

We deployed HOBO U23 Pro v2 data loggers (Onset Computer Corporation, USA) at 3373 m, 3564 m, 3763 m, and 4020 m to monitor hourly air temperature at 1 m height and calculated mean annual temperature (MAT) for the study period (2016–2018). MAT at remaining altitudes was estimated by generating standard curves (Singh et al., 2014). We estimated edaphic factors, including soil pH, moisture content, organic carbon, total nitrogen, and C/N. Soil moisture content (SMC) was measured gravimetrically from a 5 g soil sample (Rayment and Lyons, 2011). The remaining soil was air-dried and sieved through a 1 mm sieve to remove gravels, plant roots, and leaf litter. Soil pH was measured by a glass electrode pH meter (Sension 7, Hach Company, USA) in a 1:2.5 (w/v) suspension of soil and deionized water (Blakemore et al., 1987). Soil organic carbon

(SOC) was measured using the potassium dichromate (K2Cr2O7) oxidation method (Walkley and Black, 1934), and total nitrogen (TN) was determined by the Kjeldahl method (Bremner, 2018) using Kjeltec 8400 (Foss India Pvt. Ltd).

4.3.3 Bacterial α, β-diversity and composition estimation

Bacterial α, β-diversity and composition estimated in Chapter 3 were used for analysis in this chapter.

4.3.4 Data analysis

To assess the relationship of MAT and edaphic factors with bacterial richness and diversity, Multiple ordinary least square (OLS) regression analysis was performed with stepwise forward selection. For SOC and TN having high correlation ($r = 0.95$, $p < 0.001$), regressions were performed with SOC only. A model was considered most parsimonious based on Akaike's information criterion (Johnson and Omland, 2004). Mantel test with Pearson correlation was used to test the relationship of bacterial community composition with environmental variables. A forward selection of environmental variables using stepwise regression (with 999 permutations) was performed. Redundancy analysis (RDA) was conducted using Hellinger transformed bacterial abundance data to identify environmental variables that significantly explained the variation in abundant phyla. The RDA model and the environmental variables were tested by permutation test using ANOVA. Subsequently, univariate regression analyses was conducted to assess the relationship of environmental variables with Hellinger transformed relative abundance of individual bacterial phyla. Finally, structural equation model (SEM) analysis was performed to determine the direct and indirect effects of environmental variables on bacterial richness, α-diversity, and composition. The

composition was characterized by the first axis of PCoA of the Bray-Curtis dissimilarity matrix (Li et al., 2015). Based on theoretical knowledge, a path model was developed to relate environmental variables including vegetation, MAT, SMC, SOC, and pH with bacterial richness, diversity, and composition. To improve the fit between the model and the data, the initial theoretical model was modified for the correct specification of theoretical causal relationships between variables before analysis. We used Maximum likelihood estimation to compare the SEM model with the observations. The model fitness with the data was tested using Comparative Fit Index (CFI), Akaike Information Criteria (AIC), and Root Square Mean Errors of Approximation (RMSEA). Adequate model fits were indicated by a high CFI (>0.90), low AIC, and low RMSEA (<0.05) ("Structural Equation Modeling and Natural Systems by J. B. GRACE," 2007). All analyses were conducted in R 4.0.3 (http://www.R-project.org/) through RStudio 1.3.1093, 2020 (https://rstudio.com/products/rstudio/) using vegan 2.5-7 (https://cloud.r-project.org/package=vegan) and lavaan 0.6-9 (https://cloud.r-project.org/package=lavaan) (Oksanen et al., 2019; R Core Team, 2020; Wickham, 2011; Wickham and Wickham, 2017).

4.4 Results

4.4.1 Air temperature and edaphic factors across elevation-vegetation gradient

Both temperature and edaphic factors varied across the elevation gradient (Table 4.1). Mean annual air temperature (MAT) showed a monotonous decrease across the elevation gradient. In contrast, edaphic properties including SMC, SOC, and TN showed a dip in mid-elevations with similar values at low and high elevations. No significant difference was observed in the C/N ratio and pH at any altitude.

Table 4.1 Vegetation, mean annual air temperature (MAT), and edaphic properties including soil moisture content (SMC), pH, soil organic carbon (SOC), total nitrogen (TN) and C/N ratio at sampling sites across elevation.

Altitude (m.a.s.l)	Vegetation	Dominant Plants	MAT (°C)	SMC (%)	pH	SOC (g Kg^{-1})	TN (g Kg^{-1})	C/N ratio
3373	Subalpine forest	**Tree species:** *Betula utilis, Populus ciliata, Acer caesium, Sorbaria tomentosa* **Ground vegetation:** *Astragalus candolleanus*, *Anaphalis triplinervis*, *Rosularia alpestris*, *Calamogrostis emodensis,*	6.13 ± 0.16^{e}	19.87 ± 2.27^{abc}	5.34 ± 0.2^{a}	52.93 ± 10.21^{acd}	4.23 ± 0.68^{abc}	12.27 ± 1.06^{a}
3483			6.04 ± 0.03^{e}	15.87 ± 5.5^{ab}	5.77 ± 0.19^{a}	52.74 ± 9.72^{acd}	4 ± 1.06^{abc}	14.22 ± 1.62^{a}
3552			5.48 ± 0.01^{de}	22.86 ± 3.24^{abc}	5.19 ± 0.42^{a}	38.56 ± 9.33^{abc}	3.28 ± 1.01^{ab}	13.89 ± 1.18^{a}
3564			5.32 ± 0.13^{de}	13.03 ± 3.56^{ab}	5.07 ± 0.35^{a}	35.19 ± 12.8^{abc}	2.95 ± 1.31^{ab}	13.07 ± 1.04^{a}
3645	Alpine scrub	*Rosa sericea, Spiraea canescens, Artemisia santolinifolia, Lonicera obovata, Viburnum cotinifolium, Berberis jaeschkeana, Juniperus communis*	4.73 ± 0.05^{cd}	7.57 ± 3.39^{a}	5.96 ± 0.26^{a}	27.99 ± 5.29^{ab}	1.94 ± 0.27^{a}	14.28 ± 1.64^{a}
3730			4.04 ± 0.09^{bc}	7.35 ± 3.85^{a}	5.8 ± 0.39^{a}	15.44 ± 4.34^{b}	1.24 ± 0.36^{a}	13.05 ± 1.23^{a}
3763			3.42 ± 0.19^{b}	7.41 ± 3.71^{a}	5.5 ± 0.39^{a}	24.07 ± 5.56^{ab}	2.26 ± 0.51^{a}	12.47 ± 1.7^{a}
3770			3.71 ± 0.11^{bc}	8.21 ± 3.89^{a}	5.11 ± 0.3^{a}	24.19 ± 7.58^{ab}	1.99 ± 0.57^{a}	11.69 ± 0.97^{a}
3980	Alpine meadow	*Geranium himalayense*, *Aconogonum tortuosum*, *Nepeta discolor, Potentilla atrisanguinea*	2.01 ± 0.21^{a}	26.64 ± 2.32^{bc}	5.34 ± 0.4^{a}	46.02 ± 6.34^{abc}	4.74 ± 0.75^{abc}	9.83 ± 0.18^{a}
3990			1.93 ± 0.22^{a}	34.46 ± 3.01^{c}	5.14 ± 0.42^{a}	44.92 ± 5.81^{abc}	4.4 ± 0.53^{abc}	10.22 ± 0.71^{a}
4000			1.85 ± 0.22^{a}	22.54 ± 3.79^{abc}	5.54 ± 0.37^{a}	71.05 ± 4.16^{cd}	6.3 ± 0.65^{bc}	11.6 ± 0.89^{a}
4020			2.08 ± 0.43^{a}	26.95 ± 5.1^{bc}	5.22 ± 0.32^{a}	87.98 ± 3.78^{d}	7.27 ± 0.7^{c}	12.65 ± 1.54^{a}

Values are mean ± S.E of mean, n = 5. Mean values followed by different letters are significantly different ($p < 0.05$).

4.4.2 Factors affecting α and β-diversity

Multiple linear regressions showed that α-diversity was positively affected by SMC and SOC across elevation (Table 4.2). Variability in richness (r^2 = 0.50, $p < 0.001$) and diversity (r^2 = 0.36, $p < 0.001$) were significantly explained by SMC and SOC, while that in evenness by only SOC (r^2 = 0.21, $p < 0.001$). No significant relationships were observed between α-diversity and pH, C/N, and MAT. On the other hand, β-diversity was significantly correlated to MAT ($r = 0.25$, $p < 0.001$) and all the selected edaphic factors (SMC: $r = 0.28$, $p < 0.001$; SOC: $r = 0.19$, $p < 0.001$; TN: $r = 0.18$, $p < 0.001$ and pH: $r = 0.07$, $p < 0.049$) except C/N ratio ($r = 0.08$, $p = 0.07$) as revealed by Mantel test. Further, the Redundancy Analysis with 12 abundant phyla showed that MAT, SMC, and SOC explained 33% ($F(3,52) = 8.68$, $p < 0.001$) of the variability in their relative abundance across the elevation gradient (Figure 4.1).

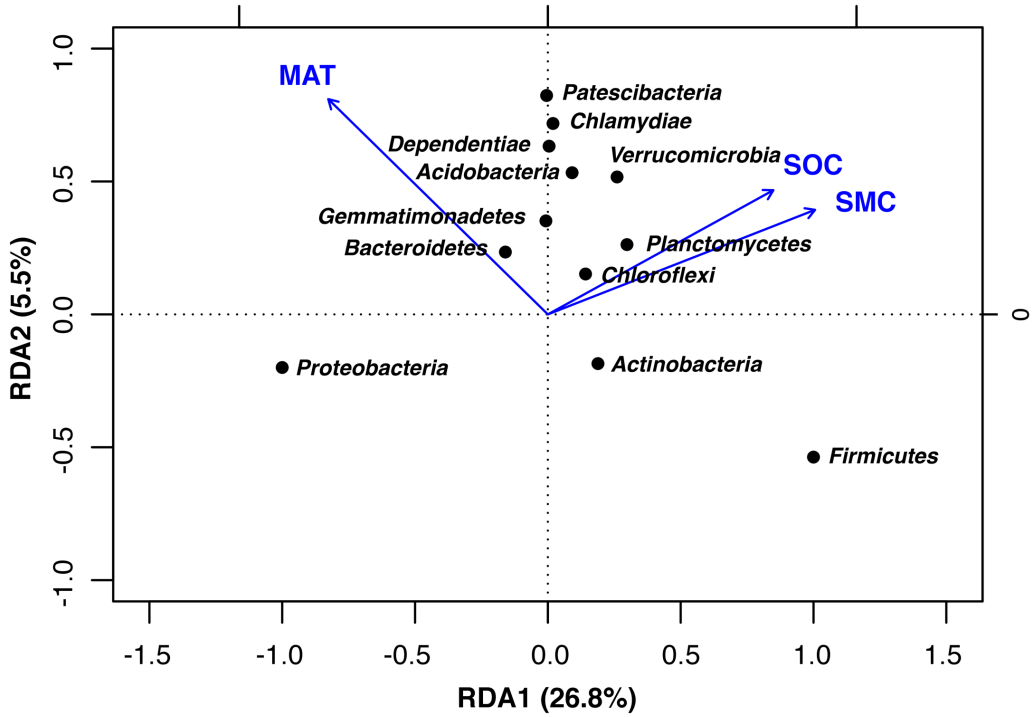

Figure 4.1 Redundancy analysis (RDA) showing significant relationships between abundant bacterial phyla and mean annual temperature (MAT), soil moisture content (SMC), and soil organic carbon (SOC).

Table 4.2 Multiple linear regression models for the relationship of richness, evenness, and diversity with mean annual temperature (MAT), soil moisture content (SMC), and soil organic carbon (SOC).

α-diversity	Predictor variables	R^2	α	β	F	p	AIC
Richness (Sobs)	SMC SOC	0.50	1473.93 (487.38)	75.66 (23.03) 38.49 (11.05)	26.35	< 0.001	836.12
Evenness	SOC	0.21	0.75 (0.02)	0.0015 (0.0003)	14.74	< 0.001	-290
Diversity (Shannon index)	SMC SOC	0.36	5.43 (0.28)	0.03 (0.01) 0.02 (0.01)	14.81	< 0.001	1.3

Values within parenthesis indicate standard error. α and β are constants. Significant at $p < 0.001$.

We performed linear regressions to understand the effect of MAT, SMC, and SOC on each abundant phylum (Figure 4.2). *Proteobacteria*, *Firmicutes,* and *Planctomycetes* were significantly affected by all the three factors, whereas *Bacteriodetes* and *Chlamydiae* by MAT and SMC; *Verrucomicrobia* and *Chloroflexi* by SMC and SOC, *Actinobacteria* and *Acidobacteria* by SOC and *Patescibacteria* and *Dependentiae* by MAT. *Gemmatimonadetes* was not significantly affected by any of the three factors. The unexplained variability in bacterial α and β-diversity may be due to factors such as belowground biomass, plant species composition, and soil nutrients (phosphorus and others) not measured in this study.

The SEM model (CFI = 0.94, AIC = 683.1, RMSEA = 0.16, $p < 0.05$) explained 36%, 89%, and 65% of the variation in bacterial richness, α-diversity and composition, respectively (Figure 4.3). Diversity was strongly related to richness ($\lambda = 0.94$, $p < 0.001$) which was affected directly by SOC ($\lambda = 0.32$, $p < 0.01$) and SMC ($\lambda = 0.49$, $p < 0.001$) and indirectly by vegetation type ($\lambda = 0.16$, $p < 0.01$). Community composition was related to richness ($\lambda = 0.77$, $p < 0.001$) and affected directly by SOC ($\lambda = - 0.36$, $p < 0.001$), pH ($\lambda = - 0.25$, $p < 0.01$) and MAT ($\lambda = - 0.16$, $p < 0.05$). Table 4.3 shows the standardized path coefficients of direct, indirect and total effects.

4.5 Discussion

The mid-elevation dip observed in this study suggests the dominance of factors other than elevation or temperature in controlling bacterial α-diversity (Fierer et al., 2011; Singh et al., 2014). Notably, the vegetation in our study shifts from the subalpine forest in lower elevations (3373–3564 m) to alpine scrub in the mid (3645–3770 m) to the alpine meadow in the higher elevations (3890–4020 m) (Table 4.1). The dip in α-diversity

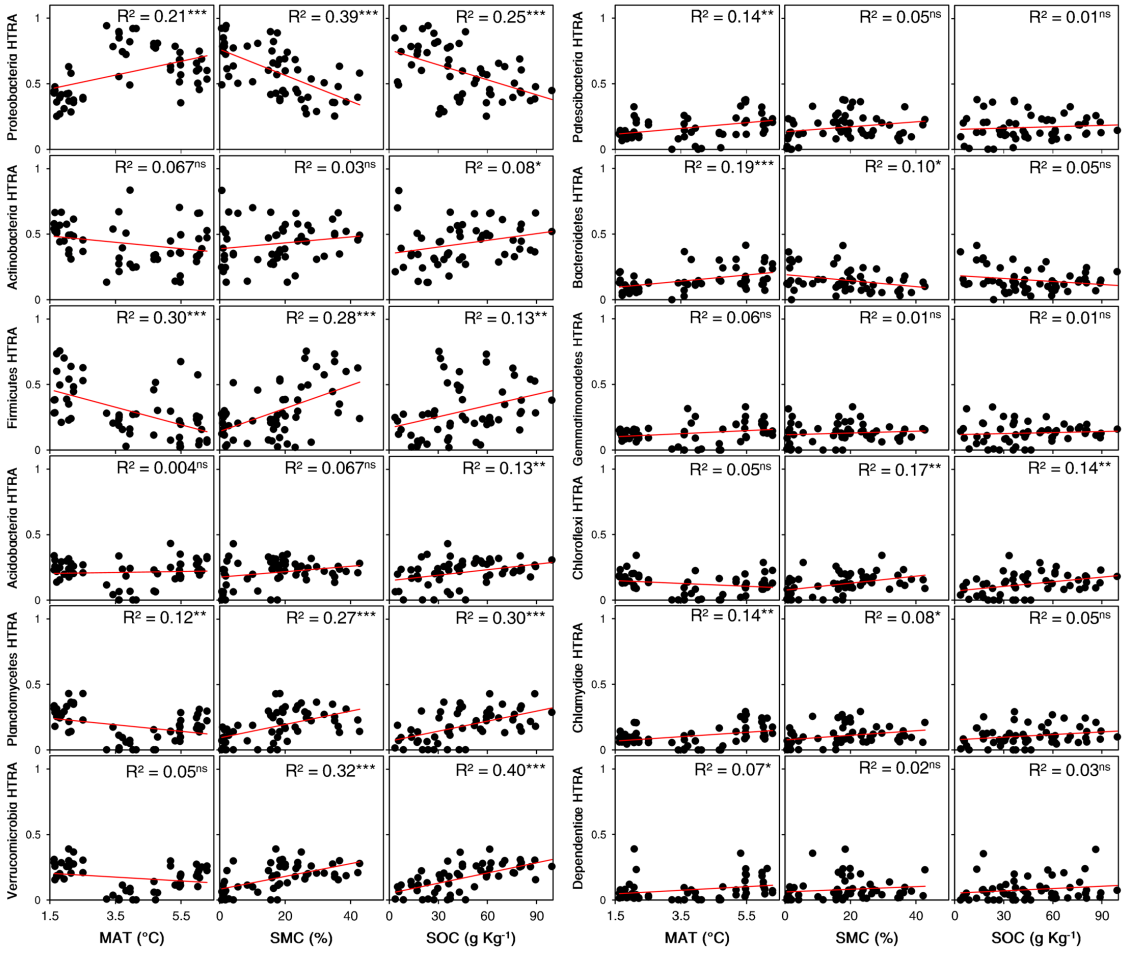

Figure 4.2 Linear relationships between Hellinger transformed relative abundance (HTRA) of bacterial phyla across elevation and mean annual temperature (MAT), soil moisture content (SMC) and soil organic carbon (SOC). Significant at ***p < 0.001, **p < 0.01 and *p < 0.05; ns represents non-significant.

corresponds to the alpine scrub vegetation having low soil moisture, SOC, and TN compared to other elevations (Table 4.1). On the contrary, subalpine forest and alpine meadow occurring in extreme climate regimes with similar edaphic characteristics (moisture, carbon, and nitrogen) had comparable α-diversity. This finding indicates that edaphic factors corresponding to different vegetation types control bacterial diversity rather than elevation or temperature. The regression analysis supports this assumption, as

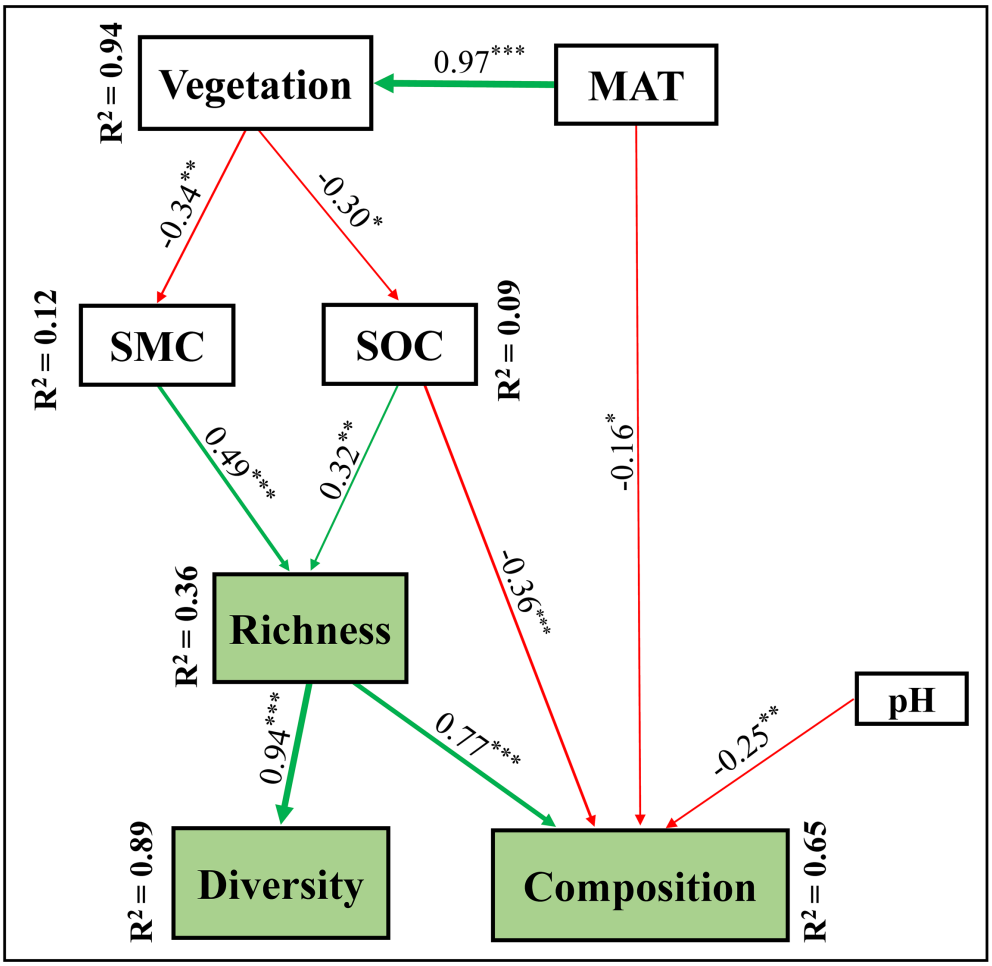

Figure 4.3 Structural equation model (SEM) showing the causal influences of vegetation, MAT, SOC, SMC, and pH on bacterial richness, α-diversity, and composition. Red and green lines indicate significant negative and positive effects, respectively. The width of the arrows is based on the standardized path coefficients indicating the strength of the causal effect. The standardize coefficients are marked above each path (* indicates significant ($p < 0.05$) effects, ** indicates significant ($p < 0.01$) effects, *** indicates significant ($p < 0.001$) effects). R^2 values represent the percentage of variance explained for each variable.

most variability in bacterial richness, evenness, and diversity were explained by SMC and SOC (and in turn TN because of its high correlation with SOC, $r = 0.95$, $p < 0.001$) and not by temperature. The SEM analysis also indicated the direct effect of edaphic properties (SMC and SOC) on the bacterial richness and, in turn, diversity. The

Table 4.3 Direct, indirect and total effect coefficients of each variable in the structural model.

Variable	Direct effect	Indirect effect	Total effect
Richness			
SOC	0.49	-	0.49
SMC	0.32	-	0.32
MAT	-	-0.16	-0.16
Vegetation	-	-0.16	-0.16
Diversity			
Richness	0.94	-	0.94
SOC	-	0.30	0.30
SMC	-	0.46	0.46
Vegetation	-	0.01	0.01
MAT	-	0.02	0.02
Composition			
Richness	0.77	-	0.77
SOC	-0.36	-	-0.36
MAT	-0.16	-0.1	-0.26
pH	-0.25	-	-0.25
SMC	-	0.38	0.38
Vegetation	-	0.11	0.11
SMC			
Vegetation	-0.34	-	-0.34
SOC			
Vegetation	-0.3	-	-0.3
Vegetation			
MAT	0.97	-	0.97

Effects were calculated using standardized path coefficients for significant relations ($p<0.05$, $p<0.01$ and $p<0.001$).

dominance of edaphic factors in governing bacterial diversity along elevation gradient has also been described earlier from Mt Changbai, the Italian Alps, the Andes, and southwest Wales (Fierer et al., 2011; Shen et al., 2015, 2013; Siles and Margesin, 2016; Xue et al., 2018). We found no effect of pH and C/N ratio on bacterial α-diversity and is in contrast to other studies where they have been identified as significant drivers of bacterial communities (Adamczyk et al., 2019; Lanzén et al., 2016; Shen et al., 2015; Yashiro et al., 2016).

The effect of edaphic properties was further displayed in the patterns of bacterial β-diversity. The overlaps found in community composition (Figure 3.4, Chapter 3) between low and high elevation suggested possible relatedness due to similarity in their edaphic properties. In contrast, the mid-elevations, having contrasting soil properties, showed different community compositions. Low moisture-induced drier conditions and low substrate availability in mid-elevations may have limited the growth of these phyla and hence reduced their relative abundance (Brockett et al., 2012; Lladó et al., 2017). Low relative abundance of these bacterial phyla led to the dominance of *Proteobacteria* (54.1–74.2%) in the mid-elevations and resulted in less evenly distributed community composition (Figure 3.4a, Chapter 3), which was also evident from low evenness (0.69–0.77) (Figure 3.5, Chapter 3).

Mantel test, RDA, and SEM showed that the community composition across elevation gradient was influenced directly by both edaphic factors (SOC and pH) and temperature (Figures 4.1 and 4.3). Linear regression also indicated the relationship of many phyla to temperature along with edaphic factors (Figure 4.2). Consequently, irrespective of mid-elevation dips, relative abundances of such phyla increased or decreased across elevation. This was expected as temperature stimulates the growth and metabolic activities of bacteria and, in turn, affects the community (Zhou et al., 2011). However, the increasing temperature is only efficient in shaping community composition when nutrient and water supply is adequate (Lladó et al., 2017; Peltoniemi et al., 2015; Rousk et al., 2012). Moreover, the quality of nutrients also determines the fate of community distribution across elevation gradients in mountain ecosystems (Xu et al., 2015; Zheng et al., 2018). For instance, sub-alpine forest in the lower altitudes provides a high amount of leaf litter rich in recalcitrant carbon compared to alpine scrub and meadows, where leaf litter input is comparatively low and primarily seasonal. High leaf litter facilitates the growth of

specific communities, such as, *Acidobacteria* that can derive energy by oxidizing the recalcitrant form of carbon (Lladó et al., 2017). On the contrary, the labile form of carbon mainly comes from root exudates and depends on the formation of root networks and carbon allocation from photosynthesis (Cleveland et al., 2007; Lladó et al., 2017). Soil carbon content also depends on soil respiration, a process where soil carbon (mainly labile form) is lost due to carbon decomposition by microbes (Bokhorst et al., 2007). Alpine scrub having low vegetation cover is exposed to warming leading to rapid soil carbon decomposition and emission (Zhao et al., 2019). These habitats also provide insufficient C supplies into the soil (Rawls et al., 2003). As a cumulative effect of high respiration and poor input, soils in these habitats are C deficient, as evident in our study (Table 3.1, Chapter 3). Low carbon in soils often reduces their ability to hold water (Fierer et al., 2007; Koch, 2001), which further reduces microbial enzyme activity of communities and facilitates the growth of only those species that can grow in carbon and moisture-limited soils (Adamczyk et al., 2019; Tiwari et al., 2021b). Despite low carbon input due to low photosynthesis, alpine meadows act as sinks as decomposition rates are limited by low temperature (Barboza et al., 2018; Lanzén et al., 2016; Lazzaro et al., 2015). Overall, we see three habitat types in our study area, (i) high moisture-nutrient-temperature (HMNT) habitat at lower elevations, (ii) low moisture-nutrient-high-temperature (LMNHT) habitat at mid-elevations, and (iii) high moisture-nutrient-low-temperature (HMNLT) habitat at higher elevations. These habitats showcase two kinds of stress, one by the temperature (HMNLT) and the other by moisture and nutrients (substrate availability) (LMNHT). Under temperature stress with adequate nutrients (HMNLT), the communities are co-operative, as seen by high positive interactions in the co-occurrence network at the high elevation range. Under nutrient stress with optimum temperature (LMNHT), communities compete for the limited substrate wherein certain

species dominate, eventually decreasing the community evenness. This was indicated by the dominance of *Proteobacteria* in the mid-elevation (Figure 3.4a, Chapter 3), having high negative interactions with the other bacterial taxa (Figure 3.7b, Chapter 3). When temperature, moisture, and nutrients are optimum (HMNT), the communities participate in both positive and negative interactions (Figure 3.7c, Chapter 3), leading to the dominance of specific taxa (*Proteobacteria* in this study, Figure 3.4a) along with high overall community evenness (Figure 3.5).

In contrast to previous studies (Mountain Research Initiative EDW Working Group, 2015)(Barboza et al., 2018; Lanz´en et al., 2016; Lazzaro et al., 2015), we found no seasonal or inter-annual variation in bacterial diversity and composition, indicating the resilient nature of bacterial communities to environmental changes over the selected time window (Figure 3.6, Table 3.2, 3.3 and 3.4). This finding also confirms the mid-elevation dip pattern across all years, thereby supporting the effect of edaphic factors over the temperature in community distribution.

Chapter 5

Soil bacterial community response to an experimental warming

5.1 Introduction

Ongoing climate change due to human activities involving fossil fuel combustion and land-use change have substantially increased greenhouse gas concentrations leading to global mean surface temperature (IPCC, 2013). The rate of increase in temperature has been more pronounced at higher altitudes, particularly alpine regions (Mountain Research Initiative EDW Working Group, 2015). These regions store a large quantity of soil organic carbon (SOC) due to low decomposition and low turnover rates under cold environment (Budge et al., 2011). Since SOC decomposition is a temperature dependant process (Zi et al., 2018a), the impact of climate warming on organic carbon decomposition will determine the strength of an alpine ecosystem to sustain as a C sink or a source (Zi et al., 2018a). The organic carbon decomposition is majorly carried out by soil bacterial communities through respiration. Although Climate-modelling has predicted a positive feedback of soil respiration under warming eventually reducing the soil C store (Heimann and Reichstein, 2008), in field experimental warming studies on alpine ecosystem soil respiration and C storage showed no consistent results. Such inconsistency stems from the uncertainties in the response of soil bacterial communities to increasing temperature and associated change in the micro-environment. Therefore, understanding the response of these communities to elevated temperature is essential for predicting effects of future temperature rise on soil C store (Schindlbacher et al., 2010).

Soil microorganisms depend on water, carbon, nitrogen and phosphorus to generate energy and synthesize cellular macromolecules. The rates of these bacterial processes are influenced by environmental factors such as temperature, soil moisture, nutrient contents, pH and salinity. Any changes in atmospheric temperature are likely to effect soil environment such as soil temperature and moisture (Zi et al., 2018a). This change in soil conditions can promote changes in soil bacterial communities (Steinweg et al., 2012) and

their activities (Sheik et al., 2011). For instance, a study by Deslippe et al. (2012) (Deslippe et al., 2012) showed that warming significantly reduced the evenness of bacterial communities in the Arctic. Further another study in an Oklahoma prairie soil reported that warming treatment significantly increased the bacterial population size by 40–150%, but decreased the alpha diversity eventually changing the composition of the community (Sheik et al., 2011a) Variations in the bacterial community composition may likely affect the degradation of different soil organic carbon pools through the production of different extracellular enzymes (Sinsabaugh, 2010). Despite of such critical role in the soil, the responses of bacterial community diversity, composition and function under warming have rarely been investigated in carbon rich soils at high elevation mountain ecosystems.

In the Himalaya, alpine region encompasses almost 33% of the geographical area and store a considerable amount of SOC (Tiwari et al., 2021b). Majority of these alpine regions are covered by herbaceous meadows dominated by graminoids i.e., grasses and sedges (Tiwari et al., 2021b). These meadows are of much ecological interest due to the presence of plant forms specially adapted to harsh climatic conditions, their ability to translocate synthesized carbon to underground parts and their sensitivity to changing climate (Körner, 1999; Rawat, 2007; Rawat and Adhikari, 2005). Soil bacterial community diversity and composition in these habitats are expected to change with rising temperature leading to change in their organic carbon decomposition rate setting positive feedback to climate warming. The Himalayan region have experienced an increase of 0.9 ºC average temperature during 1901–2003 (Shrestha et al., 2012b). However, studies focused on assessing the impacts of warming on soil bacterial community from alpine region of Himalaya are lacking. This is the first study where we investigate the effects of climate warming on soil bacterial community in the alpine region of Himalaya based on

warming experiment. The major objectives of our study were to assess the effect of experimental warming on bacterial community i) alpha diversity and composition, and ii) functional traits.

5.2 Study Area

We conducted this study in an alpine meadow of Gangotri National Park located in Western Himalaya, India (30º57′01.93″ N, 79º03′28.24″ E, 4000 m above sea level) (Figure 5.1a and 5.1b).

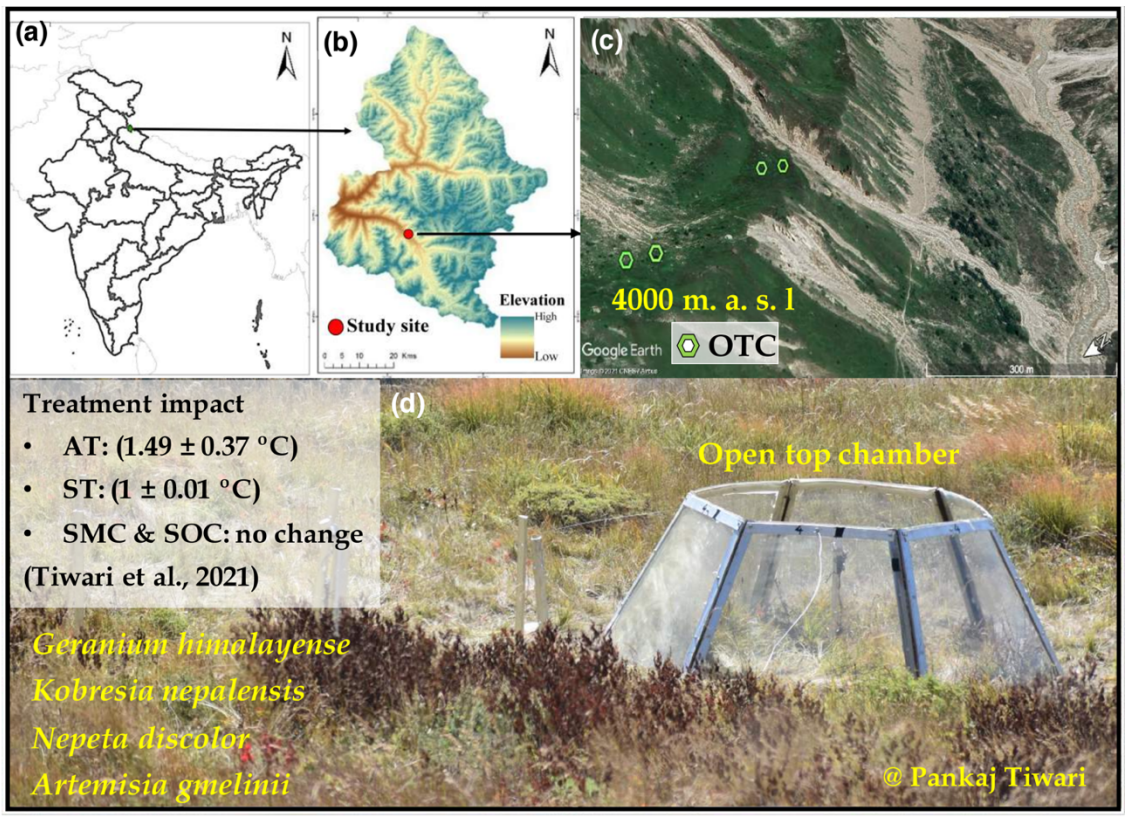

Figure 5.1 (a) State map of India, (b) Gangotri National Park in western Himalaya and (c) study site with open-top chambers at Herbaceous Meadow, and (d) an open top chamber with a control plot. Maps in figures a and b were generated with ArcGIS version 10.7 (ESRI, CA, USA, https://desktop.arcgis.com/en/arcma p/) and image in figure c was acquired using Google Earth Pro version 7.3.3.

The site was characterized by dense herbaceous vegetation and high soil organic carbon (SOC) and soil water content (SMC). Vegetation was dominated by dicotyledonous herbs such as *Geranium himalayense*, *Nepeta discolor*, *Artemisia gmelinii*, *Thalictrum alpinum*, *Cynoglossum wallichii* and *Galium rotundifolium* and few other plant types including *Polygonatum graminifolium*, *Persicaria polystachya*, *Euphorbia stracheyi* and *Astragalus candolleanus*. Mean annual precipitation was 1500 mm and mean annual temperature (MAT) measured by data loggers at the study sites from May 2017 to October 2018 was 2.92 ºC ± 0.36 ºC (Tiwari et al., 2021b).

5.3 Material and methods

5.3.1 Site selection and soil sampling

In our study site, we selected 4 homogeneous plots (2 m X 2 m) (approximately 10 m apart) with similar plant communities and soil properties in October 2016 and installed 1 open top chamber (OTC) for warming treatment at each plot (Figure 5.1c, 5.1d and 5.2). A control plot with similar vegetation adjacent to each OTC (approximately 1 m apart) was established by fencing to prevent grazing. For warming treatment, we used hexagonal OTCs that has been modified from the design developed by Molau and Alatalo (Molau and Alatalo, 1998). The chambers were built by polycarbonate sheets (3 mm) having top and bottom diameter and height as 110 cm, 170 cm and 70 cm, respectively. Since installation, the OTCs were left on plots all year around for bacterial community assessment.

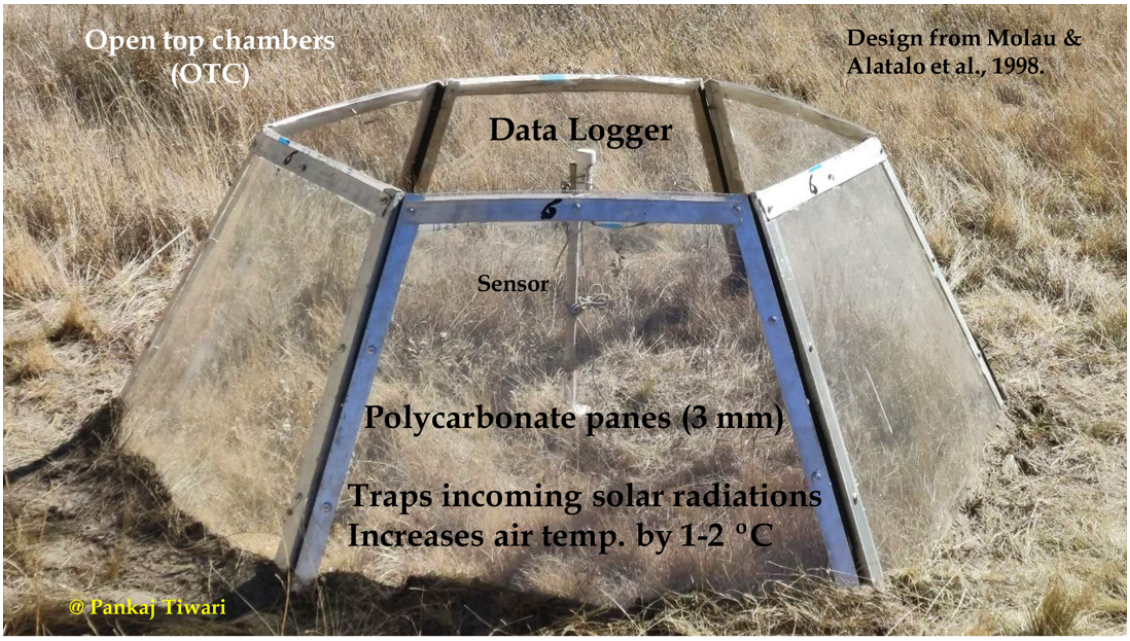

Figure 5.2 Open top chamber modified based on the design from Molau and Alatalo et al., 1998.

Figure 5.3 Soil sampling inside open top chambers.

In each warming and control plot, five 1 × 1 ft sub-plots were randomly selected for soil sampling. Sampling was performed during May and October in 2017 and May, July, September

and October in 2018. At each subplot, five soil cores (~1 g each) were collected at four corners and center from 5 cm depth using hand-held sterile soil corer (50 ml centrifuge tube of diameter 2.5 cm, Tarsons Products Pvt. Ltd, India). Before soil collection, aboveground vegetation and leaf litter were removed if present. Based on the design of Lanzen et al. (2016) (Lanzén et al., 2016), soil cores at each plot (n = 30) were pooled in a sterile zip-lock bag homogenized and stored in 100% ethanol (Merck, Germany) for molecular analyses. All samples, n = 48 (4 OTC + 4 control) x 1 composite sample per sampling time x 6 sampling time), were transported to the laboratory in a cool box.

5.3.2 DNA extraction, PCR amplification, and Illumina sequencing

Approximately 0.25 g of each soil sample was taken to extract environmental genomic DNA using a Nucleopore GDNA soil kit (Genetix Biotech Asia Pvt. Ltd, India) following the manufacturer's instructions. DNA concentrations were estimated using Qubit dsDNA HS Assay Kit (Life Technologies, USA). The bacterial V3 and V4 regions were amplified using the primer pair 338F (5′-CCTACGGGNGGCWGCAG-3′) and 806R (5′-GACTACHVGGGTATCTAATCC-3′) (Luo et al., 2019) with Illumina 16S Metagenomics Sequencing library preparation protocol. The PCR reaction was conducted with 12.5 µl of 2X Kappa Hifi Hotstart ReadyMix (Kappa Biosystems, Roche Sequencing and Life Science, USA), 1 µl each of 5 µM forward and reverse primer and 10.5 µl of the template (12.5 ng of microbial DNA). The conditions for PCR reaction included an initial denaturation of 95 °C for 3 min, followed by 25 cycles of 95 °C for 30 s, 55 °C for 30 s, and 72 °C for 30 s, followed by a final extension for 10 min at 72 °C.

A negative PCR (no template DNA) was included to monitor contamination. We purified and barcoded PCR products using Nextera XT kit (Illumina Inc., United States) and normalized amplicons to 2 nM for each library. An equal volume of each library was pooled, denatured, and diluted to 4 pM before loading onto the MiSeq flow cell (Illumina Inc., United States). Sequencing was performed at the Next Generation Genomics Facility at Center for Cellular, and Molecular Platforms (C-CAMP), Bangalore, India, using a 2×300 bp paired-end protocol on the Illumina MiSeq platform.

5.3.3 Sequence Data Processing

We used the MiSeq S.O.P. pipeline in Mothur v.1.40.5 to process Illumina-generated raw sequences (Schloss et al., 2009). We prepared full-length sequences from which good reads (> 460 bp length with no homopolymer stretches longer than 8bp) were identified and clustered (based on ≥ 97% similarity) using 16S rRNA database SILVA 132 SSU SEED. Subsequently, chimeric sequences were removed using Uchime, followed by all singletons, chloroplasts, archaea, mitochondria, and unknown origin sequences. We used high-quality sequences to estimate pair-wise distances and generate single-linkage clusters with ≥ 97% sequence similarity. The longest read from each cluster was used as the reference sequence for a taxonomic assignment against the SILVA SSU NR Ref database. Quantitative estimates of individual reads per taxonomic unit were generated from all sequences in each cluster and their replicates (≥ 97% similarity). The dataset was normalized by rarefying the sequences to the lowest sample-specific sequencing depth with maximum Good's coverage (Kozich et al., 2013). Finally, the sequences were clustered into different taxonomic levels for operational taxonomic unit (OTU) abundance and composition analysis. The data were further sorted to separate the abundant and rare taxa based on their relative abundances. OTUs with ≥1% relative

abundance was considered abundant and used for further analysis.

5.3.4 Functional analysis of the bacterial community

The genetic functional potential of the bacterial community was predicted using PICRUST (Phylogenetic Investigation of Communities by Reconstruction of Unobserved States) pipeline on the galaxy server (https://galaxyproject.org/use/langille-lab/) (Langille et al., 2013). Taxonomic classification of 16S sequences at ≥ 97% similarity was conducted against the Greengenes database. Each 16S sequence was processed to pre-computed closed-reference OTUs against the Greengenes database 13.5 to find the "nearest neighbor of the reference sequence". The OTU table was normalized according to the 16S rRNA gene copy number. The functional prediction was performed using the normalized OTU table against the Kyoto Encyclopedia of Genes and Genomes (KEGG) orthology database. The KEGG orthology (KO) assignments were performed at level 1 and 2 categories. The nearest sequence taxon index assessed the accuracy of the predicted metagenome. For our analysis, we classified the predicted functions into most abundant traits having relative abundance ≥1% at KO levels 1 and 2.

5.3.5 Data analysis

We calculated bacterial alpha diversity through three indices: OTU richness (Sobs), evenness, and Shannon diversity index for each sample using the Mothur platform. Before the analysis, we tested normality and heteroscedasticity of data by the Shapiro-Wilk and Levene tests, respectively. We used parametric t test or non-parametric Mann-Whitney U test when data was normal or not normal, respectively, to analyse the effects of warming on alpha diversity, bacterial taxa relative abundances and functional traits

between the sites. All analyses were conducted in SPSS software (version 23.0, IBM, Chicago, IL, USA) and significant differences were assessed at the level $p < 0.05$.

5.4 Results

5.4.1 Effect of warming on microclimate

Experimental warming resulted in significant and consistent increase in air temperature (AT) inside OTC at 30 cm height by 1.49 ºC ± 0.37 ºC across the seasons ($p < 0.001$) (Tiwari et al., 2021b) On the other hand soil temperature (ST) at 5 cm depth inside OTC showed low and inconsistent increase across the seasons with a mean of 1.0 ºC ± 0.36 ºC ($p = 0.03$), which was significant only during May, July and October ($p < 0.001$) of both years.

5.4.2 Effect of warming on α-diversity

Illumina sequencing across 48 samples resulted in a total of 654,842 high-quality sequences averaging 54,570 ± 8,940 sequence reads per sample. Good's coverage ranged from 83% to 99%, indicating that the sequencing was adequate and represented most of the bacterial communities at the study sites.

The alpha diversity indices indicated no significant change in bacterial community richness, evenness, and diversity due to warming across the seasons ($p>0.05$) (Figure 5.4). Bacterial richness in the control and warming plots was 6359 ± 302 and 6172 ± 219, respectively, evenness was 0.85 ± 0.12 and 0.85 ± 0.01, respectively, and diversity was 7.4 ± 0.15 and 7.4 ± 0.07, respectively.

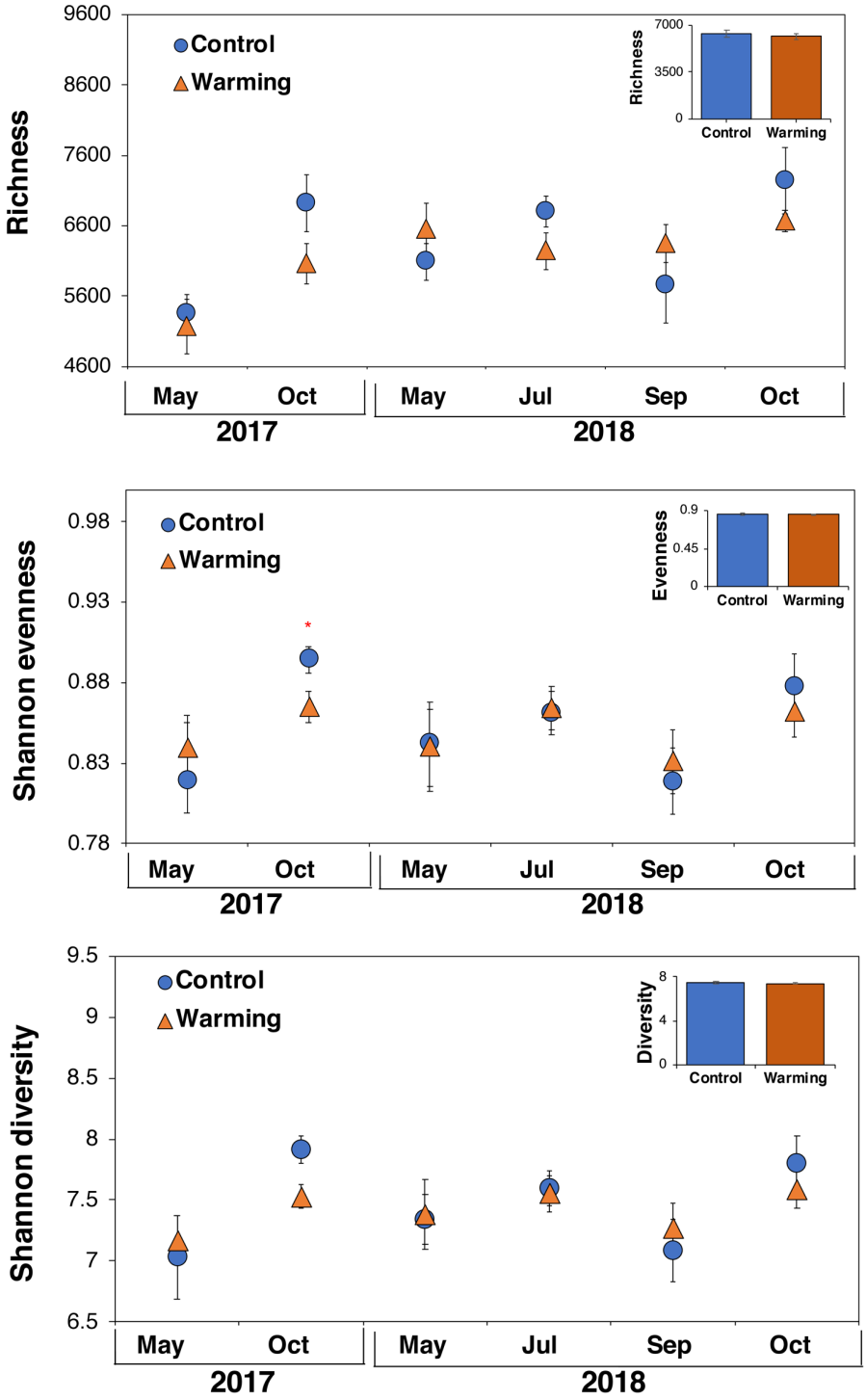

Figure 5.4 Variation in bacterial alpha diversity indices, i.e., richness, evenness and diversity under warming and control. Significant differences in alpha diversity indices was assessed by one way ANOVA followed by Tukey's honest significance difference (HSD) post-hoc test. Circles represent mean ± SE of mean of each season, n = 4. Bars represent mean ± SE of mean of all seasons, n = 24. Red star above the circle indicate a significant difference between the treatments ($p < 0.05$).

5.4.3 Effect of warming on bacterial taxa abundance

Considering a ≥ 97% sequence similarity, we identified 529,771 OTUs that were classified into 31 phyla (96.9% of the OTUs), 93 classes (96.9%), 168 orders (72.4%), 332 families (68.5%), 452 genera (57%) and 46754 species (8.8%) (Figure 5.5). Due to the low classification percentage at the species level, all further diversity analyses were conducted at phyla, class, and genera level only. Of the classified bacterial taxa we identified 12 abundant phyla, 23 abundant classes, and 30 abundant genus (Figure 5.5). Across the seasons experimental warming resulted in no significant change in the relative abundances of any bacterial taxa ($p>0.05$).

5.4.4 Effect of temperature on functional traits of the bacterial community

PICRUST predicted metagenome functions are shown in (Figure 5.6), representing the most abundant traits at levels 1 and 2 KO categories. The nearest taxon sequence index (NSTI) value of the samples ranged from 0.1 to 0.25. At level 1 KO category, we identified four abundant functional pathways of the meta-genome, i.e., metabolism, environmental information processing, genetic information processing, and cellular processes. At level 2 KO category, we identified 6 functional pathways of metabolism i.e., carbohydrate, amino acids, lipid, nucleotide, enzyme and energy, 3 pathways of genetic information processing i.e., replication, transcription and translation, and 2 pathways of environmental information processing i.e., membrane transport and signal transduction. None of these functions showed any change due to warming across the seasons ($p>0.05$).

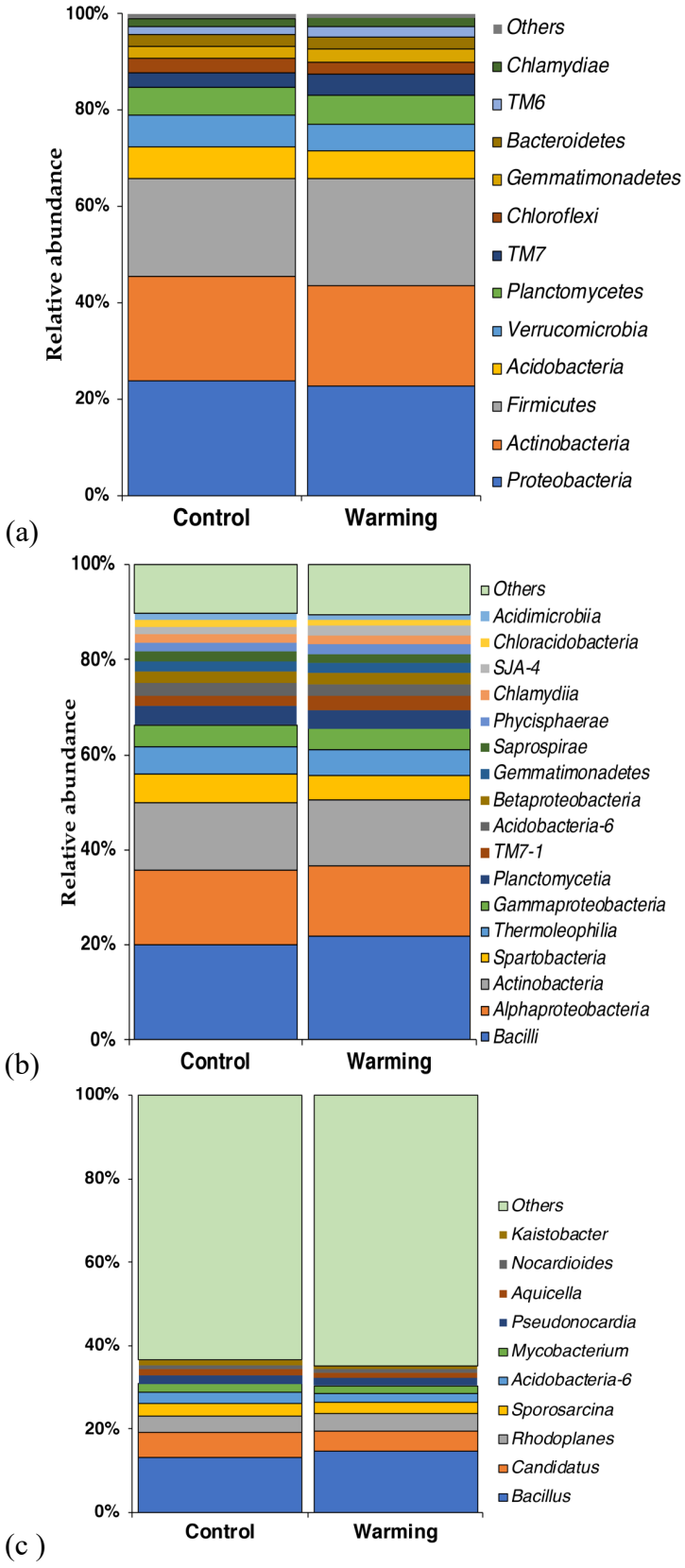

Figure 5.5 Variation in bacterial beta diversity under warming and control. Relative abundances of bacterial (a) phyla, (b) class, and (c) genera under the treatments. Here "Others" represent all taxa with relative abundances < 1%.

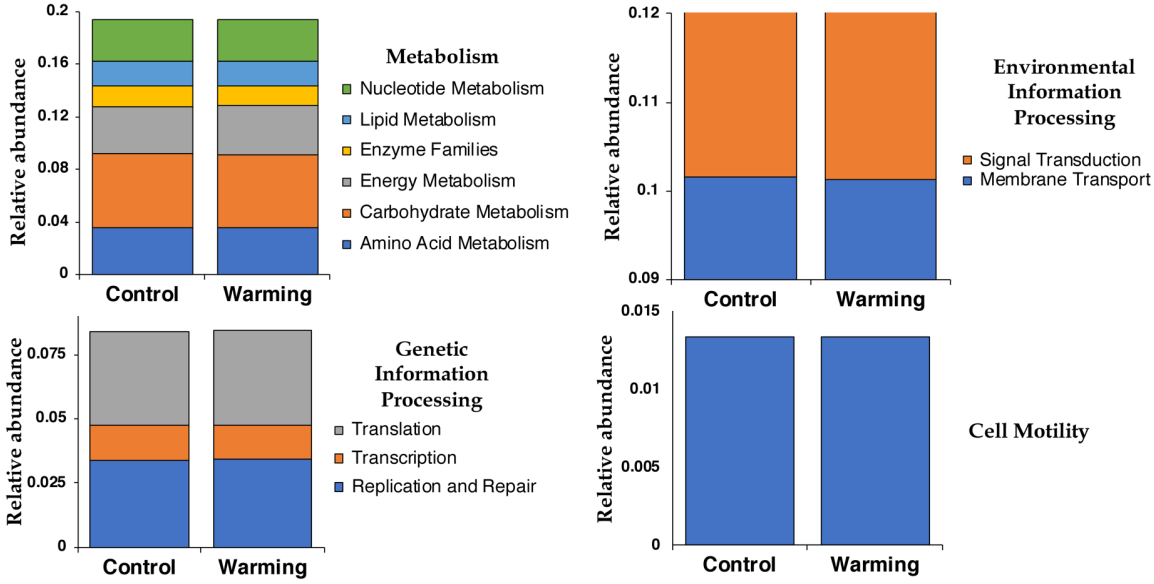

Figure 5.6 Relative abundance of most abundant predicted metagenome functions at level 1 KO category under warming and control. Each bar represents the relative abundances of all pathways associated with the abundant functions at the level 2 KO category.

5.5 Discussion

Our study provides evidence that 2 years of experimental warming resulted in no significant change in alpine soil bacterial community alpha diversity, composition and their abundant functions at 5 cm soil depth. Some recent studies have reported similar observations from alpine meadow in north western Sichuan, China (Zi et al., 2018) and Sub-Artic peatland in Sweden (Weedon et al., 2017). Notably in our study, the temperature increase inside the OTC was achieved successfully (~ 1.5 ºC), however soil moisture remained constant. Since bacterial physiological processes are dependent on both soil temperature and moisture, therefore increase in temperature solely did not affect the community diversity, composition and function (Zi et al., 2018). Similarly an earlier study on the effects of experimental warming on soil respiration from an alpine meadow in western Himalaya, also reported no change in the rate of soil respiration due to non-

significant change in soil moisture although temperature increased significantly (Tiwari et al., 2021b). Contrarily, other studies on experimental warming that resulted in change in both soil temperature, moisture and plant coverage exhibited increase in microbial biomass and their composition (Walker et al., 2006; Wang et al., 2017; Zi et al., 2018a). All these results indicate that it is only when moisture and in turn nutrient availability is altered under increasing temperature, soil microbial communities are affected.

Review of earlier experimental studies suggest three ways in which microbial communities can respond to any change or disturbance (Allison and Martiny, 2008). Firstly, microbial communities are resistant to increase in temperature only. Secondly, microbial communities particularly bacterial community composition although is sensitive to any environmental change, they are resilient and immediately return to their pre-disturbed state. Thirdly, even if composition of the community changes, the new community might have same functional as that of the original. Results obtained in our study indicates that the community might be either resistant or resilient to temperature increase. Since in our study there was no change in the community composition, we found no change in the relative abundance of abundant functions. Overall, our results implies that due to resistant and resilient nature of soil bacterial community in high altitude alpine habitats in western Himalaya, they might not experience any loss in diversity, composition and function under short-term temperature rise scenarios as long as soil moisture, plant coverage and nutrient availability remains unaltered.

Chapter 6

Key findings and implications

Increasing global average surface temperature since the past decade has led to rapid changes in terrestrial ecosystems (Cramer et al., 2001). Alpine ecosystems are particularly susceptible to more temperature rise than global average (Mountain Research Initiative EDW Working Group, 2015), and are experiencing rapid melting of ice and retreat of glacier (Venkatachalam et al., 2021; Wu et al., 2012). Soil bacterial communities in alpine ecosystems play a critical role in soil formation, plant colonization, nutrient cycling, regulation of soil carbon storage through decomposition, and mediate feedbacks between climate change and ecosystem functioning by heterotrophic respiration (Donhauser and Frey, 2018; Trivedi et al., 2013). Although a few studies have focused on macro-level deglaciation impacts, little is known about such effects on the bacterial community succession which formed the rational for this thesis 1st Chapter. This study provides the first report on soil bacterial community ecological traits associated with their succession and nutrient cycling in a newly exposed soil till a developed stage after ~300 years of post-deglaciation of Gangotri glacier, western Himalaya. Three sites were selected along a terminal moraine representing recent (~20 yrs), intermediate (~100 yrs), and late (~300 yrs) deglaciation periods. Results showed that the genus *Mycobacterium* belonging to phylum *Actinobacteria* dominated recently deglaciated land. Relative abundance of these pioneer bacterial taxa decreased by 20-50% in the later stages with the emergence of new and rising of the less abundant members of the phyla *Proteobacteria*, *Firmicutes*, *Planctomycetes*, *Acidobacteria*, *Verrucomicrobia*, Candidatus TM6, and *Chloroflexi.* The community in the recent stage was less rich and harboured competitive interactions, while the later stages experienced

a surge in bacterial diversity with cooperative interactions. The shift in α-diversity and composition was strongly influenced by soil organic carbon, carbon to nitrogen ratio, and soil moisture content. The functional analyses revealed a progression from a metabolism-focused to a functionally progressive community required for bacterial co-existence and succession in plant communities. Overall the results reveal the evolution of a simple pioneer community (dominated by *Mycobacterium* genus), mainly focused on metabolic activities, into a more diverse and functionally specialized community at the later stages. The study also demonstrates the progression in biogeochemical pathways necessary for soil fertility and plant growth post-deglaciation. This study was a single time point sampling which may not reflect the community trait variations during different seasons and years. However, as evidenced in other studies, due to the non-significant seasonal and interannual variation in the bacterial community (Bhattacharya et al., 2022; Zhu et al., 2020), results generated in this study indicate that the bacterial communities inhabit, diversify and develop specialized functions post-deglaciation leading to nutrient inputs to soil and vegetation development, which may provide feedback to climate change.

We also assessed bacterial community distribution patterns along elevation gradients as it is invaluable in understanding the underlying mechanism involved in their diversity formation, sustenance, and response to environmental changes (Donhauser and Frey, 2018; Margesin and Niklinska, 2019). However, earlier studies show contrasting patterns with different regulating factors due to habitat specificity and associated environmental conditions (Donhauser and Frey, 2018). The lack of consensus formed the basis for understanding the effects of environmental changes on soil bacterial communities and their driving factors across elevation-vegetation gradient (3373–4020 m) along the deglaciated valley of Gangotri glacier, western Himalaya in this thesis 2nd and 3rd chapter. Results demonstrates a mid-elevation dip in soil bacterial community diversity along an

elevation-vegetation gradient across three years governed primarily by edaphic properties (SOC, TN, SMC and pH) rather than temperature (Bhattacharya et al., 2022). This dip in diversity is a consequence of the shift in the bacterial socio-interactive array from co-operative to competitive under moisture and nutrient limitations. Further, the communities' seasonal and inter-annual stability confirms the mid-elevation pattern and provides evidence for their resilience towards climate shifts. By considering both spatial and temporal variability, our results enhance the reliability of the observed distribution pattern and the regulating factors. This is the first study from the temperature-sensitive high-altitude region of Himalaya that will help to understand the factors underlying bacterial diversity distribution and enhance the predictability of environmental change impacts on these communities across broader spatio-temporal scales (Bhattacharya et al., 2022).

We further established experimental warming plots in an alpine meadow of the study area to confirm the responses of bacterial community to rising temperature in the thesis last chapter. Response of these communities to warming have rarely been investigated in carbon rich soils at high elevation mountain ecosystems (Zhang et al., 2014). Results from this chapter showed that short-term increase in temperature with no change in soil moisture and nutrient content had any significant effect on bacterial alpha diversity, composition and function. The no effect of short term warming on these community functions was also reported in our earlier study where no change was observed in soil respiration under warming conditions throughout growing period of a year (Tiwari et al., 2021a). The warming experiment confirmed the neutral response of bacterial community to temperature and further established that these communities are resilient to climate warming however, a shift in edaphic properties may alter community diversity and its functional potential.

Appendix

Table A1 List of studies on effects of climate change on soil bacterial communities across mountain ecosystems of the world.

No.	Study Location	Altitude (m)	Longitude	Latitude	Reference
1	Himalaya	3700–5970	77.58 E	34.75 N	Rehakova et al., 2011; https://doi.org/10.1007/s00248-011-9878-8
2	Swiss Alps	2100	10.24 E	46.63 N	Bernasconi et al., 2011; https://doi.org/10.2136/vzj2010.0129
3	Swiss Alps	2101	8.45 E	46.60 N	Brankatschk et al., 2010; https://doi.org/10.1038/ismej.2010.184
4	Italian Alps	545-2000	11.45 E	46.58 N	Siles et al., 2017; http://dx.doi.org/10.1016/j.soilbio.2017.04.014
5	Italian Alps	545-2001	11.43 E	46.58 N	Siles and Margesin 2016; doi:10.1007/s00248-016-0748-
6	Spain	1500-2600	1 E	42.66 N	Lanzen et al., 2016; https://doi.org/10.1038/srep28257
7	Tibetan plateau	3000–3600	102.35 E	31.51 N	Tan et al., 2012; https://doi.org/10.5897/AJMR11.1537
8	Tibetan plateau	5300–5900	92.56 E	31.51 N	Janatkova et al., 2013; https://doi.org/10.1111/1462-2920.12132
9	Tibetan plateau	3400–4813	102.58 E	31.58 N	Zhang et al., 2013; https://doi.org/10.1186/1471-2180-13-72
10	Tibetan plateau	3200–3800	102.55 E	32.8 N	Yang et al., 2013; https://doi.org/10.1038/ismej.2013.146
11	Tibetan plateau	4400–5210	100.43 E	34.28 N	Yuan et al., 2014; https://doi.org/10.1111/1574-6941.12197
12	Tibetan plateau	3650	92.01 E	31.43 N	Xie et a., 2014; https://doi.org/10.1016/j.soilbio.2014.06.024
13	Tibetan plateau	3105–4556	90.21 E	28.90 N	Xu et al., 2014; https://doi.org/10.1016/j.ejsobi.2014.06.002
14	Mount Wutai	2080-3000	112.8 E	38.45 N	Luo et al, 2019; doi: 10.3389/fmicb.2019.00169
15	Chanbai mountain	2000-2500	126.91 E	41.38 N	Shen et al., 2013; https://doi.org/10.1016/j.soilbio.2012.07.013
16	Mount Gongga	2000-3000	101.48 E	29.01 N	Shen et al., 2015; doi:10.3389/fmicb.2015.00582
17	Mount Fuji	880-1830	138.86 E	35.93 N	Singh et al, 2012; https://doi.org/10.1007/s00248-011-9900-1
18	Mt. Halla	100-1950	126.53 E	33.36 N	Singh et al, 2014; http://dx.doi.org/10.1016/j.soilbio.2013.09.027
19	New Zealand	500 -1900	168.95 E	44.85 S	Wu et al., 2017; doi: 10.1093/femsec/fiw253
20	Rocky mountain	2460–3380	105.58 W	40.05 N	Bryant et al., 2008; https://doi.org/10.1073/pnas.0801920105
21	Canada	2214	111.63 W	64.83 N	Kazemi et al., 2016; https://doi.org/10.1111/mec.13835
22	Peruvian Andes	5000	71.04 W	13.46 S	Schmidst et al., 2008; https://doi.org/10.1098/rspb.2008.0808
23	Austrian Alps	2300–2530	12.69 E	47.07 N	Margesin et al., 2009; https://doi.org/10.1111/j.1574-6941.2008.00620.x
24	French Alps	2227–2818	06.63 E	45.0 N	Zinger et al., 2020; https://doi.org/10.1128/AEM.00748-09
25	Tianshan Mountains	3523	86.83 E	43.10 N	Wang et al., 2010; https://doi.org/10.1007/s00253-010-2564-9
26	Tianshan Mountains	3523	119.18 W	53.18 N	Wang et al., 2010; https://doi.org/10.1007/s00253-010-2564-10
27	Robson Glacier	3954	119.67 W	41.84 N	Hahn and Quideau 2013; https://doi.org/10.4141/cjss2012-133
28	Crooked Creek	3954	120.33 W	42.68 N	Hahn and Quideau 2013; https://doi.org/10.4141/cjss2012-134
29	Barcroft	3954	138.92 W	60.95 N	Hahn and Quideau 2013; https://doi.org/10.4141/cjss2012-135
30	Tibetan plateau	4628	102.83 E	31.23 N	Zhang et al., 2014; https://doi.org/10.1007/s12665-013-3001-z
31	Tibetan plateau	3200–3800	102.38 E	36.26 N	Yang et al., 2013; https://doi.org/10.1038/ismej.2013.146
32	French Alps	2227–2818	10.69 E	46.77 N	Zinger et al., 2011; https://doi.org/10.1371/journal.pone.0019950
33	Tibetan plateau	4400–5100	101.2 E	37.61 N	Guo et al., 2015; https://doi.org/10.1007/s00253-015-6723-x
34	Tibetan plateau	4149–5033	91.05 E	30.5 N	Liu et al., 2015; https://doi.org/10.1093/femsec/fiv078

Table A2. Number of sequences and Good's coverage at all sampling sites.

Sample no	Altitude (m)	Date of sampling	Sample ID	Total number of paired end reads	Total number of quality reads	Good's coverage (%)
1	3373	October_2016	Alt1_Oct2016	244920.87	61246	88.30
2	3373	October_2017	Alt1_Oct2017	225528.30	48170	88.37
3	3373	October_2018	Alt1_Oct2018	215173.63	55198	87.75
4	3373	May_2017	Alt1_May2017	187102.30	33101	89.24
5	3373	May_2018	Alt1_May2018	203472.26	44950	85.61
6	3483	October_2016	Alt2_Oct2016	181176.80	32997	90.14
7	3483	October_2017	Alt2_Oct2017	126680.11	34495	94.23
8	3483	October_2018	Alt2_Oct2018	239593.90	56914	88.93
9	3483	May_2017	Alt2_May2017	220650.24	43272	90.63
10	3483	May_2018	Alt2_May2018	131438.47	34333	96.97
11	3552	October_2016	Alt3_Oct2016	207662.01	50412	91.27
12	3552	October_2017	Alt3_Oct2017	359241.21	88603	83.92
13	3552	October_2018	Alt3_Oct2018	230585.93	54106	86.81
14	3552	May_2017	Alt3_May2017	197217.56	52893	91.69
15	3552	May_2018	Alt3_May2018	190304.47	37164	90.04
16	3564	October_2016	Alt4_Oct2016	186084.79	55086	94.13
17	3564	October_2017	Alt4_Oct2017	181924.97	54668	96.18
18	3564	October_2018	Alt4_Oct2018	105043.04	29768	96.56
19	3564	May_2017	Alt4_May2017	152866.05	45551	96.17
20	3564	May_2018	Alt4_May2018	174892.17	40420	89.20
21	3645	October_2016	Alt5_Oct2016	157684.27	50513	98.65
22	3645	October_2017	Alt5_Oct2017	159120.75	48436	97.28
23	3645	October_2018	Alt5_Oct2018	113153.20	31023	99.09
24	3645	May_2017	Alt5_May2017	127308.57	23821	99.91
25	3645	May_2018	Alt5_May2018	36450.83	10063	Eliminated
26	3730	October_2016	Alt6_Oct2016	134401.22	33397	99.32
27	3730	October_2017	Alt6_Oct2017	108634.25	33312	98.94
28	3730	October_2018	Alt6_Oct2018	104594.14	28278	99.60
29	3730	May_2017	Alt6_May2017	186443.91	53315	97.56
30	3730	May_2018	Alt6_May2018	149424.47	15149	Eliminated
31	3763	October_2016	Alt7_Oct2016	146491.65	42221	98.80
32	3763	October_2017	Alt7_Oct2017	127907.11	40970	98.63
33	3763	October_2018	Alt7_Oct2018	102050.36	28864	99.56
34	3763	May_2017	Alt7_May2017	146641.28	34144	99.11
35	3763	May_2018	Alt7_May2018	43872.68	10710	Eliminated
36	3770	October_2016	Alt8_Oct2016	185905.23	60098	96.68
37	3770	October_2017	Alt8_Oct2017	122550.21	39640	98.27
38	3770	October_2018	Alt8_Oct2018	114948.81	33200	96.13
39	3770	May_2017	Alt8_May2017	142750.80	35417	99.37
40	3770	May_2018	Alt8_May2018	56771.12	12440	Eliminated
41	3980	October_2016	Alt9_Oct2016	311183.64	46996	85.73
42	3980	October_2017	Alt9_Oct2017	248722.29	37630	87.18
43	3980	October_2018	Alt9_Oct2018	378050.44	56482	84.47
44	3980	May_2017	Alt9_May2017	220644.92	49711	91.24
45	3980	May_2018	Alt9_May2018	305827.34	31009	90.67
46	3990	October_2016	Alt10_Oct2016	301118.98	56895	88.22
47	3990	October_2017	Alt10_Oct2017	316280.76	63627	85.91
48	3990	October_2018	Alt10_Oct2018	365959.87	47314	90.15
49	3990	May_2017	Alt10_May2017	273905.53	37462	91.00
50	3990	May_2018	Alt10_May2018	186832.96	42392	88.67
51	4000	October_2016	Alt11_Oct2016	285827.61	54449	83.70
52	4000	October_2017	Alt11_Oct2017	254553.75	49249	82.55
53	4000	October_2018	Alt11_Oct2018	377540.88	37549	86.89
54	4000	May_2017	Alt11_May2017	294121.24	49034	86.86
55	4000	May_2018	Alt11_May2018	227742.89	27451	92.68
56	4020	October_2016	Alt12_Oct2016	235374.74	57290	88.31
57	4020	October_2017	Alt12_Oct2017	286475.55	63125	81.71
58	4020	October_2018	Alt12_Oct2018	343168.44	45733	87.34
59	4020	May_2017	Alt12_May2017	147000.40	39902	91.82
60	4020	May_2018	Alt12_May2018	187042.45	31021	90.09

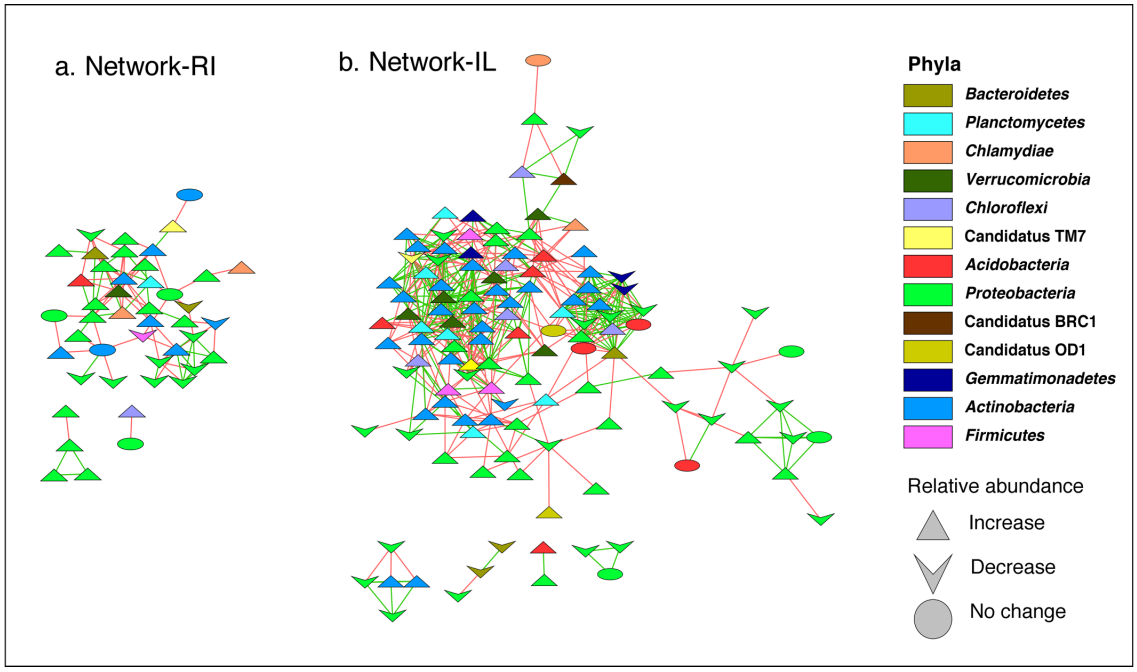

Figure A1 Organic layout of bacterial co-occurrence networks of (a) recent and intermediate communities (Network-RI) and (b) intermediate and late communities (Network-IL) based on Random Matrix Theory. Each node represents a genera, and each straight line (link) represent a significant ($p < 0.05$) correlation. Nodes of the same color represent the same phyla the genera belong to. Nodes with triangle shapes represent genera with increasing abundance, inverted triangle shapes represent decreasing abundance, and oval shapes represent genera with no change in their relative abundance. Green and red lines indicate positive and negative correlations between nodes, respectively. The figure was generated in Cytoscape 3.2.8.

References

Adamczyk, M., Hagedorn, F., Wipf, S., Donhauser, J., Vittoz, P., Rixen, C., Frossard, A., Theurillat, J.-P., Frey, B., 2019. The Soil Microbiome of GLORIA Mountain Summits in the Swiss Alps. Frontiers in Microbiology 10. https://doi.org/10.3389/fmicb.2019.01080

Ahmad, T., Gupta, G., Sharma, A., Kaur, B., El-Sheikh, M.A., Alyemeni, M.N., 2021. Metagenomic analysis exploring taxonomic and functional diversity of bacterial communities of a Himalayan urban fresh water lake. PloS one 16, e0248116.

Alfaro, F.D., Salazar-Burrows, A., Bañales-Seguel, C., García, J.-L., Manzano, M., Marquet, P.A., Ruz, K., Gaxiola, A., 2020. Soil microbial abundance and activity across forefield glacier chronosequence in the Northern Patagonian Ice Field, Chile. Arctic, Antarctic, and Alpine Research 52, 553–562. https://doi.org/10.1080/15230430.2020.1820124

Allison, S.D., Martiny, J.B., 2008. Resistance, resilience, and redundancy in microbial communities. Proceedings of the National Academy of Sciences 105, 11512–11519.

Barboza, A.D.M., Pylro, V.S., Jacques, R.J.S., Gubiani, P.I., de Quadros, F.L.F., Trindade, J.K. da, Triplett, E.W., Roesch, L., 2018. Seasonal dynamics alter taxonomical and functional microbial profiles in Pampa biome soils under natural grasslands. PeerJ 6, e4991. https://doi.org/10.7717/peerj.4991

Bardgett, R.D., Freeman, C., Ostle, N.J., 2008. Microbial contributions to climate change through carbon cycle feedbacks. The ISME journal 2, 805–814.

Bharti, A.; Kumar, V.; Gusain, O.; Bisht, G.S. (2010). Antifungal activity of actinomycetes isolated from Garhwal region. Journal of Sci. Engg. and Tech. Mgt. 2: 2.

Bhattacharya, P., Tiwari, P., Rai, I.D., Talukdar, G., Rawat, G.S., 2022. Edaphic factors override temperature in shaping soil bacterial diversity across an elevation-vegetation gradient in Himalaya. Applied Soil Ecology 170, 104306. https://doi.org/10.1016/j.apsoil.2021.104306

Bhattacharyya, T., Pal, D.K., Chandran, P., Ray, S.K., Mandal, C., Telpande, B., 2008. Soil carbon storage capacity as a tool to prioritize areas for carbon sequestration. Current science 482–494.

Blakemore, L.C., Searle, P.L., Daly, B.K., 1987. Methods for chemical analysis of soils. Lower Hutt, N.Z. : NZ Soil Bureau, Dept. of Scientific and Industrial Research.

Bokhorst, S., Huiskes, A., Convey, P., Aerts, R., 2007. Climate change effects on organic matter decomposition rates in ecosystems from the Maritime Antarctic and Falkland Islands. Global Change Biology 13, 2642–2653. https://doi.org/10.1111/j.1365-2486.2007.01468.x

Botta, C., Cocolin, L., 2012. Microbial dynamics and biodiversity in table olive fermentation: culture-dependent and -independent approaches. Front. Microbio. 3. https://doi.org/10.3389/fmicb.2012.00245

Bradford, M.A., Watts, B.W., Davies, C.A., 2010. Thermal adaptation of heterotrophic soil respiration in laboratory microcosms. Global Change Biology 16, 1576–1588. https://doi.org/10.1111/j.1365-2486.2009.02040.x

Bradley, J.A., Anesio, A.M., Arndt, S., 2017. Microbial and Biogeochemical Dynamics in Glacier Forefields Are Sensitive to Century-Scale Climate and Anthropogenic Change. Front. Earth Sci. 5. https://doi.org/10.3389/feart.2017.00026

Brady, N.C., Weil, R.R., 2002. The Nature and Properties of Soils, 13th edition, Prentice Hall. ed.

Brankatschk, R., Töwe, S., Kleineidam, K., Schloter, M., Zeyer, J., 2011. Abundances and potential activities of nitrogen cycling microbial communities along a chronosequence of a glacier forefield. The ISME Journal 5, 1025–1037. https://doi.org/10.1038/ismej.2010.184

Bremner, J.M., 2018. Nitrogen-Total, in: Sparks, D.L., Page, A.L., Helmke, P.A., Loeppert, R.H., Soltanpour, P.N., Tabatabai, M.A., Johnston, C.T., Sumner, M.E. (Eds.), SSSA Book Series. Soil Science Society of America, American Society of Agronomy, Madison, WI, USA, pp. 1085–1121. https://doi.org/10.2136/sssabookser5.3.c37

Brockett, B.F.T., Prescott, C.E., Grayston, S.J., 2012. Soil moisture is the major factor influencing microbial community structure and enzyme activities across seven biogeoclimatic zones in western Canada. Soil Biology and Biochemistry 44, 9–20. https://doi.org/10.1016/j.soilbio.2011.09.003

Bryant, J.A., Lamanna, C., Morlon, H., Kerkhoff, A.J., Enquist, B.J., Green, J.L., 2008. Microbes on mountainsides: contrasting elevational patterns of bacterial and plant diversity. Proceedings of the National Academy of Sciences 105, 11505–11511.

Budge, K., Leifeld, J., Hiltbrunner, E., Fuhrer, J., 2011. Alpine grassland soils contain large proportion of labile carbon but indicate long turnover times. Biogeosciences 8, 1911–1923. https://doi.org/10.5194/bg-8-1911-2011

Chatterjee, D., Saha, S., 2018. Response of Soil Properties and Soil Microbial Communities to the Projected Climate Change, in: Bal, S.K., Mukherjee, J., Choudhury, B.U., Dhawan, A.K. (Eds.), Advances in Crop Environment Interaction. Springer Singapore, Singapore, pp. 87–136. https://doi.org/10.1007/978-981-13-1861-0_4

Chen, H., Tian, H.-Q., 2005. Does a General Temperature-Dependent Q10 Model of Soil Respiration Exist at Biome and Global Scale? Journal of Integrative Plant Biology 47, 1288–1302. https://doi.org/10.1111/j.1744-7909.2005.00211.x

Ciccazzo, S., Esposito, A., Borruso, L., Brusetti, L., 2016. Microbial communities and primary succession in high altitude mountain environments. Annals of Microbiology 66, 43–60. https://doi.org/10.1007/s13213-015-1130-1

Cleveland, C.C., Nemergut, D.R., Schmidt, S.K., Townsend, A.R., 2007. Increases in soil respiration following labile carbon additions linked to rapid shifts in soil microbial community composition. Biogeochemistry 82, 229–240. https://doi.org/10.1007/s10533-006-9065-z

Cramer, W., Bondeau, A., Woodward, F.I., Prentice, I.C., Betts, R.A., Brovkin, V., Cox, P.M., Fisher, V., Foley, J.A., Friend, A.D., Kucharik, C., Lomas, M.R., Ramankutty, N., Sitch, S., Smith, B., White, A., Young-Molling, C., 2001. Global response of terrestrial ecosystem structure and function to CO_2 and climate change: results from six dynamic global vegetation models: ECOSYSTEM DYNAMICS, CO_2 and CLIMATE CHANGE. Global Change Biology 7, 357–373. https://doi.org/10.1046/j.1365-2486.2001.00383.x

Crowther, T.W., van den Hoogen, J., Wan, J., Mayes, M.A., Keiser, A.D., Mo, L., Averill, C., Maynard, D.S., 2019. The global soil community and its influence on biogeochemistry. Science 365, eaav0550. https://doi.org/10.1126/science.aav0550

Dash, S.K., Jenamani, R.K., Kalsi, S.R., Panda, S.K., 2007. Some evidence of climate change in twentieth-century India. Climatic Change 85, 299–321. https://doi.org/10.1007/s10584-007-9305-9

Deng, Y., Jiang, Y.-H., Yang, Y., He, Z., Luo, F., Zhou, J., 2012. Molecular ecological network analyses. BMC Bioinformatics 13, 113. https://doi.org/10.1186/1471-2105-13-113

Deslippe, J.R., Hartmann, M., Simard, S.W., Mohn, W.W., 2012. Long-term warming alters the composition of Arctic soil microbial communities. FEMS Microbiol Ecol 82, 303–315. https://doi.org/10.1111/j.1574-6941.2012.01350.x

Djukic, I., Zehetner, F., Mentler, A., Gerzabek, M.H., 2010. Microbial community composition and activity in different Alpine vegetation zones. Soil Biology and Biochemistry 42, 155–161. https://doi.org/10.1016/j.soilbio.2009.10.006

Donhauser, J., Frey, B., 2018. Alpine soil microbial ecology in a changing world. FEMS Microbiology Ecology 94. https://doi.org/10.1093/femsec/fiy099

Drake, H.L., Gößner, A.S., Daniel, S.L., 2008. Old Acetogens, New Light. Annals of the New York Academy of Sciences 1125, 100–128. https://doi.org/10.1196/annals.1419.016

Dube, J.P., Valverde, A., Steyn, J.M., Cowan, D.A., van der Waals, J.E., 2019. Differences in Bacterial Diversity, Composition and Function due to Long-Term Agriculture in Soils in the Eastern Free State of South Africa. Diversity 11, 61. https://doi.org/10.3390/d11040061

Duraipandian, V.; Sasi, A.H.; Islam, V.H.; Valanarasu, M.; Ignacimuthu, S. (2010). Antimicrobial properties of actinomycetes from the soil of Himalaya. Journal de Mycologie Medicale/Journal of Medical Mycology. 20(1): 15-20.

Dutta, H., Dutta, A., 2016. The microbial aspect of climate change. Energy, Ecology and Environment 1, 209–232. https://doi.org/10.1007/s40974-016-0034-7

Edgar, R.C., Haas, B.J., Clemente, J.C., Quince, C., Knight, R., 2011. UCHIME improves sensitivity and speed of chimera detection. Bioinformatics 27, 2194–2200. https://doi.org/10.1093/bioinformatics/btr381

Edwards, A., Pachebat, J.A., Swain, M., Hegarty, M., Hodson, A.J., Irvine-Fynn, T.D.L., Rassner, S.M.E., Sattler, B., 2013. A metagenomic snapshot of taxonomic and functional diversity in an alpine glacier cryoconite ecosystem. Environmental Research Letters 8, 035003. https://doi.org/10.1088/1748-9326/8/3/035003

Feng, W., Zhang, Y., Yan, R., Lai, Z., Qin, S., Sun, Y., She, W., Liu, Z., 2020. Dominant soil bacteria and their ecological attributes across the deserts in northern China. European Journal of Soil Science 71, 524–535. https://doi.org/10.1111/ejss.12866

Fierer, N., Bradford, M.A., Jackson, R.B., 2007. Toward an ecological classification of soil bacteria. Ecology 88, 1354–1364. https://doi.org/10.1890/05-1839

Fierer, N., McCain, C.M., Meir, P., Zimmermann, M., Rapp, J.M., Silman, M.R., Knight, R., 2011. Microbes do not follow the elevational diversity patterns of plants and animals. Ecology 92, 797–804.

Florentino, A.P., Weijma, J., Stams, A.J.M., Sánchez-Andrea, I., 2016. Ecophysiology and Application of Acidophilic Sulfur-Reducing Microorganisms, in: Rampelotto, P.H. (Ed.), Biotechnology of Extremophiles: Springer International Publishing, Cham, pp. 141–175. https://doi.org/10.1007/978-3-319-13521-2_5

Frkova, Z., Pistocchi, C., Vystavna, Y., Capkova, K., Dolezal, J., Tamburini, F., 2021. Phosphorus dynamics during early soil development in extreme environment (preprint). Soils and biogeochemical cycling. https://doi.org/10.5194/soil-2021-65

GCTE-NEWS, Rustad, L., Campbell, J., Marion, G., Norby, R., Mitchell, M., Hartley, A., Cornelissen, J., Gurevitch, J., 2001. A meta-analysis of the response of soil respiration, net nitrogen mineralization, and aboveground plant growth to experimental ecosystem warming. Oecologia 126, 543–562. https://doi.org/10.1007/s004420000544

Gilbert, J.A., Dupont, C.L., 2011. Microbial Metagenomics: Beyond the Genome. Annual Review of Marine Science 3, 347–371. https://doi.org/10.1146/annurev-marine-120709-142811

Gleason, H.A., 1920. Some Applications of the Quadrat Method. Bulletin of the Torrey Botanical Club 47, 21. https://doi.org/10.2307/2480223

Gupta, P., Sangwan, N., Lal, R., Vakhlu, J., 2015. Bacterial diversity of Drass, cold desert in Western Himalaya, and its comparison with Antarctic and Arctic. Archives of Microbiology 197, 851–860. https://doi.org/10.1007/s00203-015-1121-4

Harry, M., Gambier, B., Garnier-Sillam, E., 2000. Soil conservation for DNA preservation for bacterial molecular studies. European Journal of Soil Biology 36, 51–55. https://doi.org/10.1016/S1164-5563(00)00044-3

Hashimoto, S., Carvalhais, N., Ito, A., Migliavacca, M., Nishina, K., Reichstein, M., 2015. Global spatiotemporal distribution of soil respiration modeled using a global database. Biogeosciences 12, 4121–4132. https://doi.org/10.5194/bg-12-4121-2015

Heimann, M., Reichstein, M., 2008. Terrestrial ecosystem carbon dynamics and climate feedbacks. Nature 451, 289–292. https://doi.org/10.1038/nature06591

Hotaling, S., Hood, E., Hamilton, T.L., 2017. Microbial ecology of mountain glacier ecosystems: biodiversity, ecological connections and implications of a warming climate. Environmental Microbiology 19, 2935–2948. https://doi.org/10.1111/1462-2920.13766

IPCC Climate Change 2013, 2013. . The Physical Science Basis.

Jangid, K., Whitman, W.B., Condron, L.M., Turner, B.L., Williams, M.A., 2013. Soil bacterial community succession during long-term ecosystem development. Molecular Ecology 22, 3415–3424. https://doi.org/10.1111/mec.12325

Ji, M., Greening, C., Vanwonterghem, I., Carere, C.R., Bay, S.K., Steen, J.A., Montgomery, K., Lines, T., Beardall, J., van Dorst, J., Snape, I., Stott, M.B., Hugenholtz, P., Ferrari, B.C., 2017. Atmospheric trace gases support primary production in Antarctic desert surface soil. Nature 552, 400–403. https://doi.org/10.1038/nature25014

Johnson, J.B., Omland, K.S., 2004. Model selection in ecology and evolution. Trends in Ecology & Evolution 19, 101–108. https://doi.org/10.1016/j.tree.2003.10.013

Kasana, R.C.; Yadav S.K. (2007). Isolation of a psychrotrophic Exiguobacterium sp. SKPB5 (MTCC 7803) and characterization of its alkaline protease. Current Microbiology. 54(3): 224-229.

Kazemi, S., Hatam, I., Lanoil, B., 2016. Bacterial community succession in a high-altitude subarctic glacier foreland is a three-stage process. Molecular Ecology 25, 5557–5567. https://doi.org/10.1111/mec.13835

Kim, M., Jung, J.Y., Laffly, D., Kwon, H.Y., Lee, Y.K., 2017. Shifts in bacterial community structure during succession in a glacier foreland of the High Arctic. FEMS Microbiology Ecology 93, fiw213. https://doi.org/10.1093/femsec/fiw213

Koch, A.L., 2001. Oligotrophs versus copiotrophs. Bioessays 23, 657–661.

Körner, C., 1999. Climatic stress. Alpine Plant Life Springer, Berlin, Heidelberg.

Kozich, J.J., Westcott, S.L., Baxter, N.T., Highlander, S.K., Schloss, P.D., 2013. Development of a Dual-Index Sequencing Strategy and Curation Pipeline for Analyzing Amplicon Sequence Data on the MiSeq Illumina Sequencing Platform.

Applied and Environmental Microbiology 79, 5112–5120. https://doi.org/10.1128/AEM.01043-13

Krishnan, R., Sanjay, J., Gnanaseelan, C., Mujumdar, M., Kulkarni, A., Chakraborty, S. (Eds.), 2020. Assessment of Climate Change over the Indian Region: A Report of the Ministry of Earth Sciences (MoES), Government of India. Springer Singapore, Singapore. https://doi.org/10.1007/978-981-15-4327-2

Kshetri, L.; Thounaojam, N.; Pandey, P. (2015). Plant growth promoting Rhizobacteria (PGPR) and their application for sustainable agriculture in North Eastern Region of India. Envis Bulletin Himalayan Ecology. 23: 41.

Kuypers, M.M.M., Marchant, H.K., Kartal, B., 2018. The microbial nitrogen-cycling network. Nature Reviews Microbiology 16, 263–276. https://doi.org/10.1038/nrmicro.2018.9

Langille, M.G.I., Zaneveld, J., Caporaso, J.G., McDonald, D., Knights, D., Reyes, J.A., Clemente, J.C., Burkepile, D.E., Vega Thurber, R.L., Knight, R., Beiko, R.G., Huttenhower, C., 2013. Predictive functional profiling of microbial communities using 16S rRNA marker gene sequences. Nature Biotechnology 31, 814–821. https://doi.org/10.1038/nbt.2676

Lanzén, A., Epelde, L., Blanco, F., Martín, I., Artetxe, U., Garbisu, C., 2016. Multi-targeted metagenetic analysis of the influence of climate and environmental parameters on soil microbial communities along an elevational gradient. Scientific Reports 6. https://doi.org/10.1038/srep28257

Lazzaro, A., Hilfiker, D., Zeyer, J., 2015. Structures of Microbial Communities in Alpine Soils: Seasonal and Elevational Effects. Frontiers in Microbiology 6. https://doi.org/10.3389/fmicb.2015.01330

Li, J., Ma, Y.-B., Hu, H.-W., Wang, J.-T., Liu, Y.-R., He, J.-Z., 2015. Field-based evidence for consistent responses of bacterial communities to copper contamination in two contrasting agricultural soils. Front. Microbiol. 6. https://doi.org/10.3389/fmicb.2015.00031

Lladó, S., López-Mondéjar, R., Baldrian, P., 2017. Forest soil bacteria: diversity, involvement in ecosystem processes, and response to global change. Microbiology and Molecular Biology Reviews 81.

Longbottom, T.L., Townsend-Small, A., Owen, L.A., Murari, M.K., 2014. Climatic and topographic controls on soil organic matter storage and dynamics in the Indian Himalaya: Potential carbon cycle–climate change feedbacks. CATENA 119, 125–135. https://doi.org/10.1016/j.catena.2014.03.002

Luo, Z., Liu, J., Zhao, P., Jia, T., Li, C., Chai, B., 2019. Biogeographic Patterns and Assembly Mechanisms of Bacterial Communities Differ Between Habitat Generalists and Specialists Across Elevational Gradients. Frontiers in Microbiology 10. https://doi.org/10.3389/fmicb.2019.00169

Mancinelli, R.L., 1996. The nature of nitrogen: an overview. Life Support Biosph Sci 3, 17–24.

Mapelli, F., Marasco, R., Rizzi, A., Baldi, F., Ventura, S., Daffonchio, D., Borin, S., 2011. Bacterial Communities Involved in Soil Formation and Plant Establishment Triggered by Pyrite Bioweathering on Arctic Moraines. Microbial Ecology 61, 438–447. https://doi.org/10.1007/s00248-010-9758-7

Margesin, R., Niklinska, M.A., 2019. Editorial: Elevation Gradients: Microbial Indicators of Climate Change? Frontiers in Microbiology 10. https://doi.org/10.3389/fmicb.2019.02405

Marion, G.M., Henry, G.H.R., Freckman, D.W., Johnstone, J., Jones, G., Jones, M.H., LéVesque, E., Molau, U., MøLgaard, P., Parsons, A.N., J. Svoboda, Virginia, R.A., 1997. Open-top designs for manipulating field temperature in high-latitude ecosystems. Global Change Biology 3, 20–32. https://doi.org/10.1111/j.1365-2486.1997.gcb136.x

Masse, J., Prescott, C.E., Renaut, S., Terrat, Y., Grayston, S.J., 2017. Plant Community and Nitrogen Deposition as Drivers of Alpha and Beta Diversities of Prokaryotes in Reconstructed Oil Sand Soils and Natural Boreal Forest Soils. Applied and Environmental Microbiology 83. https://doi.org/10.1128/AEM.03319-16

Misra, A.K., 2011. Impact of Urbanization on the Hydrology of Ganga Basin (India). Water Resources Management 25, 705–719. https://doi.org/10.1007/s11269-010-9722-9

Miteva, V.I., Sheridan, P.P., Brenchley, J.E., 2004. Phylogenetic and Physiological Diversity of Microorganisms Isolated from a Deep Greenland Glacier Ice Core. Applied and Environmental Microbiology 70, 202–213. https://doi.org/10.1128/AEM.70.1.202-213.2004

Molau, U., Alatalo, J.M., 1998. Responses of subarctic-alpine plant communities to simulated environmental change: biodiversity of bryophytes, lichens, and vascular plants. Ambio 27, 322–329.

Mountain Research Initiative EDW Working Group, 2015. Elevation-dependent warming in mountain regions of the world. Nature Climate Change 5, 424–430. https://doi.org/10.1038/nclimate2563

Nemergut, D.R., Anderson, S.P., Cleveland, C.C., Martin, A.P., Miller, A.E., Seimon, A., Schmidt, S.K., 2007. Microbial Community Succession in an Unvegetated, Recently Deglaciated Soil. Microbial Ecology 53, 110–122. https://doi.org/10.1007/s00248-006-9144-7

Oksanen, J., Guillaume Blanchet, F., Friendly, M., Kindt, R., Legendre, P., McGlinn, D., 2019. Vegan: Community Ecology Package.

Ortiz-Álvarez, R., Fierer, N., de los Ríos, A., Casamayor, E.O., Barberán, A., 2018. Consistent changes in the taxonomic structure and functional attributes of bacterial communities during primary succession. The ISME Journal 12, 1658–1667. https://doi.org/10.1038/s41396-018-0076-2

Ortiz-Estrada, Á.M., Gollas-Galván, T., Martínez-Córdova, L.R., Martínez-Porchas, M., 2019. Predictive functional profiles using metagenomic 16S rRNA data: a novel approach to understanding the microbial ecology of aquaculture systems. Reviews in Aquaculture 11, 234–245. https://doi.org/10.1111/raq.12237

Padma, T.V., 2014. Himalayan plants seek cooler climes. Nature 512, 359–359. https://doi.org/10.1038/512359a

Pedrós-Alió, C., 2006. Marine microbial diversity: can it be determined? Trends in Microbiology 14, 257–263. https://doi.org/10.1016/j.tim.2006.04.007

Peltoniemi, K., Laiho, R., Juottonen, H., Kiikkilä, O., Mäkiranta, P., Minkkinen, K., Pennanen, T., Penttilä, T., Sarjala, T., Tuittila, E.-S., Tuomivirta, T., Fritze, H., 2015. Microbial ecology in a future climate: effects of temperature and moisture on microbial communities of two boreal fens. FEMS Microbiology Ecology 91. https://doi.org/10.1093/femsec/fiv062

Philippot, L., Tscherko, D., Bru, D., Kandeler, E., 2011. Distribution of High Bacterial Taxa Across the Chronosequence of Two Alpine Glacier Forelands. Microbial Ecology 61, 303–312. https://doi.org/10.1007/s00248-010-9754-y

Pollierer, M.M., Langel, R., Körner, C., Maraun, M., Scheu, S., 2007. The underestimated importance of belowground carbon input for forest soil animal food webs. Ecology Letters 10, 729–736. https://doi.org/10.1111/j.1461-0248.2007.01064.x

Pusalkar, P.K., Singh, D.K., 2012. Flora of Gangotri National Park, Western Himalaya, India. Botanical Survey of India.

Qiang, W., He, L., Zhang, Y., Liu, B., Liu, Y., Liu, Q., Pang, X., 2021. Aboveground vegetation and soil physicochemical properties jointly drive the shift of soil microbial community during subalpine secondary succession in southwest China. CATENA 202, 105251. https://doi.org/10.1016/j.catena.2021.105251

Quast, C., Pruesse, E., Yilmaz, P., Gerken, J., Schweer, T., Yarza, P., Peplies, J., Glöckner, F.O., 2012. The SILVA ribosomal RNA gene database project: improved data processing and web-based tools. Nucleic Acids Research 41, D590–D596. https://doi.org/10.1093/nar/gks1219

R Core Team, 2020. R: A language and environment for statistical computing. R Foundation for Statistical Computing, Vienna, Austria.

Rao, P., Patil, Y. (Eds.), 2017. Reconsidering the Impact of Climate Change on Global Water Supply, Use, and Management:, Advances in Environmental Engineering and Green Technologies. IGI Global. https://doi.org/10.4018/978-1-5225-1046-8

Rawat, G.S., 2007. Pastoral Practices, wild mammals and conservation status of alpine meadows in western Himalaya. The journal of the Bombay Natural History Society. 104, 5–11.

Rawat, G.S., Adhikari, B.S., 2005. Floristics and Distribution of Plant Communities across Moisture and Topographic Gradients in Tso Kar Basin, Changthang

Plateau, Eastern Ladakh. Arctic, Antarctic, and Alpine Research 37, 539–544. https://doi.org/10.1657/1523-0430(2005)037[0539:FADOPC]2.0.CO;2

Rawls, W.J., Pachepsky, Y.A., Ritchie, J.C., Sobecki, T.M., Bloodworth, H., 2003. Effect of soil organic carbon on soil water retention. Geoderma 116, 61–76. https://doi.org/10.1016/S0016-7061(03)00094-6

Rayment, G.E., Lyons, D.J., 2011. Soil chemical methods : Australasia. Collingwood, Vic. : CSIRO Publishing.

Rousk, J., Frey, S.D., Bååth, E., 2012. Temperature adaptation of bacterial communities in experimentally warmed forest soils. Global Change Biology 18, 3252–3258. https://doi.org/10.1111/j.1365-2486.2012.02764.x

Saba, I.; Qazi, P.H.; Rather, S.A.; Dar, R.A.; Qadri, Q.A.; Ahmed, N.; Shawl, S. (2012). Purification and characterization of a cold active alkaline protease from Stenotrophomonas sp. isolated from Kashmir, India. World Journal of Microbiology and Biotechnology. 28(3): 1071-1079.

Santos, R., de Carvalho, C.C.C.R., Stevenson, A., Grant, I.R., Hallsworth, J.E., 2015. Extraordinary solute-stress tolerance contributes to the environmental tenacity of mycobacteria: Extraordinary stress-tolerance of mycobacteria. Environmental Microbiology Reports 7, 746–764. https://doi.org/10.1111/1758-2229.12306

Sanyal, A.K., Uniyal, V.P., Chandra, K., Bhardwaj, M., 2013. Diversity, distribution pattern and seasonal variation in moth assemblages along altitudinal gradient in Gangotri landscape area, Western Himalaya, Uttarakhand, India. Journal of Threatened Taxa 5, 3646–3653. https://doi.org/10.11609/JoTT.o2597.3646-53

Schindlbacher, A., de Gonzalo, C., Díaz-Pinés, E., Gorría, P., Matthews, B., Inclán, R., Zechmeister-Boltenstern, S., Rubio, A., Jandl, R., 2010. Temperature sensitivity of forest soil organic matter decomposition along two elevation gradients. Journal of Geophysical Research 115. https://doi.org/10.1029/2009JG001191

Schloss, P.D., Westcott, S.L., Ryabin, T., Hall, J.R., Hartmann, M., Hollister, E.B., Lesniewski, R.A., Oakley, B.B., Parks, D.H., Robinson, C.J., Sahl, J.W., Stres, B., Thallinger, G.G., Van Horn, D.J., Weber, C.F., 2009. Introducing mothur: Open-Source, Platform-Independent, Community-Supported Software for Describing and Comparing Microbial Communities. Applied and Environmental Microbiology 75, 7537–7541. https://doi.org/10.1128/AEM.01541-09

Schütte, U.M., Abdo, Z., Bent, S.J., Williams, C.J., Schneider, G.M., Solheim, B., Forney, L.J., 2009. Bacterial succession in a glacier foreland of the High Arctic. The ISME journal 3, 1258–1268.

SchüTte, U.M.E., Abdo, Z., Foster, J., Ravel, J., Bunge, J., Solheim, B., Forney, L.J., 2010. Bacterial diversity in a glacier foreland of the high Arctic. Molecular Ecology 19, 54–66. https://doi.org/10.1111/j.1365-294X.2009.04479.x

Shannon, P., Markiel, A., Ozier, O., Baliga, N.S., Wang, J.T., Ramage, D., Amin, N., Schwikowski, B., Ideker, T., 2003. Cytoscape: A Software Environment for

Integrated Models of Biomolecular Interaction Networks. Genome Research 13, 2498–2504. https://doi.org/10.1101/gr.1239303

Sharma, S.; Kaur, M.; Prashad, D. (2014). Isolation of fluorescent Pseudomonas strain from temperate zone of Himachal Pradesh and their evaluation as plant growth promoting Rhizobacteria PGPR. The Bioscan. 9(1): 323-328.

Shao, K., Bai, C., Cai, J., Hu, Y., Gong, Y., Chao, J., Dai, J., Wang, Y., Ba, T., Tang, X., Gao, G., 2019. Illumina Sequencing Revealed Soil Microbial Communities in a Chinese Alpine Grassland. Geomicrobiology Journal 36, 204–211. https://doi.org/10.1080/01490451.2018.1534902

Sheik, C.S., Beasley, W.H., Elshahed, M.S., Zhou, X., Luo, Y., Krumholz, L.R., 2011a. Effect of warming and drought on grassland microbial communities. ISME J 5, 1692–1700. https://doi.org/10.1038/ismej.2011.32

Sheik, C.S., Beasley, W.H., Elshahed, M.S., Zhou, X., Luo, Y., Krumholz, L.R., 2011b. Effect of warming and drought on grassland microbial communities. ISME J 5, 1692–1700. https://doi.org/10.1038/ismej.2011.32

Shen, C., Ni, Y., Liang, W., Wang, J., Chu, H., 2015. Distinct soil bacterial communities along a small-scale elevational gradient in alpine tundra. Frontiers in Microbiology 6. https://doi.org/10.3389/fmicb.2015.00582

Shen, C., Xiong, J., Zhang, H., Feng, Y., Lin, X., Li, X., Liang, W., Chu, H., 2013. Soil pH drives the spatial distribution of bacterial communities along elevation on Changbai Mountain. Soil Biology and Biochemistry 57, 204–211. https://doi.org/10.1016/j.soilbio.2012.07.013

Shendure, J., Ji, H., 2008. Next-generation DNA sequencing. Nat Biotechnol 26, 1135–1145. https://doi.org/10.1038/nbt1486

Shrestha, U.B., Gautam, S., Bawa, K.S., 2012a. Widespread Climate Change in the Himalayas and Associated Changes in Local Ecosystems. PLoS ONE 7, e36741. https://doi.org/10.1371/journal.pone.0036741

Shrestha, U.B., Gautam, S., Bawa, K.S., 2012b. Widespread Climate Change in the Himalayas and Associated Changes in Local Ecosystems. PLoS ONE 7, e36741. https://doi.org/10.1371/journal.pone.0036741

Siles, J.A., Cajthaml, T., Filipová, A., Minerbi, S., Margesin, R., 2017. Altitudinal, seasonal and interannual shifts in microbial communities and chemical composition of soil organic matter in Alpine forest soils. Soil Biology and Biochemistry 112, 1–13. https://doi.org/10.1016/j.soilbio.2017.04.014

Siles, J.A., Cajthaml, T., Minerbi, S., Margesin, R., 2016. Effect of altitude and season on microbial activity, abundance and community structure in Alpine forest soils. FEMS Microbiology Ecology 92, fiw008. https://doi.org/10.1093/femsec/fiw008

Siles, J.A., Margesin, R., 2017. Seasonal soil microbial responses are limited to changes in functionality at two Alpine forest sites differing in altitude and vegetation. Scientific Reports 7. https://doi.org/10.1038/s41598-017-02363-2

Siles, J.A., Margesin, R., 2016. Abundance and Diversity of Bacterial, Archaeal, and Fungal Communities Along an Altitudinal Gradient in Alpine Forest Soils: What Are the Driving Factors? Microbial Ecology 72, 207–220. https://doi.org/10.1007/s00248-016-0748-2

Singh, B.K., Bardgett, R.D., Smith, P., Reay, D.S., 2010. Microorganisms and climate change: terrestrial feedbacks and mitigation options. Nature Reviews Microbiology 8, 779–790. https://doi.org/10.1038/nrmicro2439

Singh, D., Lee-Cruz, L., Kim, W.-S., Kerfahi, D., Chun, J.-H., Adams, J.M., 2014. Strong elevational trends in soil bacterial community composition on Mt. Halla, South Korea. Soil Biology and Biochemistry 68, 140–149. https://doi.org/10.1016/j.soilbio.2013.09.027

Singh, D., Takahashi, K., Kim, M., Chun, J., Adams, J.M., 2012. A Hump-Backed Trend in Bacterial Diversity with Elevation on Mount Fuji, Japan. Microbial Ecology 63, 429–437. https://doi.org/10.1007/s00248-011-9900-1

Spellerberg, I.F., Fedor, P.J., 2003. A tribute to Claude Shannon (1916-2001) and a plea for more rigorous use of species richness, species diversity and the 'Shannon-Wiener' Index: *On species richness and diversity*. Global Ecology and Biogeography 12, 177–179. https://doi.org/10.1046/j.1466-822X.2003.00015.x

Steinweg, J.M., Dukes, J.S., Wallenstein, M.D., 2012. Modeling the effects of temperature and moisture on soil enzyme activity: Linking laboratory assays to continuous field data. Soil Biology and Biochemistry 55, 85–92. https://doi.org/10.1016/j.soilbio.2012.06.015

Stres, B., Sul, W.J., Murovec, B., Tiedje, J.M., 2014. Correction: Recently Deglaciated High-Altitude Soils of the Himalaya: Diverse Environments, Heterogenous Bacterial Communities and Long-Range Dust Inputs from the Upper Troposphere. PLoS ONE 9. https://doi.org/10.1371/annotation/1406824c-f082-400b-8fc7-4995c97a6249

Structural Equation Modeling and Natural Systems by J. B. GRACE, 2007. . Biometrics 63, 977–977. https://doi.org/10.1111/j.1541-0420.2007.00856_13.x

Sun, H., Wu, Y., Zhou, J., Bing, H., Zhu, H., 2020. Climate influences the alpine soil bacterial communities by regulating the vegetation and the soil properties along an altitudinal gradient in SW China. CATENA 195, 104727. https://doi.org/10.1016/j.catena.2020.104727

Sun, S., Jones, R.B., Fodor, A.A., 2020. Inference-based accuracy of metagenome prediction tools varies across sample types and functional categories. Microbiome 8, 46. https://doi.org/10.1186/s40168-020-00815-y

Suyal, D.C., Joshi, D., Debbarma, P., Soni, R., Das, B., Goel, R., 2019. Soil Metagenomics: Unculturable Microbial Diversity and Its Function, in: Varma, A.,

Choudhary, D.K. (Eds.), Mycorrhizosphere and Pedogenesis. Springer Singapore, Singapore, pp. 355–362. https://doi.org/10.1007/978-981-13-6480-8_20

Tang, M., Li, L., Wang, X., You, J., Li, J., Chen, X., 2020. Elevational is the main factor controlling the soil microbial community structure in alpine tundra of the Changbai Mountain. Scientific Reports 10. https://doi.org/10.1038/s41598-020-69441-w

Tarlera, S., Jangid, K., Ivester, A.H., Whitman, W.B., Williams, M.A., 2008. Microbial community succession and bacterial diversity in soils during 77 000 years of ecosystem development: Microbial community succession in soils. FEMS Microbiology Ecology 64, 129–140. https://doi.org/10.1111/j.1574-6941.2008.00444.x

Tiwari, P., Bhattacharya, P., Rawat, G.S., Rai, I.D., Talukdar, G., 2021a. Experimental warming increases ecosystem respiration by increasing above-ground respiration in alpine meadows of Western Himalaya. Sci Rep 11, 2640. https://doi.org/10.1038/s41598-021-82065-y

Tiwari, P., Bhattacharya, P., Rawat, G.S., Rai, I.D., Talukdar, G., 2021b. Experimental warming increases ecosystem respiration by increasing above-ground respiration in alpine meadows of Western Himalaya. Scientific Reports 11. https://doi.org/10.1038/s41598-021-82065-y

Tiwari, P., Bhattacharya, P., Rawat, G.S., Talukdar, G., 2021c. Equilibrium in soil respiration across a climosequence indicates its resilience to climate change in a glaciated valley, western Himalaya. Sci Rep 11, 23038. https://doi.org/10.1038/s41598-021-02199-x

Tiwari, P., Singh, J.S., 2017. A plant growth promoting rhizospheric Pseudomonas aeruginosa strain inhibits seed germination in Triticum aestivum (L) and Zea mays (L). Microbiology Research 8. https://doi.org/10.4081/mr.2017.7233

Treseder, K.K., Balser, T.C., Bradford, M.A., Brodie, E.L., Dubinsky, E.A., Eviner, V.T., Hofmockel, K.S., Lennon, J.T., Levine, U.Y., MacGregor, B.J., Pett-Ridge, J., Waldrop, M.P., 2012. Integrating microbial ecology into ecosystem models: challenges and priorities. Biogeochemistry 109, 7–18. https://doi.org/10.1007/s10533-011-9636-5

Trivedi, P., Anderson, I.C., Singh, B.K., 2013. Microbial modulators of soil carbon storage: integrating genomic and metabolic knowledge for global prediction. Trends in Microbiology 21, 641–651. https://doi.org/10.1016/j.tim.2013.09.005

Venkatachalam, S., Kannan, V.M., Saritha, V.N., Loganathachetti, D.S., Mohan, M., Krishnan, K.P., 2021. Bacterial diversity and community structure along the glacier foreland of Midtre Lovénbreen, Svalbard, Arctic. Ecological Indicators 126, 107704. https://doi.org/10.1016/j.ecolind.2021.107704

Walker, M.D., Wahren, C.H., Hollister, R.D., Henry, G.H., Ahlquist, L.E., Alatalo, J.M., Bret-Harte, M.S., Calef, M.P., Callaghan, T.V., Carroll, A.B., 2006. Plant

community responses to experimental warming across the tundra biome. Proceedings of the National Academy of Sciences 103, 1342–1346.

Walkley, A., Black, I.A., 1934. An examination of the Degtjareff method for determining soil organic matter, and a proposed modification of the chromic acid titration method. Soil Science 37, 29–38. https://doi.org/10.1097/00010694-193401000-00003

Wang, C., Wang, G., Wang, Y., Zi, H., Lerdau, M., Liu, W., 2017. Effects of long-term experimental warming on plant community properties and soil microbial community composition in an alpine meadow. Israel Journal of Ecology & Evolution 1–12. https://doi.org/10.1080/15659801.2017.1281201

Wang, J., Soininen, J., He, J., Shen, J., 2012. Phylogenetic clustering increases with elevation for microbes: Phylogenetic clustering increases with elevation. Environmental Microbiology Reports 4, 217–226. https://doi.org/10.1111/j.1758-2229.2011.00324.x

Wang, J., Wu, Y., Li, J., He, Q., Zhu, H., Bing, H., 2021. Energetic supply regulates heterotrophic nitrogen fixation along a glacial chronosequence. Soil Biology and Biochemistry 154, 108150. https://doi.org/10.1016/j.soilbio.2021.108150

Weedon, J.T., Kowalchuk, G.A., Aerts, R., Freriks, S., Röling, W.F.M., van Bodegom, P.M., 2017. Compositional Stability of the Bacterial Community in a Climate-Sensitive Sub-Arctic Peatland. Frontiers in Microbiology 8. https://doi.org/10.3389/fmicb.2017.00317

Wickham, H., 2011. ggplot2: ggplot2. Wiley Interdisciplinary Reviews: Computational Statistics 3, 180–185. https://doi.org/10.1002/wics.147

Wickham, H., Wickham, M.H., 2017. Package tidyverse. Easily Install and Load the 'Tidyverse.

Wieder, W.R., Grandy, A.S., Kallenbach, C.M., Taylor, P.G., Bonan, G.B., 2015. Representing life in the Earth system with soil microbial functional traits in the MIMICS model. Geoscientific Model Development 8, 1789–1808. https://doi.org/10.5194/gmd-8-1789-2015

Wu, X., Zhang, W., Liu, G., Yang, X., Hu, P., Chen, T., Zhang, G., Li, Z., 2012. Bacterial diversity in the foreland of the Tianshan No. 1 glacier, China. Environmental Research Letters 7, 014038. https://doi.org/10.1088/1748-9326/7/1/014038

Xu, G., Chen, J., Berninger, F., Pumpanen, J., Bai, J., Yu, L., Duan, B., 2015. Labile, recalcitrant, microbial carbon and nitrogen and the microbial community composition at two Abies faxoniana forest elevations under elevated temperatures. Soil Biology and Biochemistry 91, 1–13. https://doi.org/10.1016/j.soilbio.2015.08.016

Xu, M., Li, Xiaoliang, Cai, X., Gai, J., Li, Xiaolin, Christie, P., Zhang, J., 2014. Soil microbial community structure and activity along a montane elevational gradient on the Tibetan Plateau. European Journal of Soil Biology 64, 6–14. https://doi.org/10.1016/j.ejsobi.2014.06.002

Xue, P.-P., Carrillo, Y., Pino, V., Minasny, B., McBratney, Alex.B., 2018. Soil Properties Drive Microbial Community Structure in a Large Scale Transect in South Eastern Australia. Scientific Reports 8. https://doi.org/10.1038/s41598-018-30005-8

Yang, Y., Fang, J., Tang, Y., Ji, C., Zheng, C., He, J., Zhu, B., 2008. Storage, patterns and controls of soil organic carbon in the Tibetan grasslands. Global Change Biology 14, 1592–1599. https://doi.org/10.1111/j.1365-2486.2008.01591.x

Yashiro, E., Pinto-Figueroa, E., Buri, A., Spangenberg, J.E., Adatte, T., Niculita-Hirzel, H., Guisan, A., van der Meer, J.R., 2016. Local Environmental Factors Drive Divergent Grassland Soil Bacterial Communities in the Western Swiss Alps. Applied and Environmental Microbiology 82, 6303–6316. https://doi.org/10.1128/AEM.01170-16

Zahran, H.H., 1999. *Rhizobium* -Legume Symbiosis and Nitrogen Fixation under Severe Conditions and in an Arid Climate. Microbiology and Molecular Biology Reviews 63, 968–989. https://doi.org/10.1128/MMBR.63.4.968-989.1999

Zhang, B., Chen, S., He, X., Liu, W., Zhao, Q., Zhao, L., Tian, C., 2014. Responses of Soil Microbial Communities to Experimental Warming in Alpine Grasslands on the Qinghai-Tibet Plateau. PLoS ONE 9, e103859. https://doi.org/10.1371/journal.pone.0103859

Zhang, B., Xue, K., Zhou, S., Che, R., Du, J., Tang, L., Pang, Z., Wang, F., Wang, D., Cui, X., Hao, Y., Wang, Y., 2019. Phosphorus mediates soil prokaryote distribution pattern along a small-scale elevation gradient in Noijin Kangsang Peak, Tibetan Plateau. FEMS Microbiology Ecology 95. https://doi.org/10.1093/femsec/fiz076

Zhao, Z., Zhang, X., Dong, S., Wu, Y., Liu, S., Su, X., Wang, X., Zhang, Y., Tang, L., 2019. Soil organic carbon and total nitrogen stocks in alpine ecosystems of Altun Mountain National Nature Reserve in dry China. Environmental Monitoring and Assessment 191. https://doi.org/10.1007/s10661-018-7138-9

Zheng, H., Chen, Y., Liu, Y., Zhang, J., Yang, W., Yang, L., Li, H., Wang, L., Wu, F., Guo, L., 2018. Litter quality drives the differentiation of microbial communities in the litter horizon across an alpine treeline ecotone in the eastern Tibetan Plateau. Scientific Reports 8. https://doi.org/10.1038/s41598-018-28150-1

Zhou, J., Deng, Y., Luo, F., He, Z., Yang, Y., 2011. Phylogenetic Molecular Ecological Network of Soil Microbial Communities in Response to Elevated CO_2. mBio 2. https://doi.org/10.1128/mBio.00122-11

Zhou, J., Xue, K., Xie, J., Deng, Y., Wu, L., Cheng, X., Fei, S., Deng, S., He, Z., Van Nostrand, J.D., Luo, Y., 2012. Microbial mediation of carbon-cycle feedbacks to climate warming. Nature Clim Change 2, 106–110. https://doi.org/10.1038/nclimate1331

Zhu, B., Li, C., Wang, J., Li, J., Li, X., 2020. Elevation rather than season determines the assembly and co-occurrence patterns of soil bacterial communities in forest

ecosystems of Mount Gongga. Applied Microbiology and Biotechnology 104, 7589–7602. https://doi.org/10.1007/s00253-020-10783-w

Zi, H.B., Hu, L., Wang, C.T., Wang, G.X., Wu, P.F., Lerdau, M., Ade, L.J., 2018a. Responses of soil bacterial community and enzyme activity to experimental warming of an alpine meadow: Effects of warming on soil microorganisms. Eur J Soil Sci 69, 429–438. https://doi.org/10.1111/ejss.12547

Zi, H.B., Hu, L., Wang, C.T., Wang, G.X., Wu, P.F., Lerdau, M., Ade, L.J., 2018b. Responses of soil bacterial community and enzyme activity to experimental warming of an alpine meadow: Effects of warming on soil microorganisms. European Journal of Soil Science 69, 429–438. https://doi.org/10.1111/ejss.12547

Annexure – I

Permits

All required permissions for the field survey and soil sampling were provided by Uttarakhand Forest Department (Permit no. 702/5-6).

Current Microbiology (2022) 79:91
https://doi.org/10.1007/s00284-022-02779-8

Shifts in Bacterial Community Composition and Functional Traits at Different Time Periods Post-deglaciation of Gangotri Glacier, Himalaya

Pamela Bhattacharya[1] · Pankaj Tiwari[1] · Gautam Talukdar[1] · Gopal S. Rawat[1]

Received: 17 August 2021 / Accepted: 20 January 2022

Abstract
Climate change causes an unprecedented increase in glacial retreats. The melting ice exposes land for colonization and diversification of bacterial communities leading to soil development, changes in plant community composition, and ecosystem functioning. Although a few studies have focused on macro-level deglaciation impacts, little is known about such effects on the bacterial community succession. Here, we provide meta-barcoding-based insight into the ecological attributes of bacterial community across different retreating periods of the Gangotri glacier, western Himalaya. We selected three sites along a terminal moraine representing recent (~ 20 yrs), intermediate (~ 100 yrs), and late (~ 300 yrs) deglaciation periods. Results showed that the genus *Mycobacterium* belonging to phylum *Actinobacteria* dominated recently deglaciated land. Relative abundance of these pioneer bacterial taxa decreased by 20–50% in the later stages with the emergence of new and rising of the less abundant members of the phyla *Proteobacteria*, *Firmicutes*, *Planctomycetes*, *Acidobacteria*, *Verrucomicrobia*, Candidatus TM6, and *Chloroflexi.* The community in the recent stage was less rich and harbored competitive interactions, while the later stages experienced a surge in bacterial diversity with cooperative interactions. The shift in α-diversity and composition was strongly influenced by soil organic carbon, carbon to nitrogen ratio, and soil moisture content. The functional analyses revealed a progression from a metabolism focused to a functionally progressive community required for bacterial co-existence and succession in plant communities. Overall, the findings indicate that the bacterial communities inhabit, diversify, and develop specialized functions post-deglaciation leading to nutrient inputs to soil and vegetation development, which may provide feedback to climate change.

Introduction

Increasing global average surface temperature since the past decade has led to rapid changes in terrestrial ecosystems [1]. The high altitude ecosystems and Polar Regions have particularly experienced higher warming rates, leading to rapid melting of ice and retreat of glaciers [2, 3]. As the glaciers retreat, new lands are exposed for colonization by pioneer bacterial communities capable of surviving in cold oligotrophic environments primarily by utilizing atmospheric carbon (C) and nitrogen (N) depositions as energy sources [4]. Increasing bacterial activity promotes mineral weathering leading to nutrient mobilization and soil formation [4, 5]. Availability of essential nutrients such as phosphorus (P), calcium, and potassium facilitates the recruitment and growth of other microbial communities and plant colonization [5, 6]. Microbial activity and primary production eventually drive biogeochemical transformations in recently exposed soils leading to the gradual accumulation of organic matter and ecosystem maturation [5, 7]. Despite the critical role of bacterial communities in initiating soil and ecosystem development, there is limited understanding of the ecological attributes of the community, including the relationship between their composition and functional traits, interspecies interactions, and environmental control on the diversity. Understanding the ecological characteristics of abundant bacterial taxa is required for insight into the crucial microbial process involved in ecosystem development.

Taxonomic classification of bacterial metagenome is gradually progressing with cost-effective next-generation sequencing techniques [8]. However, the functional traits of bacterial communities are poorly characterized due to the low similarity

✉ Gopal S. Rawat
rawatg@wii.gov.in

[1] Wildlife Institute of India, Chandrabani, Dehradun 248001, India

Published online: 07 February 2022

of environmental 16S rRNA sequence with the existing metagenome databases [8]. In addition, functional characterization of the meta-genomes using meta-transcriptomics is expensive [8, 9]. Therefore, this has inhibited understanding the functional potential of the newly evolving ecosystems post-deglaciation. Recently, efforts have been made to predict bacterial metagenome functions using various less expensive computational approaches based on 16S rRNA sequences [10]. PICRUST platform is one of the effective computational tools to predict soil bacterial functions taking into account the relationship between phylogeny and function [11]. Although these metagenome function prediction tools are widely used for environmental bacterial community function prediction, they have certain limitations [12]. Since the microbial metagenome database used for alignment of the 16S rDNA sequences majorly represents microorganisms associated with human microbiota, the predictive power of these tools for environmental samples is compromised and needs to be used with caution [12].

The Himalayan region, representing the highest mountain ranges globally, has warmed significantly in the past years and is predicted to experience a temperature rise of 3 °C by 2050 [13]. Almost 17% of the Himalayan landscape is glaciated, of which 21% have retreated over the last 50 years [14]. The Gangotri glacier is the largest in Himalaya, having a total ice cover of 200 km^2 [14]. This glacier is the primary source of the river Ganga on which 42% of the Indian population is dependent [14]. From 1935 to 1996, the glacier has retreated on an average of 19 m/year, double that of the previous century exposing 2.25 km^2 [14]. The deglaciated foreland now supports sub-alpine and alpine vegetation rich in high altitude flora that has been legally protected in the form of Gangotri National Park [15]. Quantification of soil microbial community along a temporal sequence in glacial forelands advances our understanding of the past and future trends in ecosystem functioning during deglaciation. In this study, we investigated the succession in soil bacterial community at different periods in the forelands of Gangotri glacier with the following objectives: (i) assessment of the shift in bacterial community richness, diversity, and composition at different taxonomic levels (phyla, class, and genera), (ii) assessment of bacterial co-occurrence pattern, (iii) evaluation of the shifts in the community traits associated with (a) most abundant functions and (b) biogeochemical cycles, i.e., C, N, P and sulfur (S), and (iv) evaluate the impact of environmental factors on the community diversity and composition.

Materials and Methods

Study Area

The study was conducted in an alpine glacier foreland on the southwest-facing slope of the Gangotri glacier located in Western Himalaya, India (30.95–30.99 N, 78.99–79.06 E; 4000 m above mean sea level). We selected three sites representing recent (~ 20 yrs), intermediate (~ 100 yrs), and late (~ 300 yrs) post-deglaciation periods located at increasing distance from the snout of this glacier, which is referred to as Gaumukh (Fig. 1). We calculated the time of deglaciation via Google earth imagery and previously published articles [16] (Supplementary Fig. S1 and Table S1). The recently deglaciated site was 340 m away from the snout and represented a bare surface of sand, gravel, and small rocks (Fig. 1, Table 1 and Supplementary Table S1). The intermediate site was 1.96 km away from the snout, characterized by fresh alluvial soil with sparse vegetation represented by pioneer communities such as *Calamagrostis emodensis* and other herbs. The late stage was 3.8 km away from the snout, where the soil was well developed, representing herbaceous formation. From the recent to the late stage, the soil pH ranged from 6.7 ± 0.3 to 4.9 ± 0.3 (Table 1). Soil organic carbon (SOC) and total nitrogen (TN) ranged from 0.4 ± 0.03 to 56.2 ± 11.8 g kg^{-1} and 0.1 ± 0.01 to 4.2 ± 0.3 g kg^{-1}, respectively (Table 1). The region is completely covered with snow from December to mid-May [16]. Mean annual precipitation (MAP) and mean annual temperature (MAT) close to the study sites were around 1500 mm and 2.92 ± 0.36 °C, respectively [17, 18].

Site Selection and Soil Sampling

We selected four 5×5 m plots (approximately 50 m apart) at each site. In each plot, five 1×1 m sub-plots were selected randomly to better represent habitat heterogeneity before vegetation analysis and soil sampling. Sampling was performed in autumn of 2016 between 24 and 27th October. Vegetation was estimated at each subplot by the quadrat method. At each subplot, five soil cores (~10 g each) were collected at four corners and center from topsoil to 5 cm depth using hand-held sterile soil corer (50 ml centrifuge tube of diameter 2.5 cm, Tarsons Products Pvt. Ltd, India). Before soil collection, above-ground vegetation and leaf litter were removed if present. Based on the design of Lanzen et al. [19], soil cores at each plot ($n = 25$) were pooled (~250 g) in a sterile ziplock bag and homogenized. We aliquoted 5 g soil from this pool and preserved it in 100% ethanol (Merck, Germany) for molecular analysis. The remaining soil was kept for soil physicochemical analyses. All samples ($n = 4$ per site) were transported in a cool box containing dry ice within 48 h of sampling to the laboratory for downstream analysis.

Measurement of Soil Properties

We estimated soil properties, including soil moisture content (SMC), pH, SOC, TN, and carbon to nitrogen ratio (C/N).

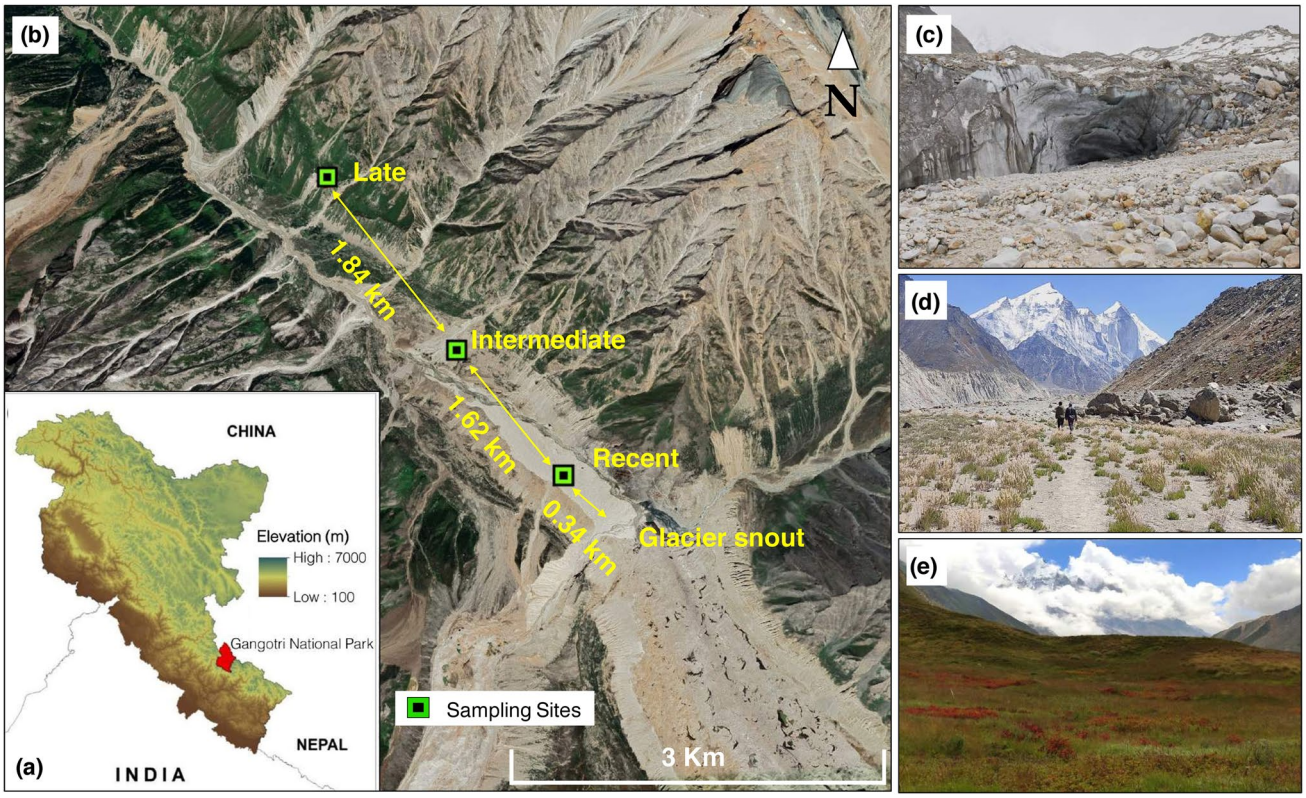

Fig. 1 Map of the study area **a** Gangotri National Park in western Himalaya, India, **b** soil sampling sites at different post-deglaciation periods from the Gangotri glacier snout, and **c**, **d**, **e** images of different deglaciation stages recent (~20 yrs), intermediate (~100 yrs), and late (~300 yrs), respectively. All maps were generated in ArcGIS version 10.7 (ESRI, CA, USA, https://desktop.arcgis.com/en/arcmap/). SRTM DEM (Shuttle Radar Topography Mission, Digital Elevation Model) data (30 m) in (**a**) was downloaded from the US Geological Survey Earth Explorer (http://earthexplorer.usgs.gov/)

Table 1 Dominant plants, mean annual temperature (MAT), and soil properties including soil moisture content (SMC), soil organic carbon (SOC), total nitrogen (TN), C/N ratio, and pH across three sites post-deglaciation of Gangotri glacier, Himalaya

Deglaciation period	Altitude (m.a.s.l)	Dominant plants	MAT	SMC (%)	SOC (g kg−1)	TN (g kg^{-1})	C/N ratio	pH
Recent	3940–4036 m	Barren land	1.8 ± 0.16^{a}	5.8 ± 1.9^{a}	0.4 ± 0.03^{a}	0.1 ± 0.01^{a}	4.3 ± 0.7^{a}	6.7 ± 0.3^{a}
Intermediate	3930–3970 m	*Calamagrostis emodensis, Saxifraga brunoniana, Anaphalis contorta, Chamerion speciosum*	2.2 ± 0.07^{a}	6.7 ± 2.9^{a}	1.5 ± 0.5^{b}	0.14 ± 0.03^{b}	10.4 ± 0.7^{b}	5.8 ± 0.4^{ab}
Late	3980–4020 m	*Geranium himalayense, Aconogonum tortuosum, Nepeta discolor, Potentilla atrisanguinea*	1.9 ± 0.05^{a}	20.1 ± 2.2^{b}	56.2 ± 11.8^{c}	4.2 ± 0.3^{c}	13.2 ± 2.2^{b}	4.9 ± 0.3^{b}

Values are mean ± SE of mean, $n = 4$. Mean values followed by different letters in superscript are significantly different ($P < 0.05$)

SMC was measured gravimetrically using 5 g soil sample immediately after soil transport to the laboratory [20]. The remaining soil was air-dried and made free of gravels, plant roots, and leaf litter by sieving through a 1 mm sieve. We measured soil pH using a glass electrode pH meter (Sension 7, Hach Company, USA) in a suspension [1:2.5 (w/v)] of soil in deionized water [21]. SOC and TN were measured using the potassium dichromate ($K_2Cr_2O_7$) oxidation method [22] and Kjeldahl method [23] using Kjeltec 8400 (Foss India Pvt. Ltd), respectively.

DNA Extraction, PCR Amplification, and Illumina Sequencing

Approximately 0.25 g of each soil sample was taken to extract environmental genomic DNA using a Nucleopore GDNA soil kit (Genetix Biotech Asia Pvt. Ltd, India) following the manufacturer's instructions. DNA concentrations were estimated using Qubit dsDNA HS Assay Kit (Life Technologies, USA). The bacterial V3 and V4 regions were amplified using the primer pair 338F (5′-CCTACG GGNGGCWGCAG-3′) and 806R (5′-GACTACHVGGG TATCTAATCC-3′) [24] with Illumina 16S Metagenomics Sequencing library preparation protocol. The PCR reaction was conducted with 12.5 µl of 2X Kappa Hifi Hotstart ReadyMix (Kappa Biosystems, Roche Sequencing and Life Science, USA), 1 µl each of 5 µM forward and reverse primer, and 10.5 µl of the template (12.5 ng of microbial DNA). The conditions for PCR reaction included an initial denaturation of 95 °C for 3 min, followed by 25 cycles of 95 °C for 30 s, 55 °C for 30 s, and 72 °C for 30 s, followed by a final extension for 10 min at 72 °C. A negative PCR (no template DNA) was included to monitor contamination. We purified and barcoded PCR products using Nextera XT kit (Illumina Inc., United States) and normalized amplicons to 2 nM for each library. An equal volume of each library was pooled, denatured, and diluted to 4 pM before loading onto the MiSeq flow cell (Illumina Inc., United States). Sequencing was performed at the Next Generation Genomics Facility at Center for Cellular, and Molecular Platforms (C-CAMP), Bangalore, India, using a 2×300 bp paired-end protocol on the Illumina MiSeq platform.

Sequence Data Processing

We used the MiSeq S.O.P. pipeline in Mothur v.1.40.5 to process Illumina-generated raw sequences [25]. We prepared full-length sequences from which good reads (>460 bp length with no homopolymer stretches longer than 8 bp) were identified and clustered (based on ≥97% similarity) using 16S rRNA reference database Greengenes (v.13_5). Subsequently, chimeric sequences were removed using Uchime, followed by all singletons, chloroplasts, archaea, mitochondria, and unknown origin sequences [26]. We used high-quality sequences to estimate pair-wise distances and generate single-linkage clusters with ≥97% sequence similarity. The longest read from each cluster was used as the reference sequence for a taxonomic assignment against the Greengenes database (v.13_5). Quantitative estimates of individual reads per taxonomic unit were generated from all sequences in each cluster and their replicates (≥97% similarity). The dataset was normalized by rarefying the sequences to the lowest sample-specific sequencing depth with maximum Good's coverage [25]. Finally, the sequences were clustered into different taxonomic levels for operational taxonomic unit (OTU) abundance and composition analysis. The data were sorted to separate the abundant and rare taxa based on their relative abundances. OTUs with ≥1% relative abundance were considered abundant, whereas ≤0.1% was considered rare [27].

Co-occurrence Network Construction

Bacterial interspecies interactions were identified by constructing co-occurrence ecological networks using Random Matrix Theory (RMT)-based method in Molecular Ecological Network Analysis (MENA) pipeline [28]. We performed the Pearson correlation ($P<0.05$) between OTUs at genus level having relative abundances >0.1% in all samples during network construction at an identical similarity threshold of 0.87 between recent and intermediate communities (network-RI) and intermediate and late communities (network-IL). Two networks (RI and IL) were constructed to understand the shift in interspecies interaction during bacterial succession from one period to the other. Various indices were calculated, including node and link numbers, average degree (avgK), average clustering coefficient (avgCC), average path distance (GD), density (D), modularity (M), and connectedness (Con) to evaluate and compare the overall topological features of the networks [28]. The networks were separated into different modules using fast greedy modularity optimization [28], and a submodule structure layout for the network graphs was visualized using Cytoscape 3.8.2 [29]. In the graphs, each node represents one genus, and each link represents one significant correlation.

Functional Analysis of the Bacterial Community

The genetic functional potential of the bacterial community was predicted using the PICRUST (Phylogenetic Investigation of Communities by Reconstruction of Unobserved States) pipeline on the galaxy server [11] (https://galaxyproject.org/use/langille-lab/). Taxonomic classification of 16S sequences at ≥97% similarity was conducted against the Greengenes database. Each 16S sequence was processed to pre-computed closed-reference OTUs against the Greengenes database 13.5 to find the "nearest neighbor of the reference sequence." The OTU table was normalized according to the 16S rRNA gene copy number. The functional prediction was performed using the normalized OTU table against the Kyoto Encyclopedia of Genes and Genomes (KEGG) orthology database. The KEGG orthology (KO) assignments were performed at level 1 and 2 categories. The nearest sequence taxon index assessed the accuracy of the predicted metagenome. For our analysis, we classified the predicted functions into most abundant traits having relative abundance ≥1% at KO levels 1 and 2. Relative abundance

of genes (Supplementary Table S2) involved in C, N, S, and P cycles was calculated from the predicted functions of the metagenome.

Data Analyses

We calculated bacterial alpha diversity through three indices: species richness (Sobs), evenness, and diversity based on Shannon's Index (H) [30] for each sample using the Mothur platform. Before the analysis, we tested normality and heteroscedasticity of data by the Shapiro–Wilk and Levene tests, respectively. We used One-way analysis of variance (ANOVA) to determine significant differences in environmental variables, alpha diversity indices, and functional traits between the sites. Further, Tukey's honest significance difference post-hoc test was applied for pair-wise comparisons of mean at 95% confidence intervals where differences were significant.

We calculated the Bray–Curtis dissimilarity matrix for beta diversity estimation after the Hellinger transformation of rarefied abundance data at phyla, class, and genus levels. For visual interpretation of differences in the bacterial community, composition principal coordinates analysis (PCoA) using the Bray–Curtis dissimilarity matrix was used. We used Multi-Response Permutation Procedure (MRPP) analysis [31] with 9999 permutations to test any significance in compositional differences.

We performed multiple ordinary least-square (OLS) regression analyses with stepwise forward selection to assess the relationship of environmental variables with bacterial richness, evenness, and diversity. Since SOC and TN showed high correlation ($r = 0.94$, $P < 0.001$) (Supplementary Fig. S2), regressions were performed with SOC only. Based on Akaike's information criterion, the most parsimonious model was selected [32]. We performed the Mantel test with the Pearson correlation to test the relationship of bacterial community composition with environmental variables. A forward selection was performed with environmental variables using stepwise regression (with 999 permutations), followed by redundancy analysis (RDA) using the Hellinger transformed bacterial abundance data to identify environmental variables that significantly explained the variation in abundant phyla. Only those environmental variables having VIF value less than 10 were included in the analysis. The RDA model and the environmental variables were tested by permutation test using ANOVA. Finally, we performed a structural equation model (SEM) analysis to determine both direct and indirect effects of environmental variables on bacterial richness, α-diversity, and composition. We used the first axis of PCoA of the Bray–Curtis dissimilarity matrix for the community composition [33]. We developed a path model based on theoretical knowledge to relate environmental variables including vegetation, MAT, SMC, SOC, C/N, and pH with bacterial richness, diversity, and composition. To improve the fit between the model and the data, the initial theoretical model was modified for the correct specification of theoretical causal relationships between variables before analysis. Maximum likelihood estimation was used to compare the SEM model with the observations. The model fitness with the data was tested using Comparative Fit Index (CFI), Akaike Information Criteria (AIC), and Root-Square-Mean Errors of Approximation (RMSEA). Good model fits were indicated by a high CFI (>0.90), low AIC, and low RMSEA (<0.05) [34]. All analyses were conducted in R 4.0.3 (http://www.R-project.org/) through RStudio 1.3.1093, 2020 (https://rstudio.com/products/rstudio/) using vegan 2.5-7 (https://cloud.r-project.org/package=vegan), lavaan 0.6–9 (https://cloud.r-project.org/package=lavaan), dplyr 1.0.5 (https://cloud.r-project.org/package=dplyr), and ggplot2 3.3.3 (https://cloud.r-project.org/package=ggplot2) [31, 35].

Availability of Data and Material

The DNA sequence dataset has been deposited to the National Centre for Biotechnology Information (NCBI) Short Read Archive (https://www.ncbi.nlm.nih.gov/sra). The BioProject accession number is PRJNA754406.

Results

Variation in Soil Properties

Soil properties varied significantly across the sites (Table 1 and Supplementary data.xlsx). SMC, SOC, TN, and C/N significantly increased ($P < 0.05$), while pH significantly decreased ($P < 0.05$) from the recent to late stage. MAT showed no significant difference ($P = 0.079$).

Variation in Bacterial α-Diversity

Illumina sequencing across 12 samples resulted in a total of 654,842 high-quality sequences averaging $54{,}570 \pm 8940$ sequence reads per sample (Supplementary Table S3). Good's coverage ranged from 0.92% to 99.9% (Supplementary Table S3), indicating that the sequencing was adequate and represented most bacterial communities at the study sites.

The alpha diversity indices indicated that bacterial community richness, evenness, and Shannon diversity increased significantly from 816 to 8008, 0.36–0.83, and 2.42–7.52, respectively, from the recent to late-stage post-deglaciation ($P < 0.05$) (Supplementary Fig. S3).

Variation in Bacterial β-Diversity

Considering a ≥97% sequence similarity, we identified 42,794 OTUs that were classified into 37 phyla (97% of the OTUs), 93 classes (96.9%), 168 orders (72.4%), 332 families (68.5%), 452 genera (57%), and 86 species (1%). Due to the low classification percentage at the species level, all further diversity analyses were conducted at phyla, class, and genera level only.

The number of abundant bacterial taxa and their relative abundances changed drastically from recent to late stages at all three taxonomic levels (Fig. 2a). At phyla level, the increasing abundant taxa were *Proteobacteria* (relative abundance from recent to intermediate to late stage: 6.8–27.2–14.5%), *Firmicutes* (1.4–0.9–24.2%), *Planctomycetes* (0.01–0.36–7.6%), *Acidobacteria* (0–1.3–6%), *Verrucomicrobia* (0.01–0.5–5.8%), Candidatus TM6 (0.003–0.12–4.1%), and *Chloroflexi* (0.04–0.17–3.6%), while the decreasing abundant taxa was *Actinobacteria* (89–62–27.5%). Increasing abundant taxa at class level were *Bacilli* (0.53–0.6–22.9%), *Thermoleophilia* (0.09–0.5–9.3%), *Alphaproteobacteria* (1.4–14.5–10.44%), *Planctomycetia* (0.01–0.27–5.5%), and *Spartobacteria* (0.01–0.43–5.4%), while *Actinobacteria* (90–62–15.7%) decreased in abundance. At genus level, *Bacillus* (0.08–0.04–16.5%), Candidatus DA101 (0.01–0.375–5.11%), *Sporosarcina* (0–0.38–3.2%), *Rhodoplanes* (0.01–1.03–3.3%), and *Pseudonocardia* (0.07–0.07–2%) became more abundant, while *Mycobacterium* decreased (89–62–0.9%). This increase in abundance of bacterial taxa led to a more evenly distributed community in the late stage compared to the recent stage, which was dominated by a single bacterial taxon at different taxonomic levels viz., *Actinobacteria* at phyla and class level (89% and 90%, respectively) and *Mycobacterium* (89%) at the genus level.

Bacterial beta diversity varied significantly between the three habitats as indicated by the MRPP analysis at phyla ($A = 0.439$ and $P < 0.001$), class ($A = 0.398$ and $P < 0.001$) and genus levels ($A = 0.357$ and $P < 0.001$). The significant change in bacterial beta diversity is visually represented by PCoA analysis (Fig. 2b), where three distinct clusters were formed at three levels.

Bacterial Co-occurrence Pattern Across the Site

The bacterial co-occurrence networks between the sites showed all features of ecological networks, including scale free (R^2 of power-law ranged from 0.57 to 0.61), small world

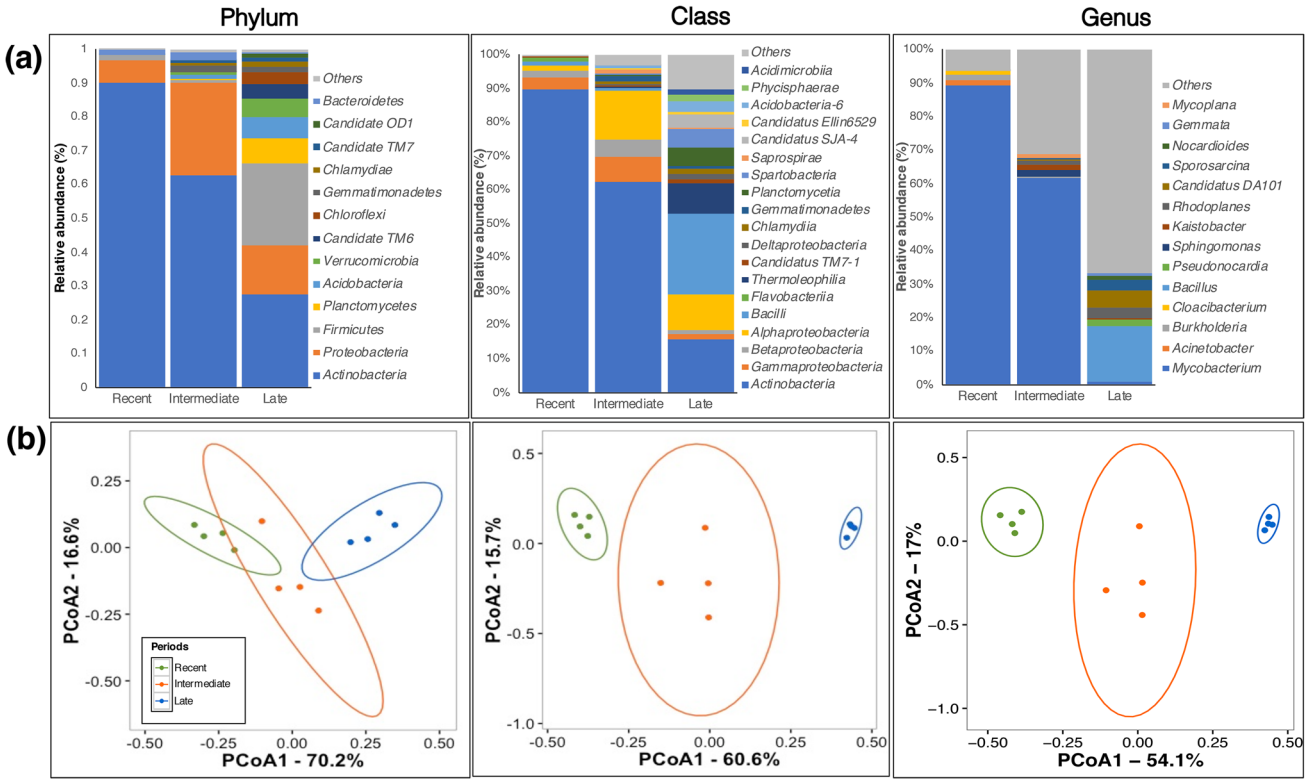

Fig. 2 Variation in bacterial beta diversity at different post-deglaciation periods. **a** Relative abundances of bacterial phyla, class, and genera across the periods. Here "Others" represent all taxa with relative abundances < 1% and **b** principal coordinates analysis (PCoA) based on Bray–Curtis dissimilarity of bacterial communities at phyla, class, and genera levels

(GD ranged from 3.1 to 3.5), non-random, and modular (modularity = 0.53) (Supplementary Table S4). Comparison of topological features showed that the number of nodes, links, and links per node were greater in the network-IL than network-RI by 168%, 455%, and 110%, respectively (Supplementary Table S4 and Fig. 3). In both the networks, 4 joint modules having nodes ≥ 6 were observed within the bigger network (Fig. 3 and Supplementary Fig. S4). The modules in network-IL showed 15% more positive interactions than network-RI. In network-RI, most genera belonging to the phyla *Proteobacteria*, *Actinobacteria, Verrucomicrobia,* and *Bacteroidetes* showed more negative interactions than positive. In network-IL, most genera of the phyla *Proteobacteria*, *Actinobacteria, Planctomycetes, Gemmatimonadetes,* and *Bacteroidetes* showed more positive interactions, while *Verrucomicrobia*, *Acidobacteria*, and *Firmicutes* showed more negative interactions. The avgK, avgCC, GD, and Con increased by 102%, 28%, 12%, and 5%, respectively, from network-RI to network-IL, whereas D decreased by 24%.

Shifts in Abundant Functional Traits of the Bacterial Community

PICRUST predicted metagenome functions are shown in Fig. 4a and b, representing the most abundant traits and biogeochemical cycles, respectively, at levels 1 and 2 KO categories. The nearest taxon sequence index (NSTI) value of the samples ranged from 0.008 to 0.24. At level 1 KO category, we identified four abundant functional pathways of the metagenome, i.e., metabolism, environmental information processing, genetic information processing, and cellular processes. Of these functions, the relative abundances of the environmental and genetic information processing (6.8–12% and 4–10%, respectively) and cellular processes (0.12–1.4%) increased significantly from the recent to late stage ($P < 0.05$). In contrast, the relative abundance of metabolism, the dominant pathway at the recent stage, decreased drastically in the later stage (38–24%, $P < 0.05$) (Fig. 4a). However, we observed an increase in the relative

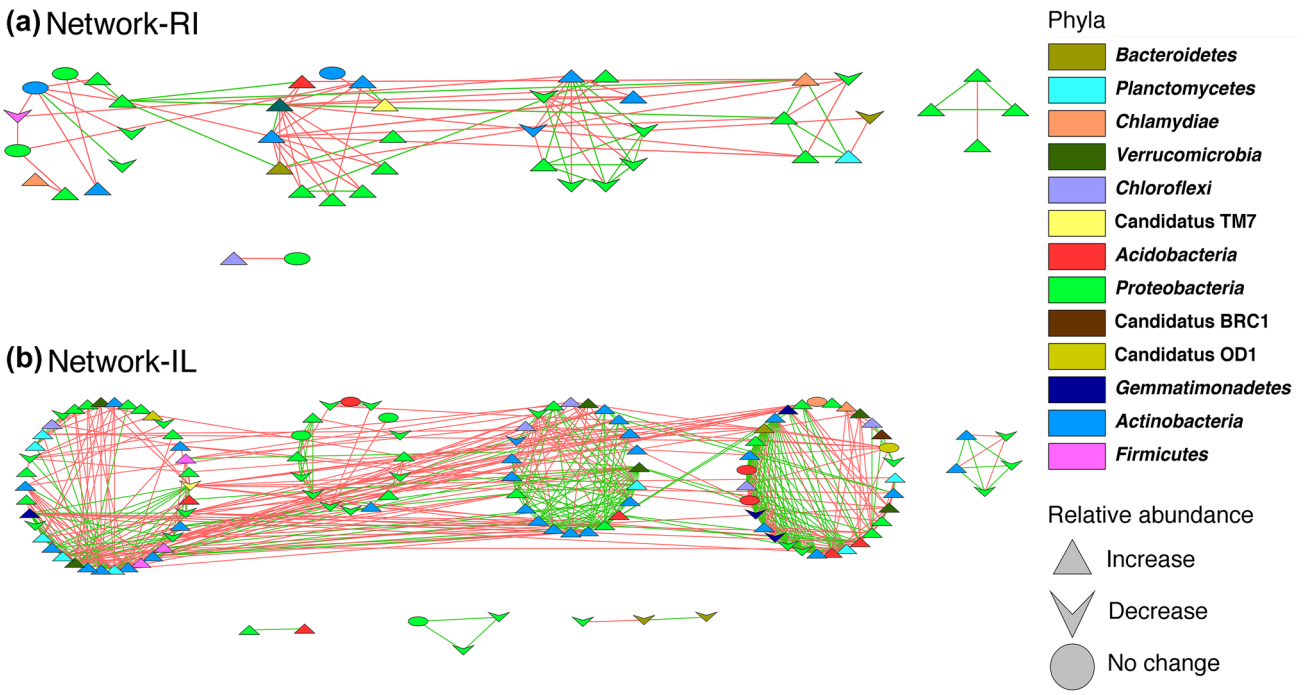

Fig. 3 Submodule structure layout of bacterial co-occurrence networks of **a** recent and intermediate communities (Network-RI) and **b** intermediate and late communities (Network-IL) based on Random Matrix Theory. Each node represents a genera, and each straight line (link) represents a significant ($P < 0.05$) correlation. Nodes of the same color represent the same phyla the genera belong to. Nodes with triangle shapes represent genera with increasing abundance, inverted triangle shapes represent decreasing abundance, and oval shapes represent genera with no change in their relative abundance. Green and red lines indicate positive and negative correlations between nodes, respectively. Each module in the network is represented by a circle composed of nodes. The figure was generated in Cytoscape 3.2.8 (Color figure online)

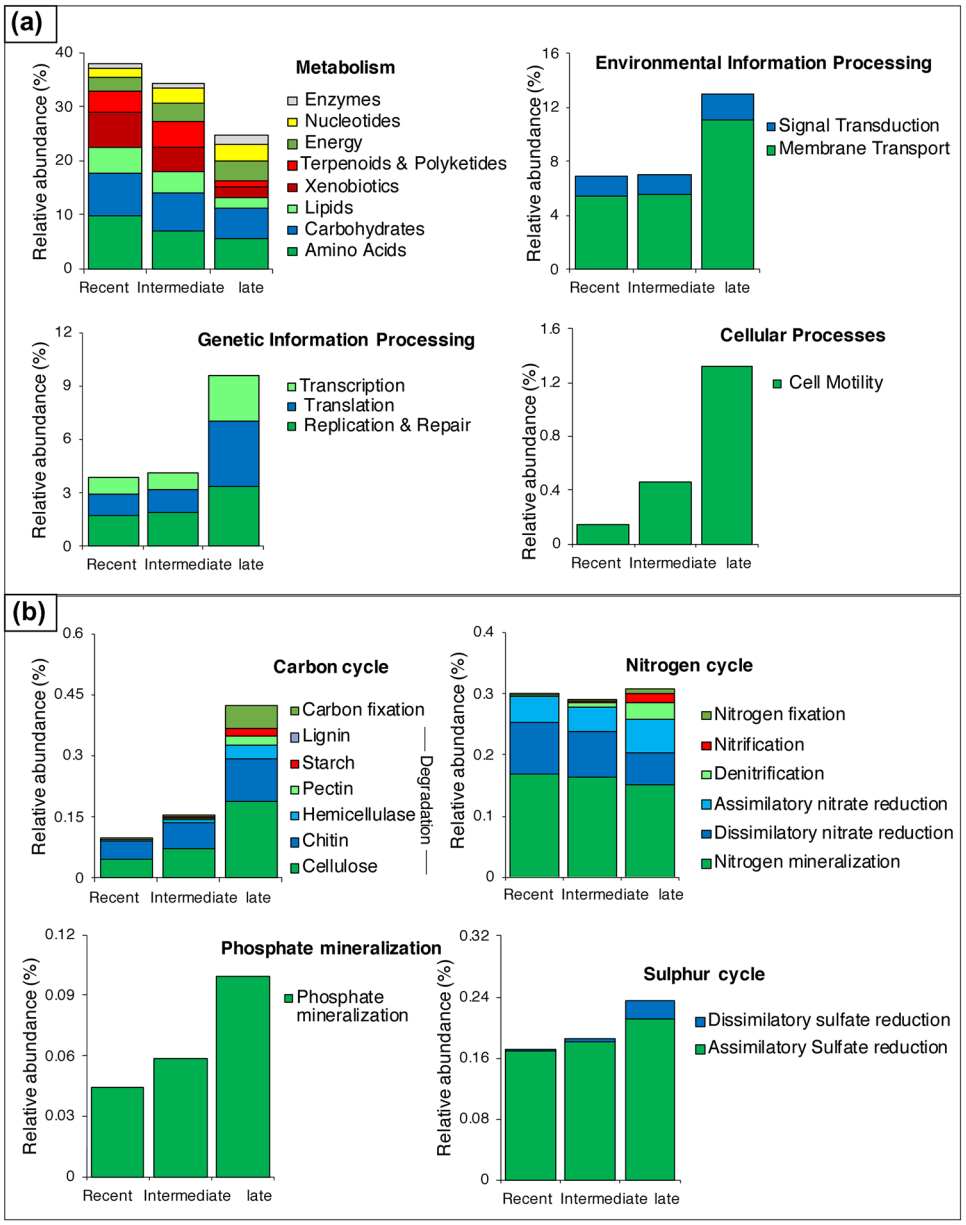

Fig. 4 Relative abundance of **a** most abundant predicted metagenome functions and **b** genes involved in C, N, P, and S cycles at level 1 KO category across different post-deglaciation periods. Each bar represents the relative abundances of all pathways associated with the abundant functions and C, N, S, and P cycles at the level 2 KO category (Color figure online)

abundance of energy and enzymes metabolism at the level 2 KO category.

Shifts in Biogeochemical Pathways of the Bacterial Community

The overall relative abundance of genes involved in each of C, S, and P cycles increased significantly ($P < 0.05$), whereas that of N remained the same from recent to late stage at level 1 KO category ($P = 0.92$) (Fig. 4b). Relative abundance of both labile (cellulose, hemicellulose, and starch) and recalcitrant (chitin and pectin) C decomposition and C fixation pathways significantly increased ($P < 0.05$) post-deglaciation at level 2 KO. Although the overall relative abundance of N cycling genes showed no change, N fixation, nitrification, and denitrification relative abundances increased. On the other hand, the relative abundance of dissimilatory N reduction pathways decreased ($P < 0.05$).

Factors Affecting α and β-Diversity

Multiple linear regressions showed that SMC, SOC, and C/N ratio positively affected α-diversity across the sites (Supplementary Table S5). Variability in richness ($R^2 = 0.8$, $P < 0.001$) was significantly explained by SMC and CN ratio, while that in evenness ($R^2 = 0.67$, $P < 0.001$) and diversity ($R^2 = 0.7$, $P < 0.001$) were significantly explained by SOC. We found no significant relationships between

α-diversity and pH, CN, and MAT. The mantel test showed that β-diversity was significantly correlated to all the measured soil properties (SMC: $r=0.565$, $P<0.001$; SOC: $r=0.66$, $P<0.01$; TN: $r=0.715$, $P<0.01$; C/N: $r=0.419$, $p<0.05$, and pH: $r=0.365$, $P<0.05$) and not MAT. The Redundancy Analysis showed that SMC and C/N explained 65% (F (2,9) = 8.5, $P<0.001$) of the variability in the relative abundances of the abundant phyla across the sites, except *Proteobacteria*, *Actinobacteria*, *Chlamydiae*, and Candidatus OD1 (Supplementary Fig. S5). The SEM model (CFI = 0.95, AIC = 78.4, RMSEA = 0.2, $P<0.05$) explained 80%, 93%, and 95% of the variation in bacterial richness, α-diversity, and composition, respectively (Fig. 5). Diversity was strongly related to SOC ($\lambda=0.24$, $P<0.05$) and richness ($\lambda=0.77$, $P<0.001$) which was influenced directly by SMC ($\lambda=0.42$, $P<0.01$) and C/N ($\lambda=0.59$, $P<0.001$) and indirectly by SOC ($\lambda=0.47$, $P<0.01$), and vegetation type ($\lambda=-0.33$, $P<0.01$). Community composition was related to richness ($\lambda=0.34$, $P<0.001$) and affected directly by SOC ($\lambda=0.46$, $P<0.001$), SMC ($\lambda=-0.46$, $P<0.001$), and C/N ($\lambda=-0.2$, $P<0.05$). The standardized path coefficients of direct, indirect, and total effects are shown in Supplementary Table S6.

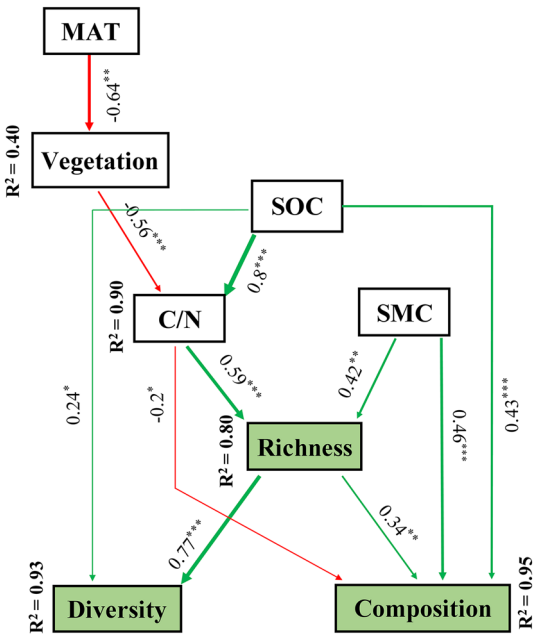

Fig. 5 Structural equation model (SEM) showing the causal influences of vegetation, MAT, SMC, SOC, and C/N ratio on bacterial richness, α-diversity, and composition. Red and green lines, respectively, represent significant negative and positive effects. The width of the arrows is based on the standardized path coefficients indicating the strength of the causal effect. The standardized coefficients are marked above each path (* indicates significant ($P<0.05$) effects, ** indicates significant ($P<0.01$) effects, *** indicates significant ($P<0.001$) effects). R^2 values represent the percentage of variance explained for each variable (Color figure online)

Discussion

This study on bacterial community succession across a temporal sequence ranging from ~ 20 to 300 years in the foreland of the Gangotri glacier provides an in-depth understanding of changes in the community diversity and functional traits during different periods' post-deglaciation. Alpha diversity measurements indicated that the community in the recently exposed site had low richness and diversity. This community possibly originates from atmospheric depositions of dust particles through precipitation and wind or from supraglacial snow (a glacier zone where sunlight penetrates) and subglacial sediments (bedrock at ice-melt water interface) through glacial runoff [4, 36]. In the cold, nutrient-poor environment, the community focuses on cell metabolism (Fig. 4) rather than growth, probably acquiring energy from atmospheric deposition of C and N sources or trace gases such as H_2 and CO [4, 37]. With time, the bacterial community shifted towards a richer and evenly distributed community from the recently deglaciated stage to late stage. A substantial increase in bacterial OTUs and their relative abundances resulted in a highly diverse community during the transition. Our results are in agreement with previous studies from other glaciated regions of the world reporting an increase in bacterial diversity during progressive stages post-deglaciation [3, 38].

The linear increase in alpha diversity suggests that environmental factors increasing across the sites might control the bacterial community diversity. In our study, the barren land in the recent stage developed into a sparsely vegetated area in the intermediate stage and a well-developed meadow in the late phase (Table 1). The increase in alpha diversity corresponds to the increase in SOC, C/N ratio, and SMC associated with developing vegetation (Supplementary Fig. S3 and Table 1), indicating that soil nutrients and their availability influence bacterial diversity post-deglaciation. This assumption was supported by the regression analysis where the majority of variability in bacterial richness (80%), evenness (67%), and diversity (70%) were explained by SMC, SOC (and in turn TN for its high correlation with SOC, $r=0.94$, $P<0.001$) and C/N ratio (Supplementary Table S5). The SEM analysis established the positive influence of soil nutrients and their availability on bacterial richness and diversity (Fig. 5). Previous studies have shown the critical role of soil nutrients in regulating bacterial diversity post-deglaciation due to its direct influence on bacterial growth, metabolism, and reproduction [39]. It is well known that soil microorganisms have a C/N ratio of 8:1 and grow optimally in soil with a C/N ratio close to 24:1 [40]. The increasing C/N ratio from recent to late stage supported more bacterial

taxa to increase due to more available organic C, which resulted in greater bacterial diversity. The crucial role of the C/N ratio was also reported by earlier studies [19].

The community composition showed rapid turnover during 300 years post-deglaciation. The community shifted from a single bacterial taxa-dominated community in the recent stage to a diverse one in the late stage, where several taxa become relatively abundant (Fig. 2a). This shift in the bacterial composition is most likely related to vegetation development and an adequate supply of nutrients [39, 41]. Under nutrient-limited conditions, communities compete for substrate resulting in competitive interaction in the community eventually leading to the dominance of specific taxa [42]. In the recent and intermediate communities, negative and competitive interactions led to the dominance of *Actinobacteria,* followed by an increasing abundance of *Proteobacteria* and *Verrucomicrobia* (Figs. 2a and 3). With adequate nutrient supply, communities become cooperative, favoring the growth of multiple taxa [42]. This cooperative nature was observed in the co-occurrence pattern between intermediate and late stages, where positive interactions led to an increase in abundance of different bacterial phyla *Planctomycetes, Gemmatimonadetes,* and *Bacteroidetes* (Figs. 2a and 3). The positive feedback influence of vegetation development and nutrients on community composition was established by mantel test, RDA, and SEM analysis (Supplementary Fig. S5 and Fig. 5).

The taxonomic analysis showed that the genus *Mycobacterium* belonging to *Actinobacteria* phyla was the pioneer bacterial taxa dominating the recent stage. This genus is abundant in many natural ecosystems, including soil, lakes, and rivers [43]. They have also been found in inorganic sediments, rocks, and dust particles and are the most stress-tolerant bacteria so far identified [43]. Due to their exceptional stress tolerance, they are ubiquitous in nature and can survive extreme environments such as hot springs, permafrost, and glaciers [43]. They generally colonize environments with low microbial diversity [43] and, in this study, have been found to inhabit an active moraine solely. This contrasts to earlier studies from polar and alpine glaciers where it is co-inhabited with other abundant taxa such as *Methylobacterium, Rhodococcus, Sphingomonas, Arthrobacter, and Frigoribacterium* [43, 44]. The phyla *Actinobacteria* is the oldest living organism with extraordinary temperature stress tolerance [43, 45]. *Actinobacteria* can predominate cold oligotrophic environments by forming mycelia required to acquire nutrients [46]. In addition, they play a crucial role in soil development through N and P mobilization, chitin degradation, and inhibition of plant pathogenic fungal species growth [47]. Consequently, they create favorable soil conditions by establishing C, N, and P pools to assist the growth of other microbes and eventually plant colonization. The role of *Actinobacteria* was evident in our study as different bacterial phyla *Proteobacteria*, *Firmicutes*, *Planctomycetes*, *Acidobacteria*, *Verrucomicrobia*, and *Chloroflexi,* gradually increased in abundance in the intermediate and late stage with the concurrent development of soil and plants communities. *Actinobacteria* were earlier reported from polar and alpine glacial forelands and lakes [2–4], cryoconite holes [48], and glacial meltwater [49], suggesting their ubiquitous nature in diverse cold habitats. Their ability to utilize atmospheric trace gases as energy sources makes them efficient to adapt and survive in low nutrient cold habitats [37].

The high degree of shift in bacterial diversity (Supplementary Fig. S3) and composition (Fig. 2) post-deglaciation led to considerable variation in the functional traits (Fig. 4). The community in the recent stage mainly depended on metabolic functions to develop resting cellular forms for sustaining life in the cold oligotrophic environment [50]. As the community diversified in the later stages, they focused more on functions that allowed them to gain mobility, sense environmental signals, and import nutrients to reproduce and grow faster for their co-existence with soil development and plant growth [49, 51]. The functional progression was evident from the high relative abundance of *Proteobacteria, Firmicutes, Planctomycetes*, and *Acidobacteria* at the later stages that are well-known copiotrophs having efficient membrane transport and signaling pathways, stress response regulatory system, and carbohydrate metabolism [49, 52].

Nutrient availability is well known to impact bacterial succession [53]. We observed a substantial increase in relative abundances of functional pathways along with the development of new ones involved in C, N, S, and P cycles post-deglaciation (Fig. 4). The increase in labile and recalcitrant C decomposition suggests functional adaptation of the bacterial community to utilize new nutrient resources such as cellulose, hemicellulose, starch, pectin, and chitin, accumulating in soil due to the growth of plants and other microbial communities [38]. The community in the later stages increased their C fixation ability, coinciding with the increase in abundance of the genus *Clostridia*, known to fix atmospheric CO_2 using the Wood-Ljungdahl pathway [54].

N mineralization and assimilatory N reduction relative frequencies showed no variation, suggesting a functional similarity between the communities. On the contrary, N fixation, nitrification, and denitrification increased from the intermediate to late stage, indicating that specific bacterial taxa display these functional abilities. For instance, bacterial genera *Allorhizobium*, *Mesorhizobium, Bradyrhizobium* known to fix N, and *Pseudomonas* and *Bacillus* known for denitrification [55] increased in abundance from the intermediate to late periods. The increase in N fixation processes most likely led to N accumulation in the ecosystem, promoting microbial and plant growth in the late stage [56]. Similarly, an increase in phosphate mineralization can enhance phosphate availability for microbial and plant growth [57],

whereas sulfur reduction pathways are used to fulfill increasing energy demand [58].

Conclusion

This study provides the first report on soil bacterial community ecological traits associated with their succession and nutrient cycling from newly exposed to late soil development stage over ~ 300 years post-deglaciation. Results reveal the evolution of a simple pioneer community (dominated by *Mycobacterium* genus), mainly focused on metabolic activities, into a more diverse and functionally specialized community at the later stages. The study also demonstrates the progression in biogeochemical pathways necessary for soil fertility and plant growth post-deglaciation. A possible limitation of our study could be the single time point sampling which may not reflect the community trait variations during different seasons and years. However, as evidenced in earlier studies, the non-significant seasonal and interannual variation in the bacterial community [39, 42] results generated in this study can improve the predictability of ecosystem development and succession models under climate change.

Supplementary Information The online version contains supplementary material available at https://doi.org/10.1007/s00284-022-02779-8.

Acknowledgements Forest Department of Uttarakhand provided necessary permits to research in Gangotri National Park. We acknowledge help from Dr. Devendra Kumar and Umed S Rana (field assistance), Arun Kumar (laboratory work), Dr. Punyasloke Bhadury (DNA sequencing), Dr. Awadhesh Pandit and Tejali Naik (NGS work), Sitendu Goswami, and Dr. Raman Kumar (Data analysis). We thank Dr. Samrat Mondol, Dr. Sathyakumar (Nodal Scientist, NMSHE), Dr. Dhananjay Mohan (Director), Dr. Y.V. Jhala (Dean), Dr. Bitapi Sinha (Research Coordinator), and Nodal Officer of Wildlife Forensics and Conservation Genetics Cell of Wildlife Institute of India for facilitating this work.

Author Contributions Conceptualization: PT and PB; Funding acquisition: GSR, GT, and PB; Resources: GSR and GT; Supervision: GSR and GT; Methodology: PT and PB; Data curation: PB; Formal analysis and investigation: PB and PT; Writing—original draft preparation: PB and PT; Writing—review and editing: GSR, GT, PB, and PT.

Funding This research is part of the project National Mission for Sustaining the Himalayan Ecosystem (NMSHE) funded by the Department of Science and Technology, Government of India (Grant No. DST/SPLICE/CCP/NMSHE/TF-2/WII/2014[G]). Partial funding for the bacterial Next Generation Sequencing was provided by the United Nations Development Programme and the Ministry of Environment, Forest and Climate Change Government of India through the Third National Communication project (Grant No. 7/2/2015-CC). Pamela Bhattacharya was supported by the Council of Scientific and Industrial Research, Government of India (Award no. 09/668(0012)/2019– EMR–I).

Data Availability The DNA sequence dataset has been deposited to the National Centre for Biotechnology Information (NCBI) Short Read Archive (https://www.ncbi.nlm.nih.gov/sra). The BioProject accession number is PRJNA754406.

Code Availability Not applicable.

Declarations

Conflict of interest The authors declare no competing interests.

Ethical Approval Not applicable.

Consent to Participate All authors gave consent to participate and publish all information provided in the manuscript.

Consent to Publish All authors gave consent to participate and publish all information provided in the manuscript.

References

1. Cramer W, Bondeau A, Woodward FI et al (2001) Global response of terrestrial ecosystem structure and function to CO_2 and climate change: results from six dynamic global vegetation models: ecosystem dynamics, CO_2 and climate change. Glob Change Biol 7:357–373. https://doi.org/10.1046/j.1365-2486.2001.00383.x
2. Venkatachalam S, Kannan VM, Saritha VN et al (2021) Bacterial diversity and community structure along the glacier foreland of Midtre Lovénbreen, Svalbard. Arct Ecol Indic 126:107704. https://doi.org/10.1016/j.ecolind.2021.107704
3. Wu X, Zhang W, Liu G et al (2012) Bacterial diversity in the foreland of the Tianshan No. 1 glacier China. Environ Res Lett 7:014038. https://doi.org/10.1088/1748-9326/7/1/014038
4. Hotaling S, Hood E, Hamilton TL (2017) Microbial ecology of mountain glacier ecosystems: biodiversity, ecological connections and implications of a warming climate. Environ Microbiol 19:2935–2948. https://doi.org/10.1111/1462-2920.13766
5. Alfaro FD, Salazar-Burrows A, Bañales-Seguel C et al (2020) Soil microbial abundance and activity across forefield glacier chronosequence in the northern Patagonian Ice Field, Chile. Arct Antarct Alp Res 52:553–562. https://doi.org/10.1080/15230430.2020.1820124
6. Frkova Z, Pistocchi C, Vystavna Y, et al (2021) Phosphorus dynamics during early soil development in extreme environment. Soils and biogeochemical cycling. Preprint.
7. Bradley JA, Anesio AM, Arndt S (2017) Microbial and biogeochemical dynamics in glacier forefields are sensitive to century-scale climate and anthropogenic change. Front Earth Sci. https://doi.org/10.3389/feart.2017.00026
8. Gilbert JA, Dupont CL (2011) Microbial metagenomics: beyond the genome. Annu Rev Mar Sci 3:347–371. https://doi.org/10.1146/annurev-marine-120709-142811
9. Feng W, Zhang Y, Yan R et al (2020) Dominant soil bacteria and their ecological attributes across the deserts in northern China. Eur J Soil Sci 71:524–535. https://doi.org/10.1111/ejss.12866
10. Ortiz-Estrada ÁM, Gollas-Galván T, Martínez-Córdova LR, Martínez-Porchas M (2019) Predictive functional profiles using metagenomic 16S rRNA data: a novel approach to understanding the microbial ecology of aquaculture systems. Rev Aquac 11:234–245. https://doi.org/10.1111/raq.12237
11. Langille MGI, Zaneveld J, Caporaso JG et al (2013) Predictive functional profiling of microbial communities using 16S rRNA marker gene sequences. Nat Biotechnol 31:814–821. https://doi.org/10.1038/nbt.2676

12. Sun S, Jones RB, Fodor AA (2020) Inference-based accuracy of metagenome prediction tools varies across sample types and functional categories. Microbiome 8:46. https://doi.org/10.1186/s40168-020-00815-y
13. Shrestha UB, Gautam S, Bawa KS (2012) Widespread climate change in the Himalayas and associated changes in local ecosystems. PLoS ONE 7:e36741. https://doi.org/10.1371/journal.pone.0036741
14. Singh RK (2018) Impact of Climate Change on the Retreat of Himalayan Glaciers and Its Impact on Major River Hydrology: Himalayan Glacier Hydrology. In Climate Change and Environmental Concerns: Breakthroughs in Research and Practice, IGI Global, pp. 681–694
15. Pusalkar PK, Singh DK (2012) Flora of Gangotri national park, western Himalaya. Botanical Survey of India, India
16. Tiwari P, Bhattacharya P, Rawat GS, Talukdar G (2021) Equilibrium in soil respiration across a climosequence indicates its resilience to climate change in a glaciated valley, western Himalaya. Sci Rep. https://doi.org/10.1038/s41598-021-02199-x
17. Sanyal AK, Uniyal VP, Chandra K, Bhardwaj M (2013) Diversity, distribution pattern and seasonal variation in moth assemblages along altitudinal gradient in Gangotri landscape area, Western Himalaya, Uttarakhand, India. J Threat Taxa 5:3646–3653. https://doi.org/10.11609/JoTT.o2597.3646-53
18. Tiwari P, Bhattacharya P, Rawat GS et al (2021) Experimental warming increases ecosystem respiration by increasing aboveground respiration in alpine meadows of Western Himalaya. Sci Rep. https://doi.org/10.1038/s41598-021-82065-y
19. Lanzén A, Epelde L, Blanco F et al (2016) Multi-targeted metagenetic analysis of the influence of climate and environmental parameters on soil microbial communities along an elevational gradient. Sci Rep. https://doi.org/10.1038/srep28257
20. Rayment GE, Lyons DJ (2011) Soil chemical methods: Australasia. CSIRO Publishing, Collingwood, Vic
21. Blakemore LC, Searle PL, Daly BK (1987) Methods for chemical analysis of soils. NZ Soil Bureau, Dept. of Scientific and Industrial Research, Lower Hutt, N.Z.
22. Walkley A, Black IA (1934) An examination of the Degtjareff method for determining soil organic matter, and a proposed modification of the chromic acid titration method. Soil Sci 37:29–38. https://doi.org/10.1097/00010694-193401000-00003
23. Bremner JM (2018) Nitrogen-Total. In: Sparks DL, Page AL, Helmke PA et al (eds) SSSA book series. Soil Science Society of America, American Society of Agronomy, Madison, WI, USA, pp 1085–1121
24. Luo Z, Liu J, Zhao P et al (2019) Biogeographic patterns and assembly mechanisms of bacterial communities differ between habitat generalists and specialists across elevational gradients. Front Microbiol. https://doi.org/10.3389/fmicb.2019.00169
25. Schloss PD, Westcott SL, Ryabin T et al (2009) Introducing mothur: open-source, platform-independent, community-supported software for describing and comparing microbial communities. Appl Environ Microbiol 75:7537–7541. https://doi.org/10.1128/AEM.01541-09
26. Edgar RC, Haas BJ, Clemente JC et al (2011) UCHIME improves sensitivity and speed of chimera detection. Bioinformatics 27:2194–2200. https://doi.org/10.1093/bioinformatics/btr381
27. Pedrós-Alió C (2006) Marine microbial diversity: can it be determined? Trends Microbiol 14:257–263. https://doi.org/10.1016/j.tim.2006.04.007
28. Deng Y, Jiang Y-H, Yang Y et al (2012) Molecular ecological network analyses. BMC Bioinformatics 13:113. https://doi.org/10.1186/1471-2105-13-113
29. Shannon P, Markiel A, Ozier O et al (2003) Cytoscape: a software environment for integrated models of biomolecular interaction networks. Genome Res 13:2498–2504. https://doi.org/10.1101/gr.1239303
30. Spellerberg IF, Fedor PJ (2003) A tribute to Claude Shannon (1916–2001) and a plea for more rigorous use of species richness, species diversity and the 'Shannon-Wiener' Index: on species richness and diversity. Glob Ecol Biogeogr 12:177–179. https://doi.org/10.1046/j.1466-822X.2003.00015.x
31. Oksanen J, Guillaume Blanchet F, Friendly M Kindt R, Legendre P, McGlinn D, Minchin PR, O'Hara RB, Simpson GL, Solymos P, Henry M, Stevens M, Szoecs E, Wagner H (2020) Vegan: community ecology package. R package version 2.5-7. https://CRAN.R-project.org/package=vegan.
32. Johnson JB, Omland KS (2004) Model selection in ecology and evolution. Trends Ecol Evol 19:101–108. https://doi.org/10.1016/j.tree.2003.10.013
33. Li J, Ma Y-B, Hu H-W et al (2015) Field-based evidence for consistent responses of bacterial communities to copper contamination in two contrasting agricultural soils. Front Microbiol. https://doi.org/10.3389/fmicb.2015.00031
34. Grace JB (2007) Structural equation modeling and natural systems. Biometrics 63:977–977. https://doi.org/10.1111/j.1541-0420.2007.00856_13.x
35. R Core Team (2020) R: A language and environment for statistical computing. R Found Stat Comput, Vienna, Austria
36. Ciccazzo S, Esposito A, Borruso L, Brusetti L (2016) Microbial communities and primary succession in high altitude mountain environments. Ann Microbiol 66:43–60. https://doi.org/10.1007/s13213-015-1130-1
37. Ji M, Greening C, Vanwonterghem I et al (2017) Atmospheric trace gases support primary production in Antarctic desert surface soil. Nature 552:400–403. https://doi.org/10.1038/nature25014
38. Jangid K, Whitman WB, Condron LM et al (2013) Soil bacterial community succession during long-term ecosystem development. Mol Ecol 22:3415–3424. https://doi.org/10.1111/mec.12325
39. Bhattacharya P, Tiwari P, Rai ID et al (2022) Edaphic factors override temperature in shaping soil bacterial diversity across an elevation-vegetation gradient in Himalaya. Appl Soil Ecol 170:104306. https://doi.org/10.1016/j.apsoil.2021.104306
40. Brady NC, Weil RR (2002) The nature and properties of soils, 13th edn. Prentice Hall, New Jersey, p 249
41. Qiang W, He L, Zhang Y et al (2021) Aboveground vegetation and soil physicochemical properties jointly drive the shift of soil microbial community during subalpine secondary succession in southwest China. CATENA 202:105251. https://doi.org/10.1016/j.catena.2021.105251
42. Zhu B, Li C, Wang J et al (2020) Elevation rather than season determines the assembly and co-occurrence patterns of soil bacterial communities in forest ecosystems of Mount Gongga. Appl Microbiol Biotechnol 104:7589–7602. https://doi.org/10.1007/s00253-020-10783-w
43. Santos R, de Carvalho CCCR, Stevenson A et al (2015) Extraordinary solute-stress tolerance contributes to the environmental tenacity of mycobacteria: extraordinary stress-tolerance of mycobacteria. Environ Microbiol Rep 7:746–764. https://doi.org/10.1111/1758-2229.12306
44. Miteva VI, Sheridan PP, Brenchley JE (2004) Phylogenetic and physiological diversity of microorganisms isolated from a deep greenland glacier ice core. Appl Environ Microbiol 70:202–213. https://doi.org/10.1128/AEM.70.1.202-213.2004
45. Johnson SS, Hebsgaard MB, Christensen TR et al (2007) Ancient bacteria show evidence of DNA repair. Proc Natl Acad Sci 104:14401–14405. https://doi.org/10.1073/pnas.0706787104
46. Gupta P, Sangwan N, Lal R, Vakhlu J (2015) Bacterial diversity of drass, cold desert in Western Himalaya, and its comparison with Antarctic and Arctic. Arch Microbiol 197:851–860. https://doi.org/10.1007/s00203-015-1121-4

47. Shao K, Bai C, Cai J et al (2019) Illumina sequencing revealed soil microbial communities in a Chinese alpine grassland. Geomicrobiol J 36:204–211. https://doi.org/10.1080/01490451.2018.1534902
48. Edwards A, Pachebat JA, Swain M et al (2013) A metagenomic snapshot of taxonomic and functional diversity in an alpine glacier cryoconite ecosystem. Environ Res Lett 8:035003. https://doi.org/10.1088/1748-9326/8/3/035003
49. Ahmad T, Gupta G, Sharma A et al (2021) Metagenomic analysis exploring taxonomic and functional diversity of bacterial communities of a Himalayan urban fresh water lake. PloS One 16:e0248116
50. Dube JP, Valverde A, Steyn JM et al (2019) Differences in bacterial diversity, composition and function due to long-term agriculture in soils in the eastern free state of South Africa. Diversity 11:61. https://doi.org/10.3390/d11040061
51. Kazemi S, Hatam I, Lanoil B (2016) Bacterial community succession in a high-altitude subarctic glacier foreland is a three-stage process. Mol Ecol 25:5557–5567. https://doi.org/10.1111/mec.13835
52. Koch AL (2001) Oligotrophs versus copiotrophs. BioEssays 23:657–661
53. Ortiz-Álvarez R, FiererRíos NA et al (2018) Consistent changes in the taxonomic structure and functional attributes of bacterial communities during primary succession. ISME J 12:1658–1667. https://doi.org/10.1038/s41396-018-0076-2
54. Drake HL, Gößner AS, Daniel SL (2008) Old acetogens, new light. Ann N Y Acad Sci 1125:100–128. https://doi.org/10.1196/annals.1419.016
55. Kuypers MMM, Marchant HK, Kartal B (2018) The microbial nitrogen-cycling network. Nat Rev Microbiol 16:263–276. https://doi.org/10.1038/nrmicro.2018.9
56. Wang J, Wu Y, Li J et al (2021) Energetic supply regulates heterotrophic nitrogen fixation along a glacial chronosequence. Soil Biol Biochem 154:108150. https://doi.org/10.1016/j.soilbio.2021.108150
57. Tiwari P, Singh JS (2017) A plant growth promoting rhizospheric *Pseudomonas aeruginosa* strain inhibits seed germination in *Triticum aestivum* (L) and *Zea mays* (L). Microbiol Res. https://doi.org/10.4081/mr.2017.7233
58. Florentino AP, Weijma J, Stams AJM, Sánchez-Andrea I (2016) Ecophysiology and application of acidophilic sulfur-reducing microorganisms. In: Rampelotto PH (ed) Biotechnology of extremophiles. Springer International Publishing, Cham, pp 141–175

Applied Soil Ecology 170 (2022) 104306

Contents lists available at ScienceDirect

Applied Soil Ecology

journal homepage: www.elsevier.com/locate/apsoil

Edaphic factors override temperature in shaping soil bacterial diversity across an elevation-vegetation gradient in Himalaya

Pamela Bhattacharya [a], Pankaj Tiwari [a], Ishwari Datt Rai [a,b], Gautam Talukdar [a], Gopal Singh Rawat [a,*]

[a] Wildlife Institute of India, Chandrabani, Dehradun 248001, India
[b] Indian Institute of Remote Sensing, Indian Space Research Organization, Dehradun, Uttarakhand 248001, India

ARTICLE INFO

Keywords:
Soil bacterial community
Metabarcoding
Elevation-vegetation gradient
Seasonal and inter-annual dynamics
Alpine region of Himalaya
Climate change

ABSTRACT

Assessment of bacterial community distribution patterns along elevation gradients is invaluable in understanding the underlying mechanism involved in their diversity formation, sustenance, and response to environmental changes. However, no consensus has been reached as studies show contrasting patterns with different regulating factors due to habitat specificity and associated environmental conditions. Moreover, limited studies have considered spatial and temporal variability in bacterial diversity simultaneously. Here, we provide three years of meta-barcoding-based insight into the effects of environmental changes on soil bacterial communities and their driving factors across elevation-vegetation gradient (3373–4020 m) in the Himalaya. We also assess their seasonal and inter-annual variations. Results indicate that extreme elevations viz., low and high, having similar edaphic factors but different climatic regimes, showed similar bacterial diversity compared to a dip at mid-elevations caused by low moisture and substrate availability. Bacterial α-diversity and relative abundances of major phyla showed mid-elevation dip mainly caused by the direct impact of edaphic factors (soil organic carbon, total nitrogen, and moisture) but not temperature. Community composition showed three distinct clusters across elevation gradient and was also influenced directly by edaphic properties in addition to temperature. Moreover, we observed no significant seasonal and inter-annual variability in α and β-diversity, suggesting stability in bacterial communities over time. The mid-elevations harbored predominantly competitive interactions, while low and high elevations exhibited co-operative interactions. Taken together, the results show the critical role of edaphic properties over the temperature in influencing bacterial diversity and indicate the community resilience towards climate warming. Our study will enhance the predictability of the community dynamics across broader spatio-temporal scales under changing climate.

1. Introduction

Bacterial communities play a crucial role in soil formation, nutrient cycling, and plant colonization (Donhauser and Frey, 2018). These communities also regulate soil carbon storage through decomposition and mediate feedbacks between climate change and ecosystem functioning by heterotrophic respiration (Trivedi et al., 2013). Recent studies have demonstrated that incorporating trophic level information of these communities in carbon dynamic-based ecosystem models has enhanced predictive power (Treseder et al., 2012; Wieder et al., 2015). However, despite their pivotal role in ecosystem functioning and environmental susceptibility (Xu et al., 2015), knowledge regarding their environmental drivers has been inconclusive due to considerable variability in observed diversity patterns (Crowther et al., 2019).

Earlier studies understanding the factors regulating bacterial diversity patterns have primarily used elevation gradient in mountain ecosystems to proxy environmental change (Donhauser and Frey, 2018). However, the distribution patterns reported in these studies are contrasting and site-specific. For instance, studies from the Italian and Swiss Alps (Adamczyk et al., 2019; Siles and Margesin, 2017), Mount Gongga, Changbai Mountain, and Colorado Rocky Mountains (Bryant et al., 2008; Shen et al., 2015; Zhu et al., 2020) showed decreasing bacterial diversity across elevation. In contrast, Tibetan Plateau and Mount Wutai exhibited an increasing trend (Luo et al., 2019; Zhang et al., 2019), and Mt Fuji showed a hump-back trend in bacterial diversity (Singh et al., 2012). Additionally, studies also observed no definite trends along

* Corresponding author.
E-mail address: rawatg@wii.gov.in (G.S. Rawat).

https://doi.org/10.1016/j.apsoil.2021.104306
Received 23 June 2021; Received in revised form 24 September 2021; Accepted 1 November 2021
Available online 10 November 2021

elevation (Siles and Margesin, 2016; Yashiro et al., 2016). The inconsistency in elevation patterns is mainly due to local edaphic and climate variability (Singh et al., 2014; Yashiro et al., 2016).

Seasonal and interannual variations in climatic and edaphic factors influence bacterial community diversity and composition (Siles et al., 2016; Siles et al., 2017). However, earlier studies have been conducted across either a single time-point or seasons within a year across different spatial scales. Small scale studies (<1000 m elevation gradient) with relatively uniform vegetation have identified the role of climate but have masked the influence of edaphic factors (Sun et al., 2020). While large scale studies (>1000 m elevation gradient) have accounted for both climatic as well as edaphic factors (Xue et al., 2018; Yashiro et al., 2016) however are limited in numbers due to logistic feasibility. To account for spatial and temporal variability simultaneously, we take advantage of a short elevation gradient with vegetation shift in the Himalaya to investigate the influence of both edaphic and climatic factors on bacterial diversity across three years. These gradients provide an array of environmental factors within small distances and are easy to monitor across multiple time points (Djukic et al., 2010; Siles et al., 2016; Tang et al., 2020; Zhu et al., 2020).

Encompassing the world's highest mountain ranges, the Himalaya represents diverse ecosystems with immense biodiversity (Padma, 2014). In addition, it retains about 33% of India's carbon stock (Bhattacharyya et al., 2008) and has a critical role in the global carbon cycle and climate warming (Longbottom et al., 2014; Yang et al., 2008). Recent assessments predict a 3 °C temperature rise in Himalaya by 2050 (Shrestha et al., 2012). High altitude habitats in the Himalaya, due to their ongoing formation in terms of soil and vegetation climax (Shrestha et al., 2012), provide climate-vegetation gradient across short elevation ranges and are ideal for studies on bacterial community dynamics. The objectives of our study were to (i) assess the patterns in bacterial α and β-diversity across an elevation-vegetation gradient, (ii) determine seasonal and inter-annual variability in bacterial diversity, (iii) assess bacterial co-occurrence pattern across the gradient, and (iv) evaluate the role of temperature and edaphic factors in shaping the community diversity and composition. We hypothesized increasing co-operative interactions between the bacterial communities with a decreasing diversity across the elevation-vegetation gradient mainly regulated by temperature.

2. Material and methods

2.1. Study site

The study was conducted along an elevation gradient on a southwest-facing slope of a glaciated valley in Western Himalaya, India (30.95–30.99° N, 78.99–79.06° E) (Fig. 1, Table 1). The entire gradient (3373–4020 m) encompasses a ~10 km trail inside a protected area (Gangotri National Park) where anthropogenic interference is limited and livestock grazing is banned. Vegetation in this region changes with increasing elevation forming elevation-vegetation gradient from a sub-alpine forest in lower elevations to alpine scrub in mid and alpine meadow at the higher elevations. The ground vegetation cover in the forest, alpine scrub, and meadow was estimated ca. 40 ± 14%, 22.5 ± 3.5%, and 70 ± 14%, respectively. Table 1 details the dominant plant species in each vegetation type. The soil is poorly formed and slightly acidic (Table 1). Mean annual precipitation is around 1500 mm, which occurs in the form of rainfall during June to September and snowfall

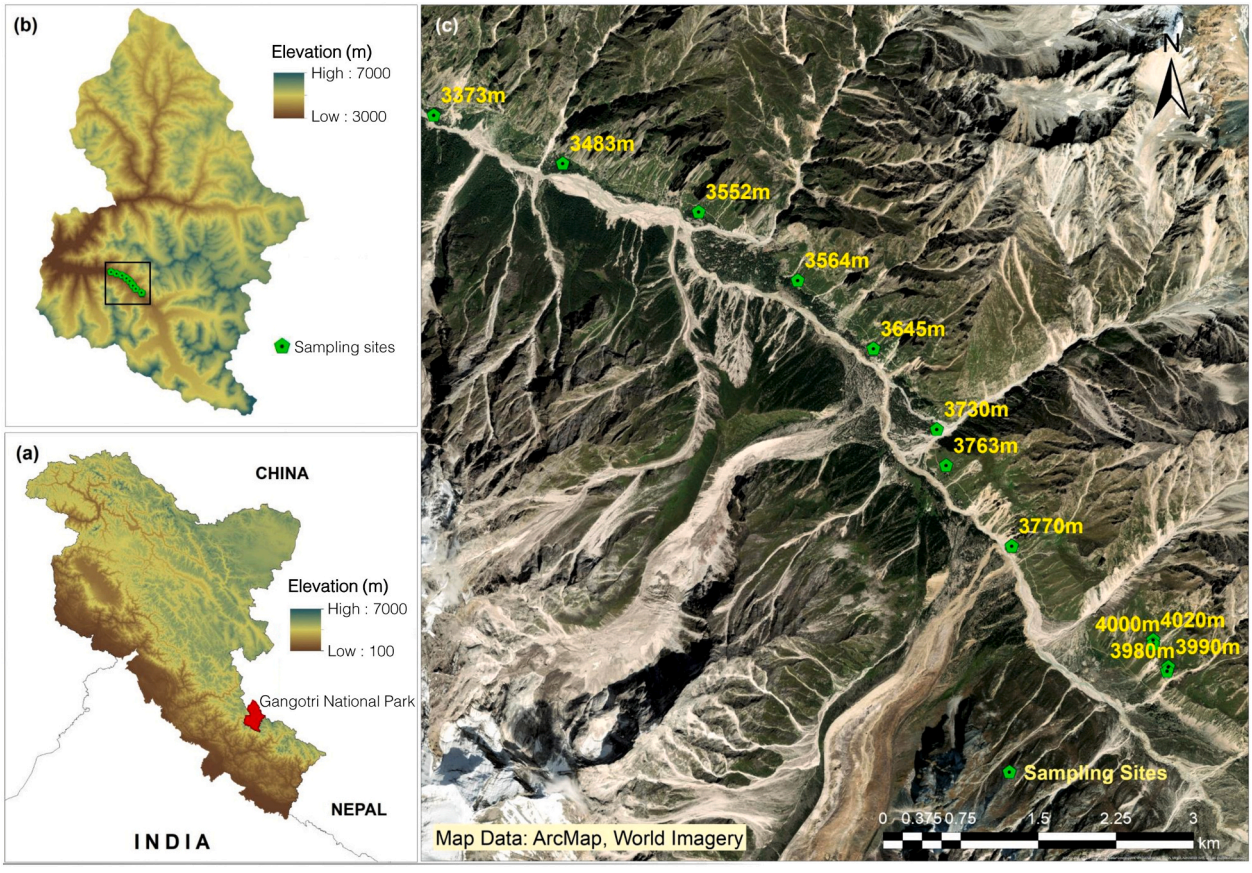

Fig. 1. Map of the study area (a) Western Himalaya, India, (b) Gangotri National Park, and (c) sampling sites along an elevation-vegetation gradient in Gangotri National Park. All maps were generated in ArcGIS version 10.7 (ESRI, CA, USA, https://desktop.arcgis.com/en/arcmap/). SRTM DEM (Shuttle Radar Topography Mission, Digital Elevation Model) data (30 m) in a and b were downloaded from the U.S. Geological Survey Earth Explorer (http://earthexplorer.usgs.gov/). The satellite imagery used in c is a base map in ArcMap 10.7 (ESRI, CA, USA, https://desktop.arcgis.com/en/arcmap/).

Table 1
Vegetation, mean annual air temperature (MAT), and edaphic properties including soil moisture content (SMC), pH, soil organic carbon (SOC), total nitrogen (TN) and C/N ratio at sampling sites across elevation.

Altitude (m. a.s.l.)	Vegetation	Dominant plants	MAT (°C)	SMC (%)	pH	SOC (g kg^{-1})	TN (g kg^{-1})	C/N ratio
3373	Subalpine forest	Tree species: *Betula utilis, Populus ciliata, Acer caesium, Sorbaria tomentosa*	6.13 ± 0.16^{e}	19.87 ± 2.27^{abc}	5.34 ± 0.2^{a}	52.93 ± 10.21^{acd}	4.23 ± 0.68^{abc}	12.27 ± 1.06^{a}
3483		Ground vegetation: *Astragalus candolleanus, Anaphalis triplinervis, Rosularia alpestris, Calamogrostis emodensis*	6.04 ± 0.03^{e}	15.87 ± 5.5^{ab}	5.77 ± 0.19^{a}	52.74 ± 9.72^{acd}	4 ± 1.06^{abc}	14.22 ± 1.62^{a}
3552			5.48 ± 0.01^{de}	22.86 ± 3.24^{abc}	5.19 ± 0.42^{a}	38.56 ± 9.33^{abc}	3.28 ± 1.01^{ab}	13.89 ± 1.18^{a}
3564			5.32 ± 0.13^{de}	13.03 ± 3.56^{ab}	5.07 ± 0.35^{a}	35.19 ± 12.8^{abc}	2.95 ± 1.31^{ab}	13.07 ± 1.04^{a}
3645	Alpine scrub	*Rosa sericea, Spiraea canescens, Artemisia santolinifolia, Lonicera obovata, Viburnum cotinifolium, Berberis jaeschkeana, Juniperus communis*	4.73 ± 0.05^{cd}	7.57 ± 3.39^{a}	5.96 ± 0.26^{a}	27.99 ± 5.29^{ab}	1.94 ± 0.27^{a}	14.28 ± 1.64^{a}
3730			4.04 ± 0.09^{bc}	7.35 ± 3.85^{a}	5.8 ± 0.39^{a}	15.44 ± 4.34^{b}	1.24 ± 0.36^{a}	13.05 ± 1.23^{a}
3763			3.42 ± 0.19^{b}	7.41 ± 3.71^{a}	5.5 ± 0.39^{a}	24.07 ± 5.56^{ab}	2.26 ± 0.51^{a}	12.47 ± 1.7^{a}
3770			3.71 ± 0.11^{bc}	8.21 ± 3.89^{a}	5.11 ± 0.3^{a}	24.19 ± 7.58^{ab}	1.99 ± 0.57^{a}	11.69 ± 0.97^{a}
3980	Alpine meadow	*Geranium himalayense, Aconogonum tortuosum, Nepeta discolor, Potentilla atrisanguinea*	2.01 ± 0.21^{a}	26.64 ± 2.32^{bc}	5.34 ± 0.4^{a}	46.02 ± 6.34^{abc}	4.74 ± 0.75^{abc}	9.83 ± 0.18^{a}
3990			1.93 ± 0.22^{a}	34.46 ± 3.01^{c}	5.14 ± 0.42^{a}	44.92 ± 5.81^{abc}	4.4 ± 0.53^{abc}	10.22 ± 0.71^{a}
4000			1.85 ± 0.22^{a}	22.54 ± 3.79^{abc}	5.54 ± 0.37^{a}	71.05 ± 4.16^{cd}	6.3 ± 0.65^{bc}	11.6 ± 0.89^{a}
4020			2.08 ± 0.43^{a}	26.95 ± 5.1^{bc}	5.22 ± 0.32^{a}	87.98 ± 3.78^{d}	7.27 ± 0.7^{c}	12.65 ± 1.54^{a}

Values are mean ± S.E of mean, n = 5. Mean values followed by different letters are significantly different ($p < 0.05$).

from December to May (Sanyal et al., 2013) while, mean annual air temperature (MAT) range from 1.85 ± 0.22 °C to 6.13 ± 0.16 °C (Table 1).

2.2. Site selection and soil sampling

We selected twelve altitudinal sites across the gradient (Fig. 1c) and marked a 5 × 5 m plot at each altitude. In each plot, we randomly selected five 1 × 1 m sub-plots for soil sampling. Five soil cores (~1 g each) were collected from 5 cm depth at four corners and center of the sub-plot using hand-held sterile soil corer (50 ml centrifuge tube of diameter 2.5 cm, Tarsons Products Pvt. Ltd, India). Before soil collection, ground vegetation was clipped, and litter was removed. Then, following the design of Lanzén et al. (2016), soil cores at each altitude (n = 25) were pooled in a sterile ziplock bag and homogenized. From this pool, 5 g soil was aliquoted and preserved in 100% ethanol (Merck, Germany) to prevent the environmental DNA from hydrolytic damage before molecular analyses (Harry et al., 2000). Both samples (one for molecular analysis and the other for soil physicochemical analyses) were transported to the laboratory in a cool box containing dry ice. Soil sampling was performed during spring (May) and autumn (October) at five time-points during October 2016, May and October 2017, and May and October 2018, giving us a total sample size of 60 (n = 5 for each altitude).

2.3. Measurement of air temperature and edaphic factors

We deployed HOBO U23 Pro v2 data loggers (Onset Computer Corporation, USA) at 3373 m, 3564 m, 3763 m, and 4020 m to monitor hourly air temperature at 1 m height and calculated mean annual temperature (MAT) for the study period (2016–2018). MAT at remaining altitudes was estimated by generating standard curves (Singh et al., 2014).

We estimated edaphic factors, including soil pH, moisture content, organic carbon, total nitrogen, and C/N. Soil moisture content (SMC) was measured gravimetrically from a 5 g soil sample (Rayment and Lyons, 2011). The remaining soil was air-dried and sieved through a 1 mm sieve to remove gravels, plant roots, and leaf litter. Soil pH was measured by a glass electrode pH meter (Sension 7, Hach Company, USA) in a 1:2.5 (w/v) suspension of soil and deionized water (Blakemore et al., 1987). Soil organic carbon (SOC) was measured using the potassium dichromate ($K_2Cr_2O_7$) oxidation method (Walkley and Black, 1934), and total nitrogen (TN) was determined by the Kjeldahl method (Bremner, 2018) using Kjeltec 8400 (Foss India Pvt. Ltd).

2.4. DNA extraction, PCR amplification, and Illumina sequencing

We extracted soil genomic DNA from approximately 0.25 g of each soil sample using a Nucleopore GDNA soil kit (Genetix Biotech Asia Pvt. Ltd, India) following the manufacturer's kit protocol. We quantified DNA concentrations using Qubit dsDNA HS Assay Kit (Life Technologies, USA). We used Illumina 16S Metagenomics Sequencing library preparation protocol to prepare sequencing libraries for bacterial V3 and V4 regions using the primers 338F (5′-CCTACGGGNGGCWGCAG-3′) and 806R (5′-GACTACHVGGGTATCTAATCC-3′) (Luo et al., 2019). The PCR reaction contained 12.5 μl of 2× Kappa Hifi Hotstart ReadyMix (Kappa Biosystems, Roche Sequencing and Life Science, USA), 1 μl each of 5 μM forward and reverse primer, and 10.5 μl of the template (12.5 ng of microbial DNA), respectively. PCR conditions included an initial denaturation of 95 °C for 3 min, followed by 25 cycles of 95 °C for 30 s, 55 °C for 30 s, and 72 °C for 30 s, followed by a final extension for 10 min at 72 °C. PCR negative (no template DNA) was included to monitor any contamination. PCR products were purified, barcoded using Nextera XT kit (Illumina Inc., United States), and normalized to 2 nM for each library. The equal volume of these libraries was pooled, denatured, and diluted to 4 pM before loading onto the MiSeq flow cell (Illumina Inc., United States). Sequencing was performed on Illumina MiSeq platform using a 2 × 300 bp paired-end protocol at the Next Generation Genomics Facility at Center for Cellular and Molecular Platforms (C-CAMP), Bangalore, India.

2.5. Sequence data processing

We processed the raw sequences using the MiSeq SOP pipeline in Mothur v.1.40.5 (Kozich et al., 2013; Masse et al., 2017; Schloss et al., 2009). Full-length sequences were prepared, and good reads (>460 bp

length with no homopolymer stretches longer than 8 bp) were identified and clustered (based on ≥97% similarity) using 16S rRNA database SILVA 132 SSU SEED (Quast et al., 2012). Uchime was used to remove chimeric sequences, followed by eliminating all singletons, chloroplasts, archaea, mitochondria, and unknown origin sequences (Edgar et al., 2011). Only high-quality sequences were used to estimate pairwise distances and generate single-linkage clusters with ≥97% sequence similarity. The longest read from each cluster was used as the reference sequence for taxonomic assignments against the SILVA SSU NR Ref database (Quast et al., 2012). All sequences in each cluster and their replicates (≥97% similarity) provided the quantitative estimates of individual reads per taxonomic unit. The dataset was normalized by rarefying the sequences to the lowest sample-specific sequencing depth with maximum Good's coverage (Kozich et al., 2013). Four samples with a sequence read less than the rarefaction depth were excluded from the downstream analyses. Finally, we clustered the sequences to phylum levels for operational taxonomic unit (OTU) abundance and composition analysis. We further classified the data into abundant taxa based on their relative abundances. OTUs with ≥1% relative abundance were considered abundant (Pedrós-Alió, 2006).

2.6. Co-occurrence network construction

To identify bacterial interspecies interactions, we constructed co-occurrence ecological networks following Random Matrix Theory (RMT)-based method through Molecular Ecological Network Analysis (MENA) pipeline (Deng et al., 2012; Zhou et al., 2011). Pearson correlation between OTUs at genus level having relative abundances >0.1% in all samples were used to construct the network with an identical similarity threshold 0.7 at three elevation ranges low (3373–3564 m), mid (3645–3770 m), and high (3980–4020 m). We calculated various indices, including node and link numbers, average degree (avgK), average clustering coefficient (avgCC), average path distance (GD), density (D), modularity (M), and connectedness (Con) to evaluate and compare the overall topological features of the networks (Deng et al., 2012). The networks were separated into different modules using fast greedy modularity optimization (Deng et al., 2012). The network graphs were visualized using Cytoscape 3.8.2 (Shannon et al., 2003), where each node represents one genus, and each link represents one significant correlation.

2.7. Data analysis

We calculated three bacterial α-diversity indices: richness (Sobs), evenness, and Shannon diversity index for each sample using the Mothur platform. We used one-way analysis of variance (ANOVA) to determine significant differences in α-diversity indices, MAT, and edaphic factors (SMC, SOC, total nitrogen, pH, and C/N) between altitudinal sites. Where differences were significant, Tukey's honest significance difference (HSD) post-hoc test was applied for pairwise comparisons of mean at 95% confidence intervals. Seasonal and inter-annual variability in α-diversity was evaluated by grouping the data into low (3373–3564 m), mid (3645–3770 m), and high elevation ranges (3980–4020 m) followed by independent sample *t*-test and ANOVA, respectively. Before the analysis, we tested normality and heteroscedasticity of data by the Shapiro-Wilk and Levene tests, respectively.

We calculated the Bray-Curtis dissimilarity matrix after Hellinger transformation of rarefied abundance data at the phyla level for β-diversity estimation. Principal Coordinate Analysis (PCoA) using the Bray-Curtis dissimilarity matrix was used to interpret differences in bacterial community composition visually. To test any significant compositional differences, we used Multi-Response Permutation Procedure (MRPP) analysis (Oksanen et al., 2020) with 9999 permutations, where chance corrected within-group agreement (a measure of effect size presented as *A* value) was calculated. The *A* value ranges between 0 and 1, where $A = 0$ indicates samples within a group are heterogeneous, and $A = 1$ depicts they are identical. We evaluated seasonal and inter-annual variability in β-diversity by grouping the data into low (3373–3564 m), mid (3645–3770 m), and high elevation ranges (3980–4020 m) followed by MRPP analysis.

Multiple ordinary least square (OLS) regression analysis with stepwise forward selection was done to assess the relationship of MAT and edaphic factors with bacterial richness and diversity. For SOC and TN having high correlation ($r = 0.95$, $p < 0.001$), regressions were performed with SOC only. A model was considered most parsimonious based on Akaike's information criterion (Johnson and Omland, 2004). Mantel test with Pearson correlation was used to test the relationship of bacterial community composition with environmental variables. We performed a forward selection of environmental variables using stepwise regression (with 999 permutations). Redundancy analysis (RDA) was conducted using Hellinger transformed bacterial abundance data to identify environmental variables that significantly explained the variation in abundant phyla. The RDA model and the environmental variables were tested by permutation test using ANOVA. Subsequently, we used univariate regression analyses to assess the relationship of environmental variables with Hellinger transformed relative abundance of individual bacterial phyla. Finally, we conducted structural equation model (SEM) analysis to determine the direct and indirect effects of environmental variables on bacterial richness, α-diversity, and composition. The composition was characterized by the first axis of PCoA of the Bray-Curtis dissimilarity matrix (Li et al., 2015). Based on theoretical knowledge, we developed a path model to relate environmental variables including vegetation, MAT, SMC, SOC, and pH with bacterial richness, diversity, and composition. To improve the fit between the model and the data, the initial theoretical model was modified for the correct specification of theoretical causal relationships between variables before analysis. We used Maximum likelihood estimation to compare the SEM model with the observations. The model fitness with the data was tested using Comparative Fit Index (CFI), Akaike Information Criteria (AIC), and Root Square Mean Errors of Approximation (RMSEA). Adequate model fits were indicated by a high CFI (>0.90), low AIC, and low RMSEA (<0.05) (Grace, 2006). All analyses were conducted in R 4.0.3 (http://www.R-project.org/) through RStudio 1.3.1093, 2020 (https://rstudio.com/products/rstudio/) using vegan 2.5-7 (https://cloud.r-project.org/package=vegan), lavaan 0.6-9 (https://cloud.r-project.org/package=lavaan), dplyr 1.0.5 (https://cloud.r-project.org/package=dplyr) and ggplot2 3.3.3 (https://cloud.r-project.org/package=ggplot2) (Oksanen et al., 2020; Team, 2020; Wickham, 2011; Wickham and Wickham, 2017).

2.8. Accession number

The DNA sequence data set has been deposited to National Centre for Biotechnology Information (NCBI) Short Read Archive (https://www.ncbi.nlm.nih.gov/sra). The BioProject accession number PRJNA705032.

3. Results

3.1. Air temperature and edaphic factors across elevation-vegetation gradient

Both temperature and edaphic factors varied across the elevation gradient (Table 1). Mean annual air temperature (MAT) showed a monotonous decrease across the elevation gradient. In contrast, edaphic properties including SMC, SOC, and total nitrogen showed a dip in mid-elevations with similar values at low and high elevations. No significant difference was observed in the C/N ratio and pH at any altitude.

3.2. Taxonomic overview

A total of 2,542,679 high-quality sequences across 60 samples were generated, averaging 42,378 ± 14,204 sequences per sample

(Supplementary Table S1). Rarefaction based on sequence reads of one of the samples (23,821) provided maximum Good's coverage (>82%) (Supplementary Table S1) for 56 samples. The remaining four samples (at altitudes 3645 m, 3730 m, 3763 m, and 3770 m in May 2018) having sequence reads less than the rarefaction depth were eliminated, and downstream analyses were performed only with 56 samples. We identified 126,667 OTUs at ≥97% similarity and were grouped into 35 phyla. Out of these 35 phyla, 34 were classified, of which 12 were abundant (relative abundance ≥1%), accounting for 98% of the total bacterial sequences (Fig. 2a). These abundant phyla were *Proteobacteria* (relative abundance 39.22%), *Actinobacteria* (20.3%), *Firmicutes* (12.4%), *Acidobacteria* (5.17%), *Planctomycetes* (4.37%), *Verrucomicrobia* (3.66%), *Patescibacteria* (3.56%), *Bacteroidetes* (3.02%), *Gemmatimonadetes* (2.17%), *Chloroflexi* (2%), *Chlamydiae* (1.58%) and *Dependentiae* (1.28%).

3.3. Bacterial α and β-diversity across elevation-vegetation gradient

Bacterial α-diversity (richness, evenness and, Shannon diversity) followed a similar trend as edaphic properties (SMC, SOC, and total nitrogen) with similarities at low and high elevation and dip in mid-elevations (Fig. 3). As a result, three distinct groups encompassing four altitudes each were visible across the gradient.

Bacterial β-diversity also showed the influence of mid-elevations. The abundant phyla decreased from 12 in the low elevations (3373–3564 m) to 5–7 across 3645–3770 m, then regained to 9–12 in higher elevations (Fig. 2a). As the number of abundant phyla decreased in mid-elevations, the communities showed less even distribution. *Proteobacteria* dominated community composition up to 3770 m with relative abundance ranging from 33 to 75%. However, *Actinobacteria* (21–29%) and *Firmicutes* (8–36%) seemed to dominate the community at higher elevations equally. We also observed the presence of

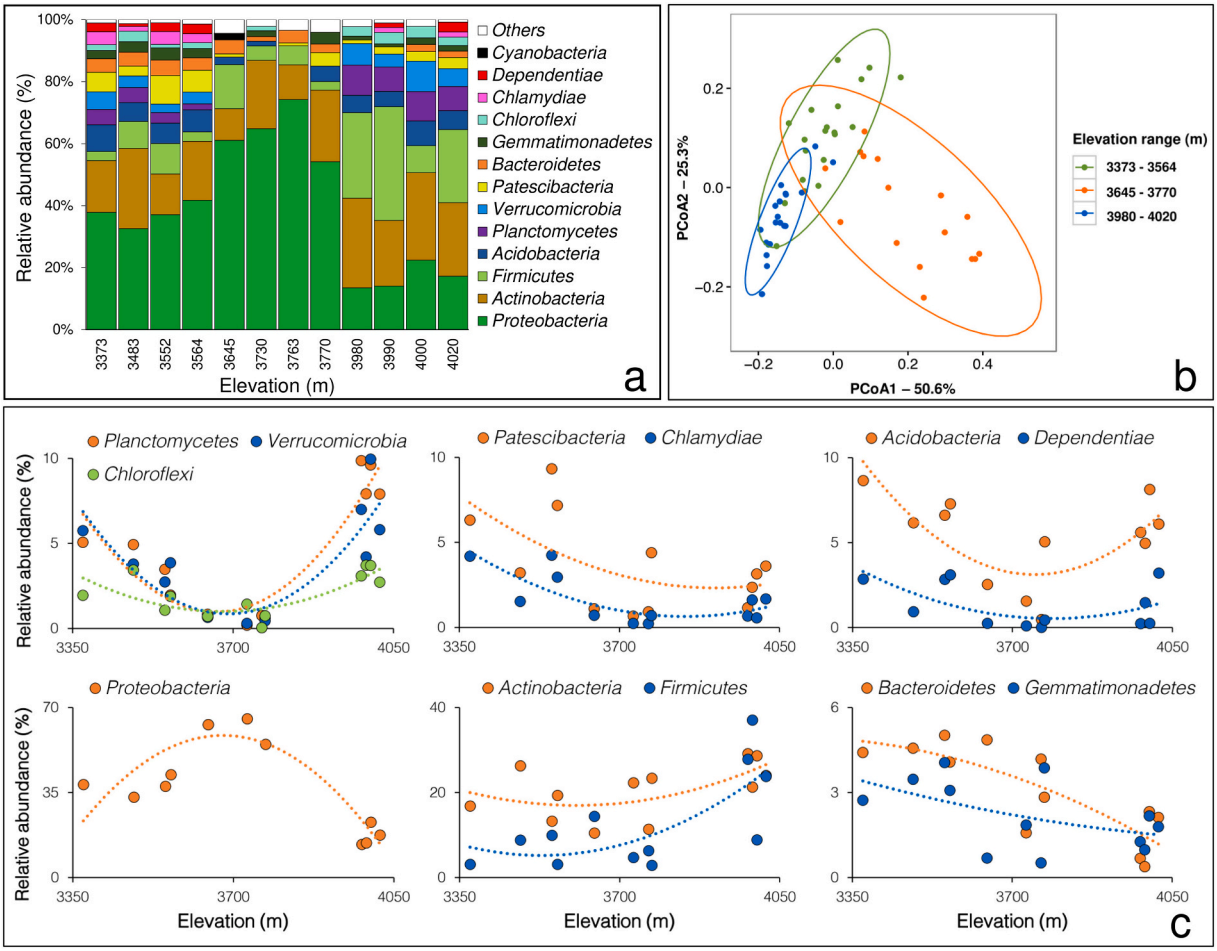

Fig. 2. Bacterial β-diversity across elevation-vegetation gradient (a) variation in relative abundances of bacterial phyla where "Others" represent all phyla with relative abundances <1%, (b) Principal Co-ordinates Analysis (PCoA) based on Bray-Curtis dissimilarity of bacterial communities and (c) variation in relative abundance of individual abundant bacterial phyla. b was generated in R 4.0.3 (http://www.R-project.org/) using vegan 2.5-7 (https://cloud.r-project.org/package=vegan), dplyr 1.0.5 (https://cloud.r-project.org/package=dplyr) and ggplot2 3.3.3 (https://cloud.r-project.org/package=ggplot2).

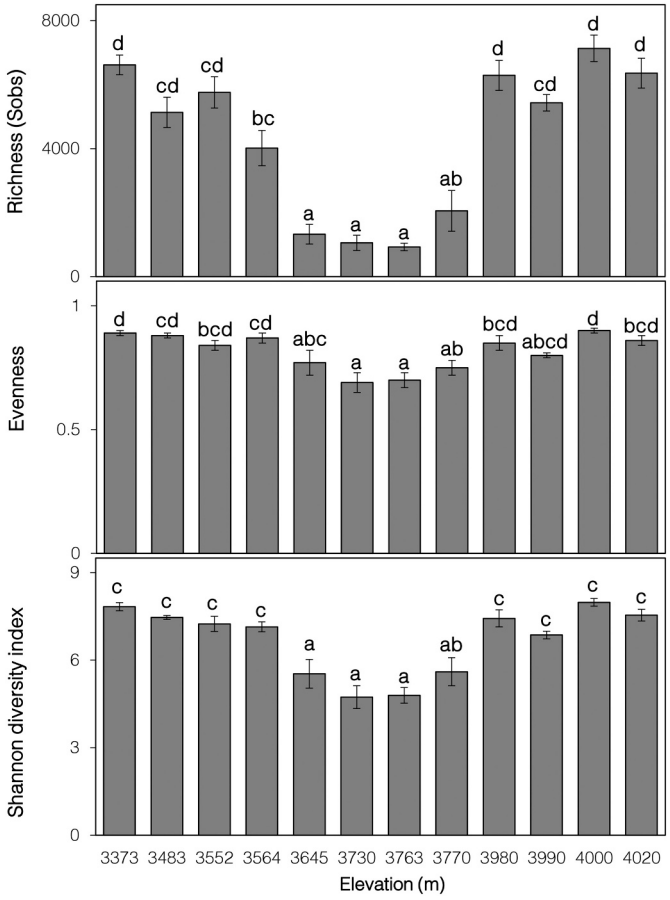

Fig. 3. Variation in bacterial richness, evenness, and diversity across the elevation-vegetation gradient. Bars represent mean ± S.E of mean, n = 5 at each altitude. Different letters (above each bar) indicate significant difference between altitudes ($p < 0.05$).

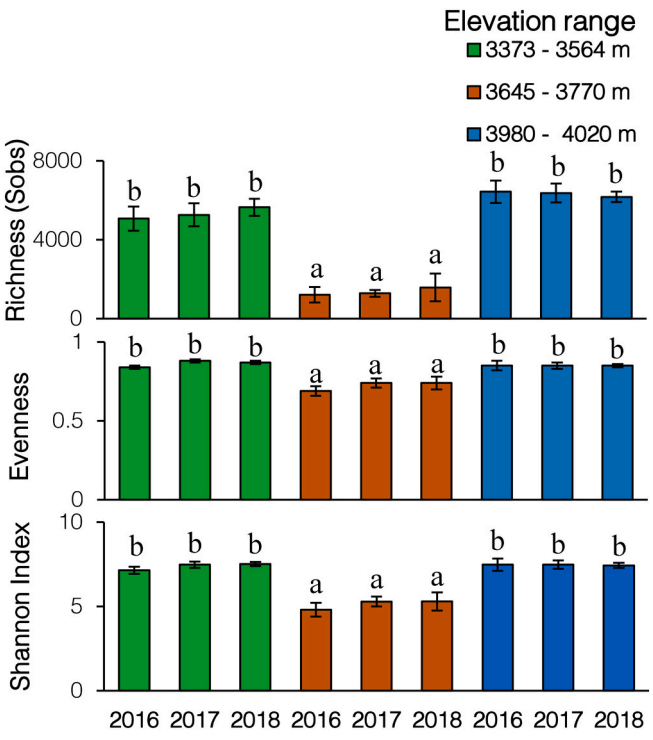

Fig. 4. Inter-annual variations in bacterial richness, evenness, and diversity. Bars represent mean ± S.E of mean, n = 5 at each altitude. Different letters (above each bar) indicate significant difference between altitudes ($p < 0.05$).

Cyanobacteria with a relative abundance of 1.98% at only 3645 m. Three significantly distinct (A = 0.26, $p < 0.001$) community clusters were observed at low, mid, and high elevation ranges (Fig. 2b). However, we observed high overlaps between the clusters at low and high elevations.

Fig. 2c shows trends in the relative abundance of abundant phyla across the elevation-vegetation gradient. Except for the most abundant *Proteobacteria*, which peaked in mid-elevations and dipped at higher elevations, several bacterial phyla showed a mid-elevation dip. Three types of curves with such mid-elevation dips were observed, one, with similar abundances at low and high elevations (*Acidobacteria* and *Dependentiae*), second, with a gradual decrease up to mid-elevations and then an abrupt increase in higher elevations (*Planctomycetes*, *Verrucomicrobia*, *Chloroflexi*), and thirdly with the highest abundance at low elevations with a dip in mid and stable towards higher elevations (*Patescibacteria*, *Chlamydiae*). On the contrary, *Actinobacteria* and *Firmicutes* increased, whereas *Bacteroidetes* and *Gemmatimonadetes* decreased across elevation.

3.4. Bacterial α and β-diversity across seasons and years

We assessed the variability in α and β-diversity across seasons (spring and autumn) and years (2016, 2017, and 2018) within 3373–3564 m, 3645–3770 m, and 3980–4020 m elevation ranges. We observed no significant difference ($p > 0.05$) in both α and β-diversity across seasons and years except for a decrease in richness during spring in the elevation range 3980–4020 m (Table 2, Fig. 4, Supplementary Tables S2 and S3).

3.5. Bacterial co-occurrence pattern across elevation-vegetation gradient

The bacterial co-occurrence networks at the three elevation ranges showed scale-free (connectivity distribution obeyed power-law model, R^2 ranged from 0.3 to 0.92), non-random, small world (average path distance ranged from 3.1 to 4.5), and modular (modularity ranged from

Table 2
Results of independent sample *t*-test for bacterial community α-diversity comparison between two seasons (Spring and Autumn) at different elevation ranges (3373–3564 m), (3645–3770 m), and (3890–4020 m).

Elevation range	Richness (Sobs)			Evenness			Diversity (Shannon Index)		
	Spring	Autumn	p-Value	Spring	Autumn	p-Value	Spring	Autumn	p-Value
(3373-3564 m)	5365 ± 534	5391 ± 382	0.96	0.86 ± 0.02	0.87 ± 0.01	0.83	7.4 ± 0.18	7.4 ± 0.18	0.86
(3645–3770 m)	1008 ± 220	1452 ± 257	0.36	0.74 ± 0.03	0.72 ± 0.02	0.773	5.1 ± 0.33	5.2 ± 0.27	0.79
(3890–4020 m)	5644 ± 226	6745 ± 301	0.016	0.84 ± 0.02	0.86 ± 0.014	0.26	7.2 ± 0.2	7.6 ± 0.2	0.143

Values are mean ± S.E of the mean. n = 8 and12 for spring and autumn, respectively. Significant at $p < 0.05$.

Table 3
Co-occurrence network topological properties at low, mid, and high elevation ranges.

	Network indices	Low (3373–3564 m)	Mid (3645–3770 m)	High (3980–4020 m)
Empirical networks	R square of power-law	0.92	0.3	0.864
	Total nodes	75	52	124
	Total links	122	112	285
	Links per node	1.6	2.2	2.3
	Positive co-occurrence (%)	63	30	86
	Average path distance (GD)	3.47	3.08	4.5
	Modularity	0.55	0.45	0.57
	Average degree (avgK)	3.25	4.31	4.6
	Average clustering coefficient (avgCC)	0.14	0.17	0.233
	Density (D)	0.044	0.084	0.037
	Connectedness (Con)	0.751	1	0.937
Randomized networks	Average clustering coefficient (avgCC)	0.06 ± 0.02	0.08 ± 0.03	0.06 ± 0.01
	Average path distance (GD)	3.36 ± 0.11	2.81 ± 0.05	3.23 ± 0.05
	Modularity (fast_greedy)	0.49 ± 0.02	0.39 ± 0.02	0.41 ± 0.01
	Connectedness (Con)	0.90 ± 0.07	0.99 ± 0.02	0.98 ± 0.03

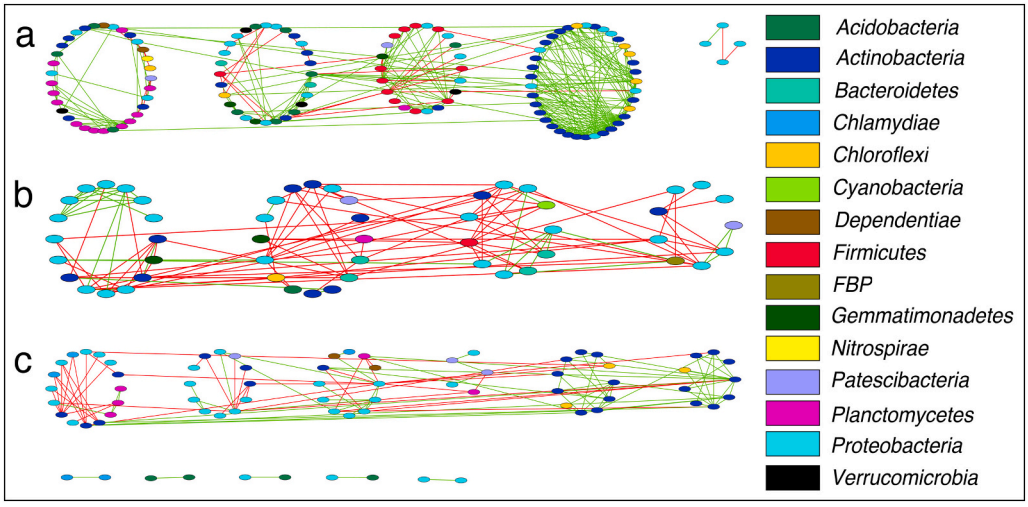

Fig. 5. Co-occurrence networks of bacterial genera at (a) high (3980–4020 m), (b) mid (3645–3770 m), and (c) low (3373–3564 m) elevation range based on Random Matrix Theory. Each genus is represented as a node having an oval shape, and each significant ($p < 0.05$) correlation (link) is represented as a straight line. Nodes of the same color represent same phyla the genera belong to. Green and red lines indicate positive and negative correlations be tween nodes, respectively. Each module in the network is represented by a circle composed of nodes. The figure was generated in Cytoscape 3.2.8.

0.45 to 0.57) features of ecological networks (Table 3) (Deng et al., 2012; Zhou et al., 2011). Comparison of topological features between the three networks revealed a dip in the number of nodes and links at the mid-elevation range with the highest value at the high-elevation range (Table 3 and Fig. 5). The low and high elevation range consisted of eleven and five modules, respectively, with most nodes connected positively (63–86%). In contrast, the mid-elevation range showed mainly negative relation (70%) among nodes of the four constructed modules. A dip in network modularity (connectivity within a module) was observed in the mid-elevation range (0.45), where the density (0.084) and connectedness (1) peaked. The average degree (3.3–4.6) and clustering coefficient (0.14–0.23) increased linearly across the elevation ranges.

3.6. Factors affecting α and β-diversity

Multiple linear regressions showed that α-diversity was positively affected by SMC and SOC across elevation (Table 4). Variability in richness ($r^2 = 0.50$, $p < 0.001$) and diversity ($r^2 = 0.36$, $p < 0.001$) were significantly explained by SMC and SOC, while that in evenness by only SOC ($r^2 = 0.21$, $p < 0.001$). No significant relationships were observed between α-diversity and pH, C/N, and MAT. On the other hand, β-diversity was significantly correlated to MAT ($r = 0.25$, $p < 0.001$) and all the selected edaphic factors (SMC: $r = 0.28$, $p < 0.001$; SOC: $r = 0.19$, $p < 0.001$; total nitrogen: $r = 0.18$, $p < 0.001$ and pH: $r = 0.07$, $p < 0.049$) except C/N ratio ($r = 0.08$, $p = 0.07$) as revealed by Mantel test. Further, the Redundancy Analysis with 12 abundant phyla showed that MAT, SMC, and SOC explained 33% ($F_{(3,52)} = 8.68$, $p < 0.001$) of the variability in their relative abundance across the elevation gradient (Fig. 6). We performed linear regressions to understand the effect of MAT, SMC, and SOC on each abundant phylum (Fig. 7). *Proteobacteria*, *Firmicutes,* and *Planctomycetes* were significantly affected by all the three factors, whereas *Bacteriodetes* and *Chlamydiae* by MAT and SMC; *Verrucomicrobia* and *Chloroflexi* by SMC and SOC, *Actinobacteria* and *Acidobacteria* by SOC and *Patescibacteria* and *Dependentiae* by MAT. *Gemmatimonadetes* was not significantly affected by any of the three factors. The unexplained variability in bacterial α and β-diversity may be due to factors such as belowground biomass, plant species composition, and soil nutrients (phosphorus and others) not measured in this study.

The SEM model (CFI = 0.94, AIC = 683.1, RMSEA = 0.16, $p < 0.05$) explained 36%, 89%, and 65% of the variation in bacterial richness, α-diversity and composition, respectively (Fig. 8). Diversity was strongly related to richness ($\lambda = 0.94$, $p < 0.001$) which was affected directly by SOC ($\lambda = 0.32$, $p < 0.01$) and SMC ($\lambda = 0.49$, $p < 0.001$) and indirectly by vegetation type ($\lambda = 0.16$, $p < 0.01$). Community composition was related to richness ($\lambda = 0.77$, $p < 0.001$) and affected directly by SOC ($\lambda = -0.36$, $p < 0.001$), pH ($\lambda = -0.25$, $p < 0.01$) and MAT ($\lambda = -0.16$, $p < 0.05$). Supplementary Table S4 shows the standardized path coefficients of direct, indirect and total effects.

4. Discussion

Earlier studies on soil bacterial communities from various mountain ecosystems of the world have described different elevation patterns of

Table 4
Multiple linear regression models for the relationship of richness, evenness, and diversity with mean annual temperature (MAT), soil moisture content (SMC), and soil organic carbon (SOC).

α-Diversity	Predictor variables	R^2	α	β	F	p	AIC
Richness (Sobs)	SMC	0.50	1473.93 (487.38)	75.66 (23.03)	26.35	<0.001	836.12
	SOC			38.49 (11.05)			
Evenness	SOC	0.21	0.75 (0.02)	0.0015 (0.0003)	14.74	<0.001	−290
Diversity (Shannon Index)	SMC	0.36	5.43 (0.28)	0.03 (0.01)	14.81	<0.001	1.3
	SOC			0.02 (0.01)			

Values within parenthesis indicate standard error. α and β are constants. Significant at $p < 0.001$.

α-diversity, such as increasing (Luo et al., 2019; Zhang et al., 2019), decreasing (Adamczyk et al., 2019; Bryant et al., 2008; Shen et al., 2015; Siles and Margesin, 2017; Zhu et al., 2020) and unimodal trends (Singh et al., 2012). In contrast, α-diversity in our study followed a hollow trend, which dipped in the mid-elevations (Fig. 3). The same trend was found across all three sampling years (Fig. 4). Upon an in-depth literature review, we came across only a single study reporting a similar mid-elevation dip in bacterial α-diversity in the southwest and northeast slopes of Mt Halla, both at 700–1300 m elevation range (Singh et al., 2014). The mid-elevation dip suggests the dominance of other factors in controlling bacterial α-diversity rather than elevation or temperature (Fierer et al., 2011; Singh et al., 2014). Notably, the vegetation in our study shifts from the subalpine forest in lower elevations (3373–3564 m) to alpine scrub in the mid (3645–3770 m) to the alpine meadow in the higher elevations (3890–4020 m) (Table 1). The dip in α-diversity corresponds to the alpine scrub vegetation having low soil moisture, SOC, and nitrogen compared to other elevations (Table 1). On the contrary, subalpine forest and alpine meadow occurring in extreme climate regimes with similar edaphic characteristics (moisture, carbon, and nitrogen) had comparable α-diversity. This finding indicates that edaphic factors corresponding to different vegetation types control bacterial diversity rather than elevation or temperature. The regression analysis supports this assumption, as most variability in bacterial richness, evenness, and diversity were explained by SMC and SOC (and in turn nitrogen because of its high correlation with SOC, $r = 0.95$, $p < 0.001$) and not by temperature. The SEM analysis also indicated the direct effect of edaphic properties (SMC and SOC) on the bacterial richness and, in turn, diversity. The dominance of edaphic factors in governing bacterial diversity along elevation gradient has also been described earlier from Mt Changbai, the Italian Alps, the Andes, and southwest Wales (Fierer et al., 2011; Shen et al., 2013, 2015; Siles and Margesin, 2017; Xue et al., 2018). We found no effect of pH and C/N ratio on bacterial α-diversity and is in contrast to other studies where they have been identified as significant drivers of bacterial communities (Adamczyk et al., 2019; Lanzén et al., 2016; Shen et al., 2015; Yashiro et al., 2016).

The effect of edaphic properties was further displayed in the patterns of bacterial β-diversity. The overlaps found in community composition (Fig. 2) between low and high elevation suggested possible relatedness due to similarity in their edaphic properties. In contrast, the mid-elevations, having contrasting soil properties, showed different community compositions. The difference in community composition at mid-elevations was reflected in most phyla's relative abundances (*Acidobacteria*, *Dependentiae*, *Planctomycetes*, *Verrucomicrobia*, *Chloroflexi*, *Patescibacteria*, and *Chlamydiae*) showing mid-elevation dips (Fig. 2c). Low moisture-induced drier conditions and low substrate availability in mid-elevations may have limited the growth of these phyla and hence reduced their relative abundance (Brockett et al., 2012; Lladó et al., 2017). Low relative abundance of these bacterial phyla led to the dominance of *Proteobacteria* (54.1–74.2%) in the mid-elevations and resulted in less evenly distributed community composition (Fig. 2a), which was also evident from low evenness (0.69–0.77) (Fig. 3).

Mantel test, RDA, and SEM showed that the community composition across elevation gradient was influenced directly by both edaphic factors (SOC and pH) and temperature (Figs. 6 and 8). Linear regression also indicated the relationship of many phyla to temperature along with edaphic factors (Fig. 7). Consequently, irrespective of mid-elevation dips, relative abundances of such phyla increased or decreased across elevation. This was expected as temperature stimulates the growth and metabolic activities of bacteria and, in turn, affects the community (Zhou et al., 2016). However, the increasing temperature is only efficient in shaping community composition when nutrient and water supply is adequate (Lladó et al., 2017; Peltoniemi et al., 2015; Rousk et al., 2012). Moreover, the quality of nutrients also determines the fate of community distribution across elevation gradients in mountain ecosystems (Xu et al., 2014; Zheng et al., 2018). For instance, sub-alpine forest in the lower altitudes provides a high amount of leaf litter rich in recalcitrant carbon compared to alpine scrub and meadows, where leaf litter input is comparatively low and primarily seasonal. High leaf litter facilitates the growth of specific communities, such as, *Acidobacteria* that can derive energy by oxidizing the recalcitrant form of carbon (Lladó et al., 2017). On the contrary, the labile form of carbon mainly comes from root exudates and depends on the formation of root networks and carbon allocation from photosynthesis (Pollierer et al., 2007). Soil carbon content also depends on soil respiration, a process where soil carbon (mainly labile form) is lost due to carbon decomposition by microbes (Cleveland et al., 2007; Lladó et al., 2017).

Alpine scrub having low vegetation cover is exposed to warming leading to rapid soil carbon decomposition and emission (Bokhorst et al., 2007). These habitats also provide insufficient C supplies into the soil (Zhao et al., 2019). As a cumulative effect of high respiration and poor input, soils in these habitats are C deficient, as evident in our study (Table 1). Low carbon in soils often reduces their ability to hold water (Rawls et al., 2003), which further reduces microbial enzyme activity of communities and facilitates the growth of only those species that can grow in carbon and moisture-limited soils (Fierer et al., 2007; Koch,

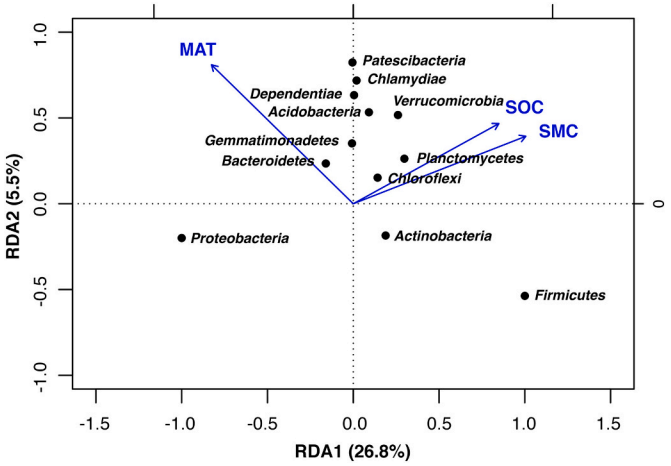

Fig. 6. Redundancy analysis (RDA) showing significant relationships between abundant bacterial phyla and mean annual temperature (MAT), soil moisture content (SMC), and soil organic carbon (SOC). The figure is generated using R 4.0.3 (http://www.R-project.org/) using vegan 2.5-7 (https://cloud.r-project.org/package=vegan).

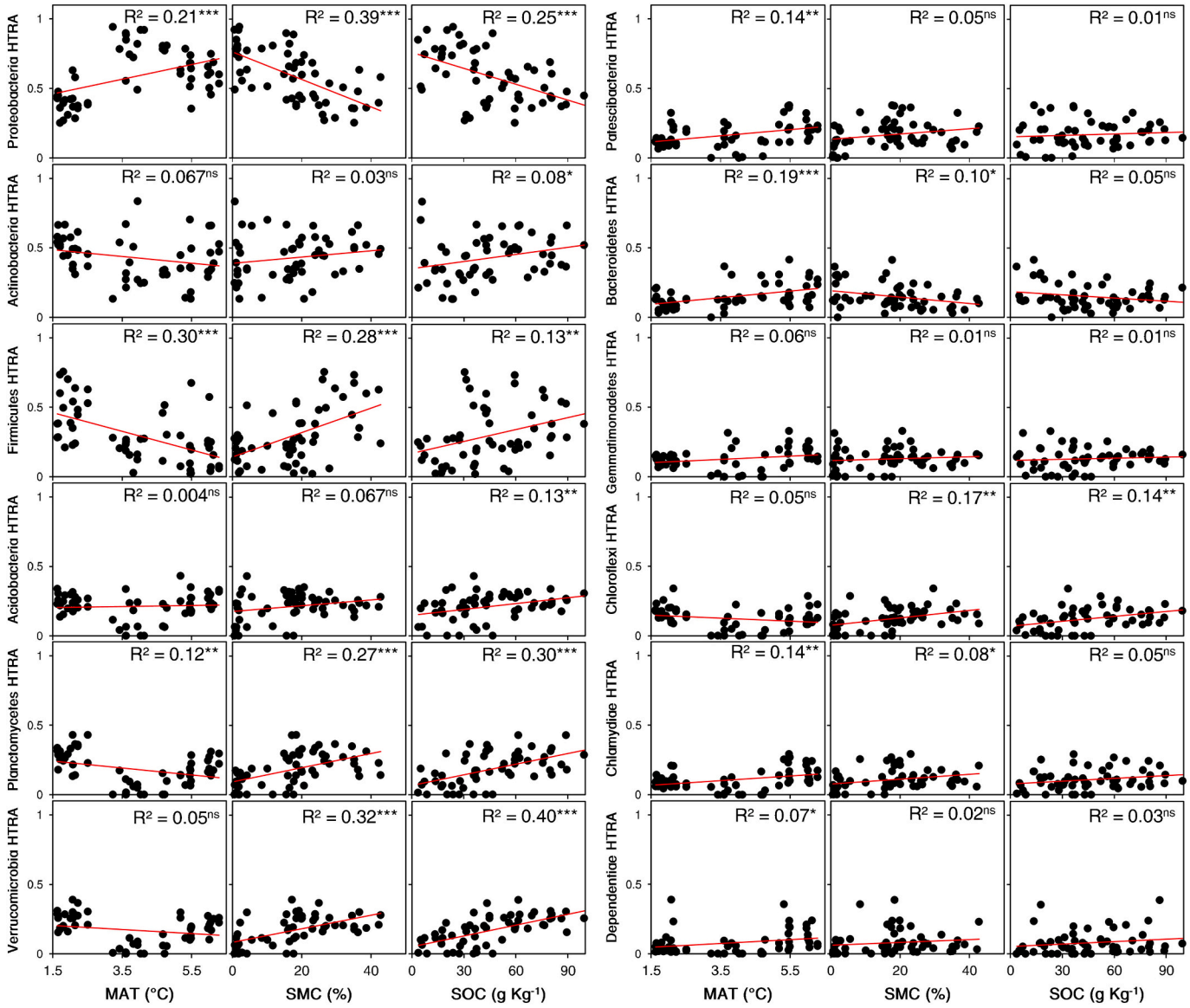

Fig. 7. Linear relationships between Hellinger transformed relative abundance (HTRA) of bacterial phyla across elevation and mean annual temperature (MAT), soil moisture content (SMC) and soil organic carbon (SOC). Significant at ***p < 0.001, **p < 0.01 and *p < 0.05; ns represents non-significant.

2001). Despite low carbon input due to low photosynthesis, alpine meadows act as sinks as decomposition rates are limited by low temperature (Adamczyk et al., 2019; Tiwari et al., 2021). Overall, we see three habitat types in our study area, (i) high moisture-nutrient-temperature (HMNT) habitat at lower elevations, (ii) low moisture-nutrient-high-temperature (LMNHT) habitat at mid-elevations, and (iii) high moisture-nutrient-low-temperature (HMNLT) habitat at higher elevations. These habitats showcase two kinds of stress, one by the temperature (HMNLT) and the other by moisture and nutrients (substrate availability) (LMNHT). Under temperature stress with adequate nutrients (HMNLT), the communities are co-operative, as seen by high positive interactions in the co-occurrence network at the high elevation range. Under nutrient stress with optimum temperature (LMNHT), communities compete for the limited substrate wherein certain species dominate, eventually decreasing the community evenness. This was indicated by the dominance of *Proteobacteria* in the mid-elevation (Fig. 2a), having high negative interactions with the other bacterial taxa (Fig. 5b). When temperature, moisture, and nutrients are optimum (HMNT), the communities participate in both positive and negative interactions (Fig. 5c), leading to the dominance of specific taxa (*Proteobacteria* in this study, Fig. 2a) along with high overall community evenness (Fig. 3).

In contrast to previous studies (Barboza et al., 2018; Lanzén et al., 2016; Lazzaro et al., 2015), we found no seasonal or inter-annual variation in bacterial diversity and composition, indicating the resilient nature of bacterial communities to environmental changes over the selected time window (Table 2, Fig. 4, Supplementary Tables S2 and S3). This finding also confirms the mid-elevation dip pattern across all years, thereby supporting the effect of edaphic factors over the temperature in community distribution.

5. Conclusion

This study demonstrates a mid-elevation dip in soil bacterial community diversity along an elevation-vegetation gradient across three years governed primarily by edaphic properties (SOC, total nitrogen, moisture, and pH) rather than temperature. This dip in diversity is a consequence of the shift in the bacterial socio-interactive array from co-operative to competitive under moisture and nutrient limitations. Further, the communities' seasonal and inter-annual stability confirms

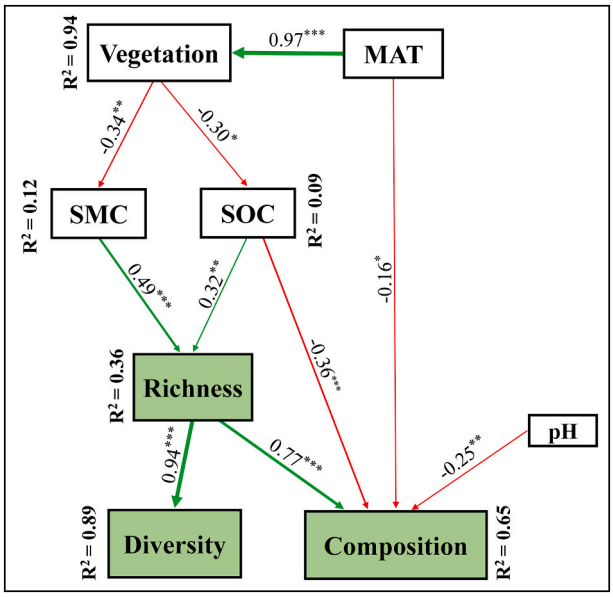

Fig. 8. Structural equation model (SEM) showing the causal influences of vegetation, MAT, SOC, SMC, and pH on bacterial richness, α-diversity, and composition. Red and green lines indicate significant negative and positive effects, respectively. The width of the arrows is based on the standardized path coefficients indicating the strength of the causal effect. The standardize coefficients are marked above each path (* indicates significant ($p < 0.05$) effects, ** indicates significant ($p < 0.01$) effects, *** indicates significant ($p < 0.001$) effects). R^2 values represent the percentage of variance explained for each variable.

the mid-elevation pattern and provides evidence for their resilience towards climate shifts. By considering both spatial and temporal variability, our results enhance the reliability of the observed distribution pattern and the regulating factors. This is the first study from the temperature-sensitive high-altitude region of Himalaya that will help to understand the factors underlying bacterial diversity distribution and enhance the predictability of environmental change impacts on these communities.

CRediT authorship contribution statement

Conceptualization and fund acquisition: G.S.R., G.T., and P.B., Supervision: G.S.R. and G.T., Study design: P.T. and P.B., Fieldwork: P.B., G.T., and I.D.R., DNA sequencing: P.B., Soil physicochemical analyses: P.B. and P.T., Data analyses: P.T. and P.B., Figures and tables preparation: P.T., P.B. and I.D.R., First draft preparation and compilation: P.B. and P.T., Reviewing and commenting: All authors.

Declaration of competing interest

The authors declare that they have no known competing financial interests or personal relationships that could have appeared to influence the work reported in this paper.

Acknowledgments

This research is part of the project National Mission for Sustaining the Himalayan Ecosystem (NMSHE) funded by the Department of Science and Technology, Government of India (grant no. DST/SPLICE/CCP/NMSHE/TF-2/WII/2014[G]). Partial funding for the bacterial Next Generation Sequencing was provided by the United Nations Development Programme and the Ministry of Environment, Forest and Climate Change Government of India through the Third National Communication project (grant no. 7/2/2015-CC). Pamela Bhattacharya was supported by the Council of Scientific and Industrial Research, Government of India (award no. 09/668(0012)/2019-EMR-I). Forest Department of Uttarakhand provided necessary permits to conduct the research in Gangotri National Park. We acknowledge help from Dr. Devendra Kumar and Umed Singh Rana (field assistance), Arun Kumar (laboratory work), Debanjan Sarkar (Maps), Dr. Punyasloke Bhadury (DNA sequencing), Dr. Awadhesh Pandit, and Tejali Naik (NGS work), Sitendu Goswami, Nilanjan Chatterjee and Dr. Raman Kumar (data analysis). We thank Dr. Sathyakumar (Nodal Scientist, NMSHE), Director, Dean, Research Coordinator, and Nodal Officer of Wildlife Forensics and Conservation Genetics Cell of Wildlife Institute of India for facilitating this work.

Appendix A. Supplementary data

Supplementary data to this article can be found online at https://doi.org/10.1016/j.apsoil.2021.104306.

References

Adamczyk, M., Hagedorn, F., Wipf, S., Donhauser, J., Vittoz, P., Rixen, C., Frossard, A., Theurillat, J.P., Frey, B., 2019. The soil microbiome of GLORIA Mountain summits in the Swiss Alps. Front. Microbiol. 10, 1–21.
Barboza, A.D.M., Pylro, V.S., Jacques, R.J.S., Gubiani, P.I., de Quadros, F.L.F., da Trindade, J.K., Triplett, E.W., Roesch, L., 2018. Seasonal dynamics alter taxonomical and functional microbial profiles in Pampa biome soils under natural grasslands. PeerJ 6, e4991.
Bhattacharyya, T., Pal, D.K., Chandran, P., Ray, S.K., Mandal, C., Telpande, B., 2008. Soil carbon storage capacity as a tool to prioritize areas for carbon sequestration. Curr. Sci. 482–494.
Blakemore, L.C., Searle, P.L., Daly, B.K., 1987. Methods for Chemical Analysis of soils. New Zealand Soil Bureau, Department of Scientific and Industrial Research, New Zealand.
Bokhorst, S., Huiskes, A., Convey, P., Aerts, R., 2007. Climate change effects on organic matter decomposition rates in ecosystems from the maritime Antarctic and Falkland Islands. Glob. Chang. Biol. 13, 2642–2653.
Bremner, J.M., 2018. Nitrogen-total. In: Sparks, D.L., Page, A.L., Helmke, P.A., Loeppert, R.H., Soltanpour, P.N., Tabatabai, M.A., Johnston, C.T., Sumner, M.E. (Eds.), SSSA Book Series. Soil Science Society of America, American Society of Agronomy, Madison, WI, USA, pp. 1085–1121.
Brockett, B.F.T., Prescott, C.E., Grayston, S.J., 2012. Soil moisture is the major factor influencing microbial community structure and enzyme activities across seven biogeoclimatic zones in western Canada. Soil Biol. Biochem. 44, 9–20.
Bryant, J.A., Lamanna, C., Morlon, H., Kerkhoff, A.J., Enquist, B.J., Green, J.L., 2008. Microbes on mountainsides: contrasting elevational patterns of bacterial and plant diversity. Proc. Natl. Acad. Sci. 105, 11505–11511.
Cleveland, C.C., Nemergut, D.R., Schmidt, S.K., Townsend, A.R., 2007. Increases in soil respiration following labile carbon additions linked to rapid shifts in soil microbial community composition. Biogeochemistry 82, 229–240.
Crowther, T.W., van den Hoogen, J., Wan, J., Mayes, M.A., Keiser, A.D., Mo, L., Averill, C., Maynard, D.S., 2019. The global soil community and its influence on biogeochemistry. Science 365, eaav0550.
Deng, Y., Jiang, Y.-H., Yang, Y., He, Z., Luo, F., Zhou, J., 2012. Molecular ecological network analyses. BMC Bioinformatics 13, 113.
Donhauser, J., Frey, B., 2018. Alpine soil microbial ecology in a changing world. FEMS Microbiol. Ecol. 94, 1–31.
Djukic, I., Zehetner, F., Mentler, A., Gerzabek, M.H., 2010. Microbial community composition and activity in different alpine vegetation zones. Soil Biol. Biochem. 42, 155–161.
Edgar, R.C., Haas, B.J., Clemente, J.C., Quince, C., Knight, R., 2011. UCHIME improves sensitivity and speed of chimera detection. Bioinformatics 27, 2194–2200.
Fierer, N., Bradford, M.A., Jackson, R.B., 2007. Toward an ecological classification of soil bacteria. Ecology 88, 1354–1364.
Fierer, N., McCain, C.M., Meir, P., Zimmermann, M., Rapp, J.M., Silman, M.R., Knight, R., 2011. Microbes do not follow the elevational diversity patterns of plants and animals. Ecology 92, 797–804.
Grace, J.B., 2006. In: Structural Equation Modeling and Natural Systems. Cambridge University Press, Cambridge, p. 365.
Harry, M., Gambier, B., Garnier-Sillam, E., 2000. Soil conservation for DNA preservation for bacterial molecular studies. Eur. J. Soil Biol. 36, 51–55.
Johnson, J.B., Omland, K.S., 2004. Model selection in ecology and evolution. Trends Ecol. Evol. 19, 101–108.
Koch, A.L., 2001. Oligotrophs versus copiotrophs. Bioessays 23, 657–661.
Kozich, J.J., Westcott, S.L., Baxter, N.T., Highlander, S.K., Schloss, P.D., 2013. Development of a dual-index sequencing strategy and curation pipeline for analyzing amplicon sequence data on the MiSeq illumina sequencing platform. Appl. Environ. Microbiol. 79, 5112–5120.
Lanzén, A., Epelde, L., Blanco, F., Martín, I., Artetxe, U., Garbisu, C., 2016. Multi-targeted metagenetic analysis of the influence of climate and environmental

parameters on soil microbial communities along an elevational gradient. Sci. Rep. 6, 28257.
Lazzaro, A., Hilfiker, D., Zeyer, J., 2015. Structures of microbial communities in alpine soils: seasonal and elevational effects. Front. Microbiol. 6, 1–13.
Li, J., Ma, Y.-B., Hu, H.-W., Wang, J.-T., Liu, Y.-R., He, J.-Z., 2015. Field-based evidence for consistent responses of bacterial communities to copper contamination in two contrasting agricultural soils. Front. Microbiol. 6.
Lladó, S., Mondéjar, R.L., Baldrian, P., 2017. Forest soil bacteria: diversity, involvement in ecosystem processes, and response to global change. Microbiol. Mol. Biol. Rev. 81, 1–27.
Longbottom, T.L., Small, A.T., Owen, L.A., Murari, M.K., 2014. Climatic and topographic controls on soil organic matter storage and dynamics in the indian himalaya: potential carbon cycle–climate change feedbacks. Catena 119, 125–135.
Luo, Z., Liu, J., Zhao, P., Jia, T., Li, C., Chai, B., 2019. Biogeographic patterns and assembly mechanisms of bacterial communities differ between habitat generalists and specialists across elevational gradients. Front. Microbiol. 10, 1–14.
Masse, J., Prescott, C.E., Renaut, S., Terrat, Y., Grayston, S.J., 2017. Plant community and nitrogen deposition as drivers of alpha and Beta diversities of prokaryotes in reconstructed oil sand soils and natural boreal Forest soils. Appl. Environ. Microbiol. 83, 1–17.
Oksanen, J., Guillaume Blanchet, F., Friendly, M., Kindt, R., Legendre, P., McGlinn, D., Minchin, P.R., O'Hara, R.B., Simpson, G.L., Solymos, P., Henry, M., Stevens, M., Szoecs, E., Wagner, H., 2020. Vegan: community ecology package. R package version 2.5-7. https://CRAN.R-project.org/package=vegan.
Padma, T.V., 2014. Himalayan plants seek cooler climes. Nature 512, 359.
Pedrós-Alió, C., 2006. Marine microbial diversity: can it be determined? Trends Microbiol. 14, 257–263.
Peltoniemi, K., Laiho, R., Juottonen, H., Kiikkilä, O., Mäkiranta, P., Minkkinen, K., Pennanen, T., Penttilä, T., Sarjala, T., Tuittila, E.S., Tuomivirta, T., Fritze, H., 2015. Microbial ecology in a future climate: effects of temperature and moisture on microbial communities of two boreal fens. FEMS Microbiol. Ecol. 91, fiv062.
Pollierer, M.M., Langel, R., Körner, C., Maraun, M., Scheu, S., 2007. The underestimated importance of belowground carbon input for forest soil animal food webs. Ecol. Lett. 10, 729–736.
Quast, C., Pruesse, E., Yilmaz, P., Gerken, J., Schweer, T., Yarza, P., Peplies, J., Glöckner, F.O., 2012. The SILVA ribosomal RNA gene database project: improved data processing and web-based tools. Nucleic Acids Res. 41, D590–D596.
Rawls, W.J., Pachepsky, Y.A., Ritchie, J.C., Sobecki, T.M., Bloodworth, H., 2003. Effect of soil organic carbon on soil water retention. Geoderma 116, 61–76.
Rayment, G.E., Lyons, D.J., 2011. Soil Chemical Methods. CSIRO Publishing, Australasia. Collingwood.
Rousk, J., Frey, S.D., Bååth, E., 2012. Temperature adaptation of bacterial communities in experimentally warmed forest soils. Glob. Chang. Biol. 18, 3252–3258.
Sanyal, A.K., Uniyal, V.P., Chandra, K., Bhardwaj, M., 2013. Diversity, distribution pattern and seasonal variation in moth assemblages along altitudinal gradient in gangotri landscape area, Western himalaya, Uttarakhand, India. J. Threatened Taxa 5, 3646–3653.
Schloss, P.D., Westcott, S.L., Ryabin, T., Hall, J.R., Hartmann, M., Hollister, E.B., Lesniewski, R.A., Oakley, B.B., Parks, D.H., Robinson, C.J., Sahl, J.W., Stres, B., Thallinger, G.G., Van Horn, D.J., Weber, C.F., 2009. Introducing mothur: open-source, platform-independent, community-supported software for describing and comparing microbial communities. Appl. Environ. Microbiol. 75, 7537–7541.
Shannon, P., Markiel, A., Ozier, O., Baliga, N.S., Wang, J.T., Ramage, D., Amin, N., Schwikowski, B., Ideker, T., 2003. Cytoscape: a software environment for integrated models of biomolecular interaction networks. Genome Res. 13, 2498–2504.
Shen, C., Ni, Y., Liang, W., Wang, J., Chu, H., 2015. Distinct soil bacterial communities along a small-scale elevational gradient in alpine tundra. Front. Microbiol. 6, 1–12.
Shen, C., Xiong, J., Zhang, H., Feng, Y., Lin, X., Li, X., Liang, W., Chu, H., 2013. Soil pH drives the spatial distribution of bacterial communities along elevation on Changbai Mountain. Soil Biol. Biochem. 57, 204–211.
Shrestha, U.B., Gautam, S., Bawa, K.S., 2012. Widespread climate change in the Himalayas and associated changes in local ecosystems. PLoS ONE 7, e36741.
Siles, J.A., Cajthaml, T., Filipová, A., Minerbi, S., Margesin, R., 2017. Altitudinal, seasonal and interannual shifts in microbial communities and chemical composition of soil organic matter in alpine forest soils. Soil Biol. Biochem. 112, 1–13.
Siles, J.A., Cajthaml, T., Minerbi, S., Margesin, R., 2016. Effect of altitude and season on microbial activity, abundance and community structure in alpine forest soils. FEMS Microbiol. Ecol. 92, fiw008.
Siles, J.A., Margesin, R., 2017. Seasonal soil microbial responses are limited to changes in functionality at two alpine forest sites differing in altitude and vegetation. Sci. Rep. 7, 2204.
Siles, J.A., Margesin, R., 2016. Abundance and diversity of bacterial, archaeal, and fungal communities along an altitudinal gradient in alpine Forest soils: what are the driving Factors? Microb. Ecol. 72, 207–220.
Singh, D., Cruz, L.L., Kim, W.S., Kerfahi, D., Chun, J.H., Adams, J.M., 2014. Strong elevational trends in soil bacterial community composition on Mt. Halla, South Korea. Soil Biol. Biochem. 68, 140–149.
Singh, D., Takahashi, K., Kim, M., Chun, J., Adams, J.M., 2012. A hump-backed trend in bacterial diversity with elevation on Mount Fuji, Japan. Microb. Ecol. 63, 429–437.
Sun, H., Wu, Y., Zhou, J., Bing, H., Zhu, H., 2020. Climate influences the alpine soil bacterial communities by regulating the vegetation and the soil properties along an altitudinal gradient in SW China. Catena 195, 1–12.
Tang, M., Li, L., Wang, X., You, J., Li, J., Chen, X., 2020. Elevational is the main factor controlling the soil microbial community structure in alpine tundra of the Changbai Mountain. Sci. Rep. 10, 12442.
Team, R.C., 2020. R: A Language and Environment for Statistical Computing. R Foundation for Statistical Computing, Vienna, Austria.
Tiwari, P., Bhattacharya, P., Rawat, G.S., Rai, I.D., Talukdar, G., 2021. Experimental warming increases ecosystem respiration by increasing above-ground respiration in alpine meadows of Western himalaya. Sci. Rep. 11, 2640.
Treseder, K.K., Balser, T.C., Bradford, M.A., Brodie, E.L., Dubinsky, E.A., Eviner, V.T., Hofmockel, K.S., Lennon, J.T., Levine, U.Y., MacGregor, B.J., Ridge, J.P., Waldrop, M.P., 2012. Integrating microbial ecology into ecosystem models: challenges and priorities. Biogeochemistry 109, 7–18.
Trivedi, P., Anderson, I.C., Singh, B.K., 2013. Microbial modulators of soil carbon storage: integrating genomic and metabolic knowledge for global prediction. Trends Microbiol. 21, 641–651.
Walkley, A., Black, I.A., 1934. An examination of the degtjareff method for determining soil organic matter, and a proposed modification of the chromic acid titration method. Soil Sci. 37, 29–38.
Wickham, H., 2011. ggplot2: ggplot2. Wiley Interdiscip. Rev. Comput. Stat. 3, 180–185.
Wickham, H., Wickham, M.H., 2017. Package tidyverse. In: Easily Install and Load the 'Tidyverse. https://tidyverse.tidyverse.org.
Wieder, W.R., Grandy, A.S., Kallenbach, C.M., Taylor, P.G., Bonan, G.B., 2015. Representing life in the earth system with soil microbial functional traits in the MIMICS model. Geosci. Model Dev. 8, 1789–1808.
Xu, M., Li, X., Cai, X., Gai, J., Li, X., Christie, P., Zhang, J., 2014. Soil microbial community structure and activity along a montane elevational gradient on the tibetan plateau. Eur. J. Soil Biol. 64, 6–14.
Xu, Z., Yu, G., Zhang, X., Ge, J., He, N., Wang, Q., Wang, D., 2015. The variations in soil microbial communities, enzyme activities and their relationships with soil organic matter decomposition along the northern slope of Changbai Mountain. Appl. Soil Ecol. 86, 19–29.
Xue, P.P., Carrillo, Y., Pino, V., Minasny, B., McBratney, A.B., 2018. Soil properties drive microbial community structure in a large scale transect in south eastern Australia. Sci. Rep. 8, 11725.
Yang, Y., Fang, J., Tang, Y., Ji, C., Zheng, C., He, J., Zhu, B., 2008. Storage, patterns and controls of soil organic carbon in the tibetan grasslands. Glob. Chang. Biol. 14, 1592–1599.
Yashiro, E., Pinto-Figueroa, E., Buri, A., Spangenberg, J.E., Adatte, T., Hirzel, H.N., Guisan, A., van der Meer, J.R., 2016. Local environmental factors drive divergent grassland soil bacterial communities in the Western swiss Alps. Appl. Environ. Microbiol. 82, 6303–6316.
Zhang, B., Xue, K., Zhou, S., Che, R., Du, J., Tang, L., Pang, Z., Wang, F., Wang, D., Cui, X., Hao, Y., Wang, Y., 2019. Phosphorus mediates soil prokaryote distribution pattern along a small-scale elevation gradient in noijin kangsang peak, tibetan plateau. FEMS Microbiol. Ecol. 95, fiz076.
Zhao, Z., Zhang, X., Dong, S., Wu, Y., Liu, S., Su, X., Wang, X., Zhang, Y., Tang, L., 2019. Soil organic carbon and total nitrogen stocks in alpine ecosystems of Altun Mountain National Nature Reserve in dry China. Environ. Monit. Assess. 191, 40.
Zheng, H., Chen, Y., Liu, Y., Zhang, J., Yang, W., Yang, L., Li, H., Wang, L., Wu, F., Guo, L., 2018. Litter quality drives the differentiation of microbial communities in the litter horizon across an alpine treeline ecotone in the eastern tibetan plateau. Sci. Rep. 8, 10029.
Zhou, J., Deng, Y., Luo, F., He, Z., Yang, Y., 2011. Phylogenetic molecular ecological network of soil microbial communities in response to elevated CO 2. MBio 2.
Zhou, J., Deng, Y., Shen, L., Wen, C., Yan, Q., Ning, D., Qin, Y., Xue, K., Wu, L., He, Z., Voordeckers, J.W., Nostrand, J.D.V., Buzzard, V., Michaletz, S.T., Enquist, B.J., Weiser, M.D., Kaspari, M., Waide, R., Yang, Y., Brown, J.H., 2016. Temperature mediates continental-scale diversity of microbes in forest soils. Nat. Commun. 7, 12083.
Zhu, B., Li, C., Wang, J., Li, J., Li, X., 2020. Elevation rather than season determines the assembly and co-occurrence patterns of soil bacterial communities in forest ecosystems of mount gongga. Appl. Microbiol. Biotechnol. 104, 7589–7602.

OPINION

Importance of monitoring soil microbial community responses to climate change in the Indian Himalayan region

Pamela Bhattacharya, Gautam Talukdar, Gopal Singh Rawat and Samrat Mondol

Increasing emission rate of carbon dioxide (CO_2) and other greenhouse gases is the major driver of global temperature increase. Soil microbial respiration is accelerating the release of CO_2 in the environment, but the mechanistic understanding of this process is still at its nascent stage. In this note, we discuss the importance of understanding the microbial responses to climate change and associated respiration process in the Indian Himalayan region. We also discuss the goals of microflora component of the ongoing National Mission for Sustaining the Himalayan Ecosystem project in tracking climate change impacts in this fragile, mountainous ecosystem.

Global climate change is currently a major challenge for modern science and society. Increasing emission rate of carbon dioxide (CO_2) from both natural and anthropogenic sources, along with other greenhouse gases is playing a major role in global warming. CO_2 emission from soil respiration (both autotrophic root respiration and heterotrophic microbial respiration) is known to be the second largest natural terrestrial flux of carbon[1]. Conversely, rising temperature leads to depletion of soil organic carbon (SOC) stocks through enhanced microbial decomposition and rapid release of CO_2, providing a positive feedback to climate change[2]. Although recent climate-carbon models support such positive feedback responses, the detailed process is still unknown due to our limited understanding of temperature sensitivity of microbial SOC decomposition[3]. Despite soil microbial decomposition of SOC results in emitting up to 25% natural CO_2 each year[4], the process of microbial community respiration with regard to climate change under varying soil environment has not been studied globally.

Soil microbial communities mediate global biogeochemical cycles (carbon, nitrogen), and any climate-driven physiological changes can affect the rates of these cyclic processes[5]. To understand patterns of temperature-induced microbial respiration at the level of ecosystems, there is a need for paradigm shift from earlier climate models which focused mainly on soil carbon pool size[6]. Particular emphasis is needed on understanding soil microbial community diversity, composition and functions for mechanistic insight into their feedback responses to climate warming[5]. A number of studies suggest that soil microorganisms either undergo functional modifications of their existing populations, or changes in their community composition in response to environmental changes, leading to altered temperature sensitivity of SOC decomposition[5,7]. Functional modifications might happen in the short-term temperature rise scenario, resulting in an increasing soil microbial respiration from faster microbial growth and physiological processes[5,7]. However, in the long-term climate change scenario, the increase or decrease in microbial respiration rate will depend on the environmental conditions and resource availability (substrate) for the existing microbial community[5,7]. Similarly, shift in microbial community composition can also be driven by environmental changes and consequently may affect soil respiration rates[5,7]. If the changed community has higher carbon efficiency (i.e. it stores more carbon than it metabolizes), then SOC decomposition will decrease along with microbial respiration rate[5]. However, in the event of community shifts towards greater diversity with microbes capable of degrading complex soil carbon, SOC decomposition will increase favouring CO_2 emission from soil and provide positive feedback to climate change[7]. Therefore, identifying different functional groups of microbes is essential in understanding the feedback responses, as they have varying capacities to decompose SOC[8]. Since such feedback responses will vary across ecosystems and regions, a clear understanding on which of these mechanisms is prevalent and how microbial diversity will affect the responses is critical in quantifying them. Although a number of studies have focused on addressing these issues in different parts of the world[9,10], data from the Indian subcontinent are completely lacking.

The Himalayan region comprising diverse and fragile ecosystems offers an excellent opportunity to study the response of changing climate on soil microbial environment, and is considered most vulnerable to increasing temperature. Harbouring a gradient of environments and ecosystems from extremely low carbon stock such as morainic soils to carbon-rich peatlands, this region plays a significant role in global carbon cycle[11]. A perusal of the literature on the Indian Himalayan region (IHR) reveals that it retains about 33% of the country's SOC[12] that changes along elevation gradient[13]. However, very few attempts have been made to quantify the rates of microbial respiration and short-term impacts of temperature and precipitation variations on SOC storage across different forest types[14]. There is a need to establish baselines on these parameters and initiate long-term monitoring. To address the information gap and also understand the impacts of climate change on the Himalayan ecosystems, the Department of Science and Technology, Government of India has initiated a dedicated National Mission for Sustaining the Himalayan Ecosystem (NMSHE) in the IHR in 2015. As part of this mission, studies on soil microflora and fauna have been initiated along an elevational gradient in the Gangotri National Park and adjoining regions to generate baseline data on soil microbial community diversity and their SOC degrading potential. With specific focus on soil bacteria, fungi, lichens and nematodes along with soil physico-chemical properties and SOC degrading enzyme activities, this component will provide valuable insights into the microbial control of soil CO_2 emission and a rapid method to track climate change impacts at ecosystem level.

Baseline data generated on soil properties, microbial biodiversity, activity and respiration in the IHR will assist in understanding the mechanisms and controlling factors of SOC decomposition in the region. Through modeling of these soil microbial community data along with other climate factors, the results will help us in developing long-term strategies to monitor climate change impacts and propose policy briefs/management strategies to manage microbial systems for mitigation of climate change.

1. Raich, J. W. *et al.*, *Global Change Biol.*, 2002, **8**, 800–812.
2. Suseela, V. *et al.*, *Global Change Biol.*, 2012, **18**, 336–348.
3. Ågren, G. I. and Wetterstedt, J. M., *Soil Biol. Biochem.*, 2007, **37**, 1794–1798.
4. Schimel, D. S., *Global Change Biol.*, 1995, **1**, 77–91.
5. Singh, B. K. *et al.*, *Nature Rev. Microbiol.*, 2010, **8**, 779–790.
6. Todd-Brown, K. E. *et al.*, *Biogeochemistry*, 2012, **109**, 19–33.
7. Pold, G. and DeAngelis, K. M., *Diversity*, 2013, **5**, 409–425.
8. Treseder, K. K. *et al.*, *Biogeochemistry*, 2012, **109**, 7–18.
9. Whitaker, J. *et al.*, *J. Ecol.*, 2014, **102**, 1058–1071.
10. Delgado-Baquerizo, M. *et al.*, *Ecol. Monogr.*, 2016, **86**, 373–390.
11. Yang, Y. H. *et al.*, *Biogeochemistry*, 2007, **84**, 131–141.
12. Bhattacharyya, T. *et al.*, *Curr. Sci.*, 2008, **95**, 482–484.
13. Longbottom, T. L. *et al.*, *Catena*, 2014, **119**, 125–135.
14. Sheikh, M. A. *et al.*, *Carbon Balance Manage.*, 2009, **4**, 1.

ACKNOWLEDGEMENTS. We thank Director, Wildlife Institute of India, Dehradun, and Nodal Officer, NMSHE project for support and DST, GoI for funding the NMSHE project. S.M. thanks DST for INSPIRE Faculty Award.

Pamela Bhattacharya, Gautam Talukdar, Gopal Singh Rawat and Samrat Mondol are in the Wildlife Institute of India, Chandrabani, Dehradun 248 001, India.*
**e-mail: samrat@wii.gov.in*

Declaring the commercial source and grade of chemicals, and equipment, in a scientific paper

Jaime A. Teixeira da Silva and Judit Dobránszki

Scientific biomedical papers widely use chemicals, reagents and/or equipment. These are described in the materials and methods section. The source of these methodological props needs to be precisely defined for scientific and proprietary reasons. The commercial source or grade of a chemical can affect the quality and outcome of an analysis, e.g. in plant tissue culture. Failure to recognize the commercial source deprives a company of its due proprietary investment in a product, reduces reproducibility and thus constitutes an incomplete or erroneous methodology. Such errors should be corrected, which should be the responsibility of authors, editors and publishers.

A methodological prop or tool (MPT) is defined here as any chemical, utensil, or equipment (CUE) that serves to support a methodology within a scientific manuscript. Not only do MPTs serve as important and fundamental tools for completing a method, their commercial source can, in select cases, also influence the outcome of a scientific manuscript. This note aims, using plant tissue culture, to (a) highlight the importance of specifying the commercial source and grade of CUEs; (b) show through select and concrete examples, how specific CUEs from different sources, or of different quality, can lead to qualitative and quantitative differences in the outcome of an experiment; (c) encourage authors, editors and publishers to correct the literature, to correct the weaknesses of traditional peer review[1], through post-publication peer review (PPPR), in a bid to make the methodological sections as accurate and precise as possible. In doing so, reproducibility of weak, unclear or unstated methodological flaws might increase. However, efforts to increase reproducibility will be in vain, unless all parties are involved[2].

Using select examples of plant tissue culture, a branch of plant biotechnology, we demonstrate how differences in the choice of MPTs and CUEs can influence the outcome of an experiment. Thus, defining these elements is a central aspect of reproducibility of a protocol. This concept is fortified by a respectable leading Society in the plant science community – The American Society for Horticultural Science[3], which states that 'In general, refer to trade or brand names only parenthetically with the active ingredient, chemical formula, purity, and diluent or solvent stated clearly in the text and emphasized in preference to the commercial product; also, include the name, city, and state/country of the company that produces the product.'

The effect of chemicals, vessels, or medium components on analytical and developmental outcome in plant tissue culture

Plant cells and tissues can grow and develop *in vitro* on different media containing inorganic and organic nutrients and plant growth regulators that are added, creating an artificial growth environment, and either benefiting or negatively affecting growth. However, such nutrients may also contain impurities in the